United States
Environmental Protection
Agency

Environmental Monitoring Systems
Laboratory
Research Triangle Park NC 27711

EPA-600/9-84-001
January 1984

Research and Development

EPA

Proceedings:

National Symposium on Recent Advances in Pollutant Monitoring of Ambient Air and Stationary Sources

Do not remove. This document should be retained in the EPA Region 5 Library Collection.

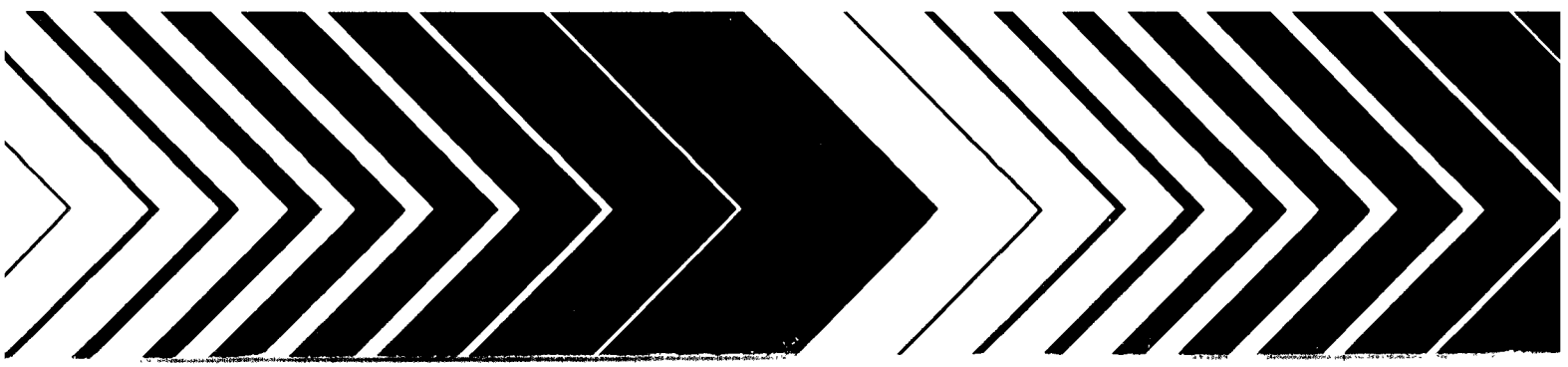

EPA-600/9-84-001
January 1984

occ 11055976

PROCEEDINGS: NATIONAL SYMPOSIUM ON RECENT ADVANCES IN POLLUTANT MONITORING OF AMBIENT AIR AND STATIONARY SOURCES

Raleigh Hilton Hotel

May 3-6, 1983

U.S. Environmental Protection Agency
Region 5, Library (PL-12J)
77 West Jackson Boulevard, 12th Floor
Chicago, IL 60604-3590

Environmental Monitoring Systems Laboratory
Office of Research and Development
U.S. Environmental Protection Agency

NOTICE

This document has been reviewed in accordance with U.S. Environmental Protection Agency policy and approved for publication. Mention of trade names or commercial products does not constitute endorsement or recommendation for use.

CONTENTS

Foreword v
Introduction vi
Session I. Inorganic Pollutants 1
Evaluation of Denuder Tubes for the Measurement of Sulfur Aerosol Composition 2
A Novel Nitrogen Dioxide Detector 13
The Use of a Tunable Diode Laser Absorption Spectrometer for Measuring Trace Gases in Trophospheric Air 23

Session II. Particulate Pollutants 33
Calibration and Testing of Inhalable Particle Samplers 34
Particulate Sampling Efficiency Dependence on Inlet Orientation and Flow Velocities 46

Session III. General and Source Oriented Monitoring 57
Metal Foil Collection/Flash Vaporization/Flame Photometry as Applied to Ambient Air Monitoring of Total Gaseous Sulfur 58
Measurement of Mercury Emissions from a Modified In-Situ Oil Shale Retort 69
Comparison of TEM and SEM Techniques for Measurement of Airborne Asbestos Fibers 83
A Pill for the Assessment of Pollution Measurement Methods 95
Sampling and Analysis of Incineration Effluents With the Volatile Organic Sampling Train (VOST) 112
Analysis of PCB's by Capillary GC/ECD for Detoxification Studies 127

Session IV. Personal Monitoring 137
Validation of a Passive Sampler for Determining Formaldehyde in Residential Indoor Air 138
Laboratory Studies of the Temperature Dependence of the Palmes NO_2 Passive Sampler 152
NIOSH-Developed Systems for Monitoring Equipment Evaluations 167
Relationships of Measured NO_2 Concentrations at Discrete Sampling Locations in Residences 177
Estimated Distributions of Personal Exposure to Respirable Particles 191
Empirical Models for Estimating Individual Exposures to Air Pollutants in a Health Effects Study 206
Carbon Monoxide Exposures in Washington, DC and Denver, Colorado During the Winter of 1982-83 220
Personal Exposure to Nitrogen Dioxide 234
Comparison of Permeation and Diffusion-Type Passive Samplers Versus Charcoal Tube Collection of Selected Gases 263

CONTENTS (Cont'd)

Session V. Acid Deposition..... 275
Automated Acquisition, Filtering and Reduction of Ion Chromatographic Data..... 276
Design and Testing of a Prototype Rainwater Sampler/Analyzer..... 290
Organic Acidity in Precipitation from Remote Areas of the World.... 300
A Field Intercomparison of Particle and Gas Dry Deposition Measurement and Monitoring Methods..... 311
A Comparison of Ambient Airborne Sulfate Concentrations Determined by Several Different Filtration Techniques..... 319
Comparison of Surrogate Surface Techniques for Estimation of Sulfate Dry Deposition..... 329

Session VI. Organic Pollutants..... 343
Evaluation of Solid Sorbents for Collection of Volatile Organics in Ambient Air..... 344
Detection of Environmental Pollutants Using Piezoelectric Crystal Sensors..... 358
Reduced-Temperature Preconcentration of Volatile Organics for Gas Chromatographic Analysis: System Automation..... 371
Detection and Determination of Polychlorinated Biphenyls in Ambient Air..... 379
A Cost-Effective Procedure to Screen Air Samples for Polyaromatic Pollutants..... 392

FOREWORD

Measurement and monitoring research efforts are designed to anticipate potential environmental problems, to support regulatory actions by developing an in-depth understanding of the nature and processes that impact health and the ecology, to provide innovative means of monitoring compliance with regulations and to evaluate the effectiveness of health and environmental protection efforts through the monitoring of long-term trends. The Environmental Monitoring Systems Laboratory, Research Triangle Park, North Carolina, has the responsibility for: assessment of environmental monitoring technology and systems; implementation of agency-wide quality assurance programs for air pollution measurement systems; and supplying technical support to other groups in the Agency including the Office of Air, Noise and Radiation, the Office of Pesticides and Toxic Substances and the Office of Solid Waste and Emergency Response.

This symposium is part of a continuing effort to explore recent advances in pollutant monitoring of ambient air and stationary sources. It serves as a forum for exchange of ideas and scientific information. In response to the Agency regulatory needs, this symposium focused on acid deposition, personal exposure and toxic substances. This publication is intended to assist those researchers interested in furthering the science of air monitoring.

Thomas R. Hauser, Ph.D.
Director
Environmental Monitoring Systems Laboratory
Research Triangle Park, North Carolina

INTRODUCTION

The third annual national symposium sponsored by EPA's Environmental Monitoring Systems Laboratory was held May 3-6, 1983 in Raleigh, North Carolina. In seven sessions over four days, papers and discussions focused on state-of-the-art systems for monitoring source emissions, ambient air, acid deposition, hazardous emissions and personal monitoring. The sessions were categorized as follows:

SESSION I	Inorganic Pollutants
SESSION II	Particulate Pollutants
SESSION III	General and Source Oriented Monitoring
SESSION IV	Personal Monitoring
SESSION V	Acid Deposition
SESSION VI	Organic Pollutants
SESSION VII	Panel Discussion

The papers are in the same order as presented by the speakers. Several papers are omitted because the speakers did not submit them in time for the agency's peer review.

SESSION I

INORGANIC POLLUTANTS

EVALUATION OF DENUDER TUBES FOR THE MEASUREMENT OF SULFUR AEROSOL COMPOSITION

David E. Layland* and Donald L. Fox

Department of Environmental Sciences and Engineering
University of North Carolina at Chapel Hill
Chapel Hill, North Carolina 27514

Abstract

Diffusion denuder tubes have been employed by a number of investigators to measure, without filtration, the H_2SO_4 component of sulfur aerosols. In this study, diffusion denuder techniques were extended to utilize thermal deammoniation in an attempt to measure the $(NH_4)_2SO_4$ component. Ammonia released from the aerosol by heating was collected on a denuder tube for analysis. The experimental apparatus consisted of WO_3, NaCl, and PbO_2 denuder tubes, an oven, a flame photometric S detector, an NH_3 convertor, and a chemiluminescent NO detector. Experimental data obtained for ammonium sulfate aerosols showed a large amount of scatter in the NH_3 collected. Furthermore, the NH_3 collected was less than expected. These results are largely explained by thermodynamic considerations. It is concluded that the collection and analysis of NH_3 is not suitable as a technique for the differential, quantitative measurement of $(NH_4)_2SO_4$. However, preliminary results do indicate the technique can be modified to provide real time measurement of the aerosol bulk ratio, NH_4/SO_4, using high temperature decomposition.

The work described in this paper was not funded by the U.S. Environmental Protection Agency and therefore the contents do not necessarily reflect the views of the Agency and no official endorsement should be inferred.

*Present address: U.S. Environmental Protection Agency (MD-14), Research Triangle Park, North Carolina, 27711

Presented at the Third National Symposium on
Recent Advances in Pollutant Monitoring of Ambient Air and Stationary Sources

Raleigh, North Carolina May 3 through 6, 1983

Introduction

A broad array of environmental effects have been associated with sulfur aerosols, ranging from human health effects to acid deposition and visibility degradation. These effects are in turn related to the chemical composition of the aerosol. Of particular interest are the ammonium salts of sulfuric acid which appear to dominate the composition of submicron continental aerosols. The need for measurement techniques which do not rely on filtration and which provide real time measurement of the composition of these aerosols has been recognized. The use of diffusion denuder tubes appears to offer some advantages in this regard.

Interest in the use of diffusion denuder tubes for measuring the aerosol composition has been mostly directed toward exploiting the thermal volatilization of sulfuric acid to determine the acid fraction of the aerosol (1-4). In this technique, the aerosol is passed through a heated tube. At the proper conditions of temperature and residence time, sulfuric acid is selectively vaporized and is removed by diffusion to the wall of a denuder tube. Thermal volatilization, however, cannot provide information on the composition of the more abundant neutralized sulfate aerosols having bulk NH_4/SO_4 ratios in the range of 1 to 2. The purpose of this investigation was to assess whether diffusion denuder techniques could be extended to utilize thermal deammoniation as a means for providing further information on the composition of these aerosols.

A number of studies have established deammoniation as the mechanism by which ammonium sulfate thermally decomposes. Working with bulk samples of ammonium sulfate, Kiyoura and Urano (5) showed that ammonium sulfate first decomposed to form triammonium hydrogen sulfate and then at higher temperatures decomposed further to form ammonium hydrogen sulfate, releasing ammonia at each

step. Tu and Kanapilly (6) found that bulk ammonium sulfate released ammonia and an ammonium hydrogen sulfate vapor. Other studies have indicated that thermal deammoniation also occurs in aerosols generated by nebulizing aqueous solutions of ammonium sulfate. Slanina et al.(4) found evidence for this by passing an ammonium sulfate aerosol through a tube heated to 130°C. The ammonia was collected for analysis on a diffusion denuder tube. Larson et al.(7) used nephelometry, together with the deliquescent properties of $(NH_4)_2SO_4$ and NH_4HSO_4, to infer the same decomposition mechanism at higher temperatures, approaching 200°C.

Experimental

The experimental apparatus is shown in Figure 1. Diffusion denuder tubes were placed along two sample manifolds and were designed to ensure laminar flow under the conditions of sampling. Along the upper manifold in Figure 1, sulfur aerosol was separated from gas phase sulfur by a lead dioxide coated tube which removed SO_2 (8). The aerosol was then passed either directly to an FPD sulfur analyzer or first through a thermodenuder tube and then to the analyzer. The thermodenuder was simply a sodium chloride coated tube located inside an oven and designed to remove sulfuric acid vapor (4). Along the lower manifold, gas phase ammonia was separated from the sample stream by diffusion to the wall of a tungsten(VI) oxide coated tube. The aerosol was then passed through a glass heater tube, also located inside the oven. Ammonia released from the aerosol by thermal deammoniation was collected on a second tungsten oxide (WO_3) tube. After sampling at 1 lpm for the desired interval, generally 15 to 30 minutes, the first WO_3 tube was heated and the desorbed ammonia was eluted by a helium carrier and converted to NO by a gold catalyst maintained at 625°C. Ammonia collected on the second WO_3 tube was also driven off by thermal desorption and converted to NO in the same way. The NO was measured with a chemiluminescent

NO_x analyzer operated at reduced pressures, appearing as a well defined peak. Further details on the WO_3 denuder technique and possible interferences have been described elsewhere (9,10).

Thermal desorption of the tungsten(VI) oxide tubes produced two peaks, as shown in Figure 2. The first peak was identified as nitric acid. In sample A, the nitric acid peak (about 40 ng) has been drawn in with a dashed line as it would appear in the absence of ammonia. Ammonia eluted from the tube next and, in contrast to nitric acid, appeared as a long tailing peak. As suggested by samples B and C in Figure 2, the presence of the nitric acid and the tendency of the ammonia peak to tail, combined to establish the effective limit of detection for ammonia. Taking sample C as a reasonable lower limit, the minimum detectable concentration was about 1 ppb.

Calibration of the tungsten(VI) oxide tubes was accomplished by sampling ammonia, produced from a low level permeation device, which was mixed with dilution air to provide concentrations in the range of 3 to 30 ppb. From this, a response curve was constructed in terms of peak area versus tube loading. Below about 50 ng, as indicated in Figure 3, the response departed from linearity. This seemed to be associated with memory effects, either from the tube coating or the sampling lines. However, due to the appearance of interfering tertiary peaks on the tail of the ammonia peak during ambient sampling, peak height was substituted for peak area as a more accurate measure of NH_3.

An ammonium sulfate test atmosphere was generated in an outdoor smog chamber. This was accomplished through the homogeneous oxidation of SO_2, forming a sulfuric acid aerosol which was subsequently neutralized by the addition of excess ammonia. The SO_2 oxidation was brought about by the dark phase reaction of ozone with propylene. Aerosol concentrations ranged from 5 to 50 ppb S (25 to 250 $\mu g/m^3$ $(NH_4)_2SO_4$). A description of the UNC outdoor smog chamber facility has been given elsewhere (11).

Results and Discussion

Experimental data for the thermal deammoniation of ammonium sulfate, taken over a range of heater tube operating temperatures, showed a large amount of scatter in the fraction of aerosol NH_4 released as ammonia and collected on the second tungsten oxide tube. If the simple first order decomposition expression held true, as given by

$$(NH_4)_2SO_{4(s)} \longrightarrow NH_4HSO_{4(s)} + NH_{3(g)}$$

then 1 mole of NH_3 should be released for every 2 aerosol NH_4 mole equivalents so that the fraction of aerosol NH_4 released as ammonia should be simply 0.5 (NH_3/NH_4). However, as shown in Figure 4, at no operating temperature did the ammonia fraction (NH_3/NH_4) cluster about this value. At higher operating temperatures, some loss of sulfate was observed in the sodium chloride thermodenuder tube, indicating that the aerosol had decomposed to form sulfuric acid vapor. The acid fraction was determined from the neutralized sulfate which passed through the thermodenuder (S_n) and the total sulfate (S_t). Simple mass conservation should require that the ammonia fraction (NH_3/NH_4) be at least as great as the acid fraction ($1 - S_n/S_t$). However, the experimental data failed to show this. Acid fractions of 0.4 and greater were associated with ammonia fractions of less than 0.4 (NH_3/NH_4). These are seen in Figure 5 as the points which fall below the minimum line.

The experimental data clearly do not fit the simple mechanism given above for the thermal deammoniation of ammonium sulfate. As an alternative, a thermodynamic model comprised of three equilibrium expressions was examined:

$$(NH_4)_2SO_{4(s)} \overset{K_1}{\rightleftharpoons} NH_4HSO_{4(s)} + NH_{3(g)}$$

$$NH_4HSO_{4(s)} \overset{K_2}{\rightleftharpoons} H_2SO_{4(s)} + NH_{3(g)}$$

$$H_2SO_{4(s)} \overset{K_3}{\rightleftharpoons} H_2SO_{4(g)}$$

The thermodynamic quantities necessary to estimate the equilibrium constants have recently been reported by Scott and Cattell (12). Employing their values, two nomograms were constructed that together describe the extent of decomposition of ammonium sulfate at equilibrium as a function of temperature. The first nomogram, Figures 6, gives the equilibrium vapor pressure of ammonia, expressed as a mixing ratio, over aerosols of increasing acidity, expressed in terms of the aerosol bulk ratio (NH_4/SO_4). The second nomogram, Figure 7, gives the vapor pressure of sulfuric acid, also expressed as a mixing ratio, in equilibrium with ammonia. When heated, an ammonium sulfate aerosol will decompose, releasing ammonia and sulfuric acid vapor, until the vapor pressure of ammonia rises to its equilibrium value, as indicated in Figure 6, and the equilibrium partial pressure of sulfuric acid is reached, as indicated in Figure 7.

Applying the thermodynamic model to the experimental system, it can be shown that heteromolecular condensation will occur downstream of the oven. Thus ammonia will recombine with sulfuric acid vapor and condense to form an aerosol which passes through the tunsten oxide denuder tube, rather than diffusing to the wall and being collected. The onset of condensation is highly sensitive to the rate of temperature drop and the rate of ammonia adsorption in the denuder, which in turn control the vapor pressures of NH_3 and H_2SO_4. This seems to explain why in the experimental data the ammonia fraction was often less than the acid fraction. Sulfuric acid had been removed by the thermodenuder in the upper manifold of Figure 1 but not in the lower manifold. Here, the acid vapor had apparently scavenged much of the ammonia released from the ammonium sulfate aerosol in the oven. This in turn suggests that the measured ammonia fraction had some dependence on the time of sampling. Adsorption sites on the warmer upstream surfaces of the tungsten oxide tube were occupied first, increasing the importance of condensation later on during the sampling interval.

Presumably, condensation could be avoided by removing the sulfuric acid vapor *in situ*, within the oven. However, the extent of aerosol decomposition, and therefore the measured ammonia fraction (NH_3/NH_4), will depend on the aerosol concentration. According to the thermodynamic model, a smaller fraction of the aerosol will decompose to release ammonia at higher aerosol concentrations. At high enough temperatures, it should be possible to completely decompose the aerosol, thereby avoiding this effect. This hypothesis was tested by raising the oven temperature to 225°C and replacing the glass heater tube in the lower manifold of Figure 1 with a sodium chloride thermodenuder to remove sulfuric acid vapor. Measured ammonia fractions were greater than 0.9, indicating good recovery of aerosol NH_4, well within experimental errors. At these temperatures, the NaCl thermodenuder in the upper manifold served as an *in situ* zero reference for the sulfur analyzer.

Summary and Conclusions

Thermodynamic analysis and our experimental data lead us to conclude that thermal deammoniation with collection of ammonia is not suitable as a technique for the differential, quantitative measurement of ammonium sulfate. This is caused by the difficulty of defining a unique set of conditions under which ammonium sulfate decomposes to form ammonium hydrogen sulfate. However, diffusion denuder tubes do appear to be a feasible approach for the measurement of the aerosol bulk ratio, NH_4/SO_4. This requires modification of the experimental technique to fully decompose the aerosol at high temperatures and to remove sulfuric acid *in situ* to avoid condensation.

References

1. Huntzicker, J.J., Hoffman, R.S., and Ling, C.S. Continuous measurement and speciation of sulfur-containing aerosols by flame photometry. Atmos. Environ. 12: 83, 1978.

2. Cobourn, W.G., Husar, R.B., and Husar, J.D. Continuous in situ monitoring of ambient particulate sulfur usir flame photometry and thermal analysis. Atmos. Environ. 12: 89, 1978.

3. Tanner, R.L. D'Ottavio, T., Garber, R., and Newman, L. Determination of ambient aerosol sulfur using a continuous flame photometric detection system. I. Sampling system for aerosol sulfate and sulfuric acid. Atmos. Environ. 14: 121, 1980.

4. Slanina, J., Lamoen-Doornenbal, L.v., Lingerak, W.A., Meilof, W., Klockow, D., and Niebner, R. Application of thermo-denuder analyzer to the determination of H_2SO_4, HNO_3, and NH_3 in air. Intern. J. Environ. Anal. Chem. 9: 59, 1981.

5. Kiyoura, R. and Urano, K. Mechanism, kinetics, and equilibrium of thermal decomposition of ammonium sulfate. Ind. Engng. Chem. Process Des. Develop. 9: 489, 1970.

6. Tu, K.W. and Kanapilly, G.M. Generation and characterization of submicron ammonium sulfate and ammonium hydrogen sulfate aerosols. Atmos. Environ. 12: 1623, 1978.

7. Larson, T.V., Ahlquist, N.C., Weiss, R.E., Covert, D.S. and Waggoner, A.P. Chemical speciation of H_2SO_4-$(NH_4)_2SO_4$ particles using temperature and humidity controlled nephelometry. Atmos. Environ. 16: 1587, 1982.

8. Durham, J.L., Wilson, W.E., and Bailey, E.B. Application of an SO_2-denuder for continuous measurement of sulfur in submicrometric aerosols. Atmos. Environ. 12: 883-1978.

9. Braman, R.S., Shelley, T.J., and McClenny, W.A. Tungstic acid for preconcentration and determination of gaseous and particulate ammonia and nitric acid in ambient air. Anal. Chem. 54: 358, 1982.

10. McClenny, W.A., Galley, P.C., Braman, R.S., and Shelly, T.J. Tungstic acid technique for monitoring nitric acid and ammonia in ambient air. Anal. Chem. 54: 365, 1982.

11. Fox, D.L., Sickles, J.E., Kuhlman, M.R., Reist, P.C., and Wilson, W.E. Design and operating parameters for a large ambient aerosol chamber. J. Air Poll. Control Assoc. 25: 1049, 1975.

12. Scott, W.D. and Cattell, F.C.R. Vapor pressure of ammonium sulfates. Atmos. Environ. 13: 307, 1979.

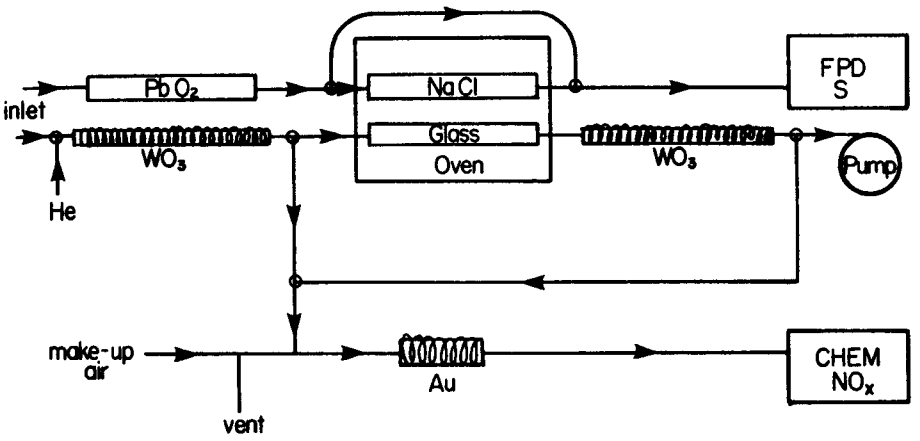

Figure 1. Diffusion denuder tube experimental apparatus.

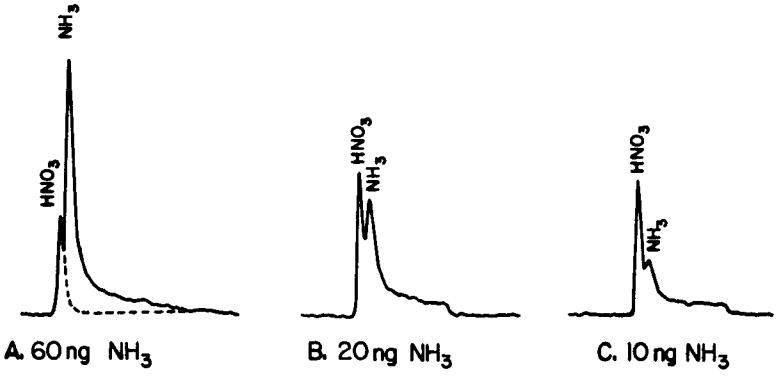

Figure 2. Tungsten(VI) oxide denuder tube thermal desorption traces.

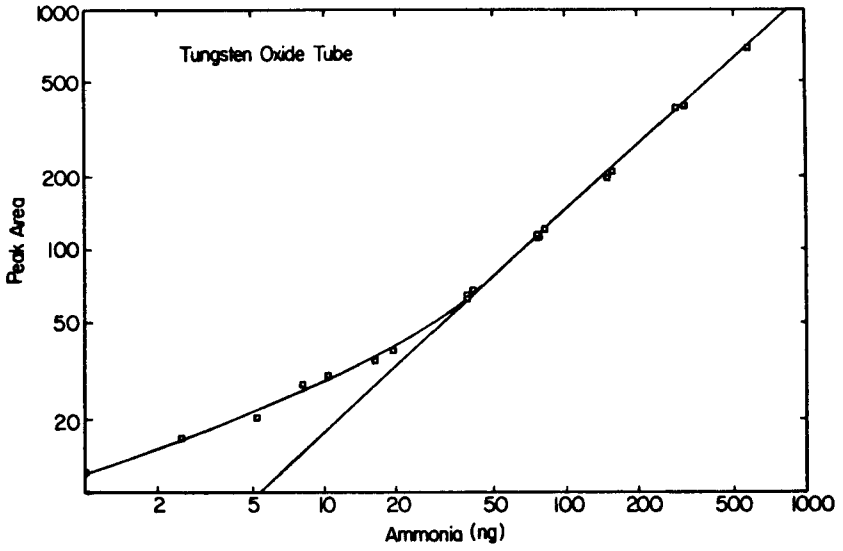

Figure 3. Tungsten(VI) oxide denuder tube response curve.

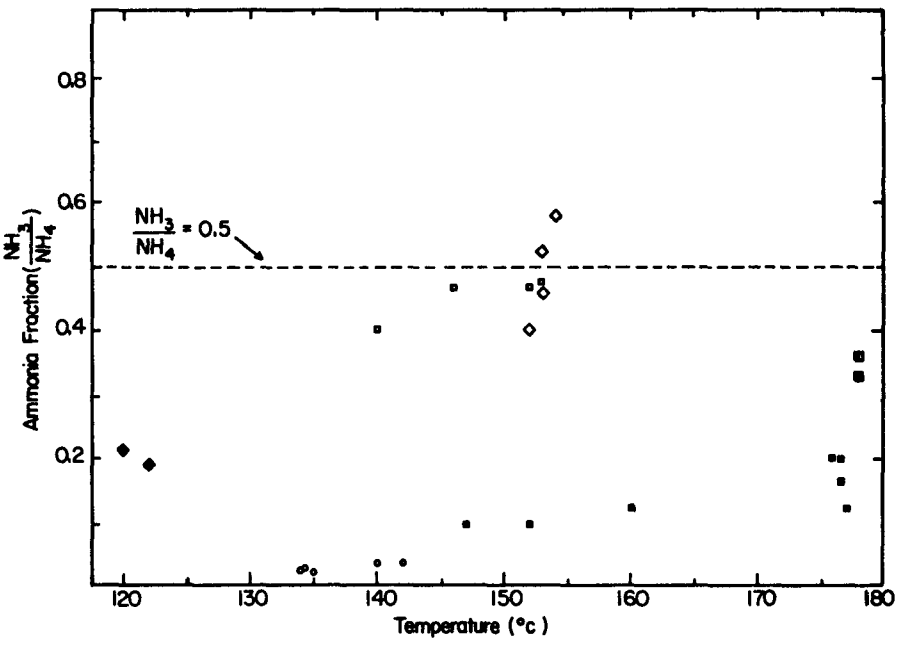

Figure 4. Measured ammonia fraction versus oven temperature.

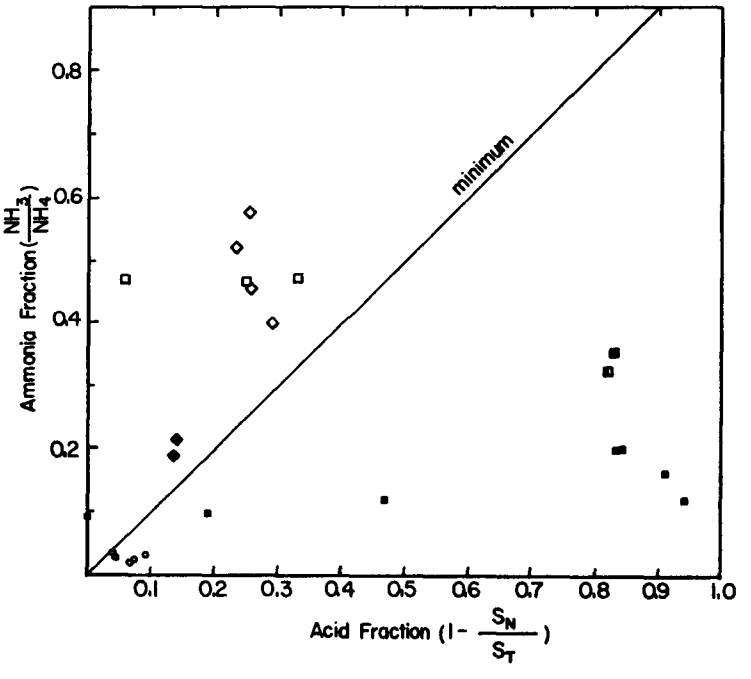

Figure 5. Measured ammonia fraction versus acid fraction.

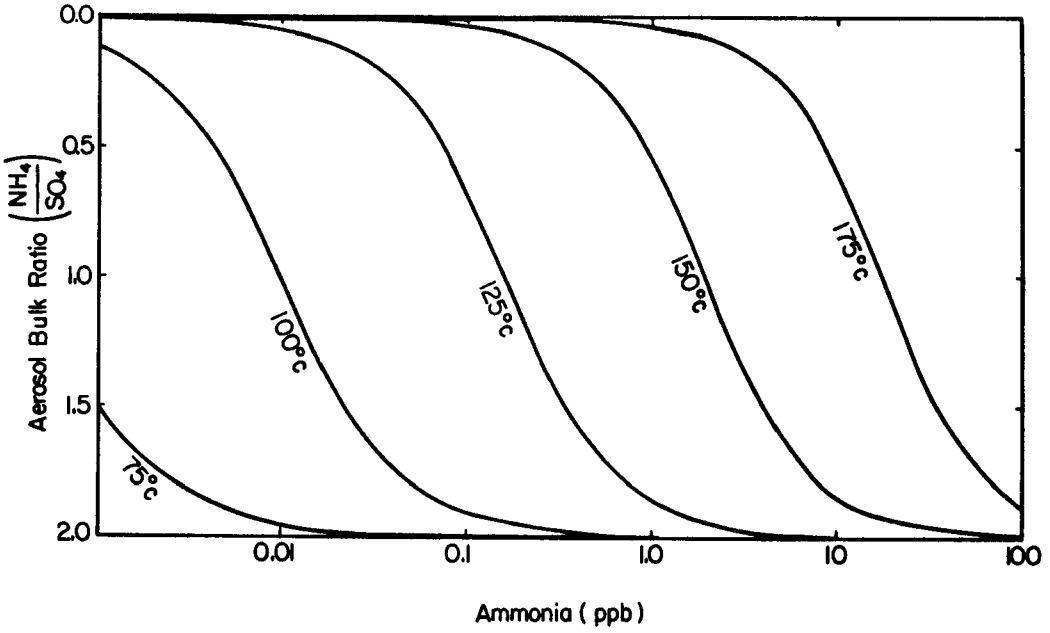

Figure 6. Predicted solid-vapor phase equilibria.

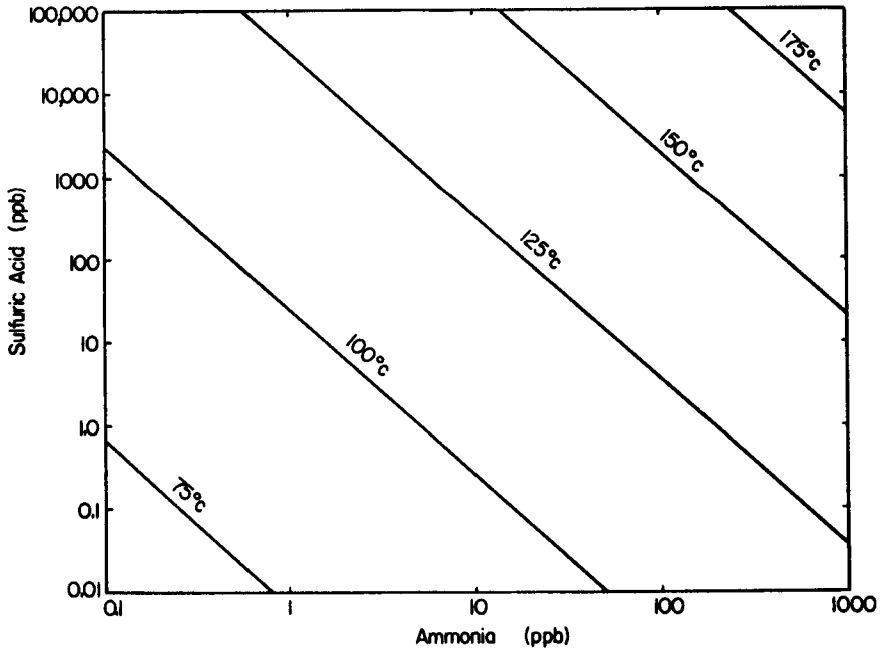

Figure 7. Predicted vapor phase equilibria.

A NOVEL NITROGEN DIOXIDE DETECTOR

D.H. Stedman
Department of Chemistry and
Atmospheric and Oceanic Science
University of Michigan
Ann Arbor, Michigan 48109

G.J. Wendel and C.A. Cantrell
Department of Chemistry
University of Michigan
Ann Arbor, Michigan 48109

L. Damrauer
Department of Chemistry
University of Colorado, Denver
Denverr, Colorado 80025

Abstract

A new NO_2 monitoring system is described which is capable of continuous measurement of ambient NO_2 from sub ppb to ppm levels using gas/surface chemiluminescence with a supported luminol solution. Response times of a few seconds were obtained. Two convertors were tested on the system for conversion of NO to NO_2. The CrO_3 trap was useful above 1-2 ppb but exhibited significant "memory" effects in cleaner air. A reaction vessel in which ozone oxidized the NO proved a simple and reliable technique. Intercomparison with a laboratory NO_x meter and results of some field measurements are presented.

A NOVEL NITROGEN DIOXIDE DETECTOR

D.H. Stedman
Department of Chemistry and
Atmospheric and Oceanic Science
University of Michigan
Ann Arbor, MI 48109

G.J. Wendel and C.A. Cantrell
Department of Chemistry
University of Michigan
Ann Arbor, MI 48109

L.Damrauer
Department of Chemistry
University of Colorado, Denver

Denver, CO 80025

In a recent issue of "Environmental Science and Technology", Hauser et al of the U.S. Environmental Protection Agency noted;

> "With current methods of continuously monitoring for nitrogen dioxide, atmospheric concentrations are found by a difference measurement - a procedure suffering from inherent variability. A continuous monitor that measures nitrogen dioxide directly and is suitable for routine monitoring situations is needed."(1)

The most common method of NO_2 monitoring is based upon the chemiluminescent reaction between NO and O_3(2,3). NO_2 is reduced to NO by several methods including hot molybdenum(4), ferrous sulfate, and photolytic reduction(5). The detection of NO_2 based upon its absorption of infra-red radiation has been reported recently using a tunable diode laser as the light source for the absorption measurement(6).

An NO_2 detector based upon the chemiluminescent reaction of NO_2 with luminol (5-amino-2,3-dihydro-1,4-phthalazine dione) has

recently been described by Maeda et al(7). The luminol system has been under study since 1928(8) and has been used for the detection of metal ions in solution in the presence of excess H_2O_2(9). The detection of H_2O_2 from biological systems(10,11) as well as ambient air samples(12,13) is accomplished with the addition of a metal ion catalyst. A detector of NO_2, O_3 and SO_2 based upon the catalysed luminol-H_2O_2 reaction has been described by Anderson et al(14,15) . In the present work, the development of a direct, continuous NO_2 detector not using H_2O_2 or a catalyst is described. The detector exhibits a 10 ppt (parts-per-trillion) detection limit and a 2Hz response speed.

Experimental

The apparatus has been discussed in detail elsewhere(16) and will therefore be described only briefly here. Figure one shows a schematic diagram of the instrument. The key feature of the instrument is the detector cell. In the original design used by Maeda et al(7), the detector cell consisted of a pool of luminol solution over which the air sample was drawn. The chemiluminescence occured at the surface of the pool and a photo-multiplier tube above the pool collected the emitted light. The pool cell was affected by noise when it was jarred and had to be leveled for optimum operation. Our new design is shown in figure two. A sheet of cellulose fiber filter paper is held in front of the photomultiplier tube and the luminol solution is supplied at the top of the filter paper and runs down the surface. The air sample is drawn over the filter paper where the chemiluminescent reaction occures. Both the air sample and luminol solution are

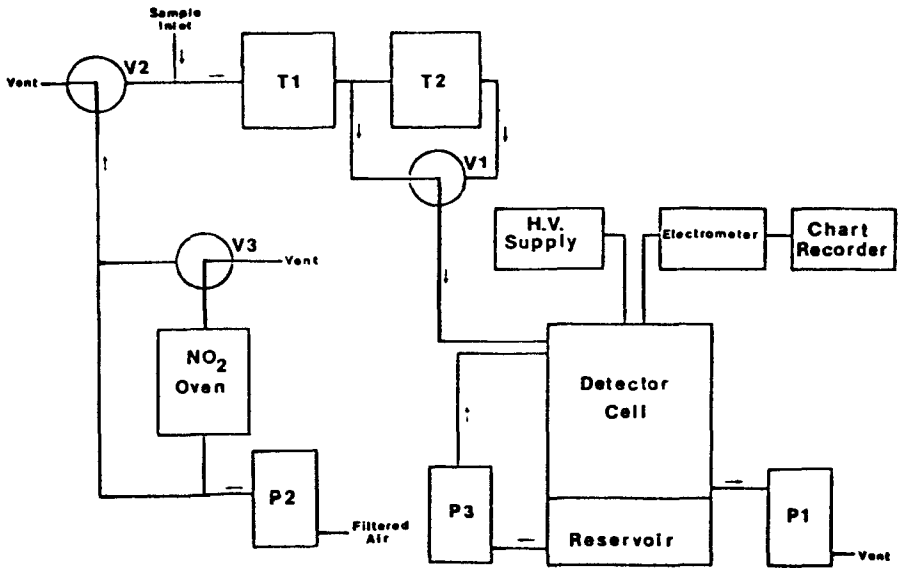

Figure 1. Block diagram of luminol NOx detector. (P1) KNF Neuberger model N79 MNP air pump; (P2) Thomas Industries model 107CA18-1 air pump; (P3) Paragon model 4465-01 liquid pump; (T1,T2) traps; (V1,V2,V3) Nacom model M223W1A three way solenoid valves. The block on the left comprising P2, V2, and V3 is the calibration system.

drawn to the bottom of the cell where the air is exhausted and the luminol solution is collected for recirculation. This design has the advantage over the pool cell used by Maeda et al(7) in that it is not sensitive to acceleration or orientation over a wide range of angles. Since the luminol solution is supported on filter paper in the new cell, these problems are alleviated.

The luminol solution is composed of NaOH, Na_2SO_3, luminol and methanol dissolved in deionized water. The luminol solution must be strongly basic for the reaction to occur and a NaOH concentration of $5X10^{-2}$ was found to give optimal results. Na_2SO_3 was added to the solution to decrease the interference

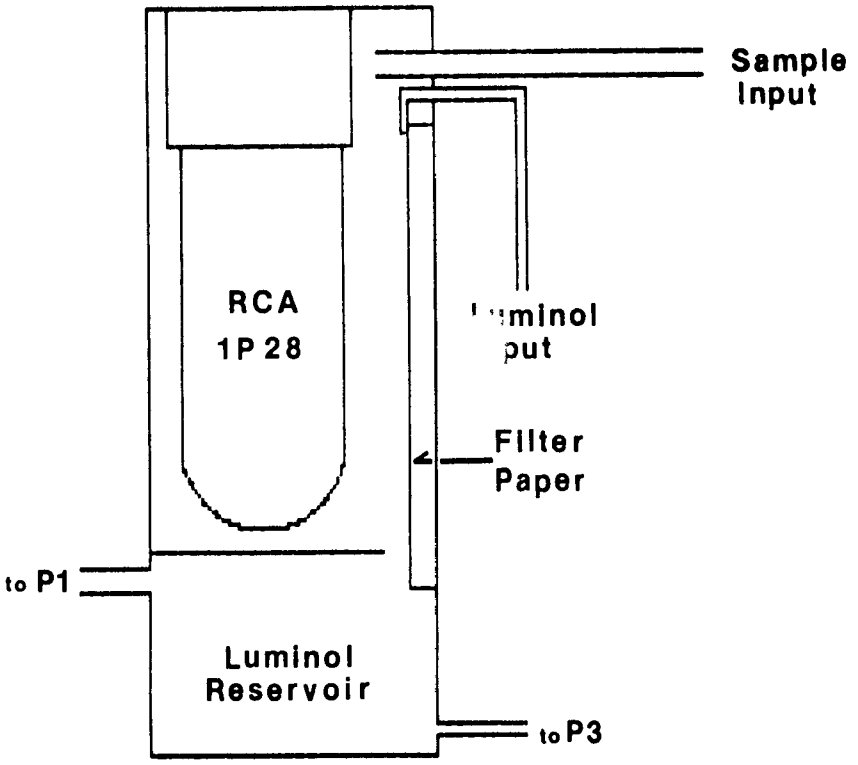

Figure 2. Schematic drawing of luminol detector cell showing the relative positioning of the 1P28 photomultiplier tube and the filter paper support.

from O_3 which also produces a chemiluminescent signal with the luminol. As was found by Maeda et al(7), a Na_2SO_3 concentration of $1X10^{-2}$ was found to give the best selectivity for NO_2. It has been found in our work with the luminol system that methanol further enhances the selectivity of the system for NO_2 over O_3. A methanol concentration of 0.05% was found to double the selectivity for NO_2 relative to O_3. With these additions to the luminol solution, the detector exhibits a sensitivity for NO_2 which is thirty times greater than that for O_3. Nevertheless, since O_3 is typically 50 ppb and NO_2 is typically 5-50 ppb, further O_3 removal is necessary.

The minimum concentration of NO_2 detectable by this technique has been tested in the laboratory and found to be 10 ppt with a signal to noise ratio of 2. In the field, with the inlet system in place, the detection limit has been measured as 30 ppt. The filter paper cell has exhibited a response speed which is greater than that measured for the pool cell. The detector, without any inlet system, has a response speed of 2 Hz, a speed which is fast enough for NO_2 flux measurements employing the eddy correlation technique if another obstacle can be overcome. The challenge is to develop an inlet system which will remove O_3 from the sample air without removing NO_2 or reducing the response speed. In the past, an O_3 removal trap filled with glass wool treated with a light coating of poly-unsaturated hydrocarbons has been used to remove the O_3. While this method is effective, it decreases the response speed to below 0.02 Hz. We are currently testing a 90 cm length of 1/4 inch stainless steel tubing heated to 100°C which in preliminary tests does not alter the response speed but removes O_3.

The luminol detector has been adapted to measure NO as well as NO_2. NO was measured by the luminol detector by first converting it to NO_2 by two different methods. The first method was oxidation by CrO_3(17). A trap filled with CrO_3 on Silica Gel was introduced into the air stream. The trap passed NO_2 but converted NO to NO_2 and the NO was measured by difference. While this scheme worked well in air containing NO_2 greater than a few parts-per-billion, memory effects and zeroing problems became overwhelming in clean air. An alternative method was to pass the

sample air through a large dark volume where the NO can react with either ambient or added O_3 to form NO_2 upstream of the O_3 removal trap. This method was found to be cleaner than the CrO_3 method and easier to zero.

Discussion

The luminol NO_2 detector has been tested against a conventional NO + O_3 chemiluminescence detector in both the laboratory and in ambient air. Figure three is a graph showing NO_2 concentrations measured in ambient air in Ann Arbor, Michigan from April 20, 1983 to April 28, 1983 by the luminol detector versus NO_2 measured by the NO + O_3 chemiluminescence detector. The NO_2 was reduced to NO for measurement by the NO + O_3 detector by FeSO4 in this experiment. As the figure shows, the two

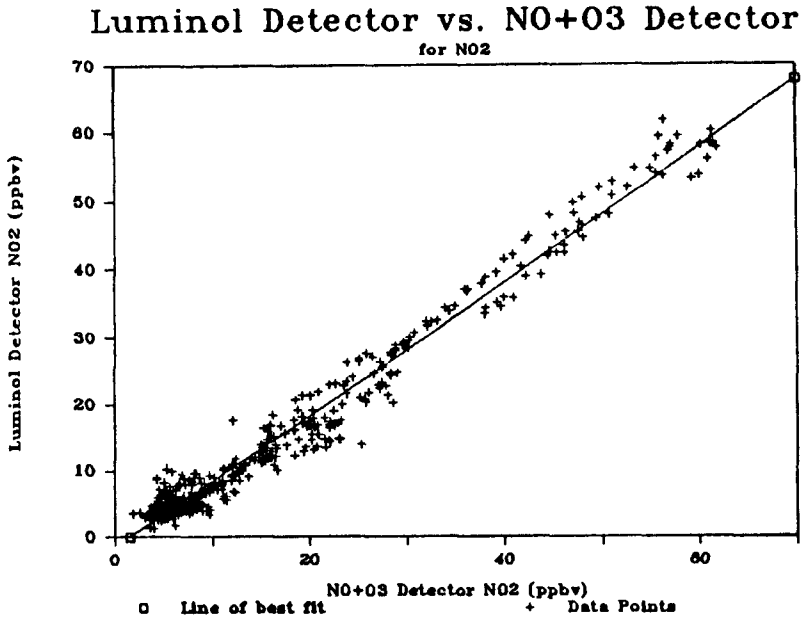

Figure 3. NO_2 concentrations measured by the luminol detector versus NO_2 concentrations measured by the NO + O_3 chemiluminescence detector in Ann Arbor, Michigan from April 20, 1983 to April 28, 1983. (slope= 0.99, intercept= -1.54 ppb, r= 0.99).

detectors are in excellent agreement. The 1.5 ppb negative intercept of the line of best fit falls within the standard error of estimate. The detector has been operated in the field for extended periods of measurements. NO and NO_2 were measured on a continuous basis for four weeks in late summer and two weeks in the winter in Bermuda. Figure four shows the average diurnal variation of NO_2 over a twenty-four hour period for each of the two measurement periods. In August, the average NO_2 concentration was on the order of 525 ppt with a diurnal variation of ±100 ppt. In the winter study, however, the average was 1.2 ppb with a variation of ±0.5 ppb. This difference is attributed to the fact that the air sampled has traveled over the

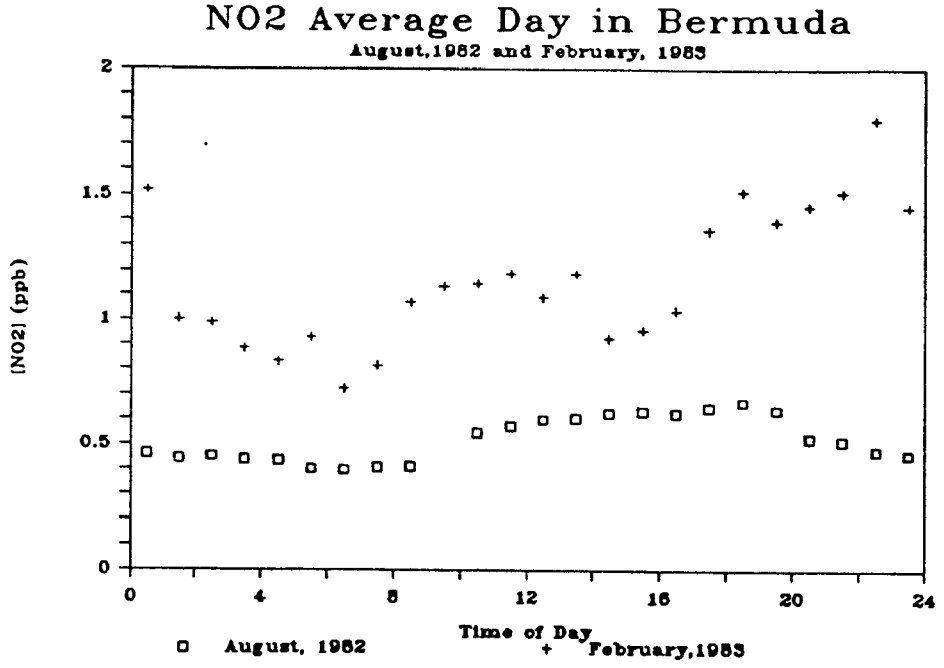

Figure 4. Average NO_2 concentrations versus time for several days in each of two time periods (August 7, 1982 to August 27,1982 and February 2,1983 to February 16, 1983)

ocean from the east coast of the United States. During winter months, there is an increased source of NO and NO_2 from home heating(18) and it is also estimated that the atmospheric removal rate is slower. The larger variability of the data in the winter months may be due to the shorter sampling period of that study.

Conclusion

The work which has been presented in this paper has shown that a direct, continuous NO_2 detector is now available meeting the needs of routine ambient monitoring as percieved by Hauser et al(1). The detector described is sensitive enough for clean air measurements and fast enough to measure NO_2 flux rates by the eddy correlation method. In additon, the detector is small and lightweight, making it ideal for most ambient air monitoring situations.

The work described in this paper was not funded by the U.S. Environmental Protection Agency and therefore the contents do not necessarily reflect the views of the Agency and no official endorsement should be inferred.

Acknowledgments

We would like to thank General Motors Research Laboratories for supporting the field trips to Bermuda.

REFERENCES

1. Hauser, T.R., Scott, D.R., Midgett, M.R. Air Monitoring:Research Needs Environ. Sci. and Tech. 17: 86a, 1983.

2. Fontijn, A., Sabadell, A.J., Ronco, R.J. Homogeneous Chemiluminescence Measurement of NO With O_3 Anal. Chem. 42: 575, 1970.

3. Ridley, B.A. Measurement of Minor Constituents in the Stratosphere by Chemiluminescence Atmosph. Tech. 9: 27, 1978.

THE USE OF A TUNABLE DIODE LASER ABSORPTION SPECTROMETER FOR MEASURING TRACE GASES IN TROPOSPHERIC AIR

H.I. SCHIFF AND G.I. MACKAY

Unisearch Associates Inc.,
222 Snidercroft, Concord, Ontario, Canada L4K 1B5

The need for accurate measurements of trace gases in tropospheric air is well recognized. An instrumental system ideally suited for such measurements should have the following characteristics: 1. Universality; it should be applicable to a wide variety of gases. 2. Specificity; it should provide positive identification of the target gas. 3. Freedom of interferences from other constituents. 4. Rapid response of one minute or less, permitting real-time measurements. 5. High sensitivity of less than 1 ppbv.

Infrared absorption affords an opportunity of meeting most of these criteria. It is a passive technique, well adapted to "in situ", real time measurements. While virtually every minor and trace constituent absorbs in this spectral region, the major gases, N_2 and O_2 are almost transparent. In fact, the absorption spectra for the trace gases are so rich that resolution of a few miliwavenumbers is required to avoid mutual interferences.

Such resolution can be obtained with FTIR spectroscopy. But because of its low sensitivity, path lengths of several

kms are required to detect constituents at the ppbv level.

Recently, tunable diode lasers have become available which provide a wavelength-tunable source with linewidths much narrower than Doppler linewidths. These diodes also have very fast response times which permit their frequencies to be scanned rapidly over the spectral range of interest.

We have recently developed a tunable diode laser absorption spectrometer (1) for tropospheric trace gas measurements. A White cell provides the long path needed to achieve the desired sensitivity. We have used this system to measure NO, NO_2 and HNO_3 in polluted and regional air .

A schematic of the spectrometer is shown in Figure 1.

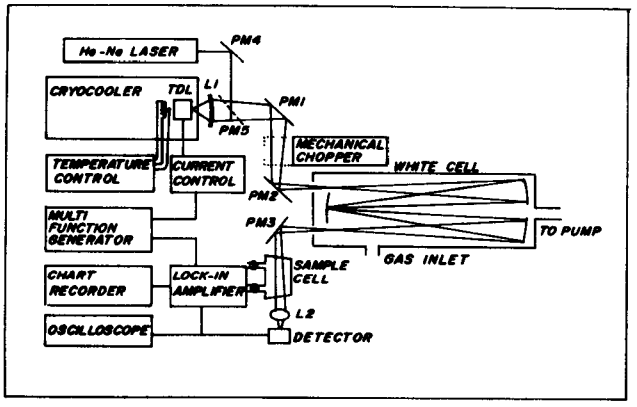

Figure 1. A schematic of the laboratory tunable diode laser system. L1 and L2 are the lenses used to focus the beam onto the White cell entrance and the detector, respectively and PMI-5 are gold coated plane mirrors for beam alignment.

The frequency at which a diode will lase depends on its temperature and the current passed through it. The appropriate temperature for a particular diode will be in the 20 to 60 K range. A helium refrigerator and a small heater maintain this

temperature to a millidegree. The frequency can be scanned over a range of about 1 wavenumber by changing the current through the diode.

The strongest absorption features of the three nitrogen compounds lie more than 1 wavenumber apart and therefore a separate diode laser is required for each. Up to four diodes can be accomodated in the assembly, but since each will operate at its own temperature only one can be used at a time. It takes about 20 minutes for temperature stability to be achieved when switching from one laser to another.

The laser beam is focussed into the White cell. A 10 cm cell containing the target gas at high concentration can be placed in the beam for initial identification and selection of the best line and to optimize the optical system. The beam is finally focussed on a HgCdTe detector. The He-Ne laser is used for initial optical alignment.

The spectrometer can be operated either in an amplitude (AM) or frequency modulated (FM) mode. In the AM mode the beam is chopped mechanically and the transmitted power detected at the chopping frequency. Figure 2 shows the AM spectrum obtained for HNO_3 and illustrates the high

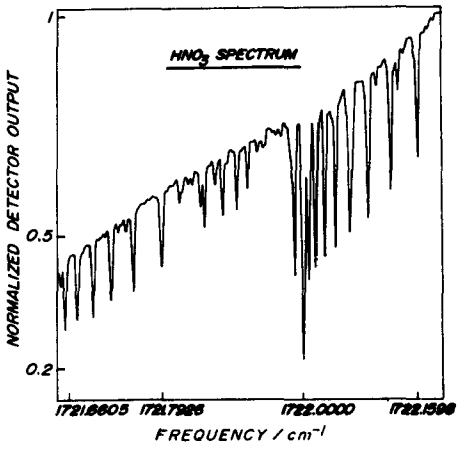

Figure 2. The HNO_3 absorption spectrum in the 1722 cm^{-1} region using the 11 cm cell.

resolution available from the spectrometer.

However, since the absorption features represent differences between two large power signals this method is limited to absorptions of about 1%.

To overcome this limitation frequency modulation is used. In the FM mode a 2 kHz sine wave is applied to the laser current which provides a frequency-modulated laser output. Detection is made at twice the applied frequency and is called 2f or second harmonic detection.

Only changes in laser power are detected and this eliminates a great deal of the noise. Absorptions as low as 10^{-5} are detectable which, for a 22 m path length corresponds to detection limits of about 0.5 ppbv. for the three nitrogen compounds. However, since information of the initial power is lost with this procedure, calibration is required to relate the signal to concentration.

Figure 3 compares the AM and FM spectra obtained for NO_2 and Figure 4 shows a repetitive scan of a single HNO_3 absorption line at 1720.000 cm^{-1}. Measurements are shown at two different concentrations. The magnitude of the signal is proportional to the mixing ratio. The scan time is about 10 sec. and the detection limit is about 0.5 ppbv. For NO and NO_2 the reponse time is about 10 sec. For HNO_3 about 5 min. is required for this gas to reach steady state with the cell.

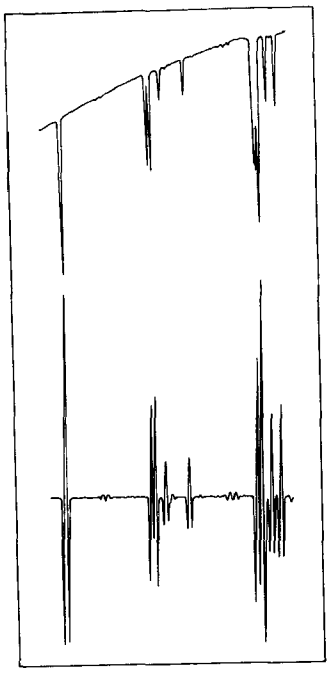

Figure 3.

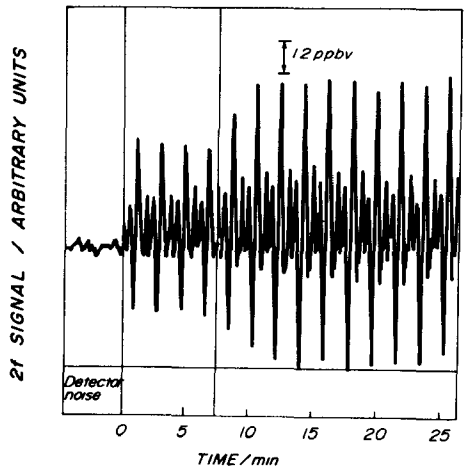

Figure 4. Repetitive scan of the 2f signal for a 25 ppb sample of NO_2 in the White cell.

Figure 5 shows a schematic of the field instrument. The air first passes through a Teflon filter to remove particles and then through an all Teflon inlet line to the White cell.

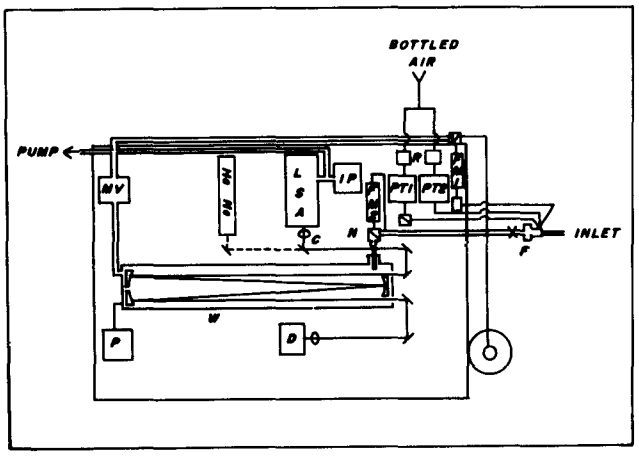

Figure 5. A schematic of the field instrument:
MV motorized valve
LSA - laser head assembly
D-HgTeCd detector
x - capillary
PM - permeation tube
FM - mass flow meters
v - 3 way valve
N - teflon needle valve
R - rotameter flowmeters
P - Baratron Pressure gauge

A restriction in the inlet and a servo valve in the outlet maintains a constant flow through and a pressure of 25 Torr in the White cell. The reduced pressure reduces pressure broadening of the absorption line which might lead to interferences from other species. The residence time in the cell is about 4 secs.

Calibration gases are added in known concentrations at the sampling inlet. Any losses that may occur in the sample line or in the White cell are thereby accounted for since they should occur equally for the sampled air and for the same air to which the calibration gas is added. For NO calibration, standard cylinder gases were used. Permeation tube sources were used for NO_2 and HNO_3 which were calibrated by titration techniques.

Figure 6 shows the signals obtained as a function of the NO calibration gas concentration. Similar linear plots were obtained for the other two gases.

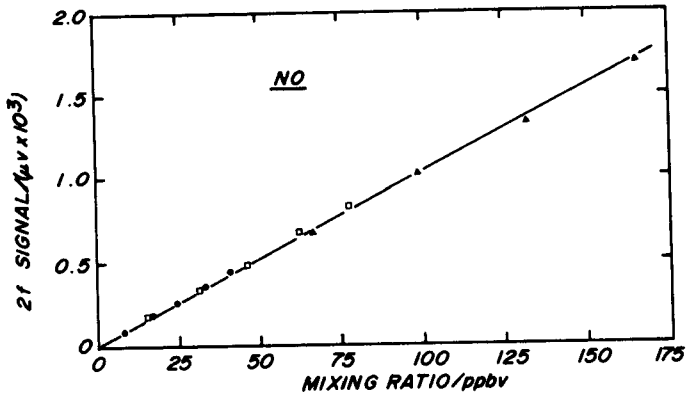

Figure 6. The observed variation of the 2f signal versus NO mixing ratios obtained by added flows of bottled 4.00 ppm NO in N_2 to measured flows of bottled air.

The field instrument was used in the autumn of 1981 in Los Angeles as part of a captive air experiment. Figure 7 shows typical NO data obtained from the roof of the Gerontology building at the University of Southern California. The scatter is real, since the precision of the measurements is better than 0.3 ppb. It shows the non-uniformity of NO in ambient urban air. These variations are much smaller in the captive air measurements.

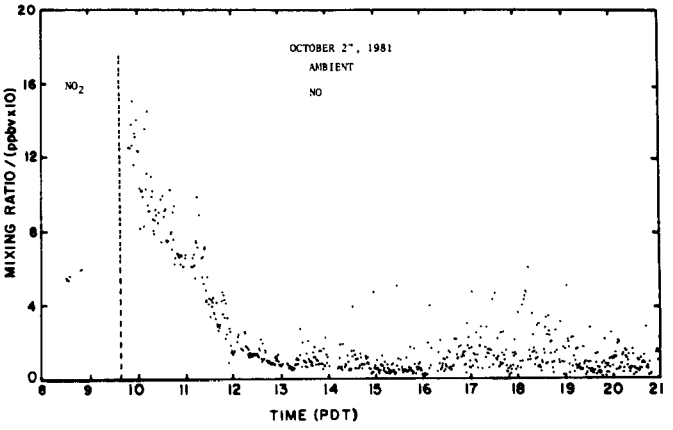

Figure 7. NO measurements taken in ambient Los Angeles air.

Figure 8 shows some NO_2 ambient air measurements. The NO_2 increases until about 13.00 hrs after which it decreases and the scatter increases. This scatter appears to correlate with the wind velocity which increased in the afternoon. The chemiluminescence measurements made by the University of Michigan group are higher than ours which can be attributed to PAN and possibly organonitrates which the chemiluminescence method cannot distinguish from NO_2.

HNO_3 data obtained during the 12 day mission. The concentration peaked about 4:00 p.m. and then decreased rather rapidly. Comparisons were made between our measurements, filter measurements by the A.E.S. and the tungstic oxide method of Braman and coworkers (2). The results of this comparison will be published shortly.

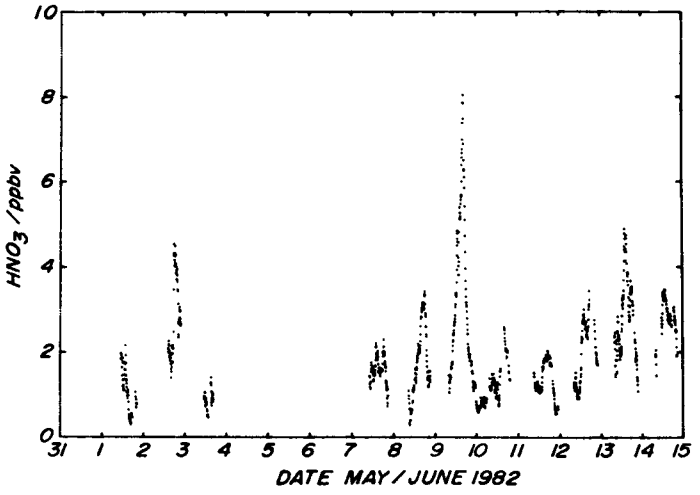

Figure 10. HNO_3 measurements taken in rural air in South-western Ontario.

These results demonstrated that the tunable diode laser spectrometer system is suitable for real time measurements in the field of NO, NO_2 and HNO_3.

We are currently developing procedures to extend this technique for measurements of H_2O_2, HCHO and NH_3.

Two other improvements in the instrumentation has recently been completed. The first is the use of two laser heads to permit measurement of more than one species at a time. With this arrangement two beams can be passed through the White cell, essentially simultaneously. Each laser head can hold 4 laser diodes permitting at least two species to be measured at

one time.

The other modification involves automation of the system for computer operation and data processing. The computer control will permit the system to operate for long periods of time unattended. The data processing system presents a number of advantages. First, it affords a method for averaging and subtracting background noise and therefore provides an improved detection limit. Second, it readily permits us to exchange sensitivity for meaurement time, with further improvement in detection limit. Finally it provides a permanent record which can be further processed at a later time.

Although the instrument has been demonstrated to operate satisfactorily under field conditions it is too expensive to be used widely in monitoring networks. Its main applications appears to provide unequivocal, fast, in situ measurements of a wide variety of tropospheric species in regional air experiments. It should also be useful in acting as a standard against which less expensive, but also less definitive methods can be compared.

REFERENCES:

1. Hastie, D.R., Mackay, G.I., Iguchi, T., Ridley, B.A. and Schiff, H.I. The use of tunable diode laser systems for measuring trace gases in tropospheric air and the sampling and calibration procedures for NO, NO#2* and HNO#3*. Environ. Science and Tech. (in press).

2. Braman, R.S., Shelly, T.J. and McClenny, W.A. Tungstic acid for preconcentration and determination of gaseous and particulate ammonia and nitric acid in ambiant air. Anal. Chem. 54: 358, 1982.

SESSION II

PARTICULATE POLLUTANTS

CALIBRATION AND TESTING OF INHALABLE PARTICLE SAMPLERS

Walter John and Stephen M. Wall
Air & Industrial Hygiene Laboratory
California Department of Health Services
Berkeley, CA 94704

Abstract

The Environmental Protection Agency has been preparing a new inhalable particle standard for the past several years. New size-selective samplers have been developed to support the standard. In the course of testing these new samplers in the laboratory, test methodology has been evolving. Since the drafts of the new standard call for the acceptance of samplers according to performance criteria, it is necessary to specify testing protocols. Progress thus far has provided a basis for a uniform approach to sampler testing, but some problems remain to be resolved.

The sampling effectiveness of an inlet is determined in a wind tunnel equipped with an aerosol generator. Liquid aerosol is used to calibrate the particle size cutoffs and to measure wall losses with the aid of a fluorescent tracer. It is also necessary to test samplers with solid particles to determine the amount of excess penetration to the after filter resulting from particle bounce and reentrainment. Methods for these measurements currently used by several laboratories are similar, but there are some significant differences. The current state-of-the-art is reviewed and remaining problems discussed.

This paper has been reviewed in accordance with the U.S. Environmental Protection Agency's peer and administrative review policies and approved for presentation and publication.

INTRODUCTION

A number of new samplers (1-4) have been developed recently to support the proposed new EPA particulate standard (5). These samplers are not only size-selective but are designed to minimize wind speed dependence. Design criterea include low internal particle losses and absence of particle bounce and reentrainment. The degree to which each of the new samplers satisfies the requirements must be determined by rigorous laboratory testing. Furthermore, the EPA plans to approve samplers according to performance criterea. This implies a specified testing protocol.

During the last few years, the development of samplers has been accompanied by improvements and innovations in aerosol testing techniques (6,7). Since these are based on current aerosol technology, there is some uniformity in the methods practiced in the various laboratories, but there are some significant differences. In fact, some difficulty is experienced in obtaining agreement between measurements made in different laboratories. The status of aerosol techniques for inlet testing in a wind tunnel and static testing of the rest of the sampler will be reviewed here.

GENERATION AND SIZING OF LIQUID PARTICLES

Liquid particles are used for measurements of sampler efficiency because aerosols of liquid particles can be generated with higher uniformity and reproducibility than in the case of solid particles. Wall losses are also measured with liquid particles because they adhere to surfaces contacted, giving upper limits to loss estimates. All of the laboratories in the EPA sampler program are using the vibrating orifice aerosol generator (8) because of its outstanding performance characteristics. In this generator, a jet of liquid is broken up by a vibrating piezoelectric crystal. Each vibration

produces a droplet, hence they are of uniform size and the rate of production is constant. Furthermore, the absolute droplet volume can be calculated by dividing the liquid flow rate by the vibrating frequency. Normally, particles smaller than the primary droplet are generated by using a solution of oil in a volatile solvent such as alcohol. For the oil, food-grade oleic acid is preferred to dioctyl phthalate (DOP) because the latter has been found to be an animal carcinogen (9).

From particle settling velocity measurements, John and Wall 10) have shown that the uncertainty of the particle diameter calculated from the vibrating orifice generator parameters can be $< 0.3\%$. Therefore, particle diameters should be based on the generator parameters. However, since the generator is subject to various malfunctions, it is necessary to have auxiliary determinations of the particle size and monodispersity. This can be accomplished with an optical particle counter which provides real time data on particle size, monodispersity and concentration. These data are indispensable for quality assurance of the test aerosol. The optical counter can be calibrated with aerosols generated from successive dilutions of a concentrated solution.

Another technique for particle sizing consists of depositing the particles on a slide for optical microscopy. The slide is coated with an oil-phobic fluorocarbon to minimize spreading. The particle diameter is obtained from the apparent diameter by multiplying by the flattening factor. Olan-Figueroa, et al., (11) have published flattening factors for oleic acid and DOP on a coating of fluorocarbon (3M Company FC 721). Their results have been confirmed by John and Wall (12). The slide method is useful only for occasional checking because the measurement accuracy is less than for the

methods discussed above. Moreover, because it is time-consuming, the method is usually limited by statistical error.

A summary of the sizing techniques for liquid particles which are recommended by the authors is presented in Table 1.

SAMPLER EFFECTIVENESS AND WALL LOSS MEASUREMENTS

The sampler effectiveness for a given wind speed and particle size is determined in a wind tunnel from the ratio of the amount of aerosol deposited on the sampler's after filter to that deposited on an isokinetic filter sampler. Static testing may be conducted in a chamber to investigate fractionating stages and internal wall losses. Aerosol deposits are quantitated from the fluorescence of a dye tracer, uranine (sodium fluorescein), added to the oleic acid solution used in the aerosol generator.

There are considerable variations in the extraction methods used by the different laboratories. We have devised procedures which are sensitive and reproducible. Teflon filters are immersed in a small amount of solvent and placed in an ultrasonic bath for 10 minutes. The extraction efficiency is 99%. Glass fiber filters are more difficult to extract and are avoided where possible. A highly efficient extraction can be achieved by placing the filter and solvent in a blender for a few minutes, followed by vacuum filtration to remove the fibers. This technique addresses the need to separate the fibers so that the deposited material can be extracted from within the filter mat. Wall losses are recovered by washing the inside surfaces of the sampler with solvent, using a squeeze bottle. Typical extraction efficiencies for oleic acid-uranine on aluminum are 90% for one wash and 99% for two washes.

An example of effectiveness measurements is shown in Figure 1 for the Size-Selective Inlet. Fairly good agreement is evident between our results

(12) for a static test using DOP and the results of Wedding (13) as well as McFarland and Ortiz (14) at 2 km/hr in wind tunnels using oleic acid. An example of wall loss measurements (12) is given in Figure 3 for the parts of the dichotomous sampler identified in Figure 2.

MEASUREMENTS WITH SPRAY-DRIED, SOLID PARTICLES

In order to compare the sampling efficiencies for solid particles to those for liquid particles, particularly near the sampler's cutpoint, it is necessary to employ monodisperse, solid particles. These may be generated conveniently by spray-drying solutions from the same vibrating orifice aerosol generator used for liquid particles. Furthermore, the unique characteristics of this generator afford a method for the determination of the aerodynamic particle diameter. Such a determination is necessary because spray-dried particles do not, in general, dry to bulk density.

As previously pointed out, the volume of the droplet produced by the vibrating orifice generator is given by the liquid flow rate divided by the vibrating frequency. Since the concentration of the solute is known, the mass of the dried particle can be calculated from the volume. The geometric particle diameter can be measured with an optical microscope. From the mass and geometric diameter, the aerodynamic diameter is readily calculated.

A direct determination of the aerodynamic diameter can be made by measuring the particle settling velocity. We have developed a Laser Settling Velocimeter (10) for this purpose. In Figure 4, three ways of relating the aerodynamic diameter to the geometric diameter are compared for solid particles of potassium biphthalate. The assumption of bulk density clearly leads to an unacceptably large error. Sizing based on optical microscopy and the

particle mass is reasonably close to the direct measurements. The difference is probably due to residual moisture in the particles.

Application of the spray-drying technique to the measurement of sampling effectiveness (12) is illustrated in Figure 1. The solid, potassium biphthalate particles show somewhat higher penetration to the after filter than do liquid particles.

TESTING WITH AEROSOLIZED BULK PARTICULATE MATERIALS

For investigation of possible excess penetration of particles much larger than the sampler cutpoint, the requirement of particle monodispersity may be relaxed. However, the size distribution of the particles must be truncated at the small end where the normal sampling efficiency is appreciable. Large particle aerosols of dry, elastic materials can be produced by suspending bulk particulate materials such as glass beads, pollen, etc. The necessary deagglomeration of the particles is efficiently accomplished in a fluidized bed. We have developed a novel Sonic Fluidized Bed (12) wherein the fluidizing action is augmented by sonic energy. This aerosol generator has the advantages of requiring less than one gram of bed particles and less than 0.5 g of test particles for a measurement.

In Figure 5, measured (12) penetrations of the Size-Selective Inlet by glass beads and A/C test dust ("Arizona Road Dust") are shown. The high value for 60 μm A/C test dust may be due to breakup of the particles which are friable. For this reason we do not regard A/C test dust as a suitable material for this work.

ASSESSMENT OF PROGRESS AND UNSOLVED PROBLEMS

Aerosol techniques for the measurement of sampling effectiveness and wall loss are well-developed. However, measurements in wind tunnels have large variances, requiring a large number of replications. A high fraction of the time is devoted to characterization of the aerosol cloud. This suggests that more use should be made of rapid monitoring methods as afforded by optical counters. Laser beams would have an obvious application here. Such beams are used in many wind tunnels to measure fluid flow.

Techniques for solid particle tests are not as advanced because of inherent difficulties. The search for better materials is still underway. For wind tunnel work the choice is further restricted by the requirement that the material be non-toxic and non-hygroscopic. A number of questions remain to be answered, including what materials best simulate ambient particles? Or, how can measurements with test particles be related to ambient particles? How much excess penetration by solid particles is acceptable in a practical sampler? Answers to these questions will be needed in the near future.

TABLE 1. METHODS FOR SIZING OF LIQUID PARTICLES

Method	Computation	Remarks
Calculation from parameters of vibrating orifice aerosol generator	$D^* = \left(\frac{6QC}{\pi f}\right)^{1/3}$, Q = Liquid flowrate; C = Vol. conc. of oil; f = vibrating frequency	Best absolute measure
Optical counter	From calibration curve, based on successive dilutions of concentrated solution	Necessary for real-time monitoring of particle size and monodispersity
Optical microscopy on coated slide	D = apparent dia. X flattening factor	For occasional checking; low accuracy

*Geometric particle diameter. The aerodynamic diameter is obtained from $D_{aero} = \sqrt{\rho}\, D$ where ρ is the particle density.

REFERENCES

1. Dzubay, T. G., Stevens, R. K. and Peterson, C. M. Application of the dichotomous sampler to the characterization of ambient aerosols. In: X-ray Fluorescence Analysis of Environmental Samples (Edited by Dzubay, T.G.) p. 95. Ann Arbor Science, Ann Arbor, MI., 1977.

2. Loo, B. W., Jaklevic, J. M. and Goulding, F. S. Dichotomous virtual impactors for large scale monitoring of airborne particulate matter. In: Fine Particles, B. Y. H. Liu, ed., Academic Press, New York, 1976. p. 311.

3. McFarland, A. R., Ortiz, C. A. and Bertch, R. W., Jr. (1979) Atmos. Environ.: 13, 761.

4. Wedding, J. B. Environ. Sci. and Technol.: 16, 154, 1982.

5. Miller, F. J., Gardner, D. E., Graham, J. A., Lee, R. E., Jr., Wilson, W. E. and Bachman, J. D. Size considerations for establishing a standard for inhalable particles. J. Air Poll. Control Assoc. 29: 610, 1979.

6. Wedding, J. B., McFarland, A. R. and Cermak, J. E. Environ. Sci. Technol.: 11, 387, 1979.

7. John, W., Reischl, G. P. and Wesolowski, J. J. (1978) Size-Selective Monitoring Techniques for Particulate Matter in California Air, AIHL/SP-12, Air and Industrial Hygiene Laboratory, California Department of Health Services, Berkeley, CA.

8. Berglund, R. N. and Liu, B. Y. H. Environ. Sci. and Technol.: 7, 147, 1973.

9 National Toxicology Program. Technical Report on the Carcinogenesis Bioassay of Di(2-ethylhexl)phthalate. U. S. Department of Health and Human Services, National Institutes of Health, National Toxicology Program, Research Triangle Park, N.C., 1982, DHHS Publication No. (NIH) 80-1768.

10. Wall, S. M., John, W. and Rodgers, D. (1982) Laser Settling Velocimeter, Paper No. 14c, First Annual Conference of the American Association for Aerosol Research, Santa Monica, CA., Feb. 17-19.

11. Olan-Figueroa, E., McFarland, A. R. and Ortiz, C. A. Am. Ind. Hyg. Assoc. J.: 43, 395, 1982.

12. John, W., Wall, S. M. and Wesolowski, J. J. Validation of Samplers for inhaled particulate matter. EPA-600/4-83-010, U.S. Environmental Protection Agency, Research Triangle Park, NC, 1983. 78 pp. (Available from the National Technical Information Service, Report No. PB83-191395).

13. Wedding, J. B. Unpublished progress report, Colorado State University, Ft. Collins, Colorado, 1981.

14. McFarland, A. R. and C. A. Ortiz. Progress Report -- Aerosol Characterization of Ambient Particulate Samplers Used in Experimental Monitoring Studies. Texas A & M University Research Foundation, College Station, Texas, October 1979.

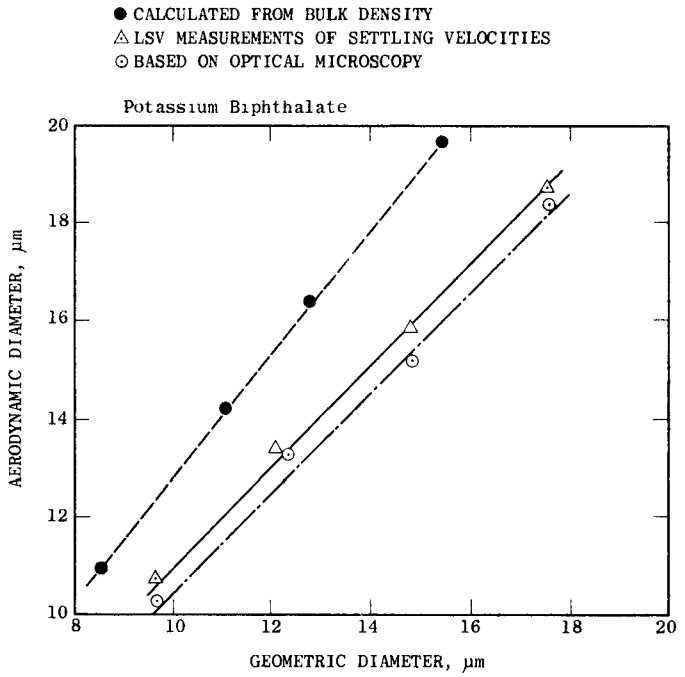

Figure 4. Comparison of three ways to obtain aerodynamic diameters of solid particles produced by the vibrating orifice aerosol generator.

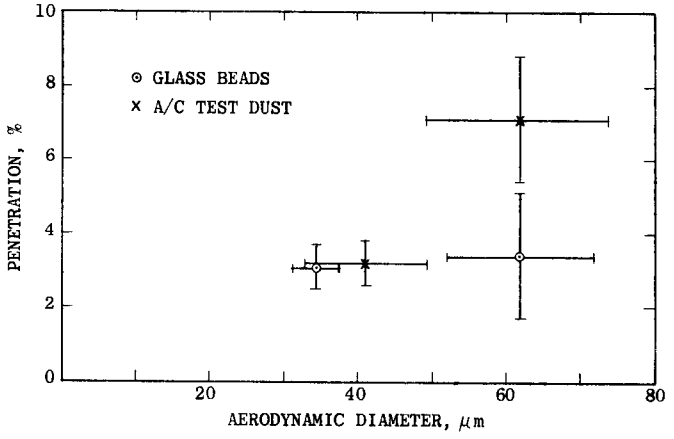

Figure 5. Penetration of the size-selective hi-vol by solid test particles.

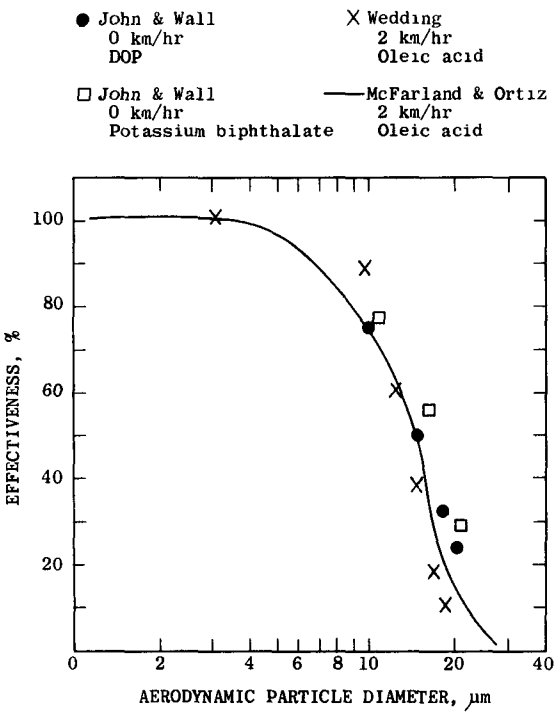

Figure 1. Sampling effectiveness of the size-selective hi-vol measured with liquid (DOP, oleic acid) and solid (potassium biphthalate) particles. Data at 2 Km/hr were taken in wind tunnels.

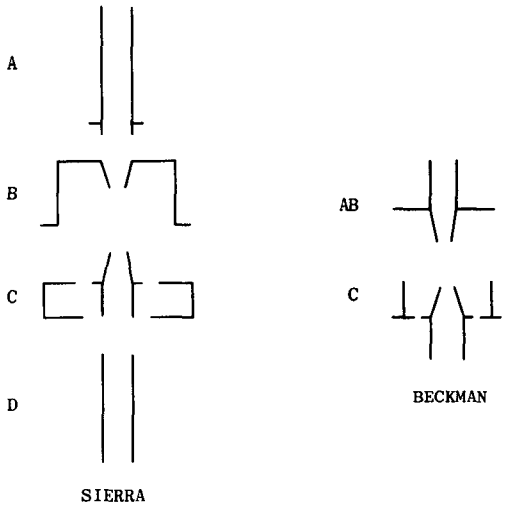

Figure 2. Identification of dichotomous sampler parts.

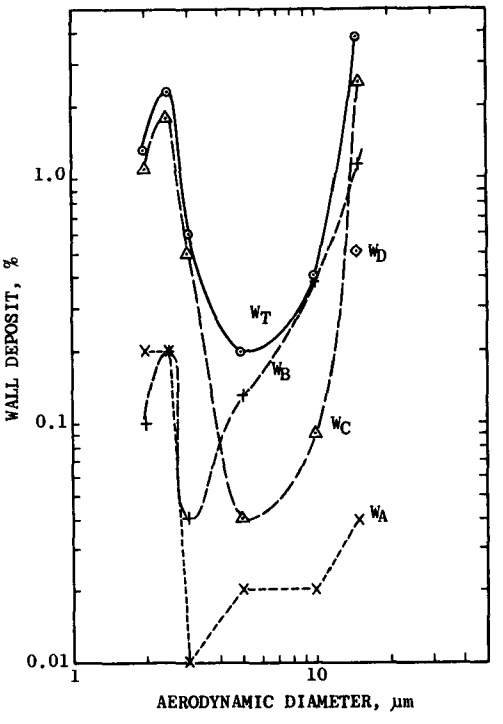

Figure 3. Wall losses measured for individual parts of the dichotomous sampler.

PARTICULATE SAMPLING EFFICIENCY DEPENDENCE ON INLET ORIENTATION AND FLOW VELOCITIES

Klaus Willeke, Pål Å. Tufto* and Lauren H. Silverman

Aerosol Research Laboratory
Department of Environmental Health
University of Cincinnati
Cincinnati, Ohio 45267

New standards on particulate air sampling for the protection of human health will have upper particle size cutoffs specified. This creates a demand for extensive testing of particulate sampling inlets. A wind tunnel has been designed and built that incorporates a new method for determining sampling efficiencies. The inlet under study is integrated into a modified optical single particle counter which records the aerosol concentration penetrated through the inlet. The penetrated aerosol concentration is thus measured dynamically and quickly for various particle sizes, sampling velocities, wind velocities and sampling angles. Extensive measurements of the overall sampling efficiency of a thin-walled sampling tube were performed at wind velocities of 250 to 1000 cm/sec, inlet velocities of 125 to 1000 cm/sec and angles of 0 to $\pm 90^{\circ}$. The sampling efficiency was found to be significantly reduced when sampling was performed at an angle to the flow. When the sampling velocity in the inlet differed from the ambient wind velocity, the sampling efficiency was increased or decreased. Solid particles with sufficient inertia bounced through the inlet and were sampled with higher efficiency than liquid particles.

---

*Current address: Division of Organization and Work Science, Norwegian Institute of Technology, University of Trondheim, Trondheim, Norway.

Introduction

When aerosols are sampled from ambient or industrial environments, air containing particles is drawn through an inlet opening to a filter or into a direct-reading instrument. Most of the theoretical and experimental studies on aerosol sampling have focused on the aspiration efficiency which considers sampling from the air environment to the face of the inlet (1-3). In addition to the particle loss or gain up to the face of the inlet, deposition of particles may occur on the inner wall of the inlet. The representativeness of the aerosol sample is thus not only dependent on the aspiration of particles to the face of the inlet, but also on particle deposition in the sampling tube upstream of the point of measurement.

In this study (4-6) we have made a thorough experimental investigation of one specific inlet in order to gain a better understanding of the dependence of overall sampling efficiency on air movements near the sampler.

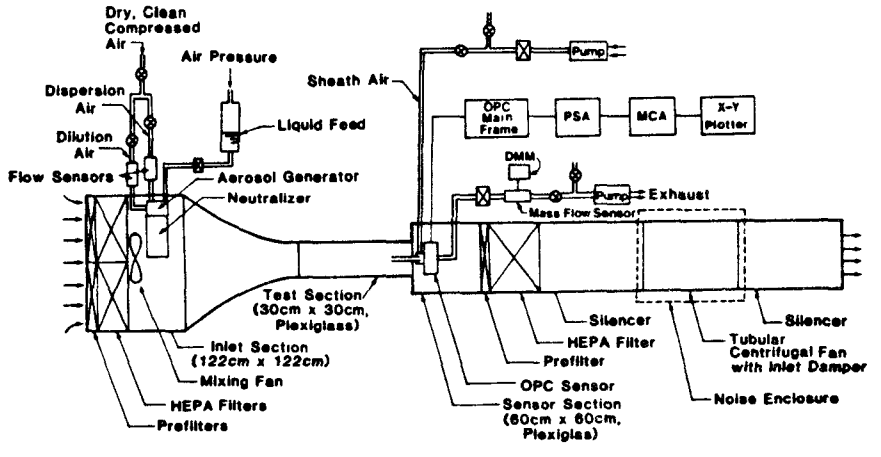

Figure 1. Wind tunnel for sampling efficiency studies: OPC = optical particle counter; PSA = pulse shaping amplifier; MCA = multichannel analyzer; DMM = digital multimeter.

Experimental Methods

We designed a special wind tunnel for sampling efficiency studies (4,7). The schematic representation of Figure 1 displays the essential elements. Laboratory air is drawn through four HEPA filters into the mixing chamber of

the wind tunnel. The air is accelerated through a tapered section which results in a constant velocity profile throughout most of the 30 cm x 30 cm test section, as measured by a thermal anemometer probe.

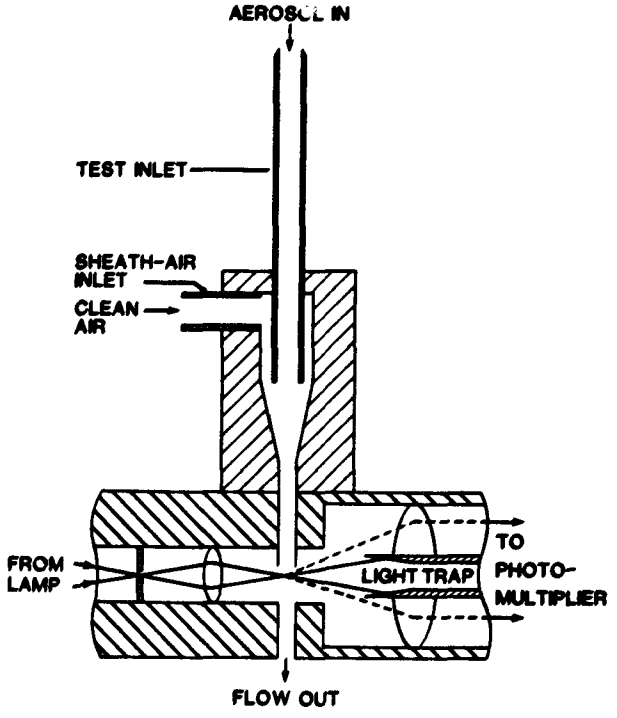

Figure 2. Schematic of test inlet integrated into a modified single-particle optical counter.

Test aerosols are injected into the mixing chamber through an aerosol generator whose design is based on the vibrating orifice principle (8). In our design the Krypton-85 charge-neutralizer section is fixed, and the vibrating-orifice section is removable as a small unit (7). The aerosol is distributed in the mixing chamber by a large disc fan as used for window exhausting in homes. This results in well-mixed aerosol concentrations in the core of the test section. The turbulence level in the wind tunnel can be varied from 3% to 8% by adjustments in the speed of the mixing fan.

The inlet under study samples from the aerosol flow in the test section of the wind tunnel. As shown schematically in Figure 2, the inlet under study is integrated into a modified single-particle counter which records the aerosol concentration that penetrates through the inlet tube. The aerosol consisted of

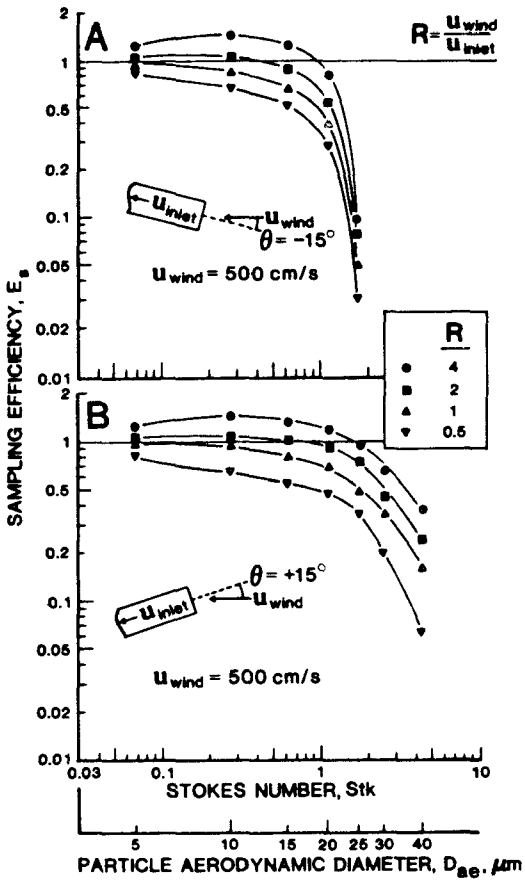

Figure 3. Sampling efficiency of a thin-walled inlet tube for upward vs. downward sampling. Test aerosol: Monodisperse liquid oleic acid. Inlet dimensions: L = 20 cm; I.D. = 0.565 cm; O.D. = 0.635 cm (1/4 inch). A: Upward sampling at $\theta = -15^{\circ}$. B: Downward sampling at $\theta = +15^{\circ}$.

liquid oleic acid and solid potassium hydrogen phthalate particles ranging in aerodynamic diameter from 5 to 40 μm. The wind velocity was varied from 250 to 1000 cm/s, and the inlet velocity from 125 to 1000 cm/s. Within these ranges of particle size and air velocity, the inlet was tested isoaxial to the wind ($\theta=0^{\circ}$) and at angles 15, 30, 60 and 90° upward and downward from the horizontal wind direction.

The penetrated aerosol concentration was measured with the optical single-particle counter for the various combinations of particle size, sampling velocity, wind velocity and sampling angle. All measurements were related to the sampled aerosol concentration at isokinetic, isoaxial conditions, for which the aerosol depositions on the inlet's inner wall were determined fluorometrically using

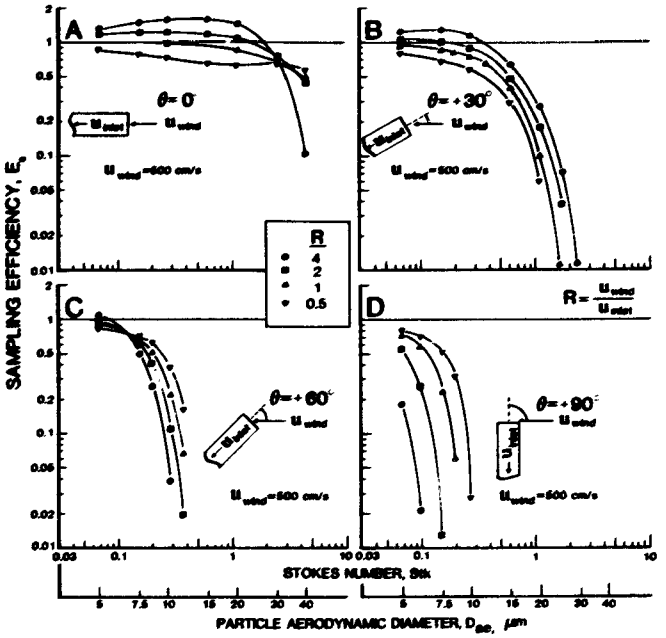

Figure 4. Sampling efficiency of a thin-walled inlet tube at constant wind velocity and different angles. Test aerosol: Monodisperse liquid oleic acid. Inlet dimensions: L = 20 cm; I.D. = 0.565 cm; O.D. = 0.635 cm (1/4 inch). A: $\theta = 0^{\circ}$. B: $\theta = +30^{\circ}$. C: $\theta = +60^{\circ}$. D: $\theta = +90^{\circ}$.

uranine-tagged particles as the test aerosol. The aerosol concentration upstream of the inlet was thus known for all the tested sampling conditions. The ratio of the particle concentration exiting from the inlet to the true particle concentration outside the sampler, defined as sampling efficiency, could thus be determined for the various sampling conditions. The particle concentration exiting from the inlet at non-isokinetic conditions relative to isokinetic conditions is termed relative sampling efficiency. The latter does not consider the particle losses inside the inlet.

In order to evaluate the distribution of particle deposition inside the sampling tube, sectional wash-offswere performed for some experiments with fluorescence-tagged aerosol.

Results and Discussions

A few sampling efficiency results obtained for the specific inlet tube tested are highlighted through Figures 3 to 5.

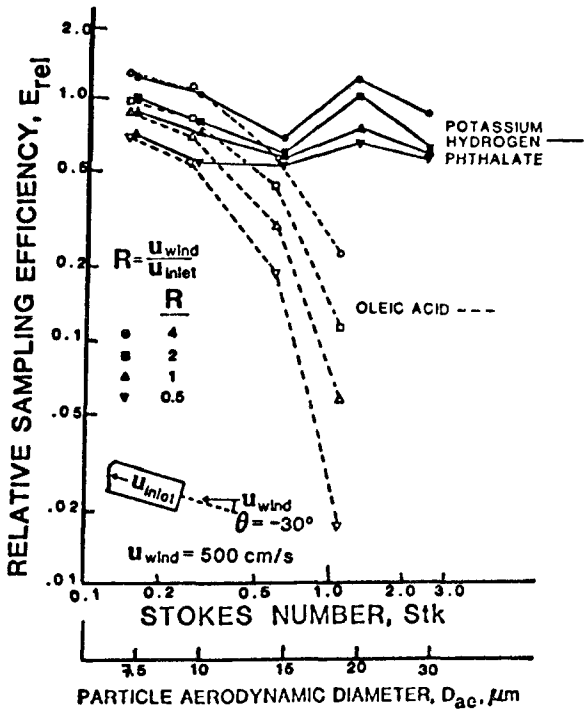

Figure 5. Relative sampling efficiency of the Figure 3 inlet tested at $\theta = -30^{\circ}$ with liquid oleic acid vs. solid potassium hydrogen phthalate particles. The relative sampling efficiency is the aerosol concentration penetrating the inlet at non-isokinetic relative to isokinetic conditions.

As seen in Figure 3 differences in sampling efficiency were found for particles above 10 μm in diameter when the aerosol was sampled 15° upward vs. 15° downward from the horizontal, downward sampling giving the higher sampling efficiency. The difference between upward and downward sampling was found to decrease as the wind velocity increased. In all cases, the difference between upward and downward sampling was found to increase with increasing particle size. A difference in sampling efficiency between upward and downward sampling was also found at $\theta = 30^{\circ}$ for particle sizes above 10 μm, although the effect was not as pronounced as for $\theta = 15^{\circ}$. At $\theta = 60^{\circ}$, the sampling efficiency for upward sampling was found to be only slightly lower than for downward sampling. At $\theta = 90^{\circ}$, no difference was found between upward and downward sampling.

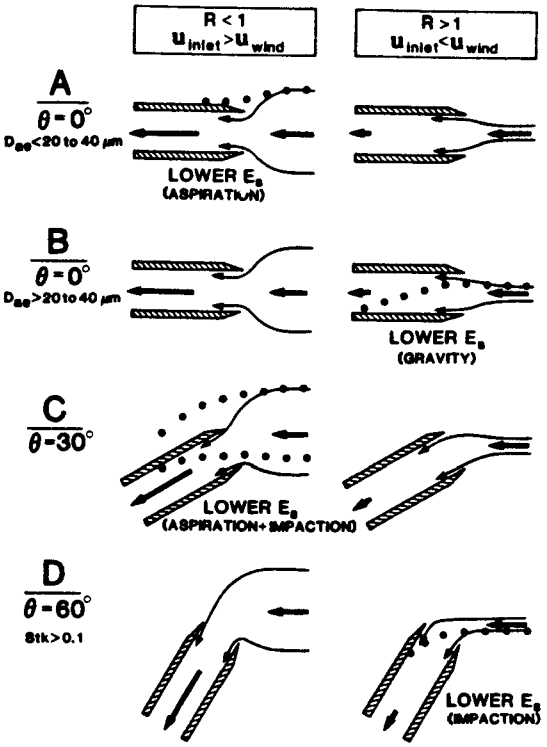

Figure 6. Dominant mechanisms for particle losses when sampling through a thin-walled inlet tube.

It is unlikely that the observed difference between upward and downward sampling is caused by differences in aspiration efficiency. Gravitational settling along the inside wall of the inlet tube should not be much different either. We propose that the differences are due to particle impaction onto the inside wall near the inlet face. When sampling downward, impaction occurs on the upper inside wall of the inlet tube and gravity pulls away from the impaction surface. When sampling upward, impaction occurs on the lower inside wall of the inlet tube and gravity pulls towards the impaction surface. Gravitational settling therefore increases impaction in upward sampling but decreases impaction in downward sampling. As the sampling angle approaches 90° to the horizontal, the component of gravitational settling velocity perpendicular to the tube wall becomes zero and no difference is observed between upward and downward sampling. However, since the magnitude of sampling efficiency decreases with increase in angle, and no particles were sampled above 10 μm for a wind velocity of 500 cm/s

and angles of $\pm 90^{o}$, gravity becomes less important with increase in angle.

Figure 4 shows the sampling efficiency as a function of particle size for various angles to the horizontal wind velocity of 500 cm/s. The data are plotted for different sampling ratios, R, defined as the ratio of wind velocity to the average air velocity in the inlet. At isoaxial sampling ($\theta = 0^{o}$) the curves for different R-values cross over each other at a particle size of about 30 µm due to the dominating effect of gravitational settling on large particles at low inlet velocities. At an angle of 60°, a different cross-over occurs at a much smaller particle size. It appears that impaction onto the inner wall increases as the angle between inside wall and wind direction increases. When impaction dominates, losses are greatest for conditions of $U_{inlet} < U_{wind}$ for which the particle trajectory has the least opportunity for turning into the inlet.

The data presented in Figure 5 demonstrate a difference between sampling liquid vs. solid particles. Small particles are sampled with similar efficiency in both cases. However, as the particle size increases, the sampling efficiency curves for the solid particles "break away" and remain high while the sampling efficiency curves for the liquid particles continue to decrease (9). We believe that the difference is due to particle bounce. As the particle size increases, so does the particle inertia: the energy of adhesion is overcome and the particle becomes airborne again, thus penetrating the inlet. A similar phenomenon has been observed in solid plate impactors. For small particles the solid and liquid particles have the same separation efficiency. However, as the particle size increases, the separation efficiency curve for solid particles breaks away from the S-shaped curve for liquid particles (10).

Figure 6 displays the dominant particle removal mechanisms as we interpret them from our data. For isoaxial sampling ($\theta = 0^{o}$) particle aspiration to the inlet face appears to affect the sampling most for small particles (Figure 6A), whereas gravitational sedimentation in the horizontal inlet tube appears to be

the dominant removal mechanism for large particles (Figure 6B). Aspiration-dominated sampling results in undersampling (i.e., lower sampling efficiencies) when the inlet velocity is higher than the wind velocity. As the orientation of the inlet is tilted away from the wind vector, particle loss due to lack of aspiration increases, but impaction onto the inside wall near the inlet face also increases. Sectional wash-off experiments indicate that most of the particles lost inside the tube are deposited just past the inlet face. At $\theta = 30^{\circ}$ both effects appear to be important, as illustrated in Figure 6C. At $\theta = 60^{\circ}$ and higher, impaction to the inner surface appears to dominate (see Figure 6D).

Acknowledgments

The initial phases of this research were supported by the U.S. National Institute for Occupational Safety and Health under Grant No. OH 00774. The latter phases were supported by the U.S. National Science Foundation under Grant No. CPE-82 13269. One of the authors (Pål Å. Tufto) was supported by the Norwegian Institute of Technology and the Royal Norwegian Council for Scientific and Industrial Research. The work described in this paper was not funded by the U.S. Environmental Protection Agency and therefore the contents do not necessarily reflect the views of the Agency and no official endorsement should be inferred.

References

1. Davies, C.N. The Entry of Aerosols into Sampling Tubes and Heads. Staub Reinhalt.Luft (English) 28:1, 1968.
2. Belyaev, S.P., and Levin, L.M. Techniques for Collection of Representative Aerosol Samples. J. Aerosol Sci. 5:325, 1974.
3. Durham, M.D., and Lundgren, D.A. Evaluation of Aspiration Efficiency as a Function of Stokes Number, Velocity Ratio and Nozzle Angle. J. Aerosol Sci. 11:179, 1980.

4. Tufto, P.Å., and Willeke, K. Dynamic Evaluation of Aerosol Sampling Inlets. Environ. Sci. Technol. 16:607, 1982.

5. Tufto, P.Å., and Willeke, K. Dependence of Particulate Sampling Efficiency on Inlet Orientation and Flow Velocities. Am. Ind. Hyg. Assoc. J. 43:436, 1982.

6. Willeke, K., and Tufto, P.Å. Sampling Efficiency Determination of Aerosol Sampling Inlets. In: V.A. Marple and B.Y.H. Liu (eds.), Aerosols in the Mining and Industrial Work Environments. Vol. I. Ann Arbor Science - The Butterworth Group, Ann Arbor, Michigan, 1983. p. 321.

7. Tufto, P.Å. Sampling Efficiencies of Particulate Sampling Inlets. Ph.D. Thesis, Department of Environmental Health, University of Cincinnati, Cincinnati, Ohio, 1981. 268 pp.

8. Berglund, R.N., and Liu, B.Y.H. Generation of Monodisperse Aerosol Standards. Environ. Sci. Technol. 7:147, 1973.

9. Silverman, L.H. Sampling Efficiencies of Solid Particles through Thin-edged Inlets. M.S. Thesis, Department of Environmental Health, University of Cincinnati, Cincinnati, Ohio 1983. 108 pp.

10. Rao, A.K., and Whitby, K.T. Non-ideal Collection Characteristics of Inertial Impactors I. Single Stage Impactors and Solid Particles. J. Aerosol Sci. 9:77, 1978.

SESSION III

GENERAL AND SOURCE ORIENTED MONITORING

METAL FOIL COLLECTION/FLASH VAPORIZATION/FLAME PHOTOMETRY AS APPLIED TO AMBIENT AIR MONITORING OF TOTAL GASEOUS SULFUR

R. A. Kagel and S. O. Farwell
Department of Chemistry
University of Idaho
Moscow, ID 83843

The analysis of gaseous samples for low part-per-million (ppm) and part-per-billion (ppb) levels of sulfur-containing vapors (H_2S, CH_3SH, SO_2, CH_3SCH_3, COS, CS_2, CH_3SSCH_3, etc.) can often be accomplished with good accuracy using a number of commercially-available instruments. In many cases, however, sample sulfur concentrations of more than one or two ppb are rarely encountered; e.g., typical concentrations in these situations range from one part-per-trillion (ppt) to around five hundred ppt. These areas of interest include: ambient air monitoring of rural atmospheres (1,2) and measurement of biogenic sulfur emission fluxes using enclosure sampling (3), plus such applications as, natural gas leak detection (i.e., via sulfur-containing taggants) and clean room air monitoring (e.g., integrated circuit manufacturing). For example, best estimates place the concentration of total sulfur-containing vapors in rural, ambient tropospheric air to be between 250 pptS and 900 pptS (W/W) (4). Nevertheless, the state of the art in sulfur-selective ambient air monitoring systems allows a practical detection limit of no better than 10 ppbS (W/W). Preconcentration schemes have been reported which do provide sub-ppb detectability; however, these previous methods have typically included such drawbacks as poor overall precision, long sampling times (i.e., no real time monitoring capability), and/or poor field sampling compatability.

Silver nitrate-impregnated filters (5) as well as metal-coated glass beads (6) and metallic foils (7) have been shown to collect, via ambient temperature chemisorption, a number of gaseous sulfur-containing compounds

present at low and sub-ppb levels in air. Recently, the collection of volatile sulfur species on a metallic foil followed by resistively-heated flash desorption has proven to be analytically useful when coupled to a flame photometric sulfur-selective detector.

This latter technique, termed metal foil collection/flash vaporization/flame photometric detection (MFC/FV/FPD), can be used to yield a total gaseous sulfur response since certain foils show nearly identical collection efficiencies and response curves toward the sulfur gases of major interest. This system has distinct advantages in terms of sensitivity, repeatability, ease of automation, and sample throughput over methods which use relatively slow, conductive thermal desorption of metallic collectors. The response of the flame photometric sulfur-selective detector is mass-flow rate dependent; therefore, a large detectability enhancement is realized by flash injection of the sample (i.e., less than 100 millisecond desorption duration). A precisely-controlled (± 0.01 V) constant voltage capacitive discharge system allows extremely repeatable desorption (± 1% of response). Since the metallic foil collector returns to its original collection characteristics after "flashing," sampling cells can be flash analyzed and prepared for the next sampling event in less than ten seconds.

The MFC/FV/FPD approach to ultratrace airborne sulfur measurements has been incorporated into a "quasi-continuous" air monitoring system capable of time-programmed sampling periods and flash desorption events via an onboard microcomputer. The programmable flash desorption system when coupled, as an inlet manifold, to a commercially available FPD sulfur monitor allows unattended operation. In this particular configuration, a pump in the FPD sulfur monitor draws the air sample through the collection cell at 200 mL/minute. Data points can be taken automatically every minute (for sample concentrations ranging from 25 ppb to 0.75 ppb [$W_{total-S}/W_{air}$]), every five

minutes (for levels from 10 ppb to 150 ppt), or every fifteen minutes (for levels from 2.5 ppb to 50 ppt). For remote field sampling application, the sampling flow rate is increased to 5 L/minute and sampling cells can be sealed, transported to the laboratory, and "flash analyzed" several weeks later. These conditions provide a detection limit of 10 ppt DMDS (V/V) for a five-minute sampling period. The precision of these measurements is approximately ± 2% over the entire LDR of 10^3.

Figure 1 illustrates the increased response obtained with the MFC/FV/FPD when compared to the response from only the FPD. The left hand portion of Figure 1 shows the response from a Meloy Labs SA-285 continuous sulfur monitor (Columbia Scientific Industries Corp., Austin, TX) to 500 ppt (V/V) of H_2S gas in air. Even under these ideal laboratory conditions and over this relatively short (about five minutes) duration, the FPD response is clearly at the detection limit. The right hand portion of Figure 1 demonstrates the significant increase in signal-to-noise response when the metal foil preconcentrator/flash vaporizer system is used with the FPD. As shown, first a 5 minute sample of zero air was passed through the collection cell (i.e. containing the metal foil) at 5 L/minute and the sulfur present in the zero air (and collected on the foil) was flash desorbed into the same FPD monitor. Next, a 1 minute sample of the 500 ppt H_2S sample was drawn through the collection cell at 5 L/minute. The corresponding MFC/FV/FPD response to this sample gave a signal-to-noise 20 times that obtained with the FPD alone. The small flash responses following the large peak are due to subsequent "clean-up" flash desorptions, illustrating that approximately 90% of the adsorbed sulfur is removed during the first flash and that the collection cell can be readied for further sampling after two cleaning flashes. Figure 2 shows triplicate

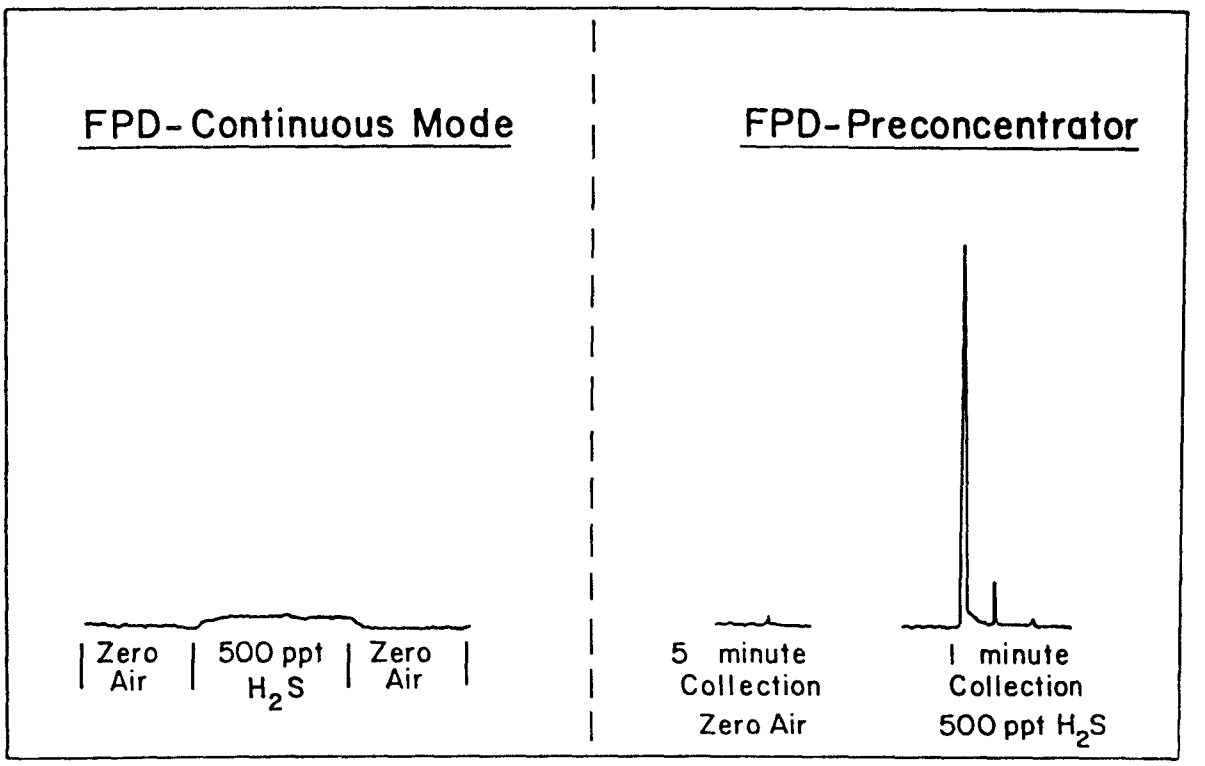

Figure 1 Meloy SA-285 sulfur monitor system response to zero air and 500 ppt H_2S (V/V) with (right) and without (left) MFC/FV preconcentrator.

MFC/FV/FPD response results for a 30 second, a 1 minute, and a 2 minute sampling of a 500 ppt (V/V) H_2S standard sample. The measurement precision is typically ± 2% of the response.

Palladium foil has been found to exhibit non-selective collection (i.e., within the precision of the standards) of all the sulfur-containing compounds tested (i.e., those compounds listed above with samples containing 0.3 ng S to 15 ng S). In Figure 3, the seven different sulfur gas standards were used separately to prepare various standard concentrations ranging from 800 pptS to 10 ppbS (W/W) (i.e., approximately 1 ngS/L to 10 ngS/L). Three concentrations from each species were sampled at 1 L/minute for 1 minute and the data combined to form the plot in Figure 3. The scatter about the regression line is well within the precision available from the calibration standards. The collection efficiency of the metal foil collector system at a sampling flow rate of 1 L/minute was determined to be approximately 40% using two different approaches. One method of estimating the collection efficiency is to compare the slopes of the standard curves (i.e., response versus ngS/sample) obtained using gaseous sulfur standards and liquid sulfur standards. The liquid standard is simply aqueous H_2SO_4 at the appropriate concentration, which is applied to the foil (e.g., in a 0.5 µL volume) and allowed to dry before flashing into the FPD. The collection efficiency of the liquid standards is placed at 100% and lesser response slopes obtained using gaseous standards attributed to less than 100% collection. These liquid standards also serve as a convenient standard for checking FPD response sensitivity. An alternate method of estimating the collection efficiency is to place two collection cells in tandem thereby, observing the "scrubbing efficiency" of the first cell by monitoring the reduced response in the second cell.

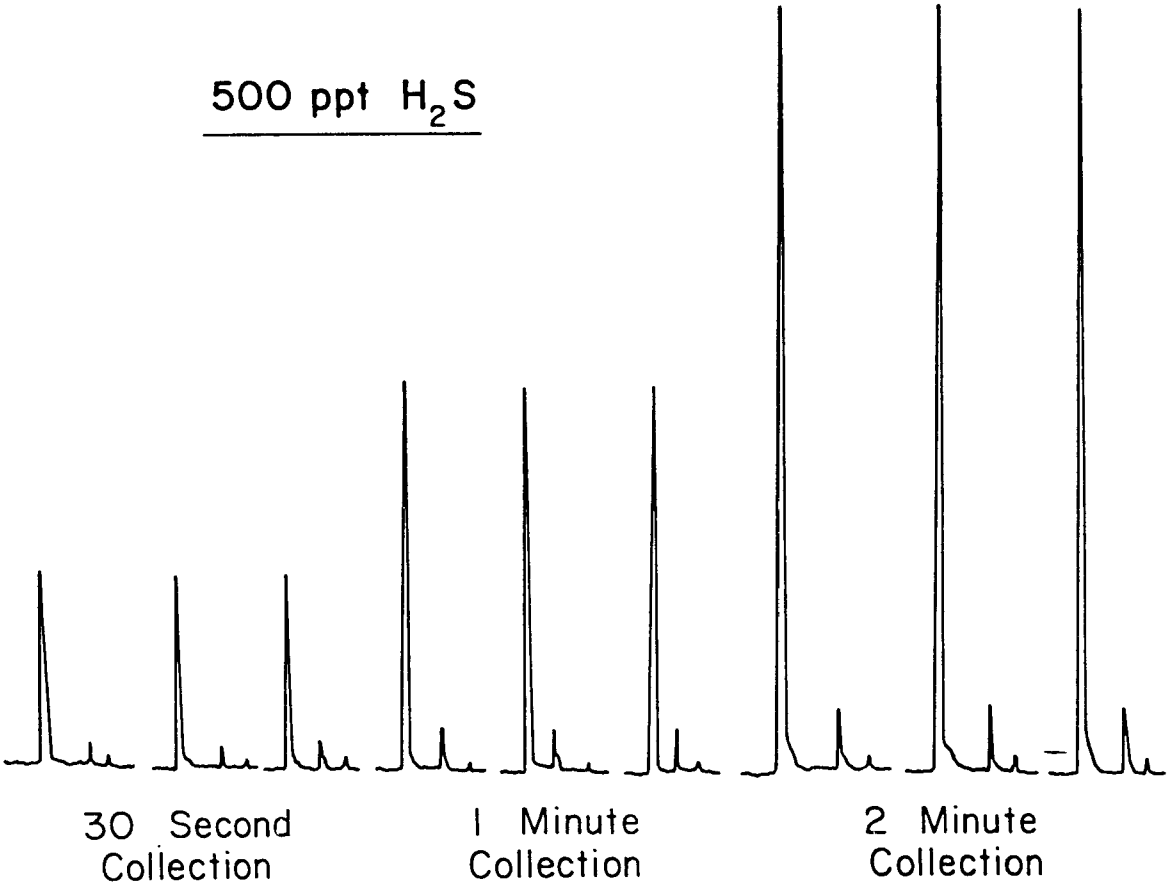

Figure 2 MFC/FV/FPD system response versus collection time of 500 ppt H_2S (V/V) with triplicate determinations shown.

Table 1 shows the collection efficiencies of various metal foils for the sulfur gases of interest over a concentration of 1 ppb and 10 ppb. Figure 4 illustrates the calibration curve for dimethyl disulfide over the concentration range of 52 ppt to 500 ppt. This figure demonstrates the sensitivity of this system and also its extreme degree of repeatability. For example, the duplicate measurements shown at each point are far more precise than the precision available between further or less diluted samples on the linear dilution curve.

To discuss potential interferences is rather meaningless without reference to a particular application or sample type. However, in the general area of air monitoring, the most common possible interferences (i.e., humidity, temperature, NO_x, and O_3) have been tested and showed no significant effect on the MFC/FV/FPD responses to known samples of the sulfur gas standards. The only significant interferent was condensing humidity, which occurs when the collector foil is below the dew point temperature of the sample. In this event the collection efficiency drops severely. The use of a Nafion sample drier or the use of a sampling cell which is heated above the sample dew point are two methods which can be used to circumvent condensation when dealing with humid, above-ambient temperature samples. Sample storage studies have been performed in which collection cells are sampled with sulfur standards or zero air and subsequently stored for a set duration before flash analysis. The results of these studies demonstrate that sample cells can be stored for periods up to several weeks without significant loss or increase in sulfur response.

Extremely high sensitivity and selectivity, field portability, ruggedness, ease of operation and calibration, and low cost make the MFC/FV/FPD system a new tool with highly desirable characteristics for numerous real world applications. The ability to make precise measurements of sulfur con-

Table 1. Percent Collection Efficiency for Various Metal Foils Toward Sulfur Gas Standards*

S-Compound	Pt	Pd	Ag	W	Ni	Rh
H_2S	41	40	38	4	0	0
CH_3SH	36	36	36	0	0	0
CH_3SCH_3	26	40	30	0	0	0
CH_3SSCH_3	39	38	36	0	0	0
SO_2	36	36	36	12	0	8
COS	7	30	1	0	0	0
CS_2	2	39	3	0	0	0

*Within the variance of the calibration standards (± 20%).

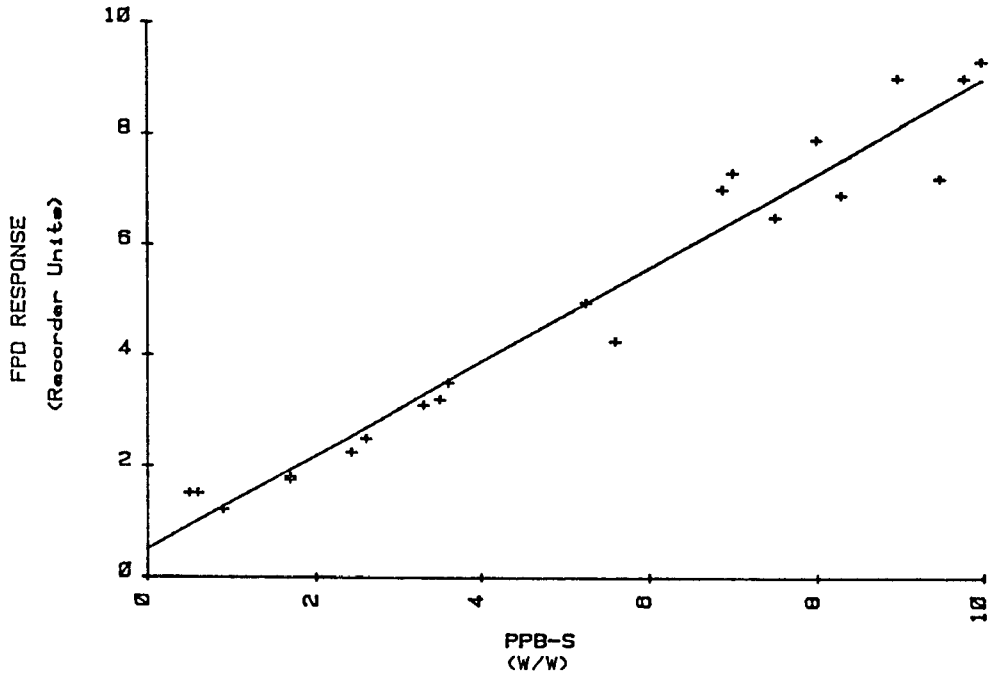

Figure 3 MFC/FV/FPD system response versus concentration using palladium foil and H_2S, CH_3SH, DMS, DMDS, COS, CS_2 and SO_2.

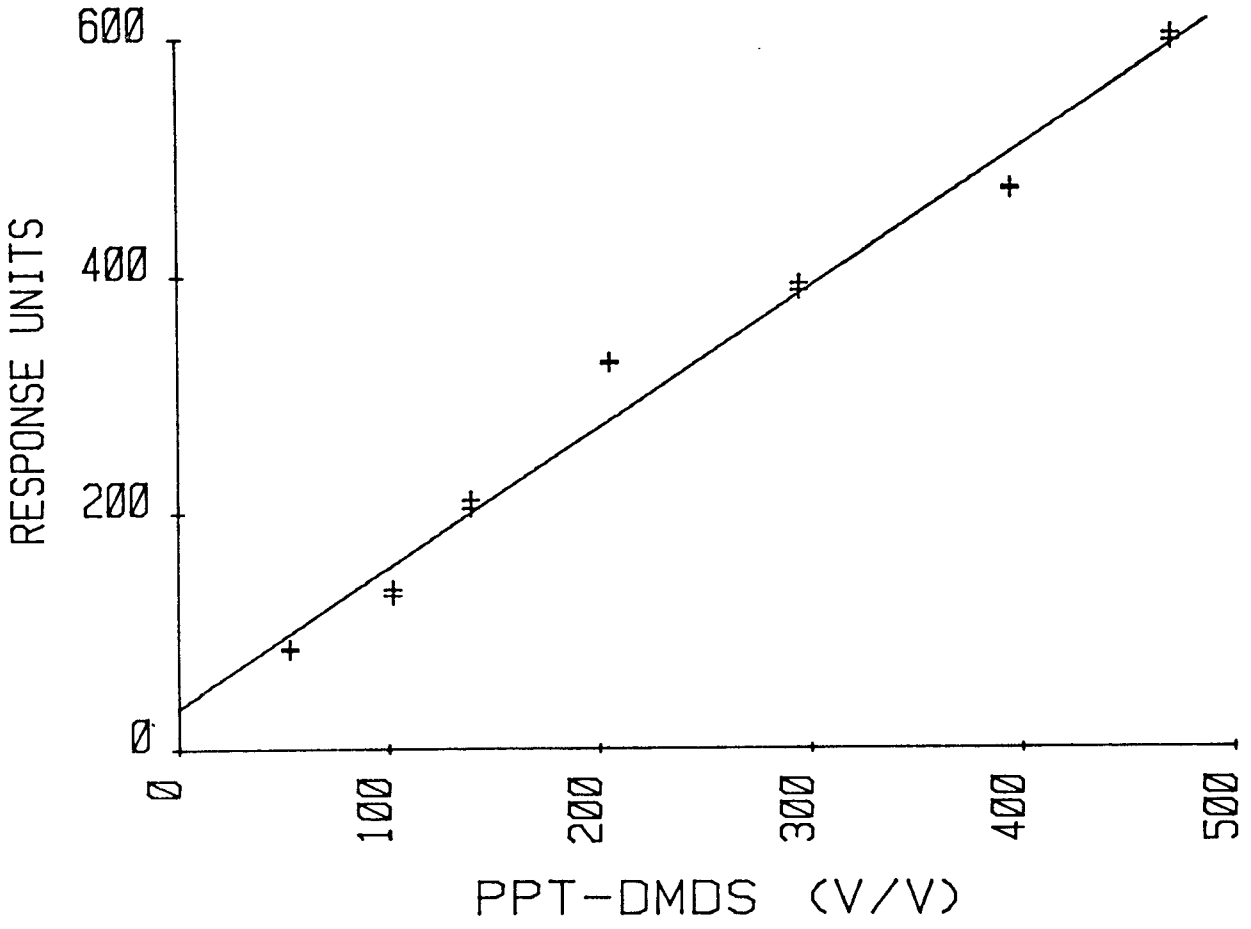

Figure 4 MFC/FV/FPD system response versus concentration of DMDS collected on platinum foil at 1 L/minute for five minutes.

centrations below 500 ppt in air will surely aid investigations into atmospheric processes involving sulfur-containing compounds.

The work described in this paper was not funded by the U.S. Environmental Protection Agency and therefore the contents do not necessarily reflect the views of the Agency and no official endorsement should be inferred.

References

1. Maroulis, P. J. and Bandy, A. R. Estimate of contribution of biologically produced dimethyl sulfide to the global sulfur cycle. Science 196: 647, 1977.

2. Harst, P. L.; Spiller, L. L.; Watts, D. M.; Spence, W.; and Miller, M. F. Infrared measurements of fluorocarbons, carbon tetrachloride, carbonyl sulfide, and other atmospheric trace gases. JAPCA 25: 1220, 1975.

3. Adams, D. F.; Farwell, S. O.; Pack, M. R. and Bamesberger, W. L. Preliminary measurements of biogenic sulfur-containing gas emissions from soils. JAPCA 29: 380, 1979.

4. Aneja, V. P.; Aneja, A. P. and Adams, D. F. Biogenic sulfur compounds and the global sulfur cycle. JAPCA 32: 803, 1982.

5. Natusch, D. F. S.; Klonis, H. B.; Axelrod, H. D.; Teck, R. J. and Lodge, J. P. Sensitive Method for Measurement of atmospheric hydrogen sulfide. Anal. Chem. 44: 2067, 1972.

6. Braman, R. S.; Ammons, J. M. and Bricker, J. L. Preconcentration and determination of hydrogen sulfide in air by flame photometric detection. Anal. Chem. 50: 992, 1978.

7. Pierce, R. W. The detection and estimation of airborne sulfur-containing compounds by means of a novel, dry, ultra-rapid, and extremely sensitive method. ISA Transactions. 13: 291, 1974.

MEASUREMENT OF MERCURY EMISSIONS FROM A MODIFIED IN-SITU OIL SHALE RETORT

Martin J. Pollard, Alfred T. Hodgson and Nancy J. Brown

Energy and Environment Division
Lawrence Berkeley Laboratory
University of California
Berkeley, California 94720

Abstract --Commercial oil shale production has the potential to release significant amounts of mercury to the atmosphere. Two techniques to measure mercury in oil shale retort offgas, Zeeman atomic absorption spectroscopy and gold bead amalgamation collection and analysis, are discussed and compared. A technique for speciating between organic and atomic forms of Hg is also discussed. The measured mercury emission rates and speciation results are presented.

This study was supported by the Assistant Secretary for Fossil Energy; Office of Oil Shale; Oil, Gas and Shale Technology Division and by the Assistant Secretary for Environment, Office of Environmental Compliance and Overview, Environmental Control Technology Division of the United States Department of Energy under Contract No. DE-AC03-76SF00098. This work was also supported by the Office of Research and Development, Industrial Environmental Research Laboratory, Energy Pollution Control Division of the United States Environmental Protection Agency under Contract No. AD-89-F-0-062-0.

Mercury is the most volatile of the toxic trace elements commonly found in oil shale. Various simulated retorting experiments have shown that most, if not all of the mercury present in the shale will be volatilized and released at typical retorting temperatures of 500–1000°C. Mercury concentrations in oil shale are only on the order of several hundred nanograms per gram. Mercury emissions from projected commercial production could be significant since an enormous mass of shale will be processed. Consequently interest in assessing potential Hg emissions prompted the development of a continuous real-time mercury monitor which was developed and tested on a laboratory scale retort to measure mercury emissions in a retorting environment.(1) The burning of a semi-commercial size modified *in-situ* (MIS) retort by the Rio Blanco Oil Shale Company ($18 \times 18 \times 122\ m^3$) between June and December 1981 provided an opportunity to test the continuous mercury monitor and to make extensive mercury concentration measurements in the offgas under actual retorting conditions.

The continuous monitoring technique is based on Zeeman atomic absorption spectroscopy (ZAA). The fundamental basis of the ZAA technique is atomic absorption spectroscopy with a unique method of background correction (2). The major difference between this technique and conventional atomic absorption spectroscopy techniques is the means by which the background correcting signal is generated. By placing a mercury lamp in a magnetic field (≈15 Kg) the atomic energy levels are split according to the Zeeman effect. Figure 1 shows the emission spectrum of the $^1S_o \rightarrow {}^3P_1$ transition corresponding to the 253.7 nm Hg line in a direction of observation perpendicular to the magnetic field. The unshifted component is designated π and the two shifted components are designated σ^+ and σ^-. The separation of the π and σ components is proportional to the magnetic field strength.

The relative transmission of the π and σ components through gaseous mercury is also shown on Figure 1. Both the π and σ components are equally absorbed and scattered by background components in the offgas such as water, oil mist, and particulates, but the π component is more strongly absorbed since it is at the resonant frequency with the Hg absorption transitions in the sample gas. By observing the difference between the π and σ transmission through the offgas we eliminate the background components of absorption and obtain a signal that corresponds only to absorption due atomic mercury.

The ZAA spectrometer is fitted with a corrosion resistant furnace-absorption tube. The sample gas flows into the furnace section of the tube, which is maintained at 800–900°C, then into a 5 cm path length absorption chamber with gas tight quartz glass windows. The total flow rate of the gas sampled through the ZAA is maintained by

an electronic flow controller which is continuously calibrated by a wet test meter and a Hewlett-Packard 85 computer and an Hewlett-Packard model 3054 Data Logger. Mercury calibration gas is generated by a device similar to the system described by Nelson (3) and is injected into the offgas line before the furnace.

A discrete sampling technique, based on mercury amalgamation on gold beads (4), was used along with the continuous mercury monitor to validate our measurements. Mercury is collected by inserting a quartz glass tube, with a 25 mm section of gold beads, into the offgas sample line for a measured flow rate and time period. The column is analyzed in the thermal desorption system shown in Figure 2. The sample collection tube, or transfer column, is quickly heated to 400°C in N_2 carrier gas; the mercury is desorbed and transferred to the analytical column downstream. The Hg is similarly desorbed from the analytical column and then analyzed by passing it into the ZAA spectrometer for detection. Calibrations are obtained by injecting gaseous Hg though the septum onto the analytical column followed by thermal desorption. Two stage desorption of samples is used since analytical response varies from column to column.

Speciation measurements of atomic and organic mercury were made using a the method adapted from Trujillo and Campbell (5). A quartz tube containing Carbosieve B is placed in front of the gold bead sampling column in the offgas sampling line. After sample collection, the atomic mercury remaining on the Carbosieve is transferred to the gold bead column by purging the Carbosieve with 10 liters of N_2 at room temperature. The organic mercury is retained on the Carbosieve B. Both the Carbosieve B and gold bead columns are analyzed in the same manner. No attempt was made to separate and identify the organic species.

A schematic of the Rio Blanco Oil Shale Company facility is shown in Figure 3. The MIS retort is an underground rubblized column of shale. The retort is burned from top to bottom with air and steam injected as shown. Shale oil is collected at the bottom of the retort and the offgas is directed to the ground surface through the offgas pipe. The primary sampling point is located in this pipe at the ground surface. The secondary sampling point is located in the offgas stack after the incinerator and desulfurization unit.

The sample offgas for the ZAA spectrometer and the discrete sampling columns were pulled from the center of the offgas pipe through a 0.63 cm Teflon tube supported by an outer stainless steel tube. It was then passed through a condenser, the sample line, the analytical instrumentation, and a peristaltic pump.

The Zeeman technique can quantitatively detect Hg in the untreated offgas and correct for background absorption due to the water vapor, oil mist, and particulates. However, sample line problems prevented the addition of mercury calibration gas in the presence of water vapor. The resistance heated stainless steel sample line (150°C) passed the water in the gas phase but condensation at the unheated fittings to the furnace-absorption tube interfered with the addition of calibration gas. The erratic addition of mercury calibration gas resulted in an extremely "noisy" calibration signal. Since we were unable to solve this problem under field conditions the offgas to the ZAA monitor was passed through a condenser. The condenser consisted of a glass bubbler packed with glass wool. It was immersed in an ice bath. This was sufficient to remove most of the water in the offgas which varied from 24 to 70% of the total offgas volume.

The stainless steel sample line was heated to prevent Hg condensation. An ambient temperature Teflon line was run in parallel to the heated stainless steel line. A comparison of the Hg signals from these sample lines showed that there were losses to the stainless steel line despite laboratory tests that showed that temperatures >100°C were sufficient to pass atomic mercury vapor with no losses to the line. The Hg signals for the Teflon and stainless steel sample lines are shown in Figure 4. The N_2 base line represents gas with no mercury vapor. When the offgas was sampled through the heated stainless steel line there was a 20-30% drop in the absorption signal relative to the Teflon line indicating loss of mercury to the stainless steel line. Since a condenser was being used to remove water, a heated line was no longer necessary. Consequently ,the Teflon sample line was used for the remaining mercury measurements.

Figure 5 shows the results of the ZAA monitor mercury measurements at the primary sampling point. The current emission rates, in g day^{-1}, were obtained by multiplying the Hg concentration in the offgas times the dry offgas flow rates from the retort. The vertical bars represent the range of emission rates obtained throughout each day. The horizontal bars are the weighted mean average emission rate for each day. The rates are highly variable within each day and between days. There is no correlation between the emission rates and the air and steam input to the retort. Laboratory experiments indicate that Hg emissions should increase toward the end of the retort burn (6,7) yet no long-term trends to the emissions rates were seen during the period of this investigation. It should be noted that the measurement period extended over 35 days during the latter part of the retort burn and that the measurements were stopped prior to termination of the burning of the retort.

Au-bead amalgamation samples were taken on one day at the secondary sampling point. After experiencing losses to our stainless steel sampling line and from experience with the laboratory retorting experiments it was expected that a significant portion of the mercury in the offgas would be lost to the surface plumbing of the retorting facility. Only an estimate of the offgas flow rate at the secondary sample point was available but qualitative results indicate that no mercury was lost to the retort plumbing.

Gold-amalgamation samples were taken on seven days. Figure 6 shows a comparison between Mercury concentrations measured by analysis of the amalgamation columns and the ZAA mercury monitor. The sample measurements used for comparison in Figure 6 were taken within one hour of each other. The error bars are two standard deviations from the measured value. The variations may be due to the non-concurrent times at which the samples were collected. Never-the-less there is generally good agreement between the two methods, and neither technique gives consistently high or low results.

The results of the speciation sample, taken on four days with the Carbosieve B columns, are shown in Table 1. The total Hg concentrations agreed well with the concentrations measured with the ZAA Hg monitor on the same days. Of the total Hg in the offgas, 52-82% of the Hg is in the form of organic compounds.

Summary

There is very good agreement between the two techniques, Zeeman atomic absorption spectroscopy and Au-bead amalgamation, for the measurement of mercury concentrations in oil shale offgas but there are a number of differences that point to the ZAA technique to be superior to Au-amalgamation columns. The primary advantage of the ZAA monitor is the ability measure Hg directly in the untreated offgas. We were unable to do this because of sample line problems that interfered with our calibrations but those problems can be solved. Au-amalgamation requires that water be removed before sampling and this water must be analyzed at a later time. Background correction is an intrinsic feature of the ZAA technique. A background correcting spectrometer should be use for the analysis of the Au-amalgamation columns. Also, successful use of the amalgamation columns requires some prior knowledge of the Hg concentration in the offgas so as not to collect too small a sample nor to exceed the breakthrough volume of the column. This is not a problem with the ZAA Hg monitor which has a large analytical range. The continuous measurement capability of the

ZAA mercury monitor makes it a superior technique for reliable measurements of daily mercury emissions rates and a superior research instrument to follow mercury emissions with the process control of the retort. In addition the technique is easily adaptable to the measurement of other atoms and some molecules.

Acknowledgements --The authors extend their appreciation to J.S. Fruchter, D.C. Girvin, and D. Sklarew of Battelle Pacific Northwest Laboratories for providing field facilities and for helpful discussions of this manuscript. Appreciation is also extended to K.L. Berry, R.L. Hutson, and J.S. Sterret of the Rio Blanco Oil Shale Company for their generous hospitality and assistance.

This study was supported by the Assistant Secretary for Fossil Energy; Office of Oil Shale; Oil, Gas and Shale Technology Division and by the Assistant Secretary for Environment, Office of Environmental Compliance and Overview, Environmental Control Technology Division of the United States Department of Energy under Contract No. DE-AC03-76SF00098. This work was also supported by the Office of Research and Development, Industrial Environmental Research Laboratory, Energy Pollution Control Division of the United States Environmental Protection Agency under Contract No. AD-89-F-0-062-0.

REFERENCES

1. Girvin D. C. and Fox J. P. (1980) "On-line Zeeman Atomic Absorption Spectroscopy for Mercury Analysis in Oil Shale Gases." U.S. Environmental Protection Agency report EPA-600/7-80-130.

2. Hadeishi T. (1972) "Isotope-shift Zeeman Effect for Trace-Element Detection: An Application of Atomic Physics to Environmental Problems. Appl. Phys. Lett. 21,438-440.

3. Nelson G. O. (1970) "Simplified Method for Generating Known Concentrations of Mercury Vapor in Air." Rev. Sci. Instrum. 41, 776-777.

4. Fitzgerald W. E. and Gill G. A. (1979) "Subnanogram Determination of Mercury by Two-Stage Gold Amalgamation and Gas Phase Detection Applied to Atmospheric Analysis." Anal. Chem. 51, 1714-1720.

5. Trujillo P. E. and Campbell E. E. (1975) "Development of a Multistage Air Sampler for Mercury." Anal. Chem. 47, 1629-1634.

6. Hodgson A. T., Pollard M. J., Harris G. J., Girvin D. C., Fox J. P. and Brown N. J. (1982) "Mercury Mass Distribution During Laboratory and Simulated In-Situ Oil Shale Retorting." Lawrence Berkeley Laboratory report LBL-12908.

7. Fox J. P. (1980) The "Partitioning of Major, Minor, and Trace Elements During Simulated In-Situ Oil Shale Retorting." Ph.D. Dissertation, Dept. of Civil Engineering, University of California, Berkeley.

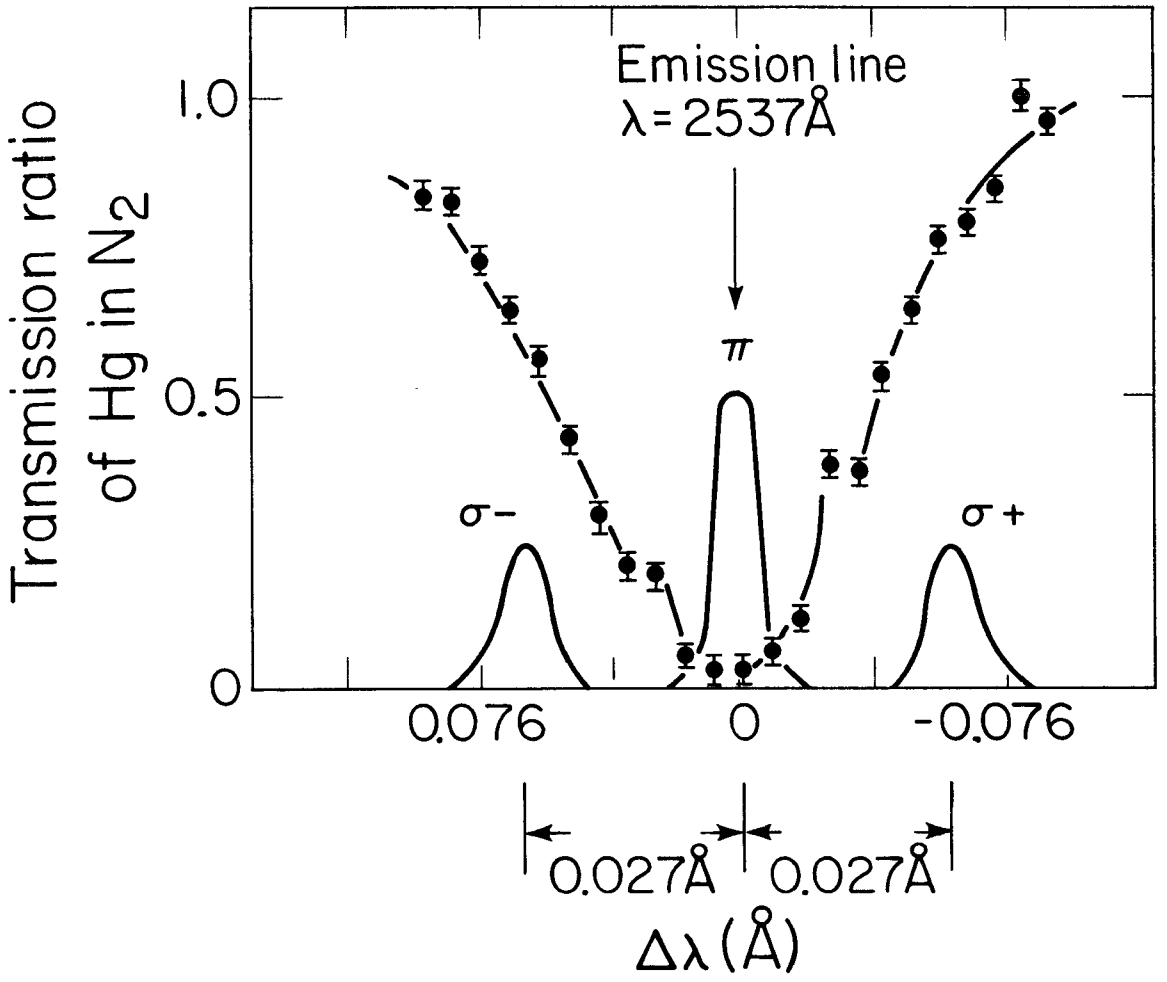

Figure 1. Mercury transmission profile

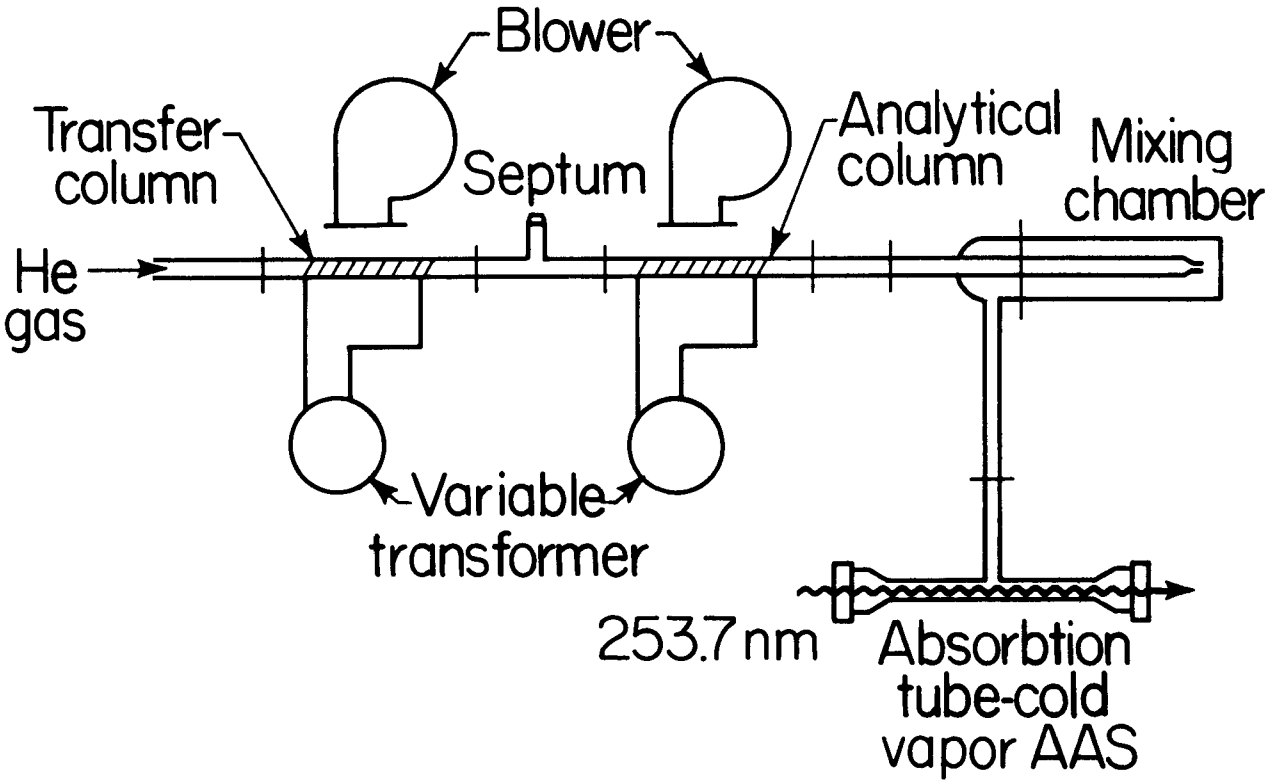

Figure 2. The two-stage thermal desorption system for the analysis of the Au-amalgamation columns.

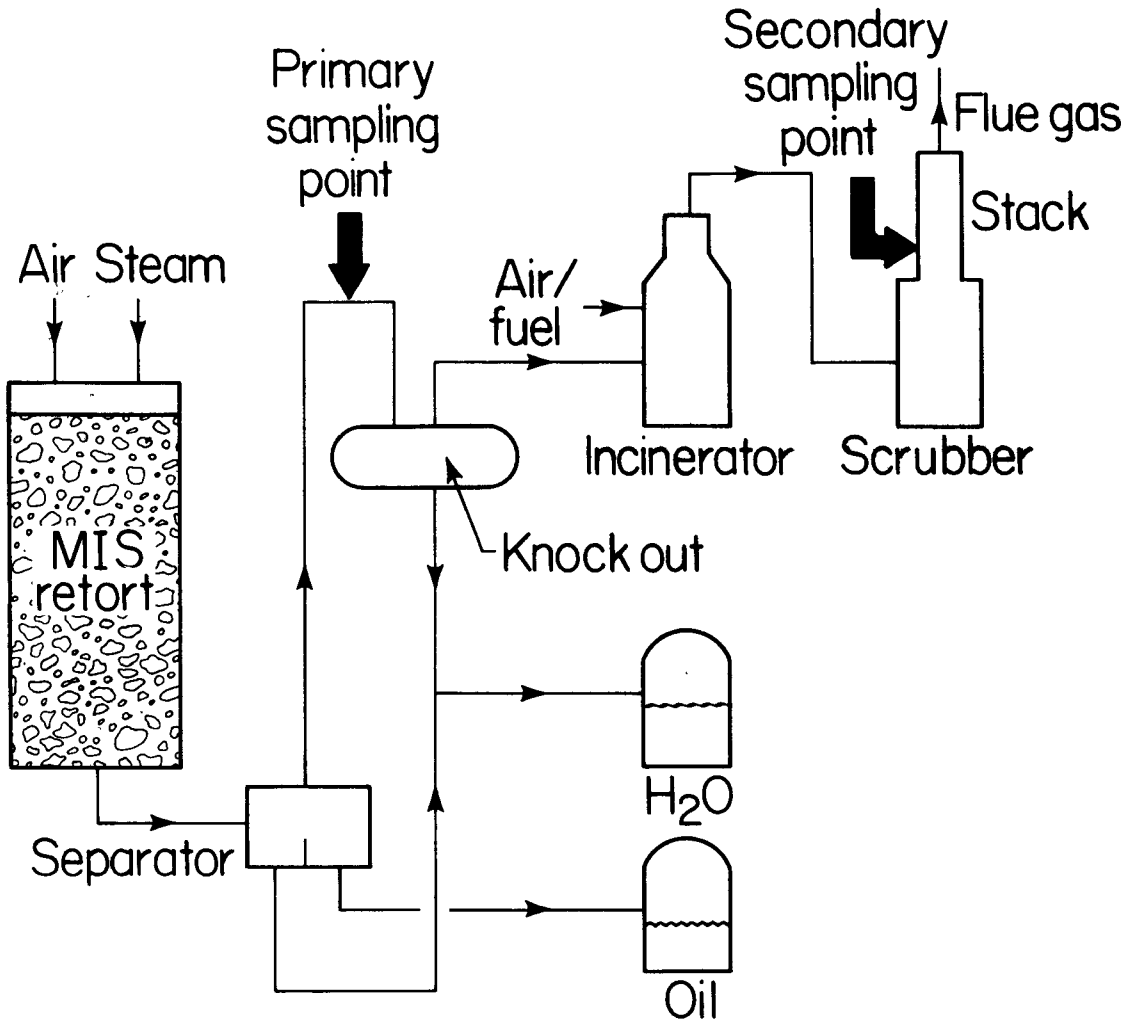

Figure 3. Schematic of the Rio Blanco Retort facility.

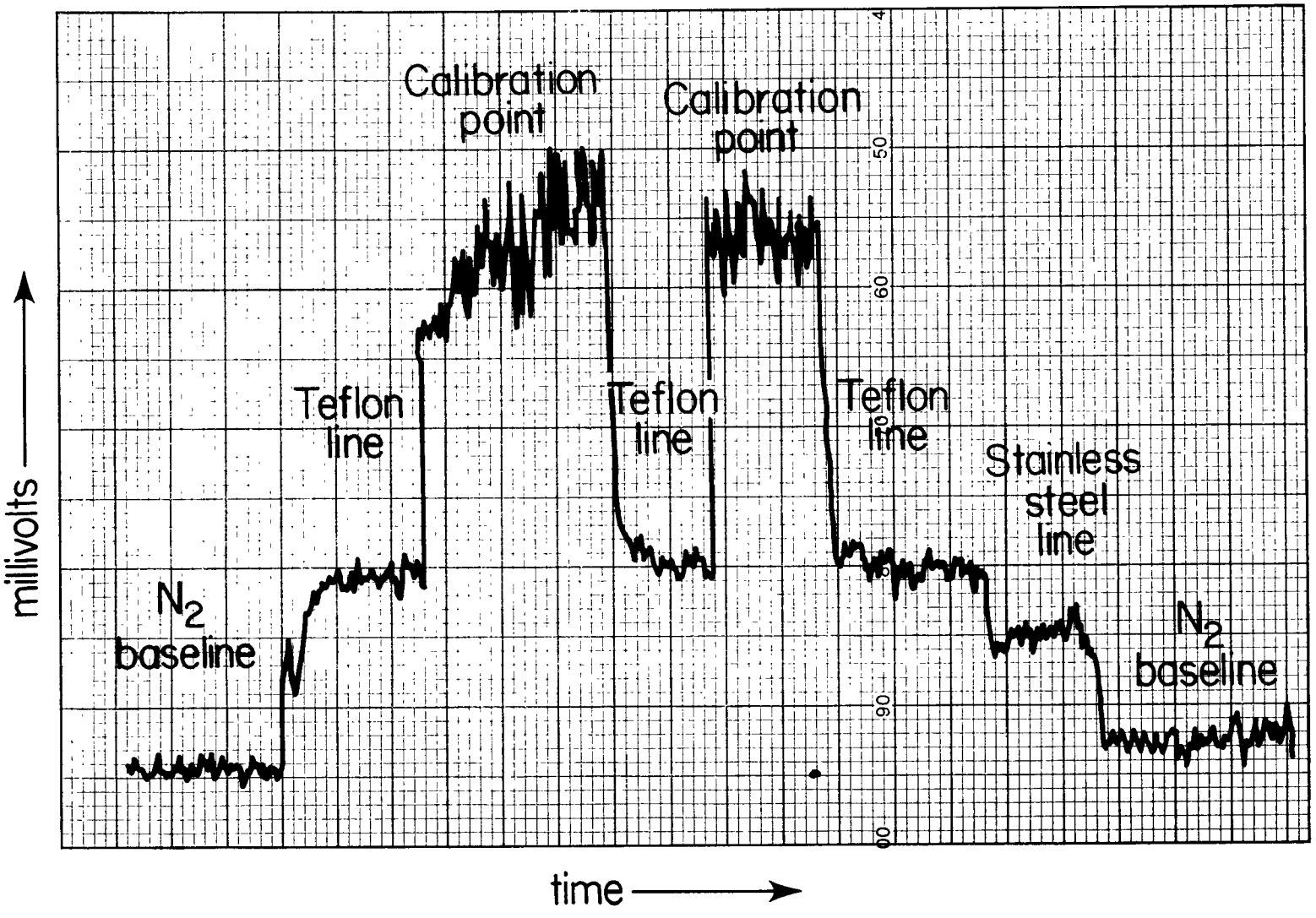

Figure 4. Typical ZAA spectrometer signal for Hg-free N_2 and for Hg in Retort 1 offgas. Standard addition calibration points and the effect of sample line material are shown.

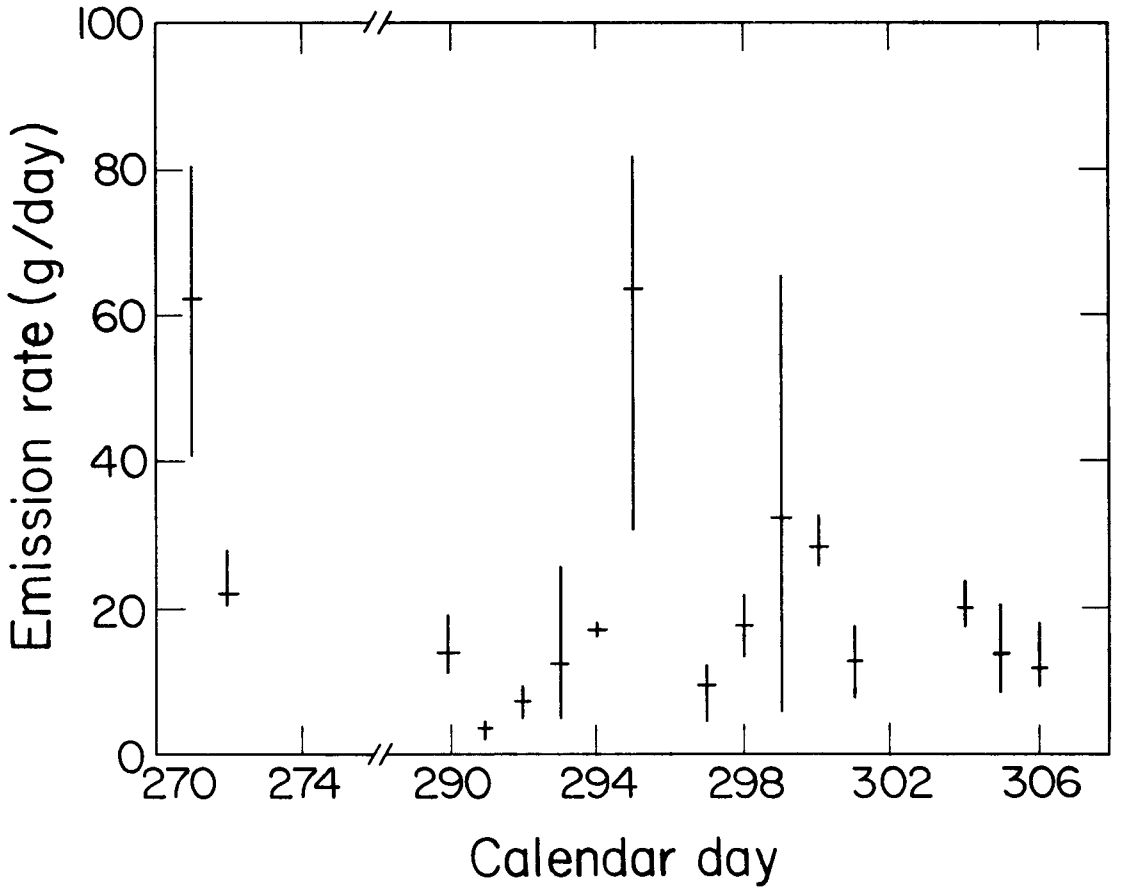

Figure 5. Mean daily Hg mass emission rates and daily mass emission rate ranges.

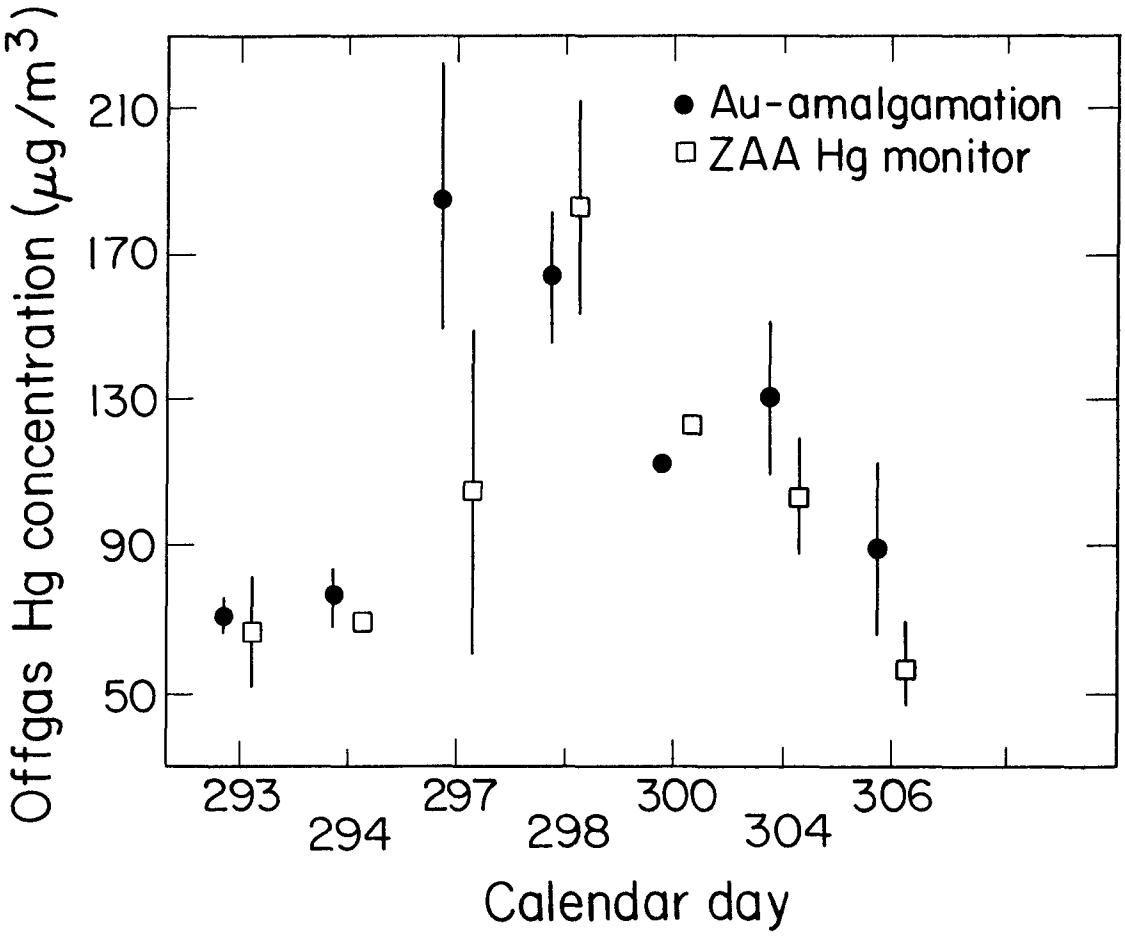

Figure 6. Comparison of Au-amalgamation and ZAA monitor mercury measurements.

Table 1. Speciation of Hg in retort offgas.

Day	n	Hg Concentration			Organic Hg (%)
		Atomic ($\mu g\ m^{-3}$)	Organic ($\mu g\ m^{-3}$)	Total	
297	2	93.5	102	196	52
298	2	30.0	138	168	82
304	3	39.9	94.9	135	70
306	3	31.3	66.2	97.5	68

ABSTRACT

COMPARISON OF TEM AND SEM TECHNIQUES FOR MEASUREMENT OF AIRBORNE ASBESTOS FIBERS

Dan Baxter

(Science Applications, Inc.)
La Jolla, CA 92038

Electron microscopy has become the accepted technique for determination of asbestos in air. Although the transmission electron microscope (TEM) is the preferred instrument for measuring airborne ambient asbestos, analysis of "workspace" environments may be accomplished using the scanning electron microscope (SEM).

Selection of any analytical method must consider the sample matrix that is being tested. Ambient air and "workspace" environments are commonly sampled and tested for asbestos. Asbestos fibers found in the ambient environment are too small for positive identification using the SEM. Limitations of the scanning electron microscope analysis, when compared to transmission electron microscopy, include lower spatial resolution and image contrast.

In lieu of these apparent shortcomings, the SEM has potential advantages over the TEM for analysis of air samples containing a large concentration of fibers in the "occupational" (>5.0 μm) size range. In addition, sample preparation for SEM is not as complex or time consuming as that required for TEM.

In order to evaluate the advantages and limitations of fiber measurement using the SEM, airborne asbestos samples were collected for analyses by

both SEM and TEM. Fibers were counted using the Environmental Protection Agency's "Provisional Methodology for Airborne Asbestos" (EPA-600/2-77-178). Over 95% of the particulate emissions collected in these samples were asbestos fibers, thus minimizing any potential matrix effects from other fibrous materials normally present in air.

Differences in fiber count and dimensions using both SEM and TEM instruments were evaluated using the following criteria: total fiber concentration, fiber dimensions (length and diameter) and calculated mass. The results of these analyses and a discussion of the limitations of both instruments are presented.

Although the Transmission Electron Microscope (TEM) is the currently accepted instrument for analysis of airborne asbestos fibers in the 'ambient' environment, the Scanning Electron Microscope (SEM) has potential advantages in monitoring locations where asbestos fiber concentrations are expected to be elevated. Due to limitations in spatial and dispersive X-ray resolution of the SEM, fibers with diameters below 0.05 μm cannot routinely be identified.

In order to compare the SEM and TEM preparation and analysis techniques for counting and sizing fibers, two samples were collected from the clean side of an asbestos mill baghouse. The two samples are typical of a workspace environment where the mean fiber sizes and relative fiber concentrations (fibers/m^3) are highly elevated. Essentially 99% of all fibers found in the two analyzed samples were asbestos. These conditions were optimal for comparison of size and mass differences due to sample preparation and imaging between the SEM and TEM. The samples were analyzed on a model ISI IIIA SEM (resolution of 70 A°) and a model Hitachi H-500 STEM (Scanning Transmission Electron Microscope) operated in the TEM mode (resolution of 1.4 A°).

Sample Preparation

The first major difference between the SEM and TEM is sample preparation. The SEM filter sample is mounted on a specimen stub and placed directly into the instrument for analysis. Because this filter section can be as large as the size of the specimen mount (10-15 mm), the field of view observed in the microscope does not have any aritifical boundary limitations. In contrast, the TEM filter sample is transferred to a 3 mm diameter 200-300 mesh copper grid using a modified Jaffe-Wick washing method. The field of view is limited by the size of the grid hole. Figure 1 presents a diagram of a 300 mesh 'grid' with examples of fibers crossing outside the field of view. The maximum fiber length that can be measured is limited by the size of the grid opening which in this case is approximately 50 μm. In situations where fibers cross the grid opening, accurate fiber length measurement is not possible. In the ambient environment concentrations of fibers are low and fiber sizes are small, therefore, the accuracy of sizing fibers is probably not impacted. In environments where the fiber concentrations are highly elevated and large

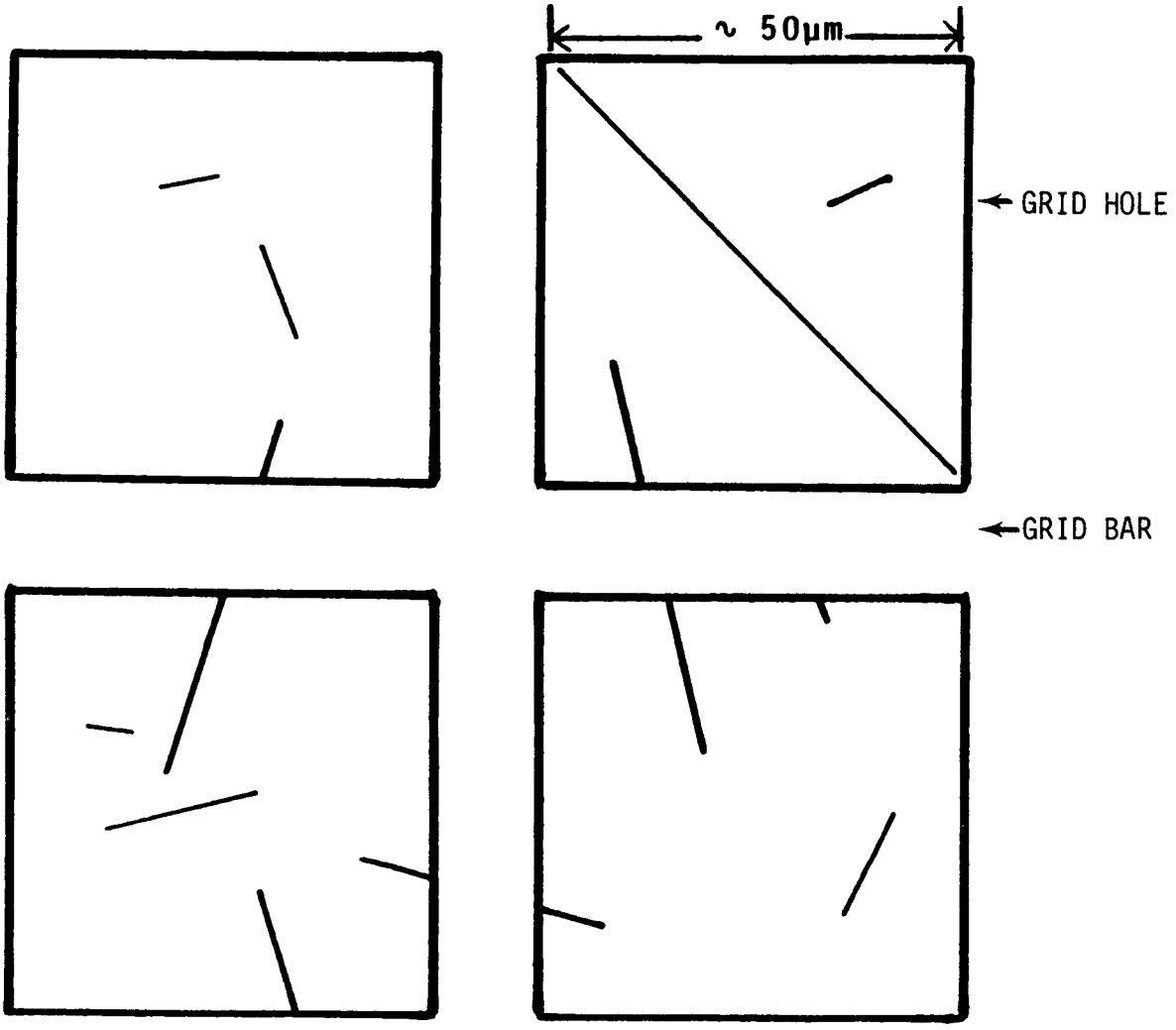

FIGURE 1. Diagrammatic representation of large Fibers on a 300 mesh TEM grid

fibers are present, significant errors in the reporting of mean fiber lengths could occur. Since mass (ng/m^3) (according to EPA protocol) is calculated by the length within the field of view, it is not affected.

Imaging Differences

The mode of sample imaging is responsible for the higher resolution of the TEM and shorter time spans required to survey a given area of a sample filter. Figure 2 is a diagramatic representation of the TEM column. The electron beam is 'transmitted' through the sample with an image generated on the phosphor screen at the base of the instrument. The image is similar to a medical X-ray in that internal structures of the sample can be viewed. Because the image is generated directly on a 'fast' phosphor screen, the sample can be moved rapidly about without any 'image recovery time'. Image recovery time is a major draw-back in using the SEM. The image in the SEM is generated in a reflected mode (Figure 3) by collecting electrons reflected off the specimen to a scintillation disc. The resultant photons are collected through a light pipe and photomultiplier tube and the amplified image is displayed on a television screen. Unfortunately, the highest resolution obtained by the SEM uses the slowest video line scan rate on the instrument (approximately 10 scans/minute). This means that each time a new field is searched, the image must be allowed to stabilize before analysis. Samples that have very low fiber concentrations may require proportionally much higher analysis time than by TEM. This is due to the proportionally large number of fields that must be analyzed.

Counting Procedures

The samples analyzed by TEM (A-9 and A-10) follow the EPA protocol outlined in the Provisional Methodology (EPA-600/2-77-178). Fibers which cross the field of view (grid bar) are counted as 'half fibers' and are assigned length values double the measured length observed within the grid hole. As explained earlier, the maximum fiber length which can be accurately

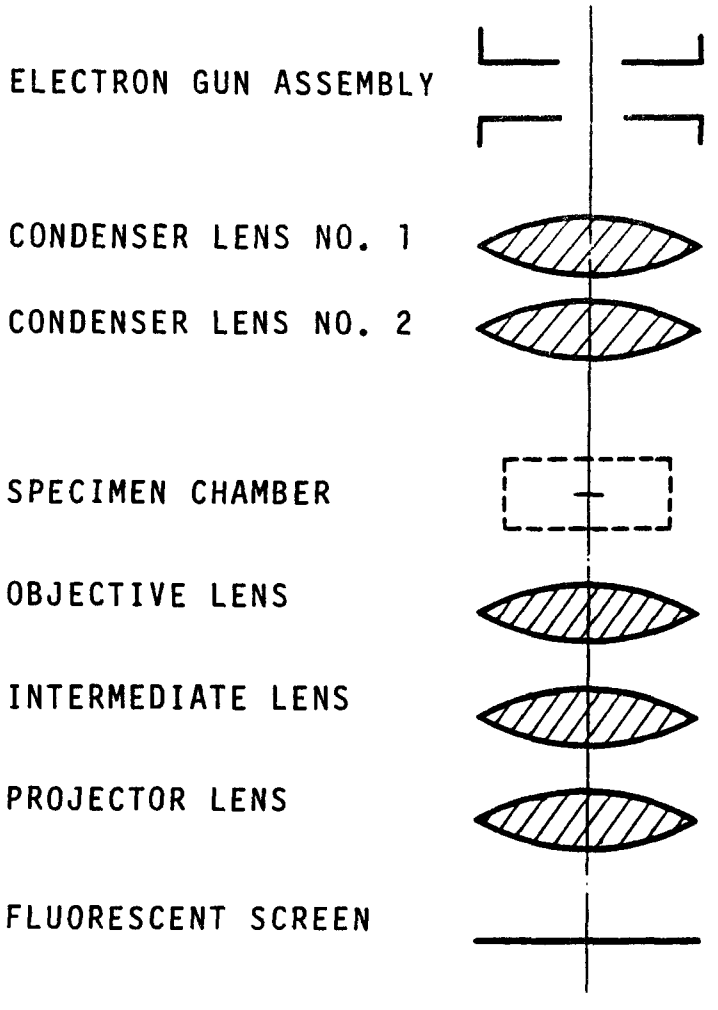

FIGURE 2. Components of the Transmission Electron Microscope

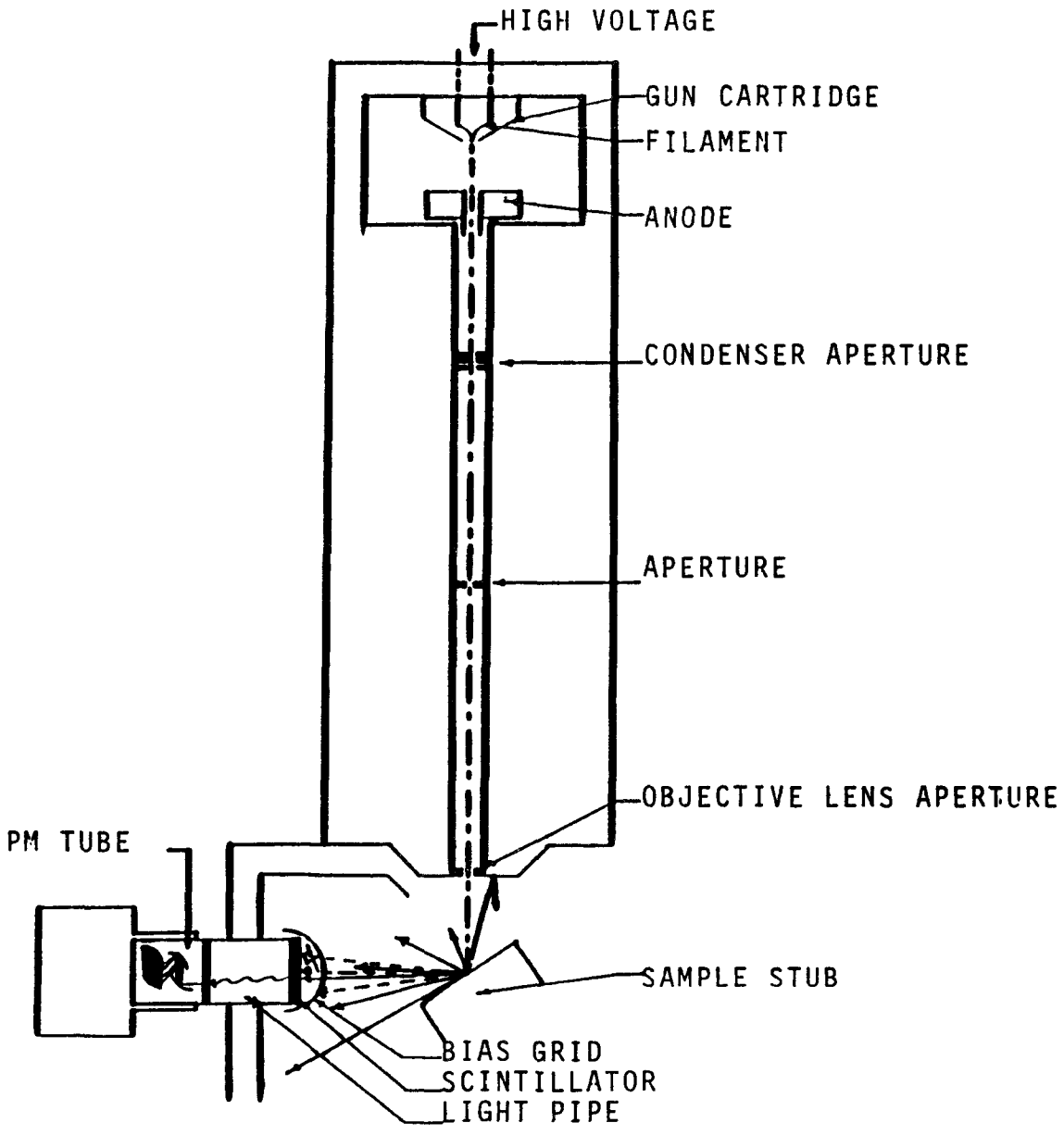

FIGURE 3. Components of the Scanning Electron Microscope

sized is artificially limited by the dimensions of the grid hole or mesh. Both samples (A-9 and A-10) analyzed by SEM were counted according to the same EPA protocol with one exception. If the fiber extended beyond the field of view, the fiber was still counted as a 'half' fiber for numerical purposes, but the true length of the fiber was actually recorded. Therefore, the sizes of large fibers are accurate in the SEM analysis. For the purpose of calculating mass, only the length of the fiber within the original field of view was used in the calculation.

Comparative Results

Table 1 gives the comparatives SEM and TEM results of analysis for total fibers/m^3, fibers greater than 5.0 µm, mean length, mean diameter, and mean mass (nanograms/m^3) in sample A-9. The results are expressed at the bottom of the table as a ratio of the SEM value divided by the TEM value. As can be observed, the total fibers/m^3 are essentially the same (610,000 fibers/m^3 for SEM and 600,000 fibers/m^3 TEM) with a comparative ratio (SEM/TEM) of approximately one. The ratio of fibers with lengths greater than 5.0 µm is 6.5 times higher in the SEM analysis than the TEM analysis. This difference is also reflected in the mean fiber lengths which are 15.5 µm and 2.6 µm respectively. The SEM mean length is 6.0 times greater than the TEM mean length. The fiber diameter in the SEM analysis is 2.5 times higher (0.38 µm versus 0.15 µm) than the TEM mean diameter. The calculated mass (ng/m^3) is surprisingly 18.5 times greater in the SEM analysis (3102 ng/m^3 verses 168 ng/m^3). The analysis of sample A-10 (Table 2) gave similar results. The ratio of SEM/TEM total fiber concentration is 1.18 (574,000 and 490,000 fibers/m^3 respectively). The number of fibers/m^3 with lengths greater than 5.0 µm is 5,8 times higher in the SEM analysis (116,000 versus 20,000). The mean length for the SEM analysis is 4 times higher than the TEM analysis 9.1 µm verses 2.3 µm). The mean diameter is 2.7 times higher in the SEM analysis (0.3 µm verses 0.13 µm) and the mass is 19.1 times higher in the SEM analysis (3730 ng/m^3 verses 195ng/m^3). As observed in both samples, the difference in mass levels is very high. Because mass is independent of the field limiting

TABLE 1. Fiber size and mass results for Sample A-9

SAMPLE A-9 ANALYSIS

	FIBERS /m^3				
	TOTAL	>5.0µm	MEAN LENGTH (µm)	MEAN DIAMETER (µm)	ng/m^3
SEM	610,000	330,000	15.5	.38	3102
TEM	600,000	51,000	2.6	.15	168
RATIO (SEM/TEM)	1.02	6.5	6.0	2.5	18.5

TABLE 2. Fiber size and mass results for Sample A-10

SAMPLE A-10 ANALYSIS

	FIBERS/m^3)				
	TOTAL	>5.0µm	MEAN LENGTH (µm)	MEAN DIAMETER (µm)	ng/m^3
SEM	574,000	116,000	9.1	.35	3730
TEM	490,000	20,000	2.3	.13	195
RATIO (SEM/TEM)	1.18	5.8	4.0	2.7	19.1

problems encountered in the TEM analysis (Figure 1), the lower mass and fiber counts (>5.0 μm) might be due to the loss of large fibers (length and diameter) in the TEM preparation procedures.

Samples A-9 and A-10 were also analyzed by size distribution. Figure 4 gives the size distribution of A-9 and A-10 normalized to fibers/mm^2 of filter area. Below 2.0 um (both samples) the SEM counts fewer fibers, and above 2.0 μm the SEM counts considerably more fibers. In both samples the TEM analysis failed to show any fibers longer than 16 μm.

Conclusions

Comparison of the two samples indicate that the SEM favorably compares with the TEM in the counting of 'total' fibers in a workspace environment. Most importantly, a transition area is observed where SEM performance improves and TEM performance declines. This is due to preparation procedures rather than instrumental resolution. The differences in mean fiber length and diameter can be accounted for by the positive skewing toward larger fiber lengths in the SEM analysis (Figure 4). What is more difficult to explain is the difference in fibers greater than 5.0 μm in length which are approximately 6 times higher in SEM analysis than TEM analysis and also the mass differential (approximately 19 times higher in SEM analysis than TEM analysis). These parameters can only be explained by an actual loss of fibers in the TEM preparation process. Further investigation into the selective loss of large fibers (length and diameter) is necessary to evaluate the upper limits of the TEM method as well as the lower limits of the SEM.

The work described in this paper was not funded by the U.S. Environmental Protection Agency and therefore the contents do not necessarily reflect the views of the Agency and no official endorsement should be inferred.

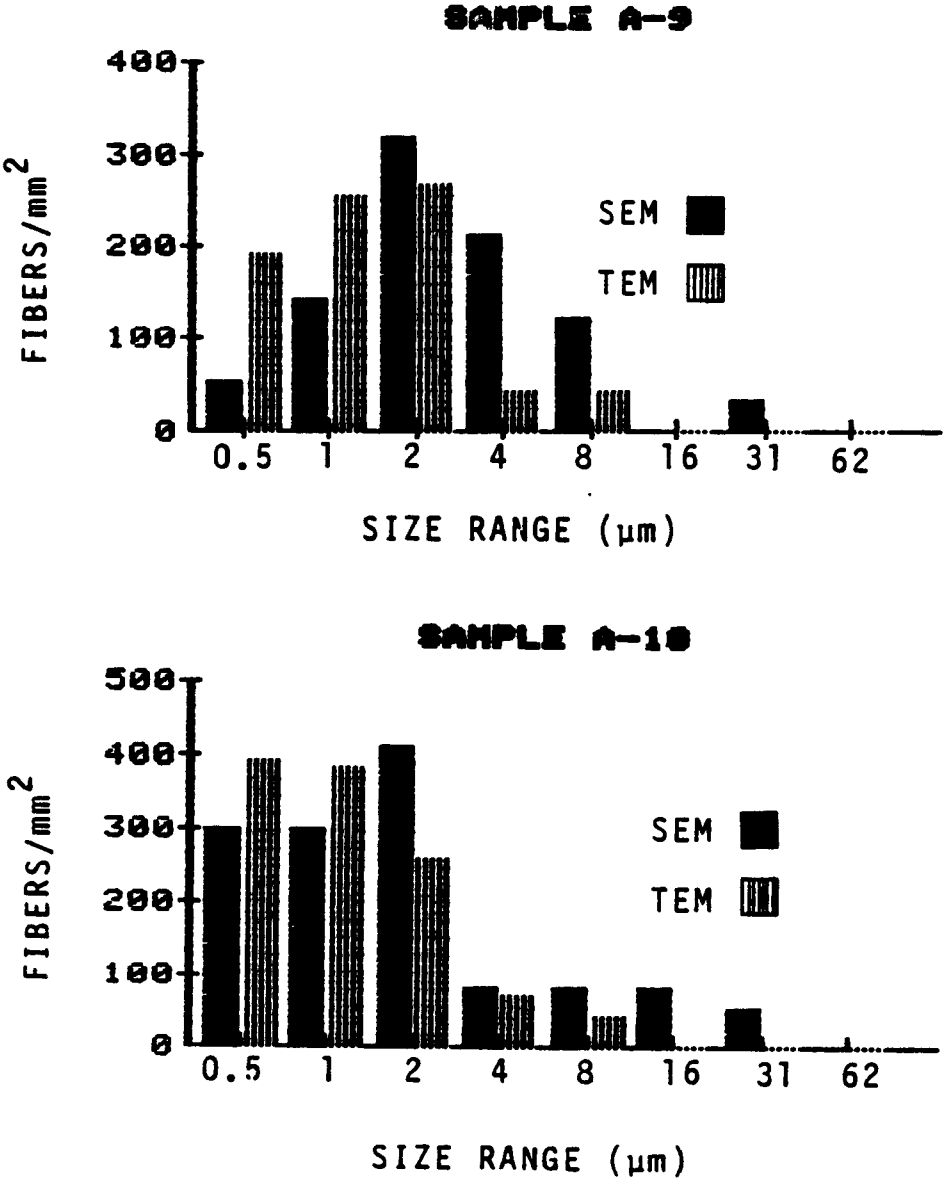

FIGURE 4. Size distribution of Fiber lengths normalized to Fibers/square millimeter

A PILL FOR THE ASSESSMENT OF POLLUTION MEASUREMENT METHODS

R. K. M. Jayanty
Research Triangle Institute
Research Triangle Park, North Carolina

and

R. G. Fuerst, T. J. Logan, and M. R. Midgett
U.S. Environmental Protection Agency
Research Triangle Park, North Carolina

A simple, inexpensive, and accurate method for evaluating and/or auditing sampling and analytical phases of the EPA Source Reference Method 6 was developed. The method uses a known amount of a chemical compound in the form of a tablet or pill (or placed in a capsule) to generate sulfur dioxide (SO_2) quantitatively by reaction with an acid. The reaction takes place in a compact glass impinger system that can be taken to the field. The SO_2 generated in test runs was collected and analyzed using the Method 6 procedure. The SO_2 generation was quantitative and recoveries were found to be 94 ± 5 percent. The time to complete the reaction was less than 15 minutes at a flow rate of 1 L/min, but the recommended sampling time was 45 minutes. The tablets prepared gravimetrically were found to be stable over a 3-month period. The interlaboratory results obtained showed close agreement with the expected concentrations based on calculations from the stoichiometric reaction. The estimates of repeatability (or within-laboratory precision), expressed as a percent of the overall average for SO_2, was 5.5 percent. The reproducibility (or between-laboratory precision estimate) for SO_2 was 13.9 percent. The overall accuracy for the method was within 0.3 percent.

This paper has been reviewed in accordance with the U.S. Environmental Protection Agency's peer and administrative review policies and approved for presentation and publication.

INTRODUCTION

The U.S. Environmental Protection Agency (EPA) is interested in developing audit materials for all EPA Source Reference Methods. These audit materials are used to conduct performance audits during stationary source measurements. EPA is currently providing liquid sulfate standards as audit materials for EPA Source Reference Method 6. EPA Method 6 is used to determine SO_2 emissions from stationary sources. These liquid sulfate audit standards, however are useful only for evaluating the analytical phase of Method 6. At present, sampling phase procedures are evaluated only by a systems audit; i.e., someone observing the sampling procedures in the field. Hence, there is a need for a method or device that can be used as an audit material for the evaluation of both the sampling and analytical phases of the source reference methods.

Recently, Research Triangle Institute (RTI) was contracted by the Quality Assurance Division of EPA's Environmental Monitoring Systems Laboratory, Research Triangle Park, North Carolina, to develop a simple method or device for evaluating/auditing both the sampling and analytical phases of various source reference methods in the field. The main objectives of this study were to develop a simple method or device for auditing both the sampling and analytical phases of EPA Method 6 and to establish the accuracy, precision, and stability for the developed method or device. Accordingly, a new audit method that is simple and inexpensive was developed for evaluating both the sampling and analytical phases of EPA Method 6. The method uses a known amount of a chemical compound (sodium bisulfite or sodium sulfite) mixed with an inert binder (polyvinyl pyrollidine) and made in the form of a tablet or pill to generate SO_2 quantitatively by reaction with sulfuric acid. The SO_2 generated in test runs was collected and analyzed using the Method 6 procedure as published in the Federal Register.[1] The audit method developed was also evaluated at two concentration levels by six different laboratories to determine its repeatability, reproducibility, and accuracy. The various activities performed during the study and the results obtained are discussed in this paper.

AUDIT METHOD SELECTION

Several methods are currently available for generation of standard atmospheres of SO_2. These include:

- Use of commercially available gas cylinders containing known blends of SO_2 in an inert balance gas
- Use of permeation tube devices containing SO_2
- Use of solid materials known to generate SO_2 upon thermal decomposition.
- Use of chemical reactions to generate SO_2 quantitatively.

The advantages and disadvantages of each method for use as an audit method in the field are discussed in a separate report.[2] It appears that out of the four possible audit systems, the use of chemical reactions to generate SO_2 quantitatively is the simplest and least expensive, especially in terms of field audit applications. Basically, the technique requires only a three-way, round-bottomed flask or an impinger, dilute sulfuric acid, and a known amount of solid material that is stable at room temperature and produces SO_2 quantitatively upon chemical reaction. The chemical reaction

well-known technique, was evaluated in the laboratory for use as a field audit method for EPA Method 6.

EXPERIMENTAL PROCEDURES

The preliminary experiments to generate SO_2 from the chemical reaction of sodium bisulfite and sulfuric acid were conducted using the experimental system shown in Figure 1. Initially, a known amount of sodium bisulfite was placed in a three-way, stoppered, round-bottomed flask and dilute sulfuric acid (10 percent) was added slowly from a burette. Dry nitrogen or air was bubbled through the solution at a flow rate of 1 L/min to sweep the released SO_2 into a glass manifold. Glass wool was used to remove the aerosol vapors. The generated SO_2 was monitored continuously with a SO_2 source analyzer (TECO Model 40 fluorescent analyzer) to determine the time of completion of the reaction. Within 10 minutes the reaction was completed. In later experiments, the SO_2 gas generated from the chemical reaction was collected into an evacuated Tedlar bag. After 30 minutes of gas flow into

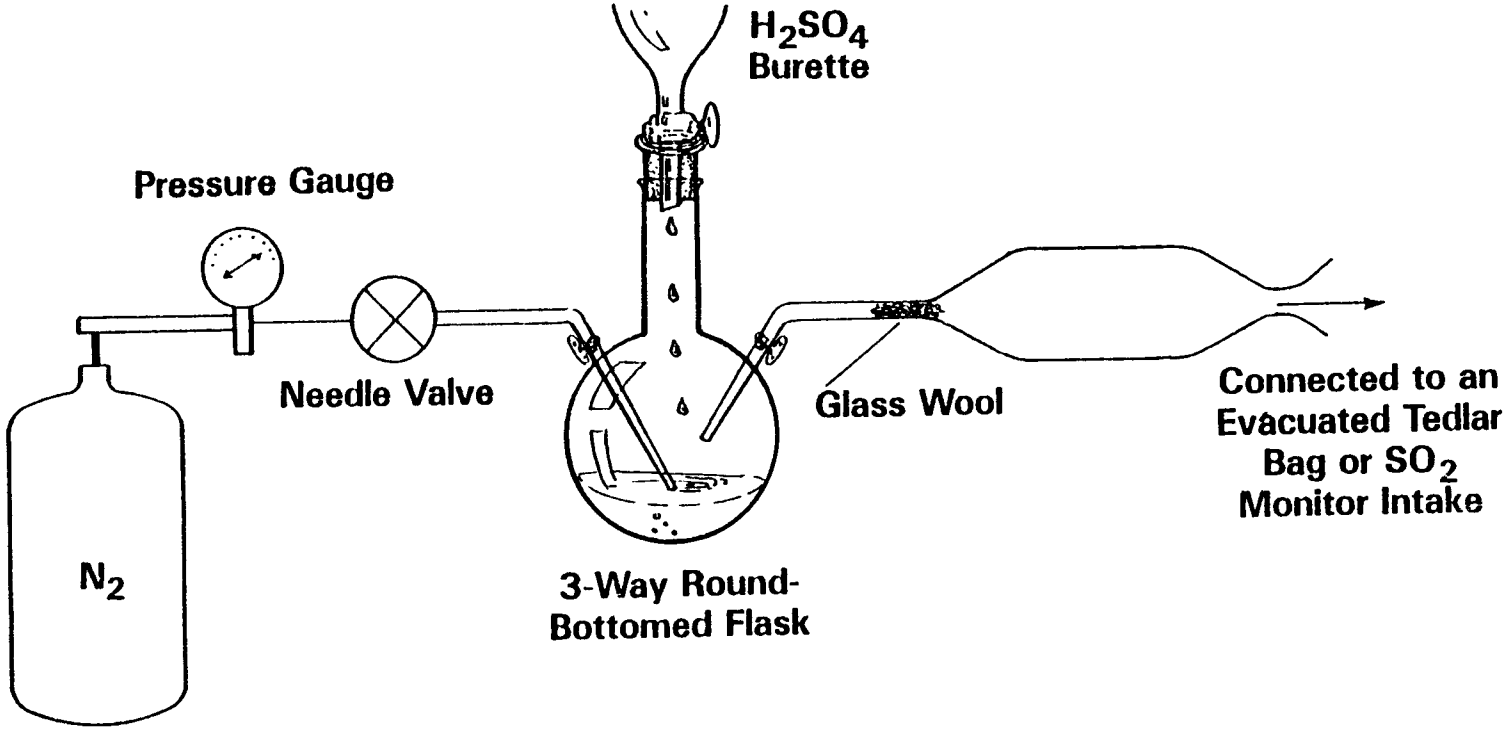

Figure 1. Preliminary SO_2 generation system.

the bag, the contents of the bag were further diluted with zero air and analyzed for SO_2 using the source analyzer. The analyzer was calibrated with a cylinder gas of SO_2 referenced to NBS-SRMs. The experiments were repeated using various amounts of sodium bisulfite and different concentrations of sulfuric acid.

The primary objective of this study was to develop a simple method or device for evaluating the sampling and analytical phases of EPA Method 6. Hence, further experiments were performed using Method 6 procedures as published in the Federal Register.[1] The sampling train component parts, except for the SO_2 gas generator, were the same as those in the EPA Method 6 train. The sampling probe was not required and hence not included in the train. A modified midget impinger (Ace Glass, Inc., Model #7544-35) was used as an SO_2 generator in place of a test-site stack sample to generate a gas sample (SO_2) from the chemical reaction (Figure 2). While the SO_2 gas was being generated, it was drawn through the sampling train according to Method 6 specifications and procedures. The preparation of tablets and SO_2 generation, analysis, and collaborative testing procedures are as follows.

PREPARATION OF TABLETS

Because the amount of sodium bisulfite or sodium sulfite required to generate source concentrations of SO_2 (~400- to 1,000-ppm levels) is so small, an inert binder (polyvinyl pyrollidine, PVP) was used for mixing. The mixture was made in the form of a tablet or pill. The tablets or pills were made using either a KBr die (which is commonly used to make KBr pellets for infrared spectrophotometric studies) or a tablet press. The tablets or pills are made by adding to the die a layer of binder, a weighed amount of sodium bisulfite, and then another layer of binder. Several hundred pounds of pressure are applied using a hydraulic press to form the tablet. The PVP binder was found to be inert and water-soluble and, because the chemical compound is contained between the two layers of binder, the tablets can be handled safely. The binder also helps reduce the rate of reaction of SO_2 generation. Tablets were made with varying amounts of sodium bisulfite to generate different concentrations of SO_2.

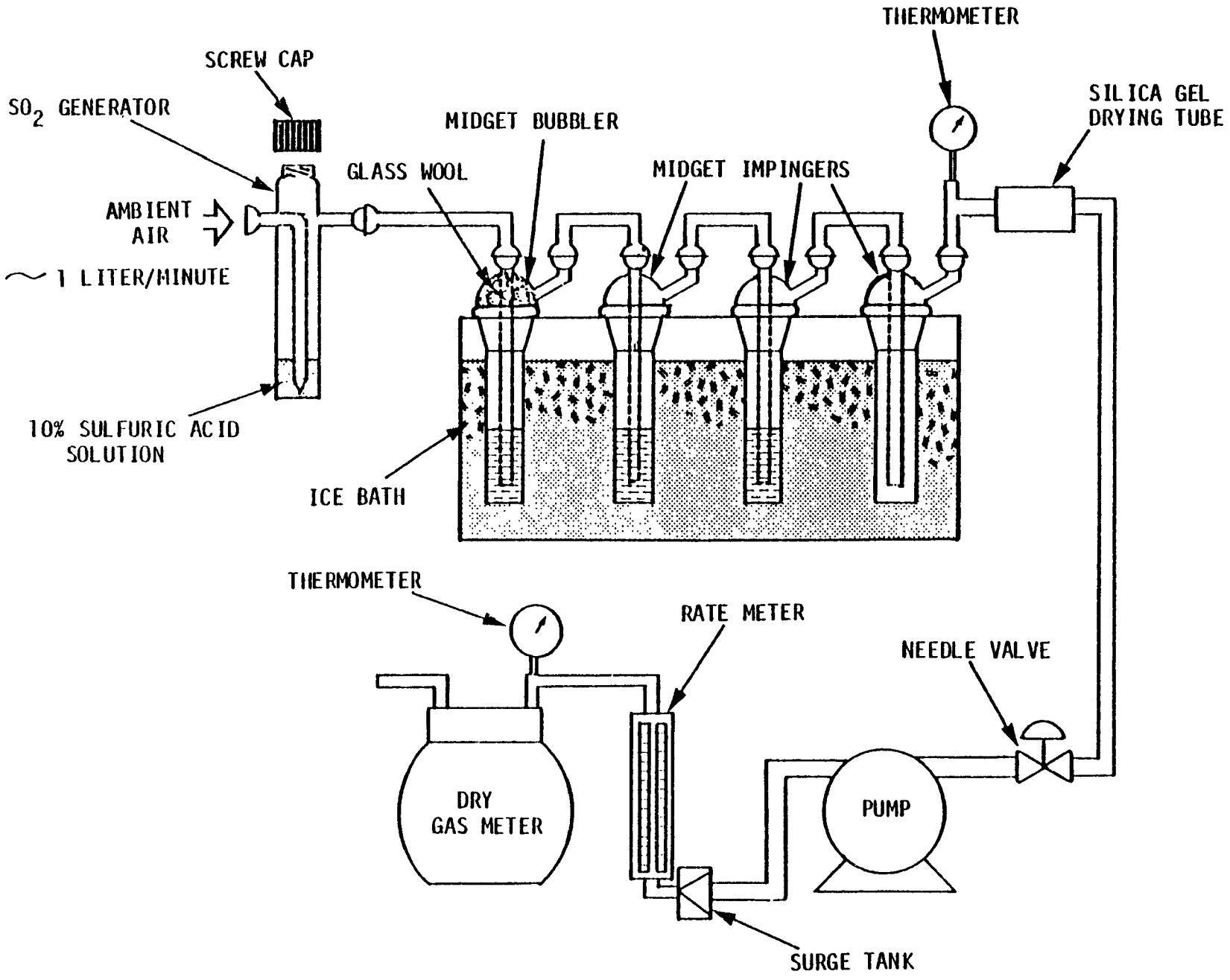

Figure 2. Sampling train with SO_2 generator.

SAMPLE GENERATION AND ANALYSIS PROCEDURES

The sampling train for the generation and collection of SO_2 is shown in Figure 2. Fifteen milliliters of 50 percent isopropanol was measured into the midget bubbler and 15 mL of 3 percent hydrogen peroxide into each of the first two midget impingers. The final midget impinger was kept dry. A leak check was performed without adding acid to the generator prior to sample generation using the leak check procedure described in EPA Method 6. After the leak check, 10 mL of 10 percent sulfuric acid solution was pipeted into the modified midget impinger (SO_2 generator). The SO_2 generator screw cap was held in one hand, the metal bellows pump was started, and the flow rate (1 L/min), which is the same as EPA Method 6, was maintained. The tablet was then dropped into the sulfuric acid solution while the pump was still running. The screw cap was replaced immediately (within a few seconds) and tightened securely. The sample collection procedure was followed as described in EPA Method 6 except for the following modifications. The gas sample was drawn through the SO_2 generator for 45 minutes. The tablet generally took 25 minutes to dissolve completely; however, the sample collection was continued for an additional 20 minutes. Since ambient air was used to draw the sample from the generator, a blank run (without a tablet) was performed for 45 minutes and impinger solutions were analyzed.

The impinger solutions were analyzed after each run for sulfate (converted form of SO_2 collected) by ion chromatography instead of barium perchlorate-thorin colorimetric titration as described in EPA Method 6. However, it was established initially that both analytical procedures gave identical results.

COLLABORATIVE TESTING PROCEDURES

Another objective of this study was to determine the accuracy and precision of the developed method. The reliability of a method is best determined by collaborative testing, the traditional means used by EPA to establish within- and between-laboratory precision of a test method. The accuracy of results obtained by a collaborative study is often more difficult to determine than the precision. In this study, however, the expected SO_2 concentrations from the stoichiometric reaction were compared to the average of measured SO_2 concentrations.

COLLABORATIVE TEST DESIGN

From those laboratories having contracts with EPA, six were selected for the collaborative study based on their past experience in source testing. They were Engineering-Science, Inc., Entropy Environmentalists, Inc., PEDCo Environmental, Inc., Radian Corporation, TRC-Environmental Consultants, Inc., and TRW-Environmental Engineering Division. Seven tablets representing two concentration levels were shipped to each of the six laboratories for analyses to evaluate the feasibility of using the described method for auditing EPA Source Method 6 in the field. Of the seven tablets, three were low concentration (60 mg SO_2) and four were high concentration (120 mg SO_2). The true concentrations of the tablets were based on theoretical concentrations calculated from gravimetric preparations and stoichiometric chemical reaction. A SO_2 generator (modified midget impinger), general instructions to perform the experiments, and a data sheet for reporting the results were also sent to each laboratory. Each laboratory was provided with the true concentration for one tablet and was asked to analyze the true concentration tablet first, then if the measured value was within ±10 percent, to analyze the remaining six tablets. The trial run was thought necessary because most laboratories had not used this method before and needed to become familiar with it. The laboratories were informed that these samples were not for an audit but only for an evaluation of the developed method. Also, the types of compounds in the tablets were not disclosed.

RESULTS AND DISCUSSION

The measured SO_2 concentrations from the preliminary Tedlar bag experiments and the corresponding expected concentrations from the stoichiometric chemical reaction are shown in Table I. The results show that the percent difference obtained ranged from 20 to 25 percent low between the concentration of SO_2 measured and the expected SO_2 concentration from the stoichiometric reaction for various amounts of sodium bisulfite. The SO_2 generation was also found to be independent of flow rate (varied 0.1-1.4 L/min) and the amount of sulfuric acid. The sulfuric acid must be slightly in excess of the amount actually required for completion of the reaction. The

Table I. Bag results.

Amount of $NaHSO_3$ (mg)	Amount of SO_2 expected[a] (ppm)	Amount of SO_2 measured (ppm)	Percent difference[b]
102.6	650	507	-21.9
199.9	804	646	-19.7
200.5	863	660	-23.5
200.6	801	604	-24.5
202.9	869	676	-22.2
201.4	799	652	-18.4
207.5	1003	794	-20.8
202.3	842	712	-15.4
202.5	739	593	-19.8
401.9	944	721	-23.6

[a]Calculated from stoichiometric chemical reaction.

[b]$\text{Percent difference} = 100 \times \frac{\text{Measured } SO_2 \text{ concentrate} - \text{Expected } SO_2 \text{ concentrate}}{\text{Expected } SO_2 \text{ concentrate}}$

lower measured SO_2 concentrations were probably due to the combination of loss of SO_2 in the bag plus loss of wet SO_2 on the glass system, but the actual reasons are neither known nor were they determined. However, the percent difference was constant within experimental error for various amounts of sodium bisulfite.

The results obtained for different amounts of sodium bisulfite (ranging from 10 to 800 mg) using the described method are shown in Table II. As the results indicate, the percent difference between the measured concentration and the expected concentration ranged from 2 to 7 percent; i.e., SO_2 recoveries obtained were between 93 and 98 percent. Lower SO_2 recoveries were obtained for small amounts of sodium bisulfite (10- to 40-mg range). Similar results were obtained for sodium sulfite. However, the SO_2 recoveries were found to be poor for sodium metabisulfite. Since ambient air was used to draw the sample from the generator, a blank run (without a tablet) was performed to test the ambient air. Analysis results showed a negligible amount of SO_2. The SO_2 generated from the material was found to be independent of flow rate and total volume of sample collection.

A study was also performed to determine the storage stability of the prepared tablets over a 3-month period at room temperature. The prepared tablets were analyzed periodically. The results of this study are shown in Table III. These results demonstrate that the tablets are stable within experimental error over the 3-month period. The stability study is still in progress.

COLLABORATIVE TEST RESULTS

The results of the analyses of the samples by the different laboratories and the expected concentrations are shown in Table IV. The analysis results, in general, showed close agreement between the expected values. For example, results of analyses of the low concentration tablets ranged from -4 to +7 percent different from the expected value. Likewise, the results of analyses of the high concentration tablets ranged from -5 to +8 percent different from the expected value. Two values reported from two laboratories were discarded during the statistical analysis because the laboratories identified problems during the SO_2 generation. Blank values reported by the laboratories were also negligible.

Table II. Results of SO_2 generated from the prepared tablets.[a] [b]

Weight of $NaHSO_3$ (mg)	Amount of SO_2 expected (mg)[c]	Amount of SO_2 measured (mg)	Percent difference[d]
12.9	7.9	5.2	-34.2
40.1	24.6	21.9	-11.0
50.6	31.1	31.3	+0.6
100.4	61.8	57.6	-6.8
101.6	62.5	61.5	-2.0
102.9	63.3	59.6	-5.8
202.9	124.9	120.3	-3.7
401.9	247.3	235.1	-2.0
802.3	493.7	464.4	-5.9
114.4[e]	38.5	23.9	-37.9
204.3[f]	103.8	105.1	+1.3

[a] Flow rate 1 L/min for 45 minutes.

[b] 3 to 5 mL of 10 percent H_2SO_4 added.

[c] Calculated from stoichiometric chemical reaction.

[d] Percent difference = $100 \times \frac{\text{Amount of } SO_2 \text{ measured - Amount of } SO_2 \text{ expected}}{\text{Amount of } SO_2 \text{ expected}}$

[e] Sodium metabisulfite was used.

[f] Sodium sulfite was used.

Table III. Stability study results.

No. of days	Amount of SO_2 expected (mg)	Amount of SO_2 measured (mg)	Percent difference[a]
0	122.7	121.9	-0.65
15	123.1	125.5	+1.95
29	123.0	124.9	+1.54
48	123.2	126.8	+2.90
68	121.7	124.4	+2.20
94	122.1	126.5	+3.55

[a]Percent difference = $100 \times \frac{\text{Amount of } SO_2 \text{ measured} - \text{Amount of } SO_2 \text{ expected}}{\text{Amount of } SO_2 \text{ expected}}$

Table IV. Interlaboratory results (mg).

		Low			High		
	Known	1	2	3	1	2	3
Lab 1							
RV	119.7	59.9	59.1	60.4	119.0	119.9	122.6
EV	121.8	60.3	60.4	60.3	122.2	122.3	122.1
Lab 2							
RV	126.5	64.5	61.5	57.9	129.4	128.0	131.7
EV	122.2	60.3	60.2	60.4	122.0	121.8	121.9
Lab 3							
RV	114.2	[a]	58.2	68.1	118.7	115.8	115.6
EV	122.2	-	60.7	60.7	121.9	122.1	122.0
Lab 4							
RV	123.2	63.0	62.3	61.9	128.4	124.9	125.6
EV	122.7	60.5	60.4	60.5	122.4	122.6	122.5
Lab 5							
RV	116.1	60.1	60.7	62.0	116.7	119.6	120.5
EV	121.8	59.9	60.0	60.3	122.1	122.1	122.2
Lab 6							
RV	116	58.3	[a]	60.2	117	118	118
EV	122.4	60.9	-	60.8	122.4	122.3	122.3

RV = Report value.

EV = Expected value.

[a]Values discarded.

STATISTICAL ANALYSIS

The primary objective of the statistical analysis was to estimate the repeatability (or within-laboratory precision) and reproducibility (or between-laboratory precision) of the audit method developed for measuring SO_2. The reproducibility of a method is a measure of the variability between measurements made in different laboratories on the same material. It takes into account the repeatability as well as the effects of differences between laboratories and the effect of those laboratory differences changing from sample to sample. These results were derived from the following variance model:

$$V(Y) = V(L) + V(ML) + V(E),$$

where

V(Y) = The total variance of a SO_2 (mg) measurement classified according to two criteria, laboratories and materials levels

V(L) = The variance of laboratory effects

V(ML) = The variance of the materials × laboratory interaction effect

V(E) = The replication error variance component.

The interaction term is included in the reproducibility estimate to allow for the difference between laboratories changing from level to level. For a two-level case where the linear line fits perfectly, a significant interaction is equivalent to nonparallel laboratory steps. The estimates of repeatability, reproducibility, and accuracy are summarized in Table V. The reproducibility of the method is also a standard deviation with the best estimate at 95 percent confidence and was calculated based on the equation:

$$\text{Reproducibility} = V(L) + V(ML) + V(E) .$$

The mean concentrations of the expected and reported values for the low, high, and overall values are included in Table V. The results indicate that the method can repeat measurements in a laboratory within ±4.99 mg about 95 percent of the time regardless of the concentration level. Also,

Table V. Statistical results (mg).[a]

	Low	High	Overall
Reported	60.5	121.6	91.1
Expected	60.4	122.2	91.3
Repeatability[a] (within laboratories)	±5.2	±5.4	±5.0
Reproducibility[a] (between laboratories)	±5.9	±23.8	±12.7
Precision (within laboratories)	60.5 ± 1.6	121.6 ± 1.8	91.1 ± 1.7
Precision (between laboratories)	60.5 ± 2.0	121.6 ± 5.4	91.1 ± 4.2
Accuracy	0.1	0.6	0.2

[a]At 95 percent confidence limits.

the method can reproduce measurements in different laboratories that lie within ±5.92 mg at the low concentration level or within ±23.8 mg at the high concentration level about 95 percent of the time. The method is not significantly biased when compared to expected values. The accuracy of the method was found to be less than 0.3 percent by comparison with the expected concentrations.

CONCLUSIONS

A new audit method that is simple and inexpensive was developed for evaluating both the sampling and analytical phases of EPA Method 6 in the field. The SO_2 generation was found to be quantitative and the recoveries were found to be 94 ± 5 percent over the 40- to 800-mg range of sodium bisulfite. The method was also evaluated at two concentration levels with six different laboratories to determine it's repeatability, reproducibility, and accuracy. The interlaboratory results obtained showed close agreement with the expected concentrations based on calculation from the stoichiometric reaction. The repeatability within a laboratory was found to be within ±4.99 mg 95 percent of the time for the two concentration levels tested. The reproducibility between laboratories was within ±5.9 mg at the low range and ±23.8 mg at the high range about 95 percent of the time. The overall accuracy of the method was within 0.3 percent by comparison with the expected concentrations. The SO_2 generation from the material was found to be independent of flow rate and total volume, and the prepared tablets were stable at room temperature over a 3-month period. It is recommended that a performance audit using this new audit method for EPA Method 6 be used during future source SO_2 emissions analyses as a routine quality assurance procedure.

ACKNOWLEDGMENTS

This project was conducted by the Research Triangle Institute, Research Triangle Park, North Carolina, under Contract No. 68-02-3767 for the Quality Assurance Division, Environmental Monitoring Systems Laboratory of the U.S. Environmental Protection Agency. Special acknowledgment is made to Mr. Jack C. Suggs of EPA for statistical analysis of the data and Dr. W. F. Gutknecht,

Dr. C. Eaton, Mr. C. E. Decker, Mr. R. Shores, Mr. L. Williams, and Ms. Ann Turner of Research Triangle Institute for technical advice and analytical support.

REFERENCES

1. Method 6--Determination of SO_2 Emissions from Stationary Sources, Federal Register, Vol. 42, No. 160, August 1977.

2. R. K. M. Jayanty, R. G. Fuerst, T. J. Logan, and M. R. Midgett, A New Audit Method for EPA Reference Method 6, Final Report, Research Triangle Institute, June 1983.

SAMPLING AND ANALYSIS OF INCINERATION EFFLUENTS WITH THE VOLATILE ORGANIC SAMPLING TRAIN (VOST)

Greg Jungclaus, Paul Gorman, and Fred Bergman
Midwest Research Institute, 425 Volker Boulevard
Kansas City, Missouri 64110

ABSTRACT

The hazardous waste incineration regulations include the requirement that a destruction/removal efficiency (DRE) of ≧ 99.99% must be achieved for selected principal organic hazardous constituents (POHCs). In order to calculate meaningful DRE values, reliable sampling and analysis methods must be available. This paper describes the sampling and analysis of incineration effluents for volatile POHCs using the volatile organic sampling train (VOST). The VOST was designed for use as an alternative to integrated gas bags and bulbs. The paper includes information on the design and evaluation of the original VOST concept, a description of the procedures and equipment used with the field version of the VOST, a description of procedures adopted to minimize sample contamination in the field, and generalizations concerning the data generated using the VOST.

This paper has been reviewed in accordance with the U.S. Environmental Protection Agency's peer and administrative review policies and approved for presentation and publication.

Introduction

Controlled incineration has been determined to be a very effective technique for destroying the components of hazardous waste without adversely affecting the environment. To test whether an incinerator is operating in a controlled manner, the EPA has developed regulations and draft protocols to test an incinerator's effectiveness by conducting trial burns.

Midwest Research Institute (MRI) has conducted trial burns at several different types of hazardous waste incinerators throughout the country. Regardless of the design of the incinerators, volatile principal organic hazardous constituents (POHCs) are generally important components of the waste feed and stack effluent. Since these volatile compounds are important constituents of the stack effluents, reliable sampling and analysis techniques are crucial in determining the effectiveness of a hazardous waste incinerator.

The traditional method for collecting stack gas samples for the analysis of volatile organics is the integrated gas bag (1). Tedlar seems to be the most common bag material. Gas bags are used with varying degrees of success by different laboratories, but generally their use suffers from several drawbacks including the need to position the bag in a large evacuated sample box which is difficult to carry up to the top of the stack, leakage problems from the bag valve after the sample is collected, loss of sample components due to adsorption onto the walls of the bag, and low sensitivity when the components are analyzed directly, or the need to concentrate the bag sample onto an adsorbent prior to analysis. However, the major drawback that MRI has experienced with bags in the field is contamination of the bag in the hostile environment of a hazardous waste incinerator.

VOST Configuration

At a meeting of EPA project officers and contractors in McClean, Virginia, in April of 1982, the basic design of the VOST was developed and vinyl chloride, carbon tetrachloride, trichloroethylene, and chlorobenzene were selected as the POHCs to test in a laboratory system. The configuration of the VOST used for the lab evaluation and in the field is shown in Figure 1. The stack gas sample was cooled by passing it through an ice-water condenser. The cooled gas and

SCHEMATIC OF VOLATILE ORGANIC SAMPLING TRAIN (VOST)

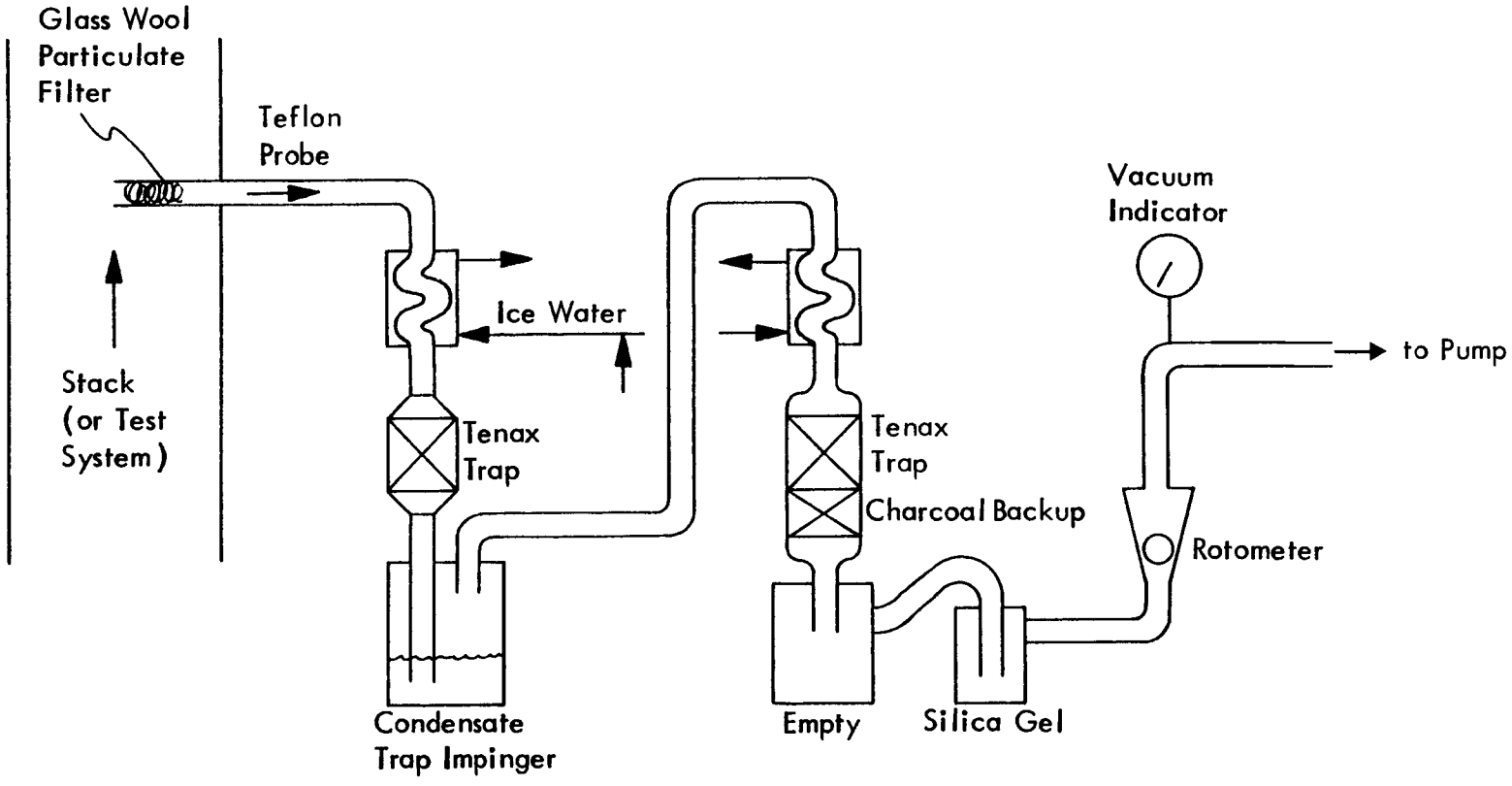

Figure 1. Configuration of volatile organic sampling train (VOST).

condensed water then passed through a front Tenax trap where most of the volatile organics were adsorbed. The water collected in an Erlenmeyer-shaped impinger where it was continually purged by the sampled gas so that most of the volatile compounds which pass through the front Tenax trap are purged from the water, passed through a second ice-water condenser and then through a back-up adsorbent trap containing a front section of Tenax and a backup section of charcoal. The purpose of the charcoal was to adsorb very volatile compounds which may break through both sections of Tenax, and is analogous to the charcoal used as a backup in the analytical adsorbent trap when analyzing water samples for volatile priority pollutants by the purge-trap-desorb GC/MS technique according to EPA Method 624 (2). It is expected that compounds which are volatile enough to pass through both Tenax traps are also volatile enough to be thermally desorbed back off the charcoal when the traps are thermally desorbed for analysis. The original VOST concept prescribed sampling with each pair of traps for 20 min at 1 L/min and then changing the pair of traps five additional times with each pair of traps used to collect 20 L of sample. This way, single pairs of traps can be analyzed for high concentration level samples, but the option exists to combine the contents of several pairs of traps onto one pair of traps prior to analysis for low concentration level samples.

VOST Trap Analysis Procedure

One thing to note about this particular sampling train is that it generates wet traps which require a special analysis technique. The contents of the wet traps are simply thermally desorbed into the bottom of a water column which is the sample container for analyzing water samples for volatile organics by purge-trap-desorb GC/MS according to EPA Method 624 (2). The thermally desorbed

steam condenses in the water column while most of the thermally desorbed volatile organics from the trap are purged out of the water and are collected on the analytical adsorbent trap for subsequent thermal desorption into the GC/MS system for analysis. The thermal desorption is performed in a commercial Nutech thermal desorption system. The glass adsorbent tubes are first spiked with 50 ng of D_4-1,2-dichloroethane, D_6-benzene, and D_{10}-ethyl benzene internal standards and bromofluorobenzene (BFB) to monitor the mass spectrometer tuning. The spiking is done by flash vaporizing a methanol calibration standard solution of the compounds onto the sample traps using a gas chromatograph injection port. The traps are analyzed by dropping them into the heated chamber and immediately closing the lid. Purified nitrogen gas passes through the heated trap, transferring the contents of the trap, including the water and the adsorbed organics, into the purge tower. The water condenses and remains in the tower while the volatile organics are purged into the analytical system.

Laboratory Evaluation of the VOST

A synthetic stack gas generator was used for the lab evaluation of the VOST (3). The synthetic stack gas generator utilized the nitrogen vapor from a tank of liquid nitrogen as the source of gas for the system since it provided a large volume of organic-free gas which could not be readily obtained by any other technique. The nitrogen gas was then heated to about 150°C and rendered wet by vaporizing deionized charcoal-filtered water into the nitrogen through a quartz tube heater. Also near the same point a syringe pump was used to spike a methanolic solution of the four volatile POHCs into the hot, wet gas stream. Four different methanolic concentrations of the POHCs were used for the laboratory evaluation yielding stack gas concentrations ranging from 0.1 ng/L to 100 ng/L in increments of a factor of 10. Three identical sampling trains were used to

collect the stack gas. Each pair of traps in each train was sampled at 1 L/min for 20 min. At the end of 20 min, the two traps were removed and placed into screw-cap tubes. Another pair of traps was then inserted into each train, the traps were leak checked and the sampling was resumed.

A large amount of data was generated during the lab evaluation. Some of the low level data were generated by combining the contents of several pairs of traps onto one pair of traps prior to analysis, while at the higher levels, the data were generated by analyzing single pairs of traps. The amounts on the front and back trap were simply added.

The data from the pairs of traps were scattered at both higher and lower values than the expected (known) value. However, when the results from three VOST trains were averaged (the procedure normally followed for incineration trial burns), the observed results for all four compounds at all four levels generally spanned the range of 50 to 150% of the expected value. These results were considered quite good; however, before the VOST could be used in the field, several important changes had to be made because of:

- The difficulty in changing and leak-checking the traps under field conditions compared to the laboratory.
- The lack of ruggedness of the laboratory sampling train.
- The high potential for contamination on the outside surfaces of the glass adsorbent traps in the hostile environment of the hazardous waste incinerator and also from the handling of the traps.

Field VOST Development

The first modification in the field VOST to simplify the changing of the traps and to reduce the likelihood of contamination, was development of a field

carrier for the traps. Figure 2 shows the components of the field carrier for the VOST traps. The adsorbent tube is held within a larger glass tube with a pair of Viton O-rings. The purpose of the outer glass tube is to protect the outside of the adsorbent-containing tube from contamination. Each of the glass tubes butts against another pair of O-rings in the metal end pieces. The assembly is held together by three cylindrical rods soldered into one end piece assembly and fastened by threaded nuts to the other metal end piece. The end caps also are fitted with a Viton O-ring to seal the traps.

The Tenax and charcoal are held in the 10 cm x 1.6 cm ID glass tubes with a fine-mesh screen supported by a C-clip, both made of stainless steel. These supporting materials hold the adsorbents more uniformly inside the tubes than glass wool (used during the lab evaluation) resulting in a lower likelihood of channeling and lower retention of water in the trap.

Figure 3 shows a photograph of the current field version of the VOST. Several items to note in the photograph are the following:

- Glass entrance tube attached to a Teflon® probe which is inserted into the stack (or quartz-lined stainless steel probe for hot stack gases).
- The front condenser.
- The front Tenax trap.
- The Erlenmeyer impinger where condensed water collects and is purged by the sampled gas.
- The backup condenser.
- The backup Tenax/charcoal trap.
- The air sampling pump.
- The bottom portion of the case. Ice water is added which is circulated by the small water pump. The VOST folds up in the case when not in use.

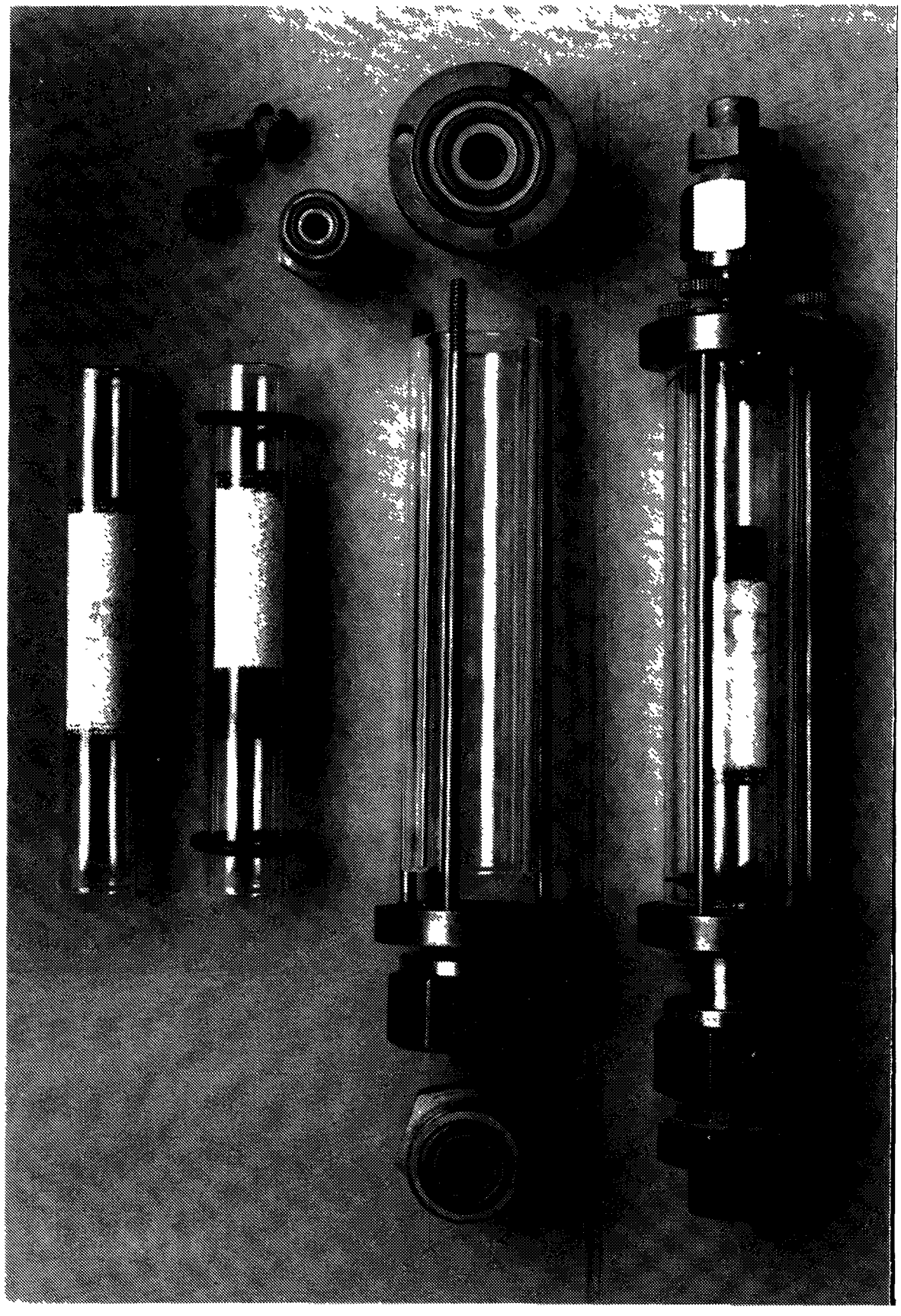

Figure 2. Components of field carrier for the VOST traps.

Figure 3. Photograph of field version of the VOST.

Trap Preparation and Contamination-Prevention Procedures

During development and evaluation of the field VOST, it was discovered that the traps were sometimes severely contaminated with volatile organic compounds. Several possible sources of contamination were identified, including the hostile ambient environment and contaminated metal carriers, O-rings, and adsorbents. In order to avoid contamination, stringent trap preparation procedures were tested and adopted which have proved very effective in eliminating the contamination during field sampling with the VOST by ensuring that the traps are clean at the time of trap preparation and by avoiding contamination of the traps at any later time with the volatile analytes which are likely to be present in the ambient atmosphere around the hazardous waste incinerator.

The procedures that are used to prepare the components of the field VOST are presented in Table 1.

TABLE 1. FIELD VOST TRAP COMPONENT CLEANUP PROCEDURES

Components	Procedures
O-rings	Condition at 200°C for 48 h in vacuum oven.
Tenax and charcoal	Thermally condition packed tubes at 250°C for 4 h two times each.
Glass tubes	Wash in Alconox, sonify, rinse, oven-dry.
Metal parts (end plugs, C-clips, screens)	Wash in Alconox, sonify, rinse, oven-dry.

Once the component parts of the field carrier have been prepared, the following procedures are followed to check the cleanliness of the traps and protect the traps from contamination until they are analyzed:

- Assemble components in organic-free room.
- Log trap numbers and trap history in laboratory record book (LRB).

- Leak check traps by attaching to source of purified gas and placing under water.
- Connect leak-tight traps to source of purified gas (i.e., manifold), inside a 190°C oven.
- Check trap effluent using gas chromatography with a flame ionization detector. Traps are considered to be clean when trap effluent leves are < 20 ppb.
- Store clean traps under ice water. (The purpose of the ice water is to protect the traps from contaminants in the air and also to keep the Tenax cold to slow the gradual aging of the Tenax which results in benzene and toluene being desorbed during analysis.)
- Transport traps to field for sample collection under ice water.
- Return traps to laboratory, disassemble, and analyze.

Two different types of blank traps are generated during field incineration tests. One type of blank is called a trip or travel blank. These traps remain under ice water during transport and during the incineration test. Another group of blank traps are taken up on the stack, and the end caps are removed and the traps exposed to the ambient air for just the time that it takes to change the traps in the sampling train. These blanks, called field blanks, may adsorb small amounts of compounds from the air. These data are then used to correct the results for the actual sample traps.

Sampling Parameters

During field sampling the VOST trap pairs are generally replaced with fresh traps at selected intervals (i.e., every 20 min or 20 L of sample) over a 2-h sampling period. There are two basic reasons for changing the traps at selected intervals:

- At sample volumes of greater than 20 L, some of the very volatile POHCs may break through both the front and backup adsorbent traps.
- The changing of the traps allows an initial analysis of one pair of traps. Analysis of a single pair of traps lowers the possibility of collecting too much sample and overloading the GC/MS system. However, if the POHCs are not detected or are present at low levels in the single pair, the option exists of combining the contents of the remaining pairs of traps onto one pair of traps with a concomitant increase in sensitivity. (The need to combine the contents of traps has not occurred under field sampling conditions.)

A "SLOW VOST" is also being evaluated during which only two or three pairs of traps are used for sample collection. The slow VOST, which generally samples only 5 L of stack gas over a 40-min sampling period, has the following advantages:

- The slower sampling rate reduces the likelihood of breakthrough and serves as a check on breakthrough for the regular VOST.
- A more integrated sample is obtained. This is very advantageous in situations where the stack gas composition changes during the incineration test.

The main disadvantage of the slow VOST is the decreased sensitivity.

Data Considerations

An important aspect of using the VOST is to know how good the field VOST data are. The lab evaluation suggested that the determined values should be in the range of about 50 to 150% of the true value. In the field we now have much additional experience working for us, but also a much more complex sample matrix working against us. However, we can test for breakthrough loss from the traps

by sampling the stack gas at two different flow rates and comparing the concentrations of the collected volatiles. Also, the distribution of the compounds on the front and backup traps would be expected to provide some indication of whether breakthrough is occurring.

Table 2 shows some typical front/back trap distribution data for VOST traps run at two different sampling rates. The fast VOST was run at 1 L/min for 20 min. The slow VOST was run at 0.25 L/min for the same 20 min. The front/backup trap distribution generally favors the front trap although it is not consistent from run to run or compound to compound. Table 3 shows the stack gas concentrations calculated for the slow and fast VOST from the data in Table 2. The data agree quite well with each other although less well at the lower concentration levels, near the detection limit of the method.

Conclusions

The conclusions from the lab evaluation of the VOST and the field use of the VOST for incineration trial burns thus far are the following:

1. The VOST concept is valid and adaptable to field use.

2. Stringent trap preparation and storage procedures are needed to avoid contaminating the traps.

3. The front Tenax trap collects most of the mass of the volatile PHOCs.

4. The backup Tenax/charcoal trap is needed for very volatile compounds and also collects more of the compounds in high level samples.

5. Breakthrough of volatile POHCs through both traps is generally not occurring, as evidenced by the distribution of compounds on the front and back traps and the near equivalency of concentrations using a fast and slow VOST.

6. In actual field incinerator sampling and analysis with the VOST, it has never been necessary to combine the contents of several pairs of traps onto one pair of traps to achieve requisite sensitivity for GC/MS analysis.

TABLE 2. DISTRIBUTION OF VOLATILE POHCs ON FRONT TENAX (T) AND BACKUP TENAX/CHARCOAL (T/C) TRAPS FOR FAST AND SLOW VOST AT AN INCINERATION TRIAL BURN

Compound	Amount detected, ng											
	1st Pair				3rd Pair				6th Pair			
	Fast*		Slow†		Fast		Slow		Fast		Slow	
	T	T/C	T	T/C	T	T/C	T	T/C	T	T/C	T	T/C
Chloroform	280	8.2	88	< 1	330	8.9	100	< 1	310	39	93	2.1
Carbon tetrachloride	55	7.8	18	4.6	47	4.7	22	< 2	4.8	29	15	< 2
Trichloroethylene	8.3	4.1	2.2	10	6.3	1.3	4.0	2.5	-	3.1	4.4	5.6
Tetrachloroethylene	44	1.6	5.4	< 1	30	< 1	7.7	< 1	5.5	1.3	9.8	< 1

*Fast VOST collected 20 L of stack effluent over 20 min.
†Slow VOST collected 5 L of stack effluent over same 20 min.

TABLE 3. CONCENTRATIONS OF VOLATILE POHCs DETERMINED FROM ANALYSIS OF FAST AND SLOW VOST AT AN INCINERATION TRIAL BURN

Compound	Concentration, ng/L					
	1st Pair		3rd Pair		6th Pair	
	Fast*	Slow†	Fast	Slow	Fast	Slow
Chloroform	14	17	16	19	16	18
Carbon tetrachloride	3.1	4.5	2.6	4.4	1.7	3.0
Trichloroethylene	0.6	2.4	0.4	1.3	-	2.0
Tetrachloroethylene	2.1	0.3	1.3	0.7	2.6	1.2

*Fast VOST collected 20 L of stack effluent over 20 min.
†Slow VOST collected 5 L of stack effluent over same 20 min.

7. The slow VOST has the advantage of yielding a more integrated sample if run at a slower flow rate and longer time than the original fast VOST concept, is less expensive because of the need to prepare and analyze fewer traps, but is slightly less sensitive.

Acknowledgement

We wish to acknowledge the EPA Office of Solid Waste and Office of Toxic Substances in Washington and the Industrial Environmental Research Lab in Cincinnati for sponsoring this work. We would also like to acknowledge Dr. Larry Johnson of the EPA Industrial Environmental Research Laboratory at Research Triangle Park and Mr. David Friedman of the EPA Office of Solid Waste in Washington who served as project officers during the laboratory evaluation of the VOST.

REFERENCES

1. Rechsteiner, C., Harris, J.C., Thrun, K.E., Sorlin, D.J., and Grady, V. Sampling and analysis methods for hazardous waste incineration. A.D. Little, Inc., in support of Guidance Manual for Evaluating Permit Applications for the Operations of Hazardous Waste Incineration Units. EPA Contract No. 68-02-3111, EPA/IERL, Research Triangle Park, North Carolina. 1981.

2. EPA Method 624 - Purgeables. U.S. Environmental Protection Agency. Federal Register 44:69532-69539, 1979.

3. Jungclaus, G. and Gorman, P. Evaluation of a volatile organic sampling train. Draft final report, Midwest Research Institute, EPA Contract No. 68-01-5915, 1982.

ANALYSIS OF PCB'S BY CAPILLARY GC/ECD FOR DETOXIFICATION STUDIES

BY

ALSTON L. SYKES

TRW ENERGY & ENVIRONMENTAL DIVISION

INDUSTRIAL HYGIENE &

TRACE SUBSTANCES LABORATORY

PO BOX 13000

RESEARCH TRIANGLE PARK, N.C. 27709

ABSTRACT

Recent efforts have been undertaken to determine the best practical methods for disposing of hazardous materials such as polychlorinated biphenyls (PCB's). Disposal in approved solid waste landfills and incineration have been the most used and studied methods. Questions concerning long term problems of landfills have brought about a need for alternate methods of disposal. One method being studied is chemical detoxification.

One common need in all of the methods used and under study is documentation of the presence and amount of PCB's. This determination is needed to calculate efficiencies of destruction or combustion of the PCB compounds. Therefore, the most critical part of these studies is the analysis. PCB's were analyzed by gas chromatography with electron capture detection utilizing a SE-54 fused silica capillary column for the purposes of determining PCB detoxification efficiency.

TEXT

Due to the recent local and national interest in occurance of Polychlorinated Biphenyl's (PCB 's) in the environment, much work has focused on identifing and quantifing trace levels in air, water, soil, and waste products. Studies are in progress to determine the efficiency of incineration, chemical detoxification, and amount of leaching from waste disposal sites. PCB's are normally distributed as Aroclor mixtures, which are variations of percent chlorination of biphenyl. PCB's are normally found in capacitor oil, transformer oil, or hydraulic oil. These Aroclor mixtures are composed of various fractions of over 200 individual isomers. The analysis of these PCB's is very complex due to their many possible isomers, but also due to the interferences present. Use of packed columns for the analyses usually requires exhaustive clean-up procedures to remove the interferences such as pesticides, oxyengenated and other strongly electron capturing species. During incineration and detoxification of the PCB's many of these interferences are formed, and the Aroclor patterns can be altered. Waste PCB oils are many times combined resulting in mixtures of the Aroclors, which are very difficult to resolve and quantify using packed GC.

The purpose of this paper is to discuss the use of fused silica capillary columns vs. packed columns in the analysis of PCB's in transformer oil used to demonstrate the efficiency of detoxification. Acurex Waste Technologies, Inc. of Mountain

View, California has developed a process for chemically detoxifying PCB's in oil. A demonstration project was conducted for EPA to obtain permits for this process. Transformer oil was spiked with an amount of PCB's and subjected to the process. Samples of the waste were taken before the process and after to determine the efficiency of detoxification. In the process the raw PCB/transformer oil was reacted with a solution of sodium to dechlorinate the molecule. The reaction was stopped in a quench tank of water, which was later separated from the oil. The laboratory analysis of the samples consisted of the following:

1) washing an aliquot of oil with organic free water to remove any sodium salts present,

2) making appropriate dilutions of the raw waste sample to within an ECD calibration curve,

3) injecting the samples onto a fused silica capillary column, with electron capture detection.

4) comparing selected peaks of the samples to those of standards for identification and quantification.

ANALYSIS CONDITIONS

The instrument used for these these analyses was a Varian 3700 GC equiped with a Nickel 63 electron capture detector, and data collection and plotting using a Varian Vista 401 data system. An SE-54 (J & W Scientific) fused silica capillary column, 30 meters by 0.25mm, was used with the split flow set at 30 ml/min. The carrier gas was nitrogen, but hydrogen can also

be used to obtain faster elution. The pressure on the column was 15 psig, which produced approximately one ml/min. flow. The split injection proceedure was used which incorported a 3 sec. hot needle and solvent flush injection technique. The injection port timperature was 290 degrees C., and the electron capture detector temperature was 320 degress C. Various oven conditions and temperatures are available to the chromatographer depending on whether or not a screening proceedure or high resolution is needed. For quick screening an initial temperature of 200 degrees C is used, then programmed to 270 degrees at 4 dgs/min. Adequate resolution is acheived in a 20 min. chromatogram that allows the chemist to determine which Aroclors are present and if interferences exist. Often it may not be necessary to improve resolution. If needed, high resolution is achieved by starting the temperature program at 100 degrees C, and programming to 270 at 3 dgs./min. for an hour chromatogram. The detection limit in either set of conditions remains at 50 picograms/microliter of Aroclor 1260. Table 1 summarizes the analysis conditions.

Examples of packed column analysis of Aroclors 1254 and 1260 in figure 1 show resolution of about 10 peaks in a 30 min. chromatogram at 200 degrees C. This is about the best on would expect from packed columns. Notice how the baseline drifts in the 1260 run. This baseline drift causes many problems with most integrators. Problems such as negative peaks, which are common with ECD's, will cause a negative baseline to be established. The integrator then includes this additional area

in each peak, resulting in a positive bias. Data systems such as The Varian Vista 401 allow the chemist to store all raw data, substract baseline drifts, force baseline to baseline integration, and replot the chromatogram to see where the baseline was drawn. These features, coupled with the ability to integrate capillary peaks faster than one-half sec., allow the chromatographer to obtain precision of injections of 3 to 5 percent. In a mixture of Aroclor 1254 and 1260 for example the chemist using a packed column may easily identify only 1260. The response of 1254 is approximately one-half of the response of 1260, due to the different isomers present. The chemist that mis-identifies an Aroclor component in a mixture and reports total PCB's could be in error as much as 50 to 100 percent. Capillary GC's high resolution capabilities offer a much more reliable analysis of PCB's, without loss of sensitivity. The detection limits for Aroclor 1260 is approximately 50 picograms per microliter. The identification of PCB isomers is becoming very important in many samples because of the problems just mentioned. This can reduce greatly the wide range of errors in reporting. Standards of individual isomers can be obtained that represent each group of the mono to decachloro biphenyls and average response ratios determined for each group. These response ratios are then used to quantify isomers found in a sample. The detection limits for individual isomers vary from approximately 10 to 20 pg/ul for the mono to tri's to less than 1 to 5 pg/ul for the tetra's to deca's.

Figure 2 shows capillary chromatograms of Aroclor 1260 in transformer oil ,5800 ppm (top), and the results of the detoxification , less than 0.5 ppm (bottom). Figure 3 shows another sample which is a mixture of Aroclor 1254 and 1260 at concentrations of 525 ppm and 170 ppm. The bottom section of figure 3 shows that after the detoxification process less than 0.5 ppm total Aroclors are present. Notice that in these examples that other compounds are formed that elute ealier. Utilizing the longer higher resolution analysis would allow futher investigation of those components.

Figure 4 shows the results of the high resolution analysis. Even with this kind of resolution there are still peaks that interfere, as can be seen. The chemist can chose peaks that do not co-elute, and achieve excellent precision and accuracy.

Figure 5 is Aroclor 1254 and 1260 combined, which demonstrates that carefull examination is still necessary for accurate identification.

Figure 6 also demonstrates the necessity of high resolution capillary chromatography. This is an example of a typical raw waste that labs usually see. This contains a mixture of Aroclor 1254, 1260, and many components that are electron capture responsive.

This paper has been reviewed in accordance with the U.S. Environmental Protection Agency peer and adminstrative review policies and approved for presentation and publication.

TABLE 1. **ANALYSIS CONDITIONS**

- GC/Ni63 ECD
- SE-54 Fused Silica Capillary
  30m x 0.25mm
- Carrier: N2 or H2 Make-up: N2
  split flow: 30 mL/min.
- Program Temperature
  screen: 200C to 270C at 4/min
  high resolution: 100C to 270C at 3/min
- Detection Limit: 50pg/uL Arocior 1260

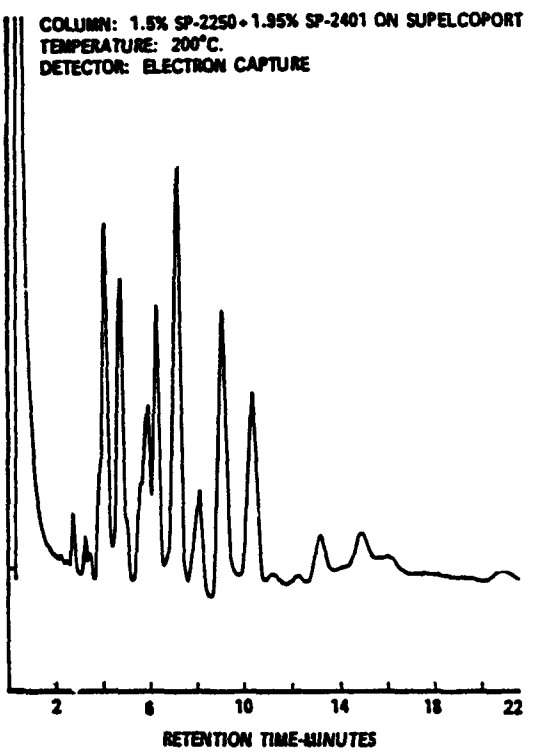

GAS CHROMATOGRAM OF PCB-1254

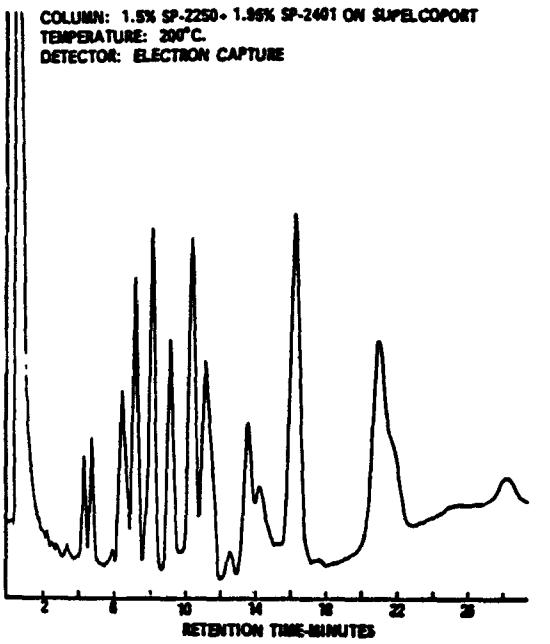

GAS CHROMATOGRAM OF PCB-1260

Figure 1. Packed column analysis.

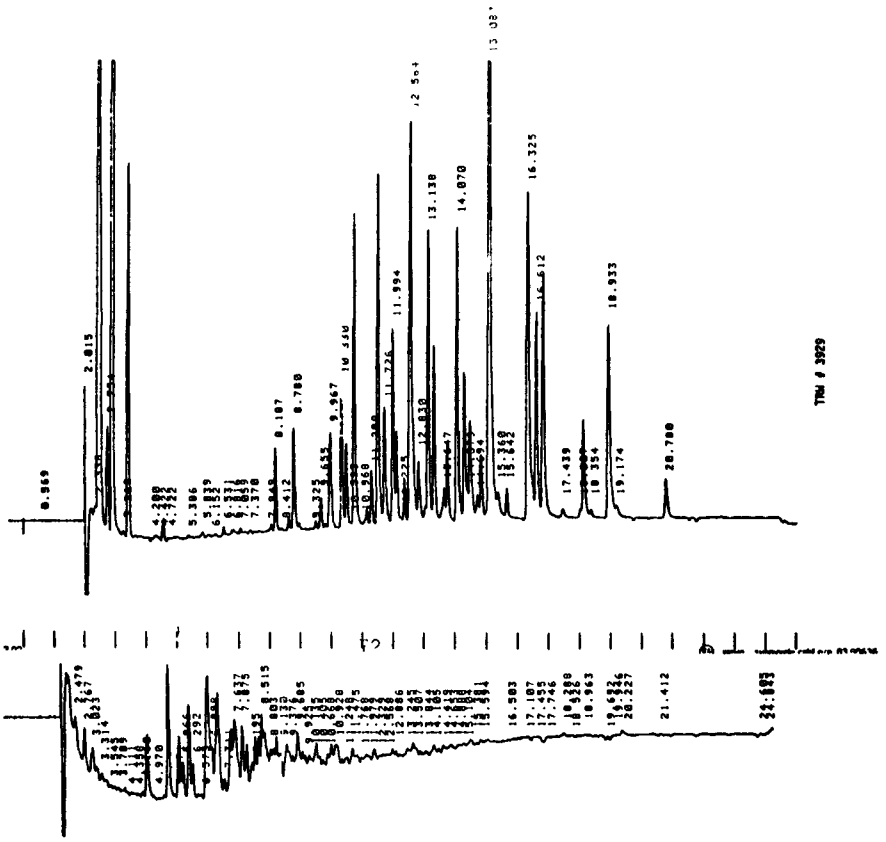

Figure 2. Aroclor 1260, 5800 ppm and <0.5 ppm.

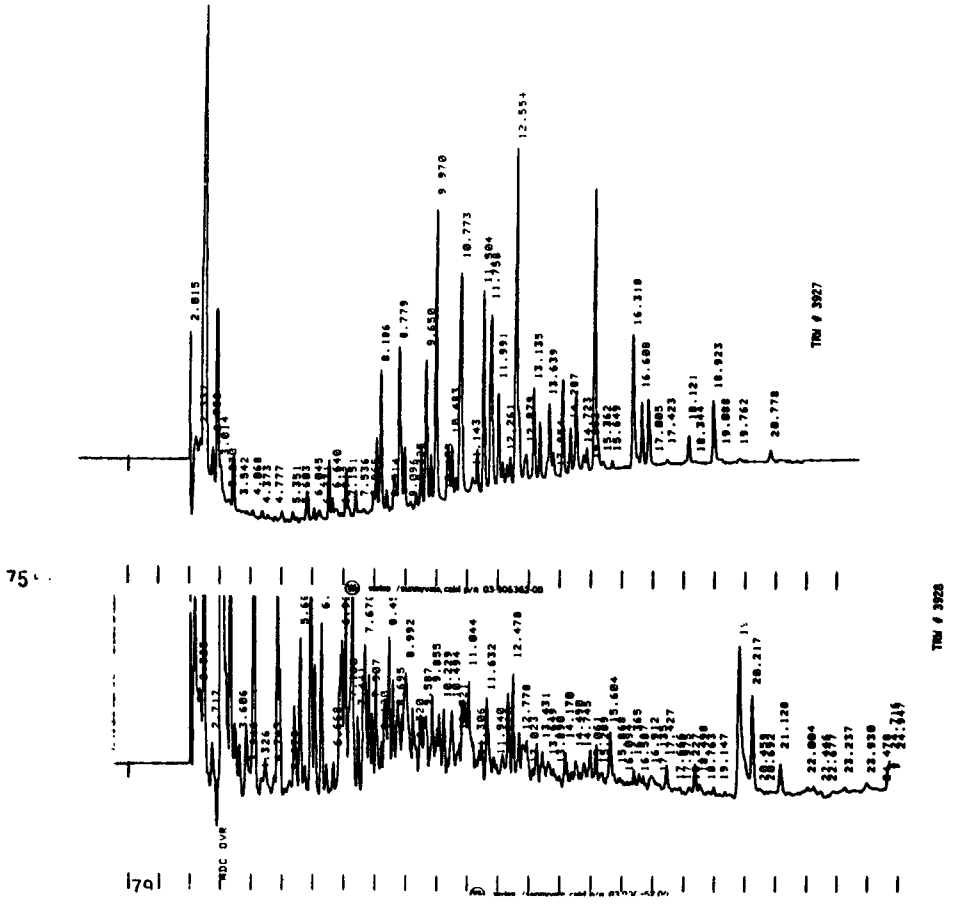

Figure 3. Aroclor 1254 (525 ppm), 1260 (170 ppm) mixture, and <0.5 ppm.

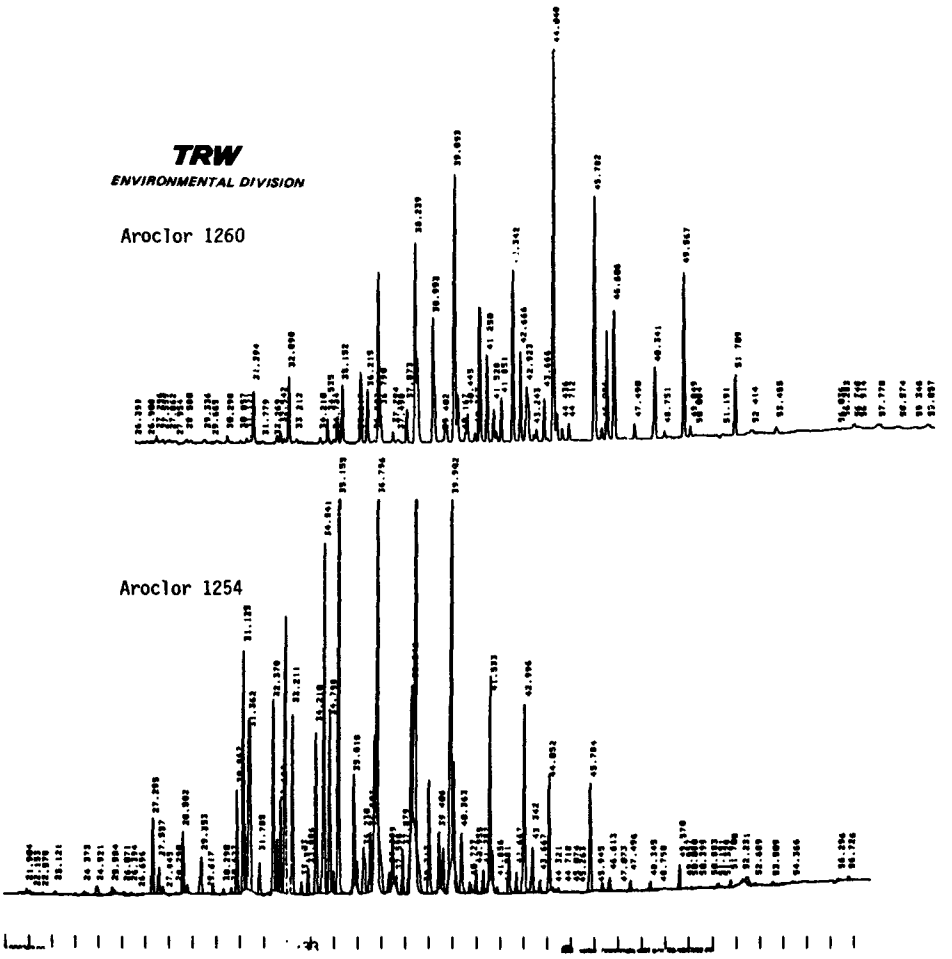

Figure 4. High resolution GC of Aroclor 1254 and 1260.

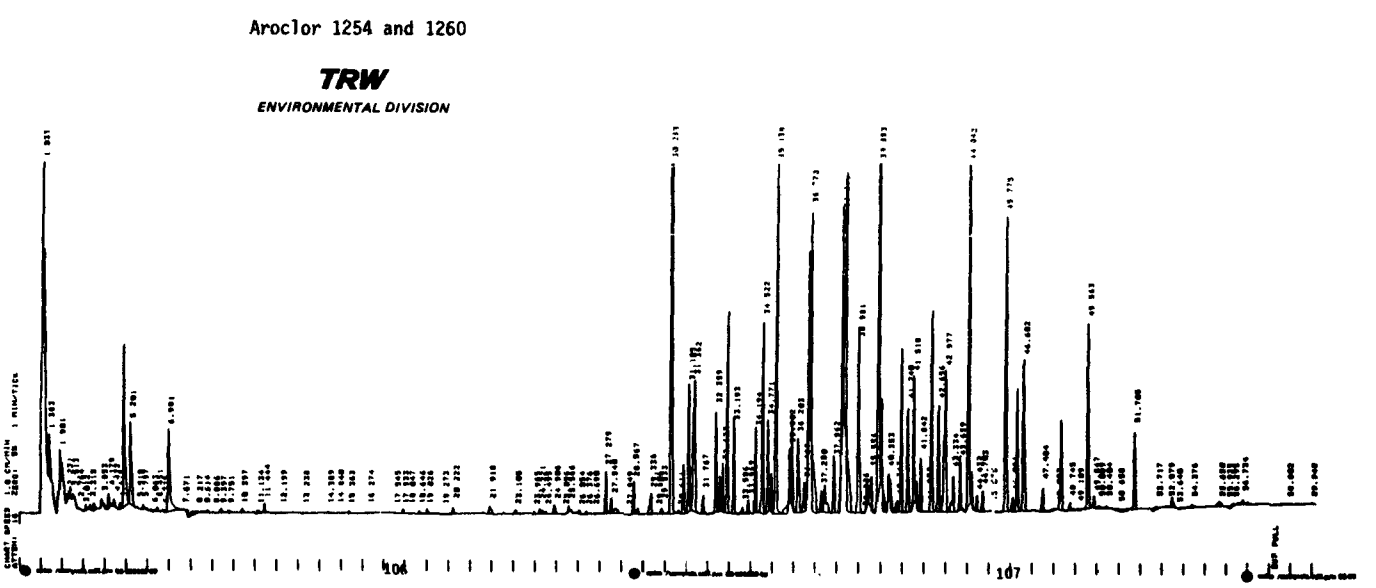

Figure 5. High resolution GC of Aroclor 1254 and 1260 combined.

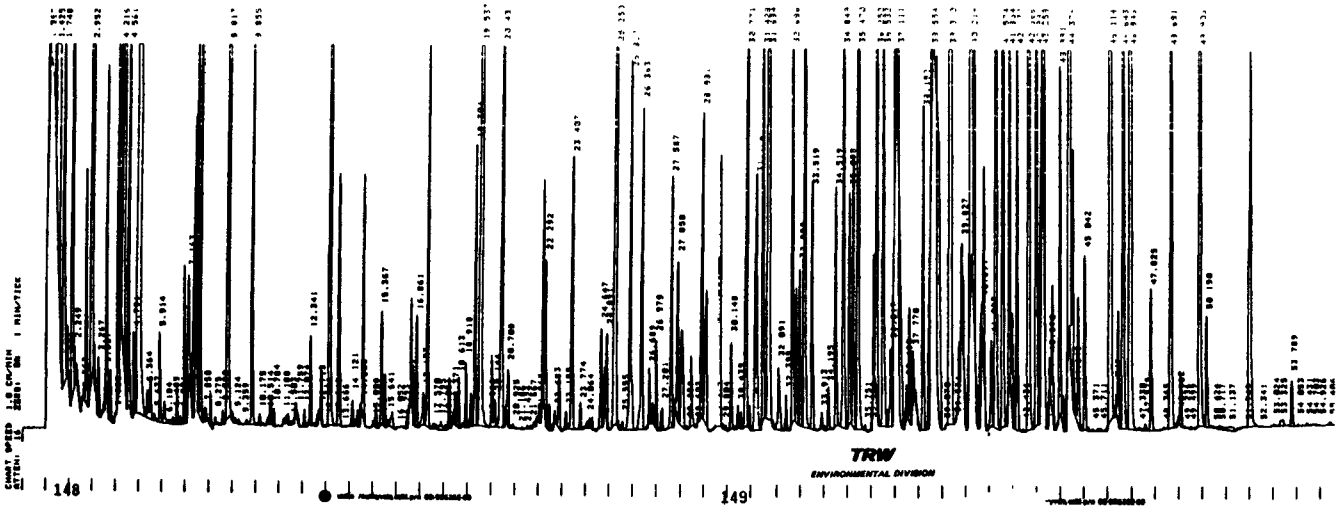

Figure 6. High resolution GC of raw waste sample.

SESSION IV

PERSONAL MONITORING

VALIDATION OF A PASSIVE SAMPLER FOR DETERMINING FORMALDEHYDE IN RESIDENTIAL INDOOR AIR

A.T. Hodgson, K.L. Geisling, J.R. Girman, and B. Remijn

Building Ventilation and Indoor Air Quality Program
Lawrence Berkeley Laboratory
University of California
Berkeley, California 94720

ABSTRACT

A passive sampling device based on the principle of diffusion has been developed specifically for the determination of formaldehyde in residential indoor air. The device, which is inexpensive and easy to use, is capable of measuring one-week time-weighted average concentrations of formaldehyde from as low as 0.018 ppm to over 1 ppm. The sampler was validated by laboratory tests and a field study conducted in occupied residences and an office. The performance of the passive sampler compared favorably to that of the reference pump/bubbler sampler. The evaluated parameters were: sampling rate; quantification limits; relative humidity effects; chemical interferences; storage stability; precision; and accuracy.

The work described in this paper was not funded by the U.S. Environmental Protection Agency and therefore the contents do not necessarily reflect the views of the Agency and no official endorsement should be inferred.

INTRODUCTION

It has recently been demonstrated that relatively low concentrations of formaldehyde (HCHO) in air potentially have adverse health effects[1,2] In addition, it has been shown that significant chronic exposures to

HCHO can occur in residential indoor environments.[3] Sources of HCHO are prevalent in the residential environment since HCHO is used as a component of many construction materials and consumer goods and is a combustion byproduct. Reduction of building air exchange rates for energy conservation has the potential to result in deleterious increases in concentrations of HCHO and other indoor-generated air pollutants. At present, data on HCHO concentrations in the residential environment are severely limited, in part, due to the lack of simple and inexpensive methods to accurately quantify low concentrations of HCHO in air.

Lawrence Berkeley Laboratory (LBL) has developed a passive sampling device based on the principle of diffusion specifically for the determination of HCHO in residential indoor air.[4] The device, which is inexpensive and easy to use, is capable of accurately measuring time-weighted average concentrations of HCHO from as low as 0.018 ppm to over 1 ppm for a period of one week. The one-week sampling period is ideally suited for quantification of chronic HCHO exposures since HCHO concentrations vary with ventilation rate, temperature, humidity, and use of combustion appliances. These, in turn, are largely determined by occupant activities, which typically have a 7-day cyclic pattern.

DESCRIPTION

The HCHO passive sampler is shown in Figure 1. It consists of a glass vial approximately 2 cm in diameter and 9.5 cm in length. A glass fiber filter, treated with a solution of sodium bisulfite and thoroughly dried under vacuum, is positioned in the bottom of the vial. When the sampler is not is use, the vial is sealed with a plastic cap. Formaldehyde is collected by the absorbent through the formation of the

addition product, sodium formaldehyde bisulfite. The specificity of the absorbent for HCHO minimizes chemical interferences. Sample analysis is by water desorption and the spectrophotometric chromatropic acid procedure described in P&CAM No. 125.[5]

The sampler is deployed in residences by taping it out of the reach of small children with the open end down to exclude dust. If the attachment surface is a wall, samplers are taped so the mouth of the sampler extends about 2 cm out from the wall. Samplers are not attached to suspected HCHO emitting sources. Sampling locations near open windows and ventilation openings are also avoided. Replicate samplers are placed at each sampling location and are spaced approximately 2 cm apart.

LABORATORY VALIDATION

Since the diffusion coefficient of HCHO in air is not known, it was necessary to empirically determine sampling rate by exposing the passive samplers to known HCHO concentrations for a period of one week.[4] Test atmospheres at approximately 1 atm, 25 ^{o}C and 30 to 45% relative humidity were produced with a HCHO gas generation/dilution system.[6] The mass of HCHO collected by the samplers is plotted against HCHO exposure in Figure 2. The sampling rate is defined by the slope of the linear regression line. This rate is calculated to be 0.296 μg/ppm-h or 4 cm^3 per minute.

The theoretical detection limit of the method is defined as the HCHO concentration that produces an analytical absorbance that is statistically distinct from the absorbance of the blank. This limit is calcu-

lated to be 0.006 ppm. Since field experience has shown that precision is often considerably reduced at this concentration, we recommend the adoption of a lower quantification limit of 0.018 which is three times the theoretical limit.

The sampler's linearity of response has not been determined for exposures in excess of 168 ppm-h (1 ppm for 168 h). However, the sampler has a large capacity for HCHO, and the upper quantification limit theoretically could be extended to at least 5 ppm for 168 h by sample dilution during analysis.

The precision of the analytical method alone, expressed as a coefficient of variation, was determined to be 3.2% from routine replicate analyses of aqueous HCHO standards on different days. The most realistic estimate of overall precision is obtained from actual field samples. For 15 determinations with 4 or 5 adjacent replicate samplers, the mean coefficient of variation was 6.7%.

The mass of HCHO collected by the sampler is standardized at 1 atm and 25 ^{o}C since the sampling rate was empirically established at these conditions. For kinetic theory, we know that in real gas diffusion processes the mass of a gas collected is a function of the square root of the absolute temperature and is independent of pressure.[7] The temperature dependence is small and can be ignored for most residential applications.

Water vapor is one of the most difficult environmental parameters to accommodate in the design of a passive sampler for HCHO. Sampling rate was determined at 25 ^{o}C with relative humidities ranging from 30 to 45%.

Additional one-week tests were performed at constant, higher relative humidities. Sampling rate as a function of relative humidity is shown in Figure 3. Statistical uncertainty increases with increasing humidity, but, most importantly, sampling rate decreases drastically at relative humidities in excess of 60%. Consequently, the sampler should not be used in high humidity environments. In actual practice, the use of the sampler is only partially restricted by its humidity response. Relative humidities in residences in most parts of the country do not usually exceed an average of 60% in the winter months. In western states, this limit is usually not exceeded at any time during the year.

The known chemical interferences for the chromatropic acid analysis of bubbler samples are considered to be of minor consequence since they are normally present in air at lower concentrations than those of HCHO.[5] The possibility that these compounds would interfere in the analysis of the passive sampler is even more remote since they are not expected to be collected by the sampler. One exception is acrolein, an unsaturated aldehyde which is a component of cigarette smoke. However, no significant difference was observed in the amount of HCHO detected in samplers with and without acrolein spikes when acrolein was in an approximate 10:1 excess of HCHO.

Samplers have been stored for a period of two weeks prior to use without any effect on sampling efficiency; after samples were collected, no HCHO was lost from samplers stored at room temperature for two weeks.[4] These estimates of storage stability are conservative. Although the times are relatively short, they are adequate for residential HCHO surveys.

The laboratory tests were conducted at an apparent linear air velocity of about 1 cm/sec which is near the lowest velocities expected to be found in residences. Attempts to determine if sampling rate varied over a velocity range of 0.5 to 5 cm/sec were inconclusive. Nevertheless, sampling rate should only vary slightly over this range since the sampler has a long diffusion path length.[8]

FIELD COMPARISON

It is virtually impossible to adequately determine the effects of the many probable combinations of environmental parameters on sampler performance in laboratory tests. In addition, the use of relatively small volume exposure chambers can impose unrealistic conditions on these tests. These limitations can be avoided by field testing.

We modified the NIOSH standard method for HCHO in air[5] to collect one-week long samples. Using this technique concurrently with the collection of passive samples, we were able to evaluate the performance of the passive sampler under actual field conditions. Twenty-one individual sampler comparisons were made over a period of three months in a variety of buildings which included new energy-efficient houses, weatherized houses, urea-formaldehyde foam insulated houses, conventional houses, and a prefabricated office. Formaldehyde concentrations at these locations ranged from about 0.03 to 0.15 ppm.

Four replicate bubbler samples were collected at each site with a refrigerated pump/bubbler sampler.[9] This device collects samples by pulling air through two bubblers in series, each containing 15 ml of water. Sample temperature is maintained at approximately 5 ^{o}C. Flow

rates are controlled near 0.14 L/min by hypodermic needle critical orifices and a vacuum pump unit. The ability to maintain low temperatures and constant low flow rates permits the collection of week-long samples. Bubbler samples were also analyzed by the chromatropic acid method. Five passive samplers were deployed at each site. The sample inlet tube for the refrigerator sampler was located approximately 30 cm from the passive samplers. Sampling periods for both devices were concurrent. Bubbler sample flow rates were measured at the beginning and end of the one-week sampling period. Average flow rates, corrected to standard conditions, were used in the concentration calculations. At the termination of the sampling period, passive samplers were capped and bubbler samples were packed in an ice chest. All samples were quickly returned to the laboratory for analysis.

The results of the field comparison are presented in Figure 4. The relationship between the two variables is quantitatively defined by the use of Bartlett's three-group method for regression.[10] This regression technique, rather than the standard linear regression, is appropriate when both variables are subject to measurement error. Inspection of Figure 4 shows that the fit of the data to the regression line is very good. The equation for the regression line indicates the passive sampler concentrations have about a 15% positive bias relative to the bubbler sampler concentrations. A two-way analysis of variance demonstrates that there is a highly significant statistical difference between the two methods.

The bubbler sample method was carefully evaluated to determine if it was the source of the 15% discrepancy. In laboratory exposure tests,

bubbler sample concentrations agreed with concentrations calculated for the test atmosphere from measured diffusion rates. Average concentrations for 7 consecutive 24-h bubbler samples agreed with concentrations of concurrently collected 7-day bubbler samples. Bubblers spiked with HCHO and then bubbled with clean air for 7 days did not lose HCHO.

Nitrates and nitrites are known interferents in the chromatropic acid analysis. They are produced when NO_2 is bubbled through water. The potential for a NO_2 induced interference was examined. Possible error, even assuming worse case conditions for NO_2, was found to be positive and to be no more than about 2%.

The weight of this evidence suggests that the bubbler sample values are correct. We can conclude that the laboratory experimental apparatus does not correctly simulate the real world and has introduced a consistent bias. The regression equation, $Y = 0.87X$, can be used to convert passive sampler concentrations (X) to bubbler sample concentrations (Y).

ACKNOWLEDGEMENT

This work was supported by the Assistant Secretary for Conservation and Renewable Energy, Office of Building Energy Research and Development, Building Systems Division of the U.S. Department of Energy under Contract No. DE-AC03-76SF00098, and by the Bonneville Power Administration, Portland, Oregon 97208.

REFERENCES

1. Gunby, P., 1980, "Fact or fiction about formaldehyde," J. Am. Med. Assoc. 243:1697-1703.

2. Svenberg, J.A., W.D. Kerns, R.I. Mitchell, E.J. Gralla, and K.L. Parkov, 1980, "Indication of squamous cell carcinomas of the rat nasal cavity by inhalation exposure to formaldehyde vapor," Cancer Res. 40:3398-3402.

3. National Research Council, 1981, Indoor Pollutants, National Academy Press, Washington, D.C.

4. Geisling, K.L., M.K. Tashima, J.R. Girman, R.R. Miksch, and S.M. Rappaport, 1982, "A passive sampling device for determining formaldehyde in indoor air," Environ. Int. 8:153-158.

5. National Institute of Occupational Safety and Health, 1977, NIOSH Manual of Analytical Methods, 2nd ed., Publication No. 77-157A, National Institute of Occupational Safety and Health, Cincinnati, OH.

6. Geisling, K.L., R.R. Miksch, and S.M. Rappaport, 1982, "Generation of dry formaldehyde at trace levels by the vapor-phase decomposition of trioxane," Anal. Chem. 54:140-142.

7. Palmes, E.D., A.F. Gunnison, J. DiMattio, and C. Tomczyk, 1976, "Personal sampler for nitrogen dioxide," Am. Ind. Hyg. Assoc. J. 37:570-577.

8. Tompkins, E.C. and R.L. Goldsmith, 1977, "A new personal dosimeter for the monitoring of industrial pollutants," Am. Ind. Hyg. Assoc. J. 38:371-377.

9. Miksch. R.R., D.W. Anthon, L.Z. Fanning, C.D. Hollowell, K. Revzan, and J. Glanville, 1981, "Modified pararosaniline method for the determination of formaldehyde in air," Anal. Chem. 53:2118-2123.

10. Sokal, R.R. and F.J. Rohlf, 1969, Biometry, W.H. Freeman and Company, San Francisco, CA.

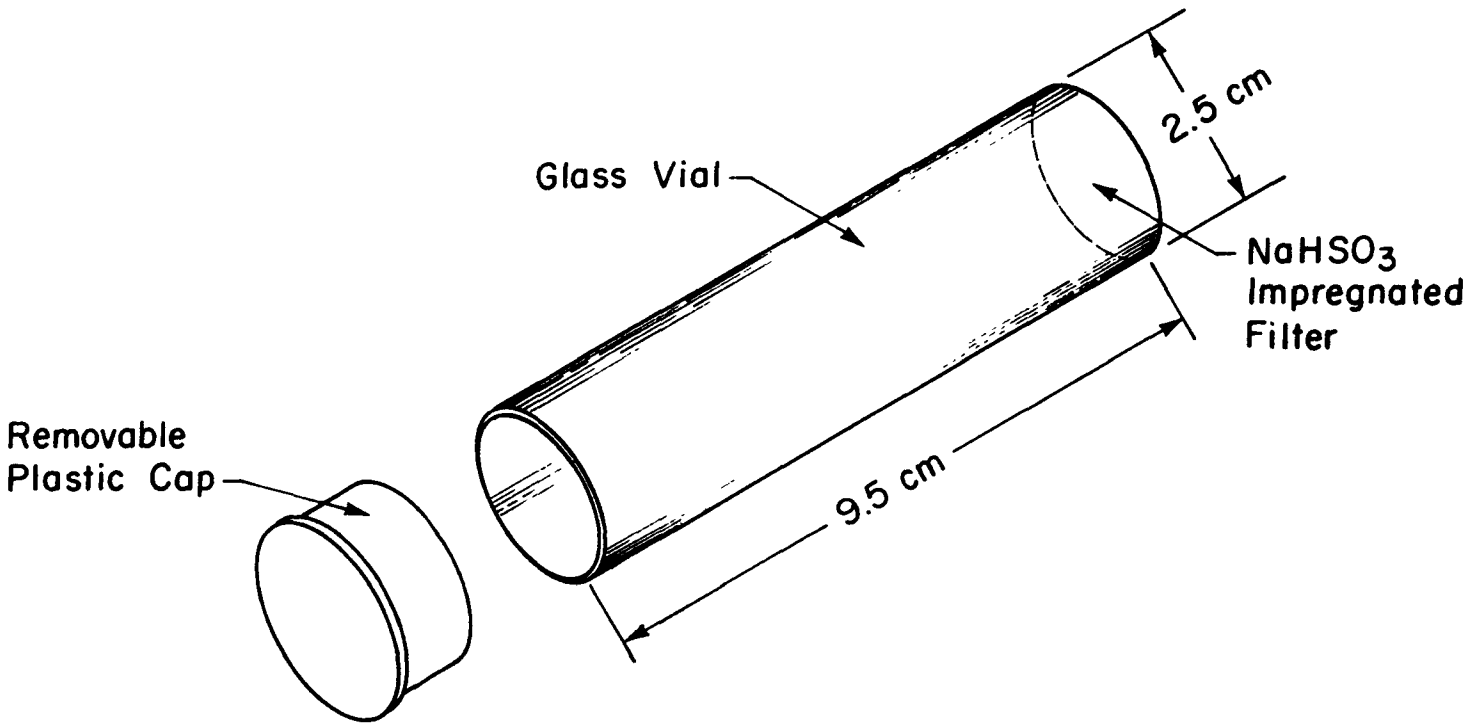

Figure 1. HCHO passive sampler.

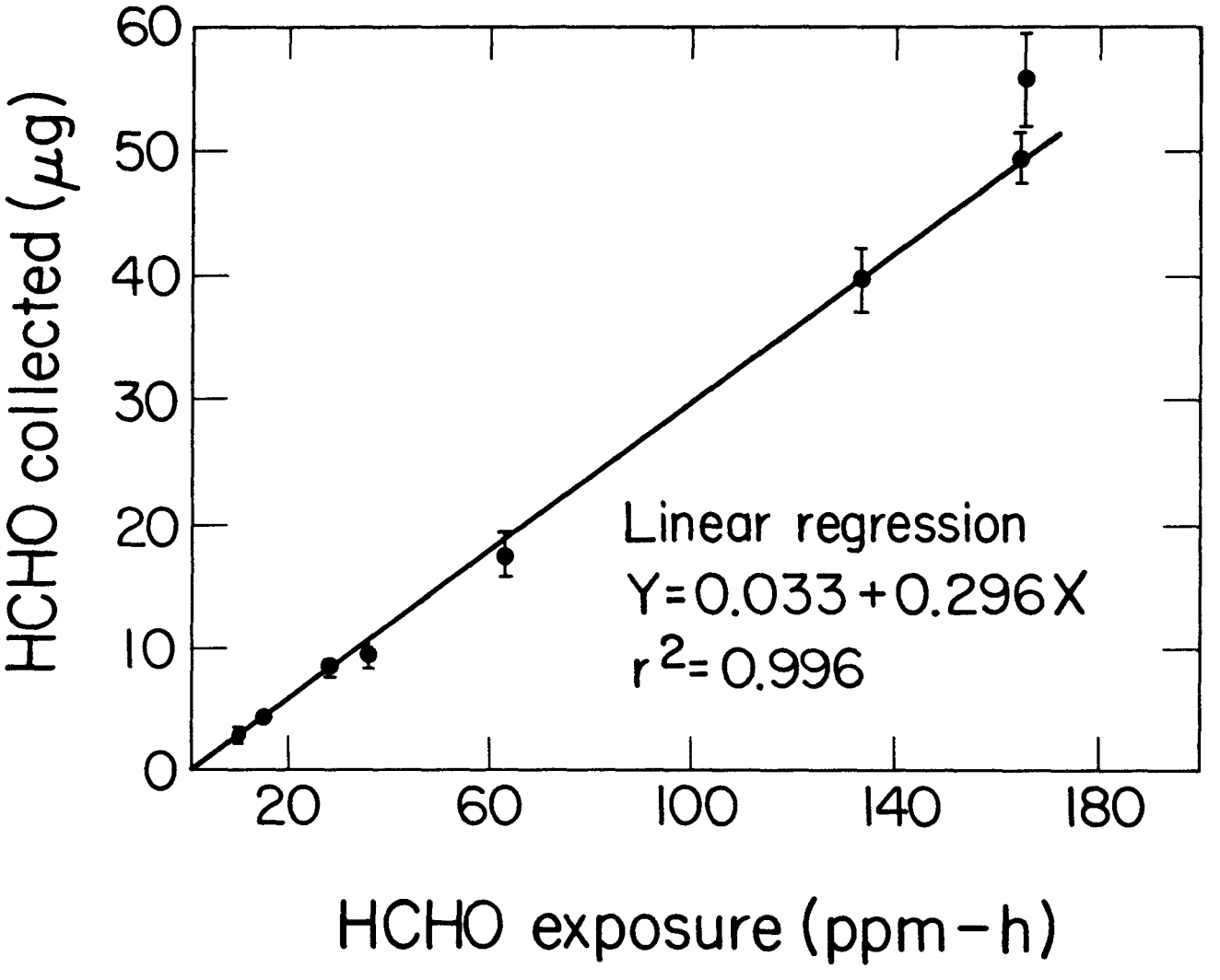

Figure 2. Mass of HCHO collected versus HCHO exposure.

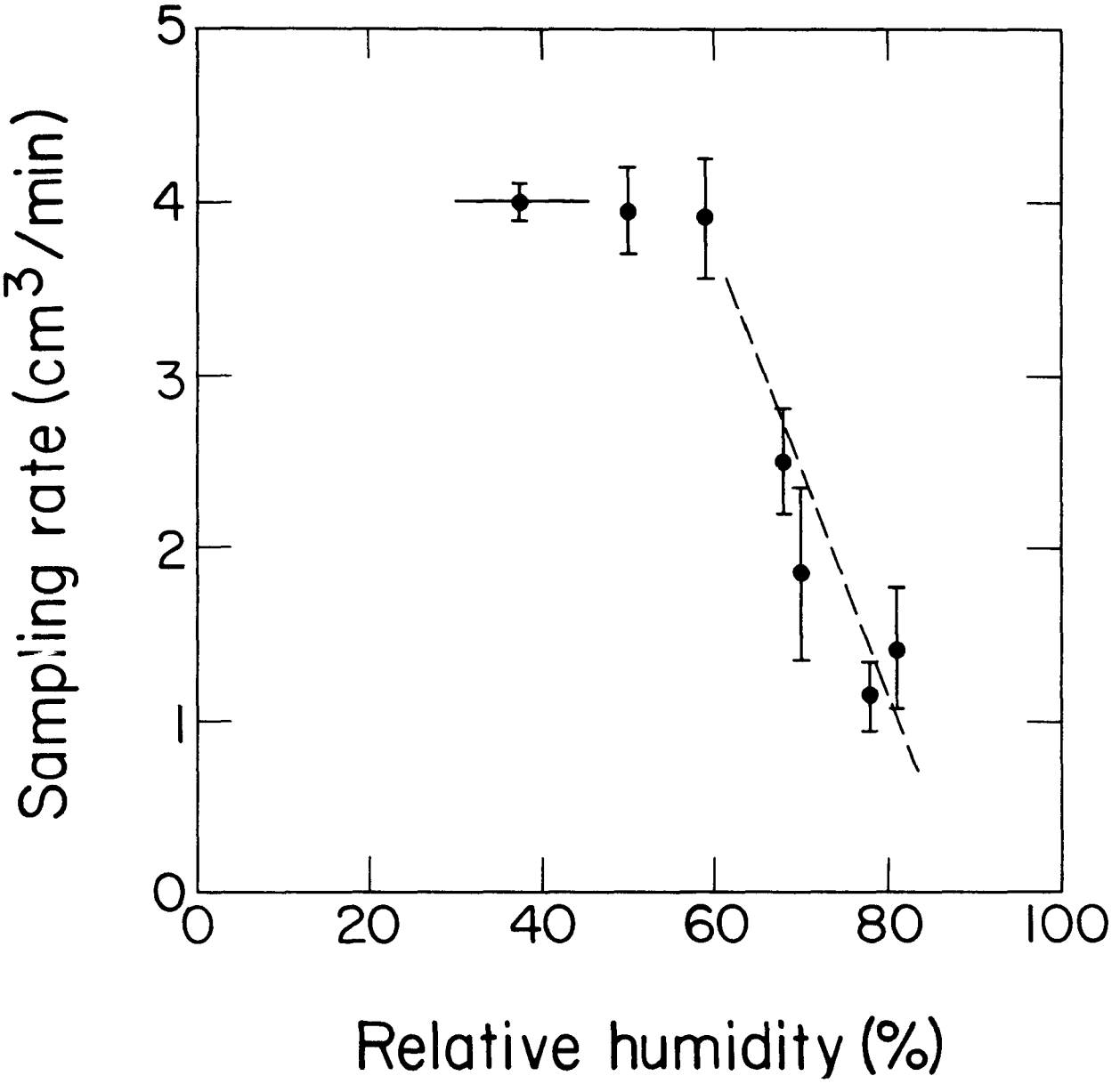

Figure 3. Sampling rate versus relative humidity at 25 °C and 0.25 ppm HCHO.

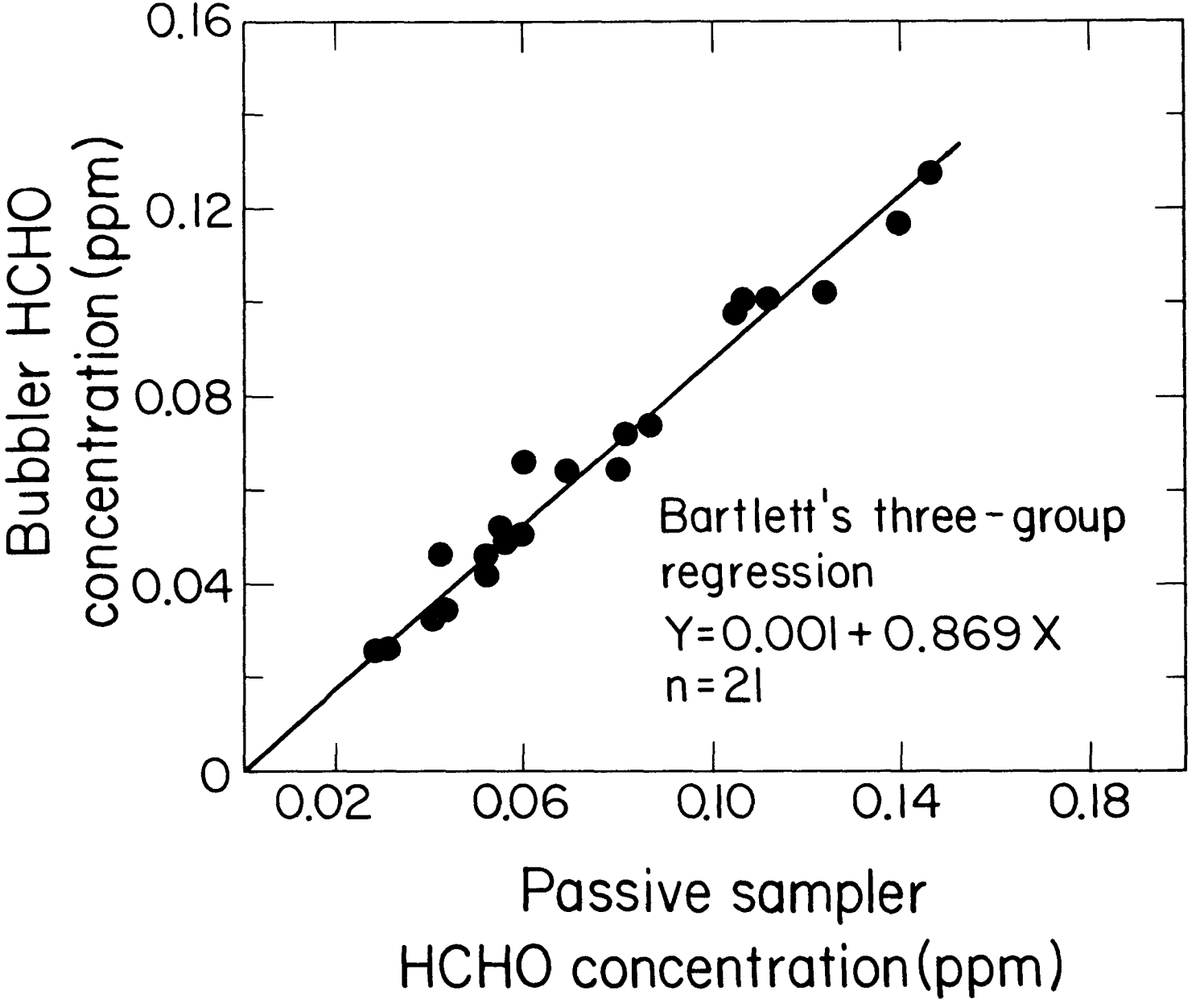

Figure 4. Passive sampler versus pump/bubbler sampler concentrations for 21 field comparisons.

LABORATORY STUDIES OF THE TEMPERATURE DEPENDENCE OF THE PALMES NO_2 PASSIVE SAMPLER

John R. Girman, Alfred T. Hodgson, Brad K. Robison, and Gregory W. Traynor

Building Ventilation and Indoor Air Quality Program
Lawrence Berkeley Laboratory
University of California
Berkeley, CA 94720

ABSTRACT

Passive samplers for air pollution measurement have been used in a variety of applications, e.g., the assessment of personal exposures to pollutants, the determination of area concentrations, and the comparison of indoor and outdoor pollutant concentrations. In some of these applications, samplers have been used under conditions for which they have been inadequately tested. Diffusion theory predicts only a 1.7% change in the sampling rate with a $10^{o}C$ change in temperature at $21^{o}C$; however, triethanolamine, the NO_2 absorbent employed in the Palmes NO_2 sampler, has a liquid-solid phase transition at $21^{o}C$. Because this phase change occurs at a typical ambient temperature, the effect of temperature upon the performance of the sampler was investigated. During this investigation, the NO_2 concentration, exposure time, and face velocity were held constant while the temperature of the sampled air was varied from $7^{o}C$ to $38^{o}C$. The collection efficiency of the Palmes NO_2 passive sampler was found to decrease by 15% when the temperature decreased from $27^{o}C$ to $15^{o}C$. This study illustrates the need for careful evaluations of passive samplers under controlled conditions that closely approximate actual use conditions.

INTRODUCTION

The use of passive samplers for air pollution measurements has become widespread. Passive samplers have been used in a variety of applications, e.g., the assessment of personal exposures to pollutants (1), the determination of area concentrations (2) and the comparison of indoor and outdoor pollutant concentrations (3). In some of these applications, passive samplers have been used under conditions for which they have been inadequately tested.

The Building Ventilation and Indoor Air Quality Group at Lawrence Berkeley Laboratory has used an instrumented mobile laboratory (4), to study indoor air pollution in a variety of residences (3,5-9). These studies provided the opportunity to compare, under field conditions, the performance of the Palmes NO_2 passive sampler (10) with that of an accepted reference method, a chemiluminescent, continuous NO_2 analyzer. One anomaly became apparent during this comparison: agreement was better between the two methods for indoor measurements than for outdoor measurements. One obvious difference between indoor and outdoor conditions was the temperature at which the measurements were taken.

From diffusion theory, we know that temperature effects the sampling rate of a passive sampler. Because diffusion theory predicts only a 1.7% change in the sampling rate with a 10 ^{o}C change in temperature at 21 ^{o}C (10), temperature corrections have generally been ignored. However, the NO_2 absorbent employed in the sampler, triethanolamine (TEA), has a liquid-solid phase transition at 21 ^{o}C (11). Because this phase change occurs at a typical ambient temperature, the effect of temperature on the performance of the NO_2 passive sampler was investigated. We

anticipated one of two possible effects: constant collection efficiencies if the TEA phases have the same response to NO_2; or a step function centered at 21 °C, if their responses differ.

EXPERIMENTAL

The passive sampler test facility employed in these studies is shown schematically in Figure 1. This facility allows for rapid set-up of a wide range of experimental conditions. The gas streams are temperature-preconditioned before entry into either of two temperature-controlled exposure chambers, each of which can hold up to 16 passive samplers. Extensive microprocessor control extends flexibility and allows automatic data logging.

For the temperature dependence tests, experimental conditions were as follows: NO_2 concentrations were either 0.301 ppm or 0.349 ppm at 2 Lpm depending on which of two NO_2 permeation tubes were used; face velocity was 0.25 cm/s; relative humidity was less than 20%; exposure time was 24 h; and temperature was varied from 7 to 38 °C.

For each series of tests, a lot of samplers was prepared. Groups of 16 samplers were exposed to the NO_2 test atmosphere at different temperatures until all samplers from a lot were exposed. All samplers from a lot were analyzed together.

For reasons explained below, an additional test to determine the effect of face velocity was conducted under the following conditions: NO_2 concentration was 0.151 ppm; relative humidity was less than 20%; exposure time was 48 h; temperature was 21 °C; and flow rate through the chamber was varied from 0.25 to 4.5 Lpm to produce apparent linear face

velocities from 0.03 to 0.6 cm/s. Calculated velocities were confirmed by visually timing the progress of injections of "smoke" from Draeger smokesticks. When velocities were below 0.1 cm/s, the flow was well described as plug flow; when velocities were greater than 0.1 cm/s, there was some turbulence and a correspondingly greater uncertainty in face velocities.

RESULTS AND DISCUSSION

The results of the temperature dependence study are illustrated in Figure 2. Each data point represents the mean value of 14 to 16 samplers with a relative standard deviation of the mean of approximately 1%. Each symbol type represents a different lot of samplers with the exception of the open circles and triangles which represent samplers from the same lot. All collection efficiencies were corrected for the temperature effect calculated from diffusion theory.

The NO_2 passive samplers have a storage stability of several months. Nevertheless, we were concerned that differences in the pre-exposure or post-exposure storage time (a single series of tests lasted up to twelve days) could introduce a small systematic bias which might diminish our ability to detect temperature effects.

To check for this bias, 16 samplers from a lot, represented by the open triangles in Figure 2, were exposed at successive temperatures from 7 ^{o}C to 38 ^{o}C. Next, 16 samplers from the same lot, represented by open circles, were exposed to successively decreasing temperatures from 38 ^{o}C to 7 ^{o}C. This same ordering was maintained during analysis. As is evident in Figure 2, no bias with respect to order of either exposure or

analysis was found.

While the data shows some scatter and some minor variation among sampler lots, the collection efficiency is fairly constant below 15 ^{o}C, averaging 82%, and then gradually rises to approximately 96% at temperatures above 27 ^{o}C. The overall change in collection efficiency from 15 to 27 ^{o}C is approximately 15% or 1% per degree C.

The temperature response occurred gradually over a larger temperature range than anticipated. TEA as actually used in the sampler, i.e., contaminated with residual acetone used as a solvent in sampler preparation, was found to melt over a wide range, 16 to 21 ^{o}C. This may, in part, account for the range of the sampler's temperature response. However, since TEA is hydroscopic, in humid atmospheres the liquid range of TEA may be extended, diminishing any temperature effects.

(The cause of the variation in collection efficiency with phase is unknown. If it is due to the kinetics of absorption, the possibility exists that the sampling rate is concentration dependent at low temperatures.)

The measured collection efficiency at 21 ^{o}C, 87%, is lower than the efficiencies, 92 to 95%, reported or calculated from data in other reports (12-14). Since precision in our study was typically better than 1%, possible systematic causes for the discrepancy in collection efficiency were examined. The mass-flow controlled, permeation tube oven which serves as the NO_2 source was calibrated by an independent laboratory; the measured NO_2 permeation rate agreed with the manufacturer's rate to within 1%. Sampler preparation was checked by preparing and

sending samplers to researchers at the Agricultural University, Wageningen, the Netherlands. They exposed our samplers simultaneously with samplers they had prepared. Agreement was better than 4% between the two sets of samplers (15). Using our facility, we exposed samplers prepared by Columbia University and then returned half of the samplers to them for analysis. Collection efficiency of these samplers was 88% (16).

Having eliminated the NO_2 source, sampler preparation and analysis as causes of the discrepancy, we next examined the effect of low face velocities. When face velocities are low, convective transport in the volume just external to the sampler opening is no longer very large with respect to diffusive transport. In effect the concentration in this volume becomes depleted of the pollutant being sampled and is no longer representative of the larger volume to be characterized. This condition, sampler starvation, was examined theoretically by Tompkins and Goldsmith (17).

The results of our preliminary study of the effects of low face velocity are illustrated in Figure 3. Each of the four points represents the mean of 16 samplers. The solid line is the solution of the Tompkins and Goldsmith equation for the NO_2 passive sampler. While the results do not definitively prove the theory, they tend to support it, especially for plug flow conditions.

Because adequate instrumentation for measuring low air velocities is presently lacking, these velocities in residences are not well known. However, typical air velocities in residences are expected to be smaller than velocities encountered in industrial or outdoor environments. Air velocities were measured in 20 houses by Oak Ridge National Laboratory

(18). All houses were closed and the air conditioner fans were turned on to circulate air without cooling. Measurements were made by timing the movement of puffs of "smoke" from Draeger smokesticks. Most velocities were between 5 and 10 cm/s, though extremes of 1 cm/s and 20 cm/s were not infrequent. Since these measurements were made with mechanical fans circulating the air, it is possible that even lower air velocities often occur in house interiors.

Using Tompkins and Goldsmith's equation, correction for the theoretical sampling efficiencies caused by the low face velocities can be applied to the results of the temperature dependence study to obtain the results shown in Figure 4. When this correction is applied, the collection efficiency at 21 ^{o}C is 95%, in agreement with results of other researchers. At temperatures about 27 ^{o}C, the collection efficiency is greater than 100%. Possible causes of this could include the uncertainty in the theoretically-derived diffusion coefficient of NO_2 in air used to calculate the sampling rate (10) or a systematic bias of the experiment.

CONCLUSIONS

This study illustrates that even simple devices such as passive samplers have the potential for error if not adequately evaluated for actual use conditions. We have measured a temperature dependence of the Palmes NO_2 passive sampler of 1% per ^{o}C over the temperature range of 15 to 27 ^{o}C. The overall variation of 15% is not large for a device with an accuracy of approximately 10%. However depending upon the resolution of the study, corrections for the variation with respect to temperature should be taken into account when comparing indoor and outdoor NO_2

concentrations and, in certain cases, when comparing concentrations in different rooms of the same house, since e.g., bedrooms and kitchens are often at different temperatures. Because people have elevated surface temperatures relative to their surroundings, temperature corrections may also be warranted in comparisons of personal and area concentrations.

One factor for which we cannot establish appropriate test conditions is face velocity. At present we do not know the range of typical air velocities in residential environments. Without this knowledge the potential exists for deploying passive samplers, especially industrial hygiene samplers with high sampling rates, under conditions where sampler starvation can occur.

ACKNOWLEDGEMENTS

The work described in this paper was not funded by the U.S. Environmental Protection Agency and, therefore, the contents do not necessarily reflect the views of the Agency and no official endorsement should be inferred. This work was supported by the Assistant Secretary for Conservation and Renewable Energy, Office of Building Energy Research and Development, Building Systems Division of the U.S. Department of Energy under Contract No. DE-AC03-76SF00098. We also acknowledge the contributions of J.R. Allen and P. Persoff.

REFERENCES

1. Dockery, D.W., Spengler, J.D., Reed, M.P., and Ware, J. Relationships among personal, indoor and outdoor NO_2 measurements. Environ. Int.5:101, 1981.

2. Melia, R.J.W., du V. Flores, C., Darby, S.C., Palmes, E.D., and Goldstein, B.D. Differences in NO_2 levels in kitchens with gas or electric cookers. Atmos. Environ.12:1279, 1978.

3. Offermann, F.J., Hollowell, C.D., Nazaroff, W.W., Roseme, G.D., and Rizzuto, J.E. Low infiltration housing in Rochester, New York: a study of air-exchange rates and indoor air quality. Environ. Int. 8:435, 1982.

4. Berk, J.V., Hollowell, C.D., Lin, C., and Pepper, J.H. Design of a mobile laboratory for ventilation studies and indoor air pollution monitoring. LBL-7817 Rev. Lawrence Berkeley Laboratory, Berkeley, CA, 1978.

5. Berk, J.V., Hollowell, C.D., Lin., C., and Young. R.A. Indoor air quality measurements in energy efficient buildings. LBL-8894 Rev. Lawrence Berkeley Laboratory, Berkeley, CA, 1980.

6. Berk, J.V., Hollowell, C.D., Pepper, J.H., and Young. R.A. The impact of reduced ventilation on indoor air quality on residential buildings. LBL-10527. Lawrence Berkeley Laboratory, Berkeley, CA, 1980.

7. Berk, J.V., Young, R.A., Brown, S.R., and Hollowell, C.D. Impact of energy-conserving retrofits on indoor air quality in residential housing. LBL-12189. Lawrence Berkeley Laboratory, Berkeley, CA, 1981.

8. Berk, J.V., Breen, M., Brown, S., Ko, I., Koonce, J., Loo, B., Pepper, J., Robb, A., Strong, P., Turiel, I., and Young, R. Field

monitoring of indoor air quality. In: Energy and Environment Division Annual Report 1980, LBL-11985, Lawrence Berkeley Laboratory, Berkeley, CA, 1981.

9. Young, R.A., Berk. J.V., Brown. S.R., and Hollowell, C.D. Energy-conserving retrofits and indoor air quality in residential housing. LBL-12847. Lawrence Berkeley Laboratory, Berkeley, CA, 1982.

10. Palmes, E.D., Gunnison, A.F., Di Mattio, J., and Tomczyk, C. Personal sampler for nitrogen dioxide. Am. Ind. Hyg. Assoc. J. 37:570, 1976.

11. Weast, R.C. (ed.) Handbook of Chemistry and Physics. 55th Ed., Chemical Rubber Co., Cleveland, Ohio, 1974, p. C-104.

12. Cadoff, B.C., Knox, S.F., and Hodgeson, J.A. Personal exposure samplers for nitrogen dioxide. NBS Draft Report to the EPA on FY-79 Activities, Washington, D.C., 1979.

13. McMahon, R., Klingner, T., Ferber, B., and Schnakenberg, G. New technology for personal sampling of NO and NO_x in the workplace. MDA-M-FS-4. MDA Scientific, Glenview, IL, 1980.

14. Woebkenberg, M.L. A comparison of three passive personal sampling methods for NO_2. Am. Ind. Hyg. Assoc. J.3:1553, 1982.

15. Boleij, J.S.M., Department of Environmental Science, Agricultural University, Wageningen, the Netherlands, personal communication, January 1983.

16. Andrews, L.R., School of Public Health, Columbia University, New York, NY, personal communication, March 1983.

17. Tompkins, Jr., F.C., and Goldsmith, R.L. A new personal dosimeter for the monitoring of industrial pollutants. Am. Ind. Hyg. Assoc. J.38:371, 1977.

18. Gammage, R.B., Health and Safety Research Division, Oak Ridge National Laboratory, Oak Ridge, TN, personal communication, April 1983.

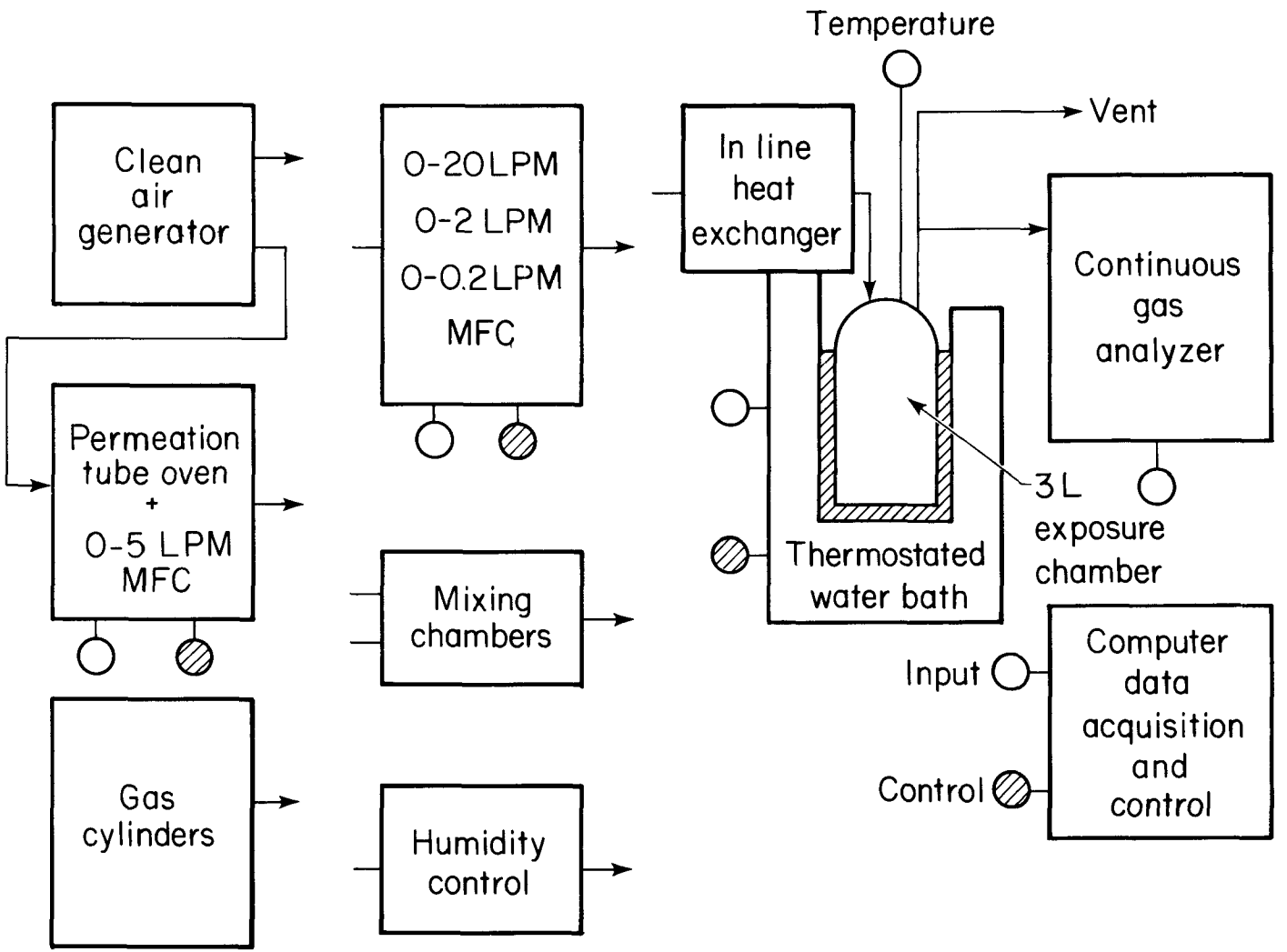

Figure 1. The passive sampler test facility is composed of modular components which are connected with teflon tubing and quick-disconnect couplings. (XBL 834-1567)

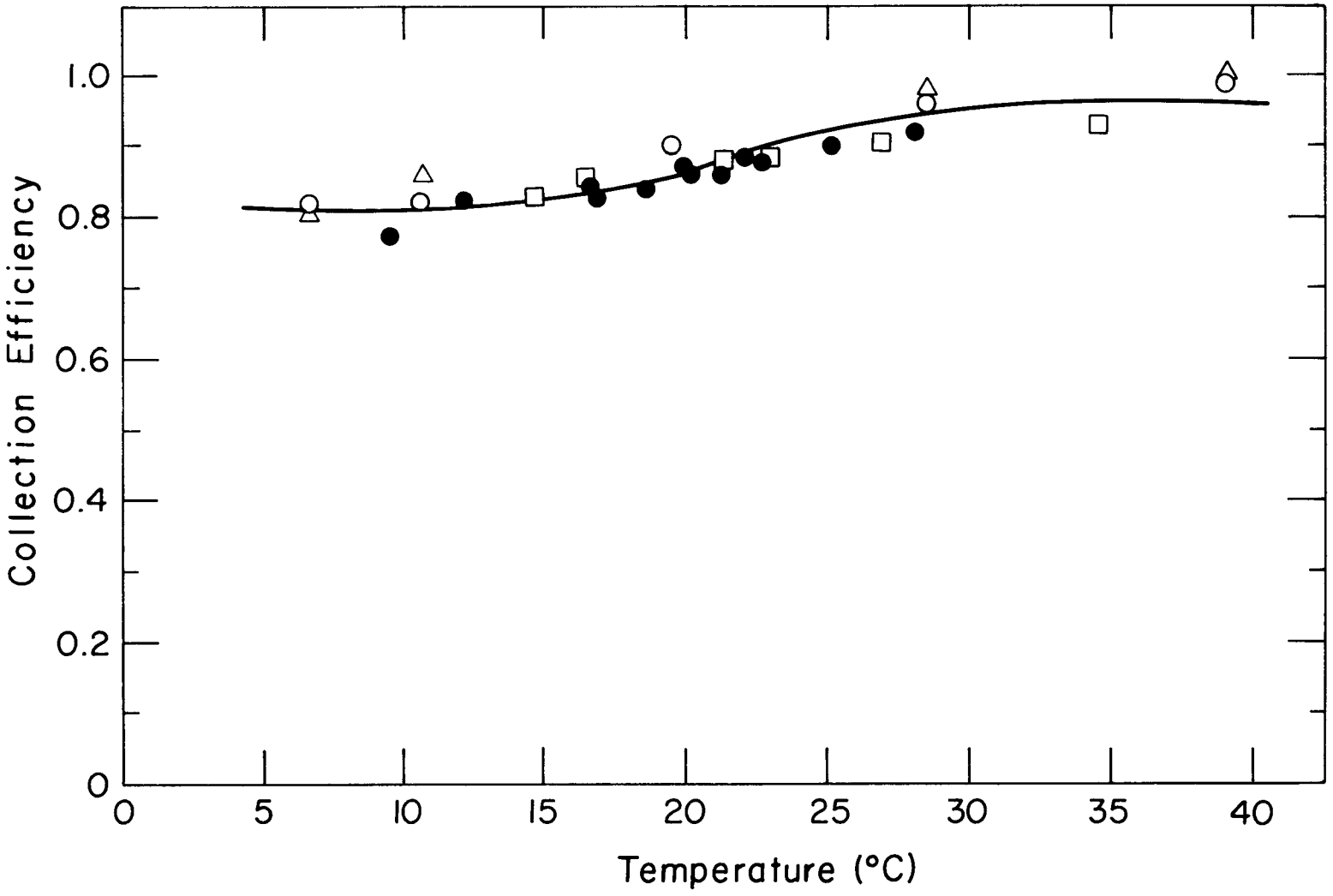

Figure 2. Measured collection efficiencies of the Palmes NO_2 passive sampler versus temperature. Efficiencies are corrected for theoretical temperature dependence. See text for explanation of symbols and experimental conditions. (XBL 828-1078)

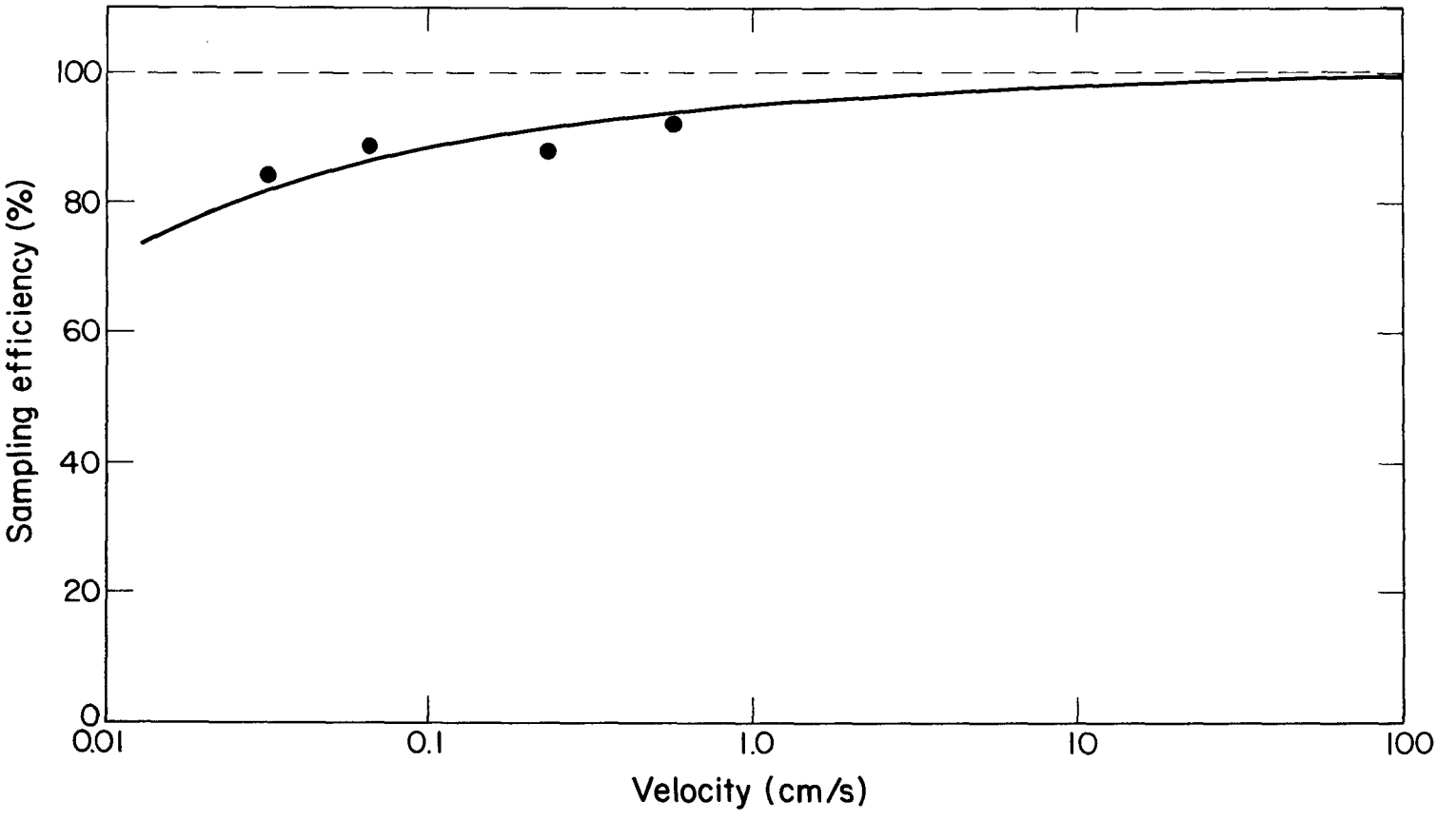

Figure 3. Theoretical and measured sampling efficiency of the Palmes NO_2 passive sampler versus face velocity. See text for explanation of symbols and experimental conditions. (XBL 834-1569)

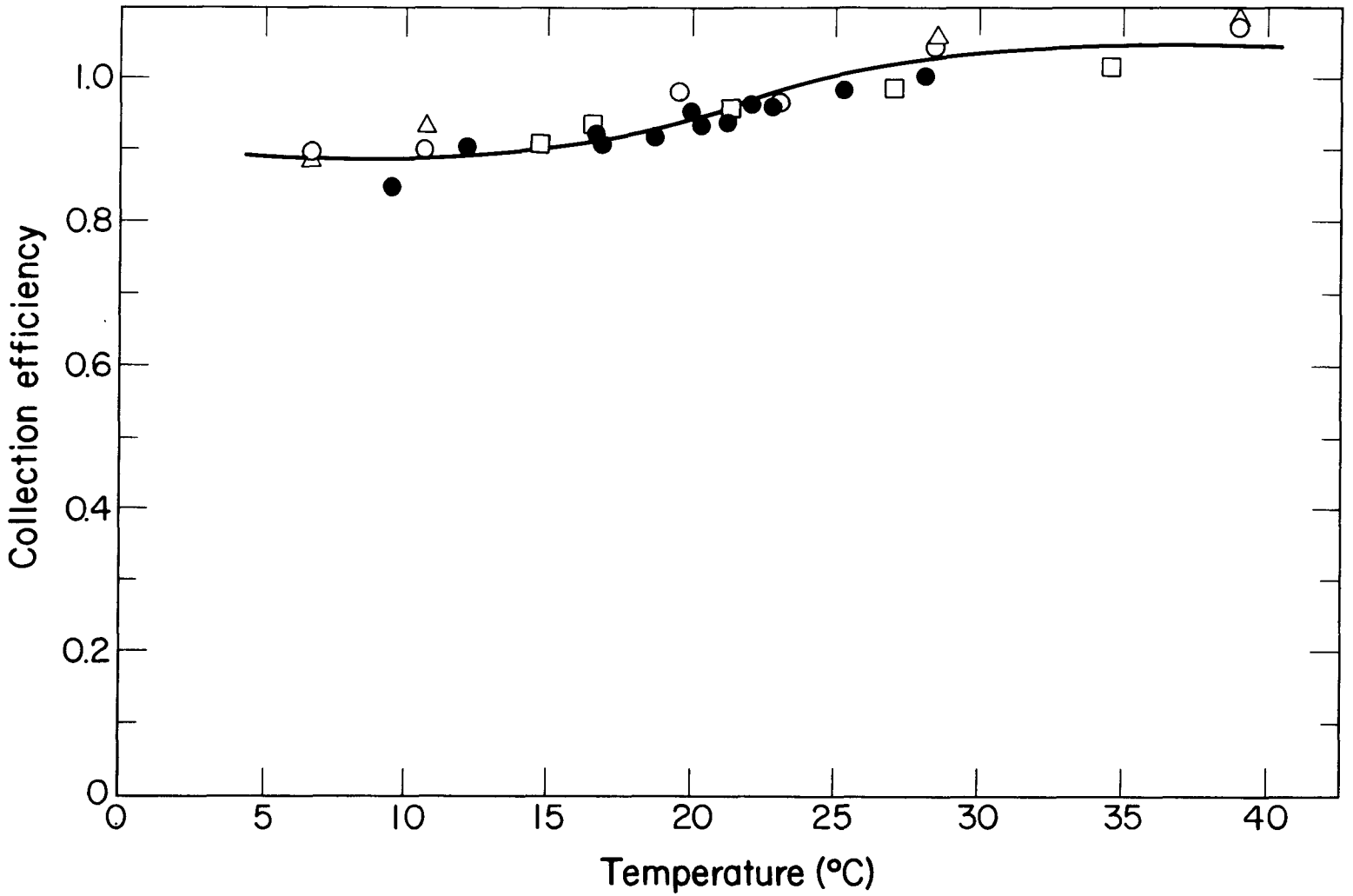

Figure 4. Collection efficiencies versus temperature of the Palmes NO_2 passive sampler after correction for face velocity effects. Efficiencies are also corrected for the theoretical temperature dependence. See text for explanation of symbols.

(XBL 834-1570)

Title: NIOSH-DEVELOPED SYSTEMS FOR MONITORING EQUIPMENT EVALUATIONS

Authors: Mary Lynn Woebkenberg and W. James Woodfin

National Institute for Occupational Safety and Health
Division of Physical Sciences and Engineering
4676 Columbia Parkway
Cincinnati, Ohio 45226

The National Institute for Occupational Safety and Health (NIOSH) has an active program in the evaluation of workplace monitoring devices and personnel exposure monitors. In addition, NIOSH frequently writes evaluation criteria, performance specifications and testing protocols for instruments and monitors. Specialized systems are sometimes needed to carry out the exacting experimentation required for both the evaluations and to demonstrate the efficacy of developed specifications and protocols. This paper will describe a specialized system consisting of a gas and vapor generation system with programmed automatic cyclic output, a recirculating exposure chamber and a multiple, variable sampler. The generation system can use vapor pressure, syringe injection, permeation/diffusion tubes or gas cylinders as the contaminant source while automatically repeating a preprogrammed generation cycle over a time period from a few minutes to several days. The exposure chamber, with a 1 M^3 internal volume, can house portable instruments as well as personal monitors (e.g. sorbent tubes and passive monitors) for evaluations. Six paired samplers allow up to twelve samples of equal or variable time and contaminant loading to be obtained on the multi-sampler. This total system can be used for the generation and sampling of complex atmospheres down to the sub-parts-per-million range.

Introduction

The National Institute for Occupational Safety and Health (NIOSH) has an active program in the evaluation of workplace monitoring devices and personnel exposure devices. In addition, NIOSH frequently writes evaluation criteria, performance specifications, and testing protocols for instruments and monitors. Specialized systems are sometimes needed to carry out the exacting experimentation required for both the evaluations and to demonstrate the efficacy of developed specifications and protocols. One of these specialized systems consists of a programmable automatic cyclic output controller for gas and vapor generation systems, a recirculating exposure chamber and a multiple, variable sampler. This paper will discuss the three components of this system and show data obtained from this system.

Programmable Automatic Cyclic Output Controller (PACOC)

The programmable automatic cyclic output controller system (Figure 1) consists of a dynamic generation system (e.g. vapor pressure, syringe injection, permeation tube or cylinder dilution) generating at a constant rate. The generation system is coupled with a modified mass flow controller (Teledyne, Hastings-Raydist) and interfaced with a time-based programmable signal generator (Data-Trak Model 5310). The final output of the generation system can be controlled over a range of concentrations with the concentration versus time profile being reproduced at preset intervals (from 1 minute to 6 days) assuming constant temperature and pressure.

In actual practice, the operator must know both the needed amount and the desired concentrations of the contaminant of interest. From this information, the operator chooses an appropriate generation system. The PACOC has mass flow controllers (identical except for the flow rate of the meters) on both the contaminant stream and the dilution air stream allowing the operator to vary the flow of either stream. Variation of the stream is accomplished by by-passing one flow meter potentiometer and substituting

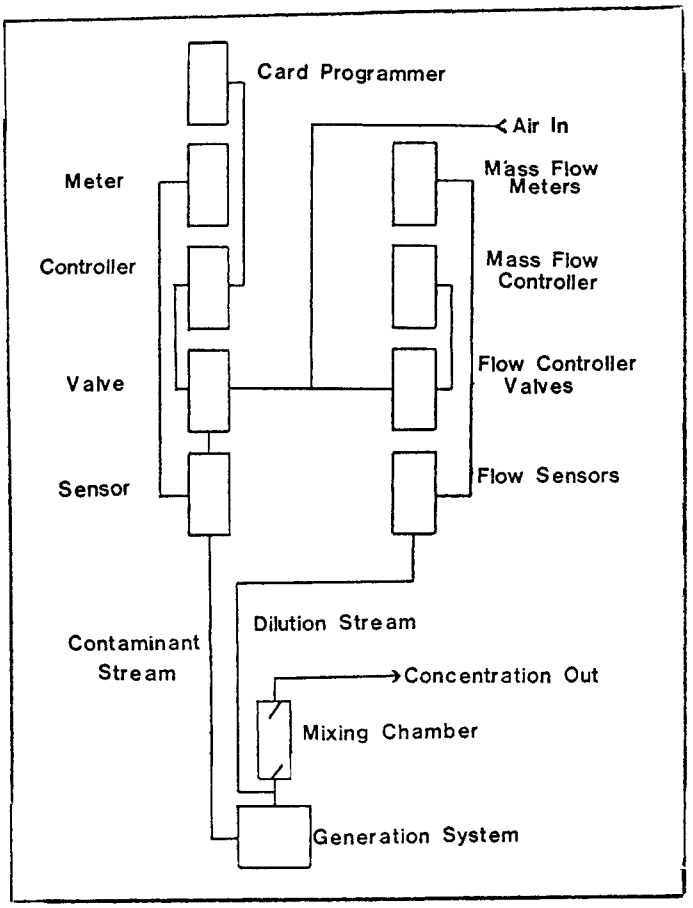

Figurel. Schematic diagram of Programmable Auotmatic Controller (PACOC)

for it the output signal from the signal generator. The signal generator provides an output signal compatible with the full scale input of the flow controller. The signal generator is regulated by a program manually etched onto a card where the abscissa represents time and the ordinate represents percent full scale output to the flow controller valve.

For example, let us assume an operator is generating toluene vapor by the vapor pressure method, that he chooses to control the dilution air and that he wants concentrations ranging from 100 ppm to 1200 ppm over a specified time period. A card as shown in Figure 2 would give such tracings. As the cycle began, the concentration of toluene was 100 ppm increasing to 1200 ppm midway through the cycle. Figures 3 and 4 show the monitored results of this experiment. Figure 3 is three repeats of the cycle with the output from the generation system measured by a continuous flame ionization detector while Figure 4 is three repeats of the same with the output measured by gas chromatography with a gas sampling valve and a flame ionization detector.

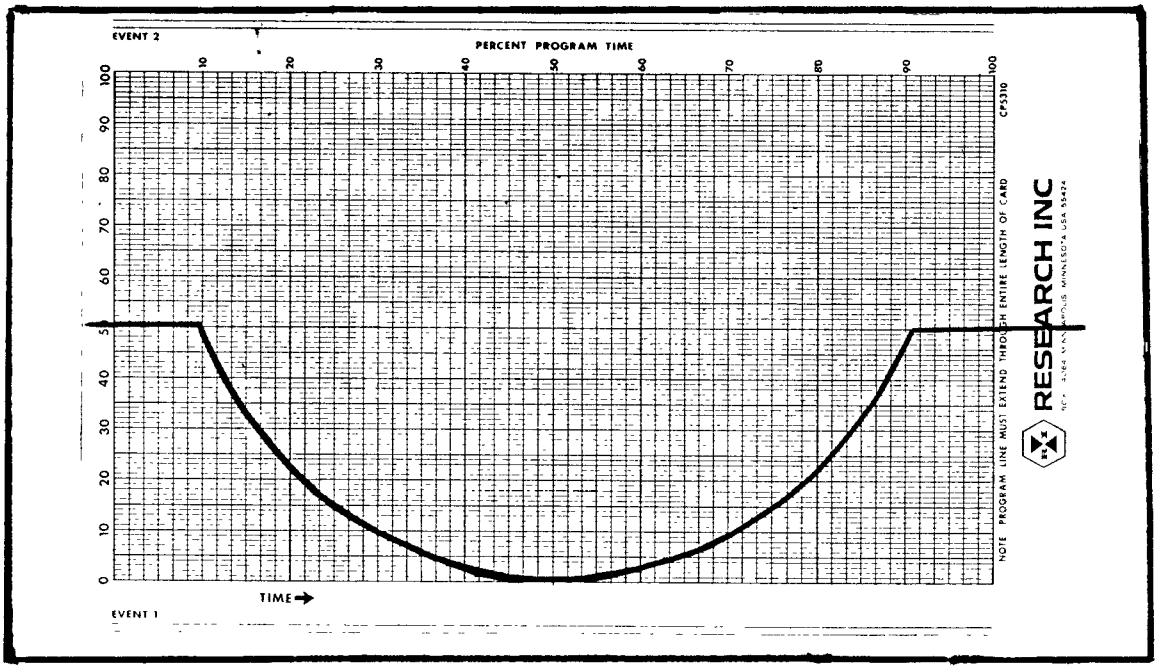

Figure 2. Sample card program for PACOC. Time 100% = 30 minutes.

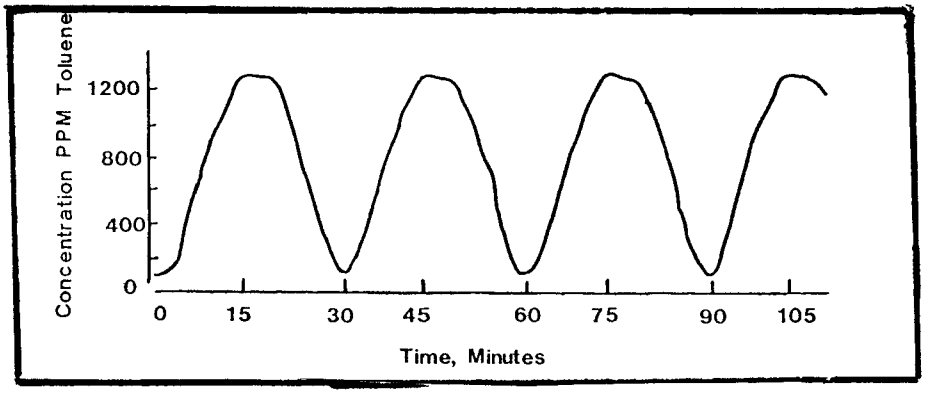

Figure 3. Continuous FID trace of PACOC-controlled toluene generation.

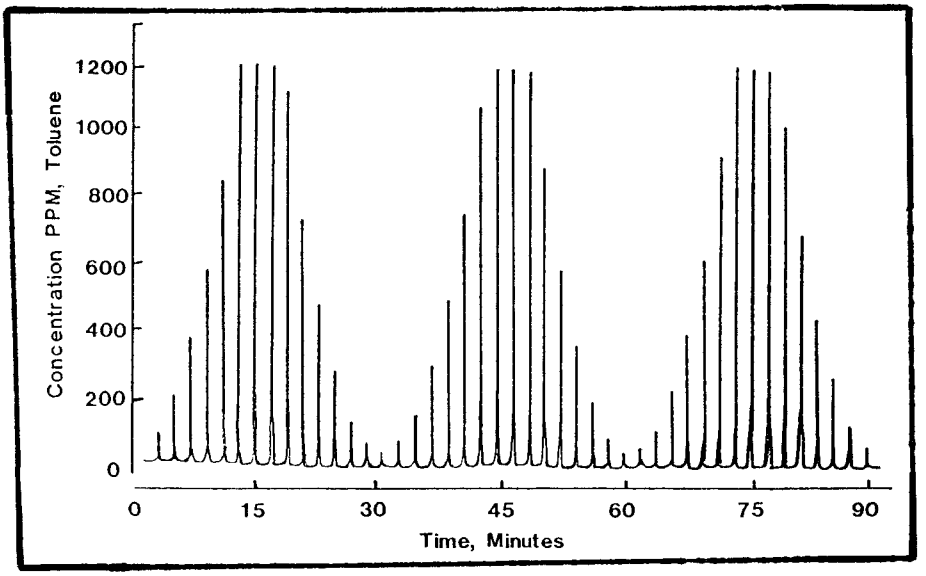

Figure 4. Gas chromatographic tracing of PACOC-controlled toluene generation.

Recirculating Exposure Chamber (REC)

For evaluations of instruments or evaluations of large numbers of monitors, the effluent from the PACOC can be directed into a recirculating exposure chamber, as shown in Figure 5. The chamber has an internal exposure volume of 1 m^3 and features:

* a recirculating stream to reduce required quantities of reagents necessary to establish and maintain desired contaminant concentrations.

* turbulence barriers to insure homogeneous mixing of exposure atmosphere components.

* "honeycomb" flow straighteners.

* glove-ports to allow access to on-going experimentation without perturbing the exposure system.

* access points for measuring individual face velocities or the complete Pitot tube traverse.

* continuous monitoring of exposure chamber temperature and relative humidity.

* access ports for external instrumental monitoring of chamber contaminant concentration.

* variable mounts for exposure devices: a multi-holed flatbed plate for instruments or a removable grid-design drawer for passive monitors, sorbent tubes and impingers. Sample pump connections may be made internally or external to the chamber.

* a dampered blower system to allow variation in the overall flowrate.

The Division of Physical Sciences and Engineering now has three such chambers; the one shown in this presentation, an externally insulated chamber for performance of non-ambient temperature experimentation and a Teflon /Teflon-coated chamber for experimentation with highly reactive species such as formaldehyde.

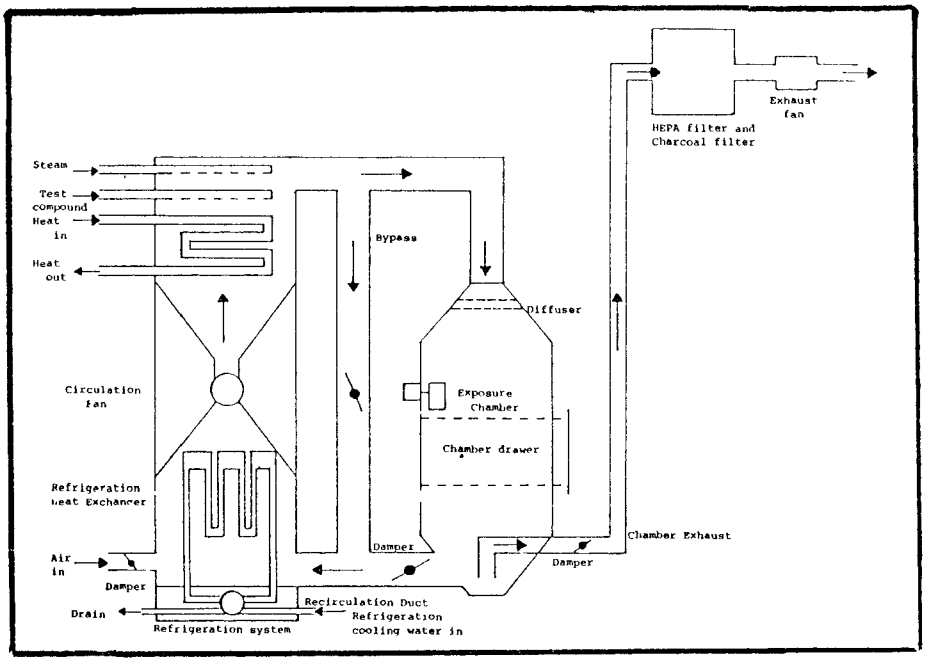

Figure 5. Schematic drawing of Recirculating Exposure Chamber (REC).

Multiple Variable Sampler (MVS)

The third component of this system, serving to complement the PACOC and the REC is a multiple, variable sampler. The MVS consists of six pairs of sampling ports all pulled by a single vaccuum pump. This allows the operator to take 12 identical samples, up to six pairs of samples or a variety of concurrent, different time duration samples. Each member of the pair in a given sampling port consists of the sample holder/inlet, a needle valve, an access for measuring pressure drop and an on/off toggle valve. The samples are paired by matching the impedence across the samples through the use of the needle valve. Needle valves were chosen over critical orifices to allow for portability of the MVS and render it useful for field work. The true utility of the MVS is seen in the following example: Assume three charcoal tube samples of the same atmosphere are to be taken concurrently but for different total time durations: 15 minutes, 30 minutes, and 60 minutes. Sample pairs 1, 2, and 3, as depicted in Figure 6, can be used. The charcoal tubes can be placed in port A of pair 1, 2, and 3 with port B of each pair left empty. With the charcoal tubes in place, the impedence across each pair of sample ports is matched using the needle valves of the empty ports to compensate for the pressure drop of the charcoal tubes. Once the impedences are matched, sampling is begun by opening the valves to allow flow through the charcoal tubes but not through the empty sampling ports. After 15 minutes (the time duration of the first

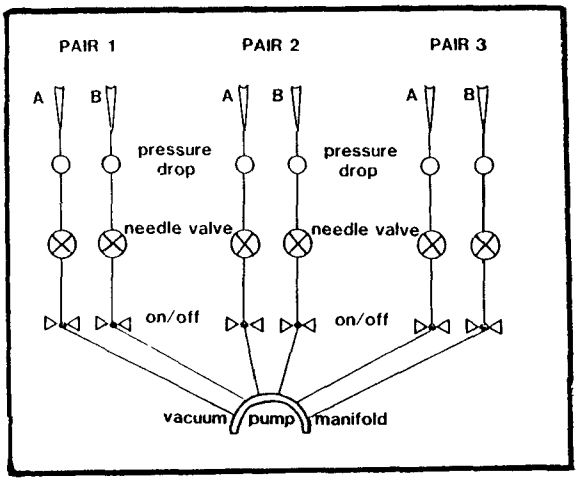

Figure 6. Schematic of three of six sample pairs of the Multiple Variable Sampler (MVS).

sample), sampling through one charcoal tube (port A, pair 1) is truncated concurrently with the start of sampling through the empty side of pair 1 (port B). After thirty minutes, the same simultaneous start/stop is performed on pair 2, ports A and B, and after sixty minutes the same is done with pair 3. In this manner all required samples are obtained during the time it would have taken to obtain just the one hour sample.

The total system: PACOC, REC and MVS required 2 person-months for construction and another four months for testing. The total materials cost did not exceed $10,000 and the trio is now routinely used.

Data

The total system is useful over a full range of experimental conditions and contaminant concentrations. To date, the system has been most widely used for carbon monoxide, toluene, and trichloroethylene. The following data, generated using this system, is offered for your consideration. In a New York City field study, a trace (see Figure 7) of carbon monoxide was obtained using an Ecolyzer 2000 and a strip chart recorder. To simulate this type of exposure in the laboratory, a program card was etched as shown in Figure 8. The resultant CO generation profile, obtained from cylinder gas diluted with house air and monitored with the Ecolyzer 2000, is shown in Figure 9.

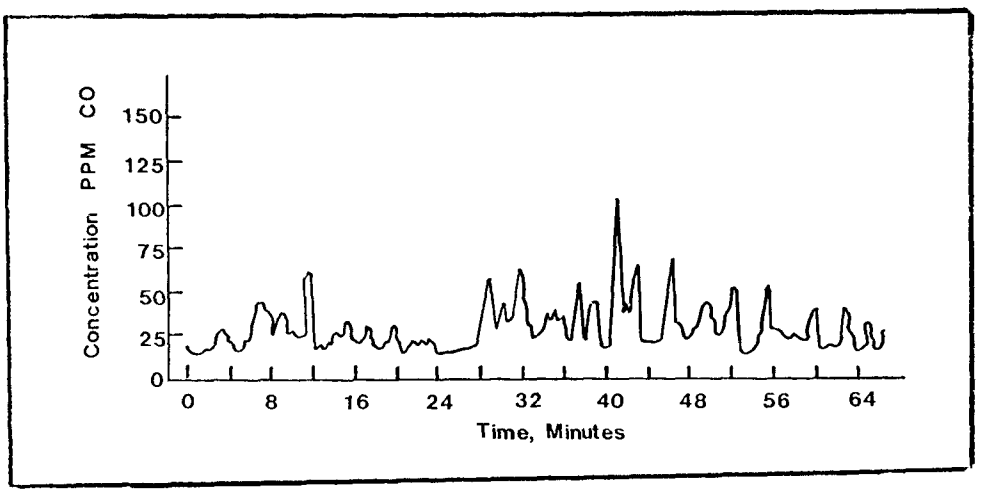

Figure 7. Carbon monoxide concentrations measured in New York City.

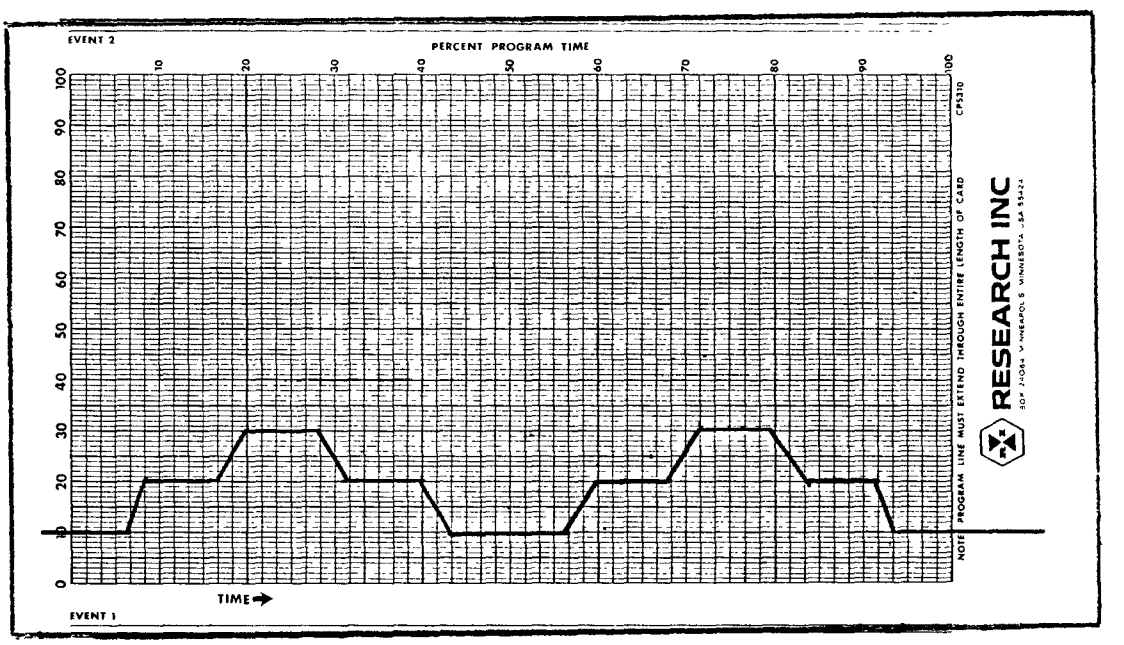

Figure 8. PACOC card program to simulate field CO concentrations.

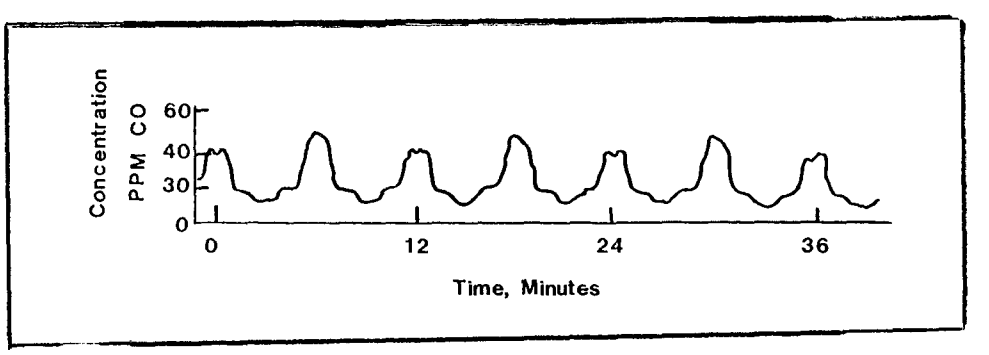

Figure 9. PACOC-controlled carbon monoxide concentrations.

The final series of figures also involve CO generation but they serve to illustrate the effect of running the program over two different time intervals. Figure 10 in this series is the program card. Figure 11 is three replicates of the program, each taking 6 minutes and Figure 12 shows the effect of doubling the time interval to 12 minutes.

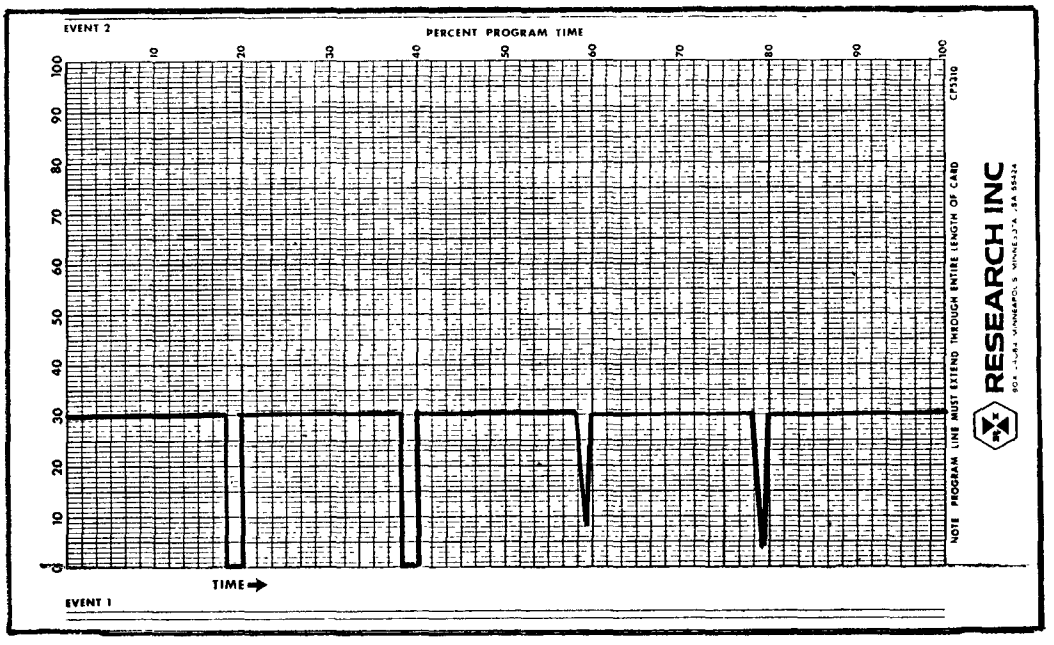

Figure 10. PACOC card program for time interval study.

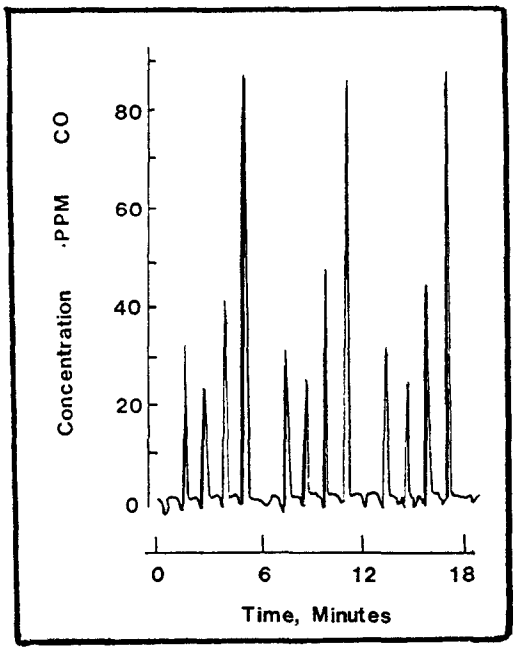

Figure 11. Gas chromatographic trace of 6-minute cycle.

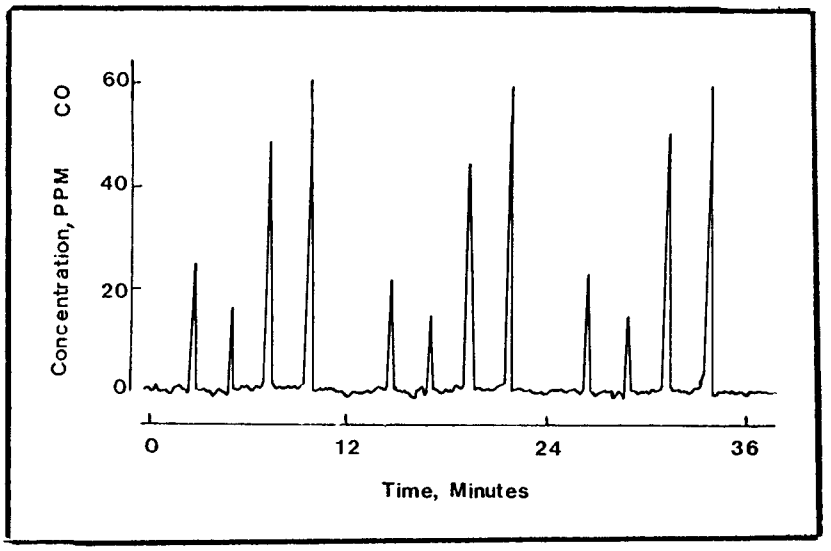

Figure 12. Gas chromatographic trace of 12-minute cycle.

Summary

The system described in this paper represents a highly versatile laboratory exposure/generation capability. Now in routine use, the system is currently being used in evaluation of portable gas chromatographs.

The work described in this paper was not funded by the U.S. Environmental Protection Agency and therefore the contents do not necessarily reflect the views of the Agency and no official endorsement should be inferred.

RELATIONSHIPS OF MEASURED NO_2 CONCENTRATIONS AT DISCRETE SAMPLING LOCATIONS IN RESIDENCES

R. Letz [1], D.P. Miller [2] and J.D. Spengler [1]
[1] Department of Environmental Science and Physiology

Harvard School of Public Health
Boston, MA 02115

[2] Department of Chemistry
Washburn University
Topeka, KS 66621

INTRODUCTION

The results presented in this paper are part of a larger ongoing study of the relationship between air pollution and pulmonary health conducted by the Harvard School of Public (1). An earlier study in Portage, Wisconsin (2) measured the nitrogen dioxide (NO_2) concentration over a one year period in a large number of homes. NO_2 concentrations inside homes with gas cooking stoves were much higher than NO_2 concentrations both outdoors and inside homes with electric cooking stoves. The current study, with a design similar to the Wisconsin project, sought to develop a data base in Topeka, Kansas. The specific objectives were to provide data for the purpose of comparison, and also to improve the understanding of how home characteristics and seasonal factors influence indoor NO_2 concentrations.

FIELD SAMPLING

Homes were selected from a list of over 1500 children participating in the Harvard Air Pollution Health Study. Families were solicited from the list at random, until seventy gas-cooking and seventy electric-cooking homes were enlisted. A team then visited each home, discussed the details of the program, and selected suitable locations for the placement of the NO_2 samplers. Thereafter, the NO_2 samplers were sent and returned by mail.

Each home was sampled in three locations, the kitchen, the bedroom of the child participating in the Harvard Study, and outside the house on the north side. Each home was sampled eight times for a period of one year, two times in each season. Each sample was collected for a one-week period. Kitchen samplers were placed approximately 10 feet from the stove and 4 to 6 feet above the floor. Both kitchen and bedroom samplers were kept away from vents, windows, and doorways

and obvious stagnant zones. Replicate samplers were taped together before sending, and participants recorded the dates and times the samplers were uncapped and recapped. Each sampler had a permanently marked unique serial number and all data were referenced to that number.

LABORATORY METHODS

Passive diffusion tubes (3) were used to collect 168 hour integrated concentrations of NO_2. Stainless steel screens, located at the closed end of a 7.1 cm long cylindrical acrylic (.95 cm inside diameter) were coated with a collecting medium (triethanolamine). A concentration gradient of NO_2 developed between the open end of the tube and the screens during exposure to the ambient air. Fick's First Law was used to calculate the average ambient concentration of NO_2. These diffusion tubes have been independently evaluated by the National Bureau of Standards (4), Warren Springs Laboratory (5), and Lawrence Berkeley Laboratory (6). In the Wisconsin study (2) the precision of the samplers was less than 2 $\mu g/m^3$.

The samplers were prepared in batches, and the replicates and blanks were selected randomly from each batch. After exposure, each batch was analyzed all at one time. A Perkin-Elmer Model 552 Spectrophotometer was used. A calibration curve prepared from stock sodium nitrite solutions and spanning the range of zero to one absorbance units was run first. A three point calibration check was run after every tenth sample. The data, including the home site identifier, sampler location identifier, tube serial number, dates and times of uncapping and recapping, and absorbances, were entered into a computer data file. The calibration curve for each batch was calculated using a linear least squares fit through the origin (7), and the absorbances for each batch were converted to nanomoles of NO_2 collected. The average amount of NO_2 in the blanks of the respective batch was subtracted, and using the exposure time and the tube parameters, the average

concentration of NO_2 at the collection site was calculated. Recent work by Girman, *et al.* (8), indicates that over normal temperature ranges and low air movement, collection efficiencies may range from .85 to 1.0. All measurements were standardized to unit absorption efficiency. No corrections for temperature, humidity, and ambient air movement were applied.

RESULTS

Table 1 gives the observed mean NO_2 concentration at the three locations in the homes with electric stoves and with gas stoves. In homes with electric stoves, the mean NO_2 concentrations were very similar at the two indoor locations, and the indoor levels were lower than the mean levels at the outdoor location. These values are low when compared with the mean values for homes with gas cooking stoves, given in Table 1. The mean indoor levels were four times the levels found in the electric stove homes. The mean outdoor NO_2 levels for both the gas and electric cooking homes were essentially identical. In homes with gas cooking stoves, the mean concentration in the kitchen was almost twice the concentration found in the child's bedroom, and almost four times the concentration found outdoors.

The mean NO_2 concentrations (in $\mu g/m^3$) at the three locations for all the homes with electric cooking stoves are plotted as a function of the month of the year in Figure 1. There was very little variation throughout the year. Note that the outdoor concentration was always higher than the kitchen concentration, which was higher than the bedroom concentration. This pattern in the means was evident in virtually every set of samples for every home with a gas cooking stove.

The pattern in Figure 1 can be contrasted with Figure 2, in which the corresponding monthly average NO_2 concentration for homes with gas cooking stoves are presented. The outdoor levels were fairly constant throughout the year,

but the levels at the two indoor locations both varied seasonally. Figure 2 also shows that in gas cooking homes, the NO_2 levels in the kitchen were always greater than the mean levels in the bedroom for all months of the year. This was the same trend found in the overall mean mentioned above. The monthly variation shows the bedroom concentration remained slightly more than half the kitchen concentration.

Annual average NO_2 concentrations were calculated for each home having five or more valid samples for the eight sampling periods. Summary statistics for these annual averages are presented in Table 2. The maxima of kitchen and bedroom concentrations were close to the mean values and indicate that in spite of other NO_2 sources within these homes, e.g., gas water heaters, gas furnaces, gas clothes dryers, the NO_2 levels were relatively uniform in homes with electric cooking stoves. The large standard deviations and maxima for kitchen and bedroom concentrations inside homes with gas cooking stoves indicates a flat distribution skewed to the right. The distributions of annual average NO_2 concentrations are presented in Figure 3. Note that there is almost no overlap between the two distributions. Figure 4 is a plot of the annual average kitchen NO_2 level versus the annual average outdoor level for homes with gas and electric cooking stoves. The indoor and outdoor levels were not well correlated, and a similar scatter plot of the mean bedroom levels versus the mean outdoor levels (not shown) exhibited even less correlation.

Correlation matrices of the annual average NO_2 concentrations in the three locations within the home are presented separately for homes with gas and electric cooking stoves in Table 3. Consider the homes with electric cooking stove first. The correlation between the outdoor level and the bedroom level was low, indicating little penetration of NO_2 from the outside air. The correlation between kitchen and outdoor levels was between the bedroom-kitchen and bedroom-outdoor

correlations, which indicates that more NO_2 penetrated from the outdoor air into the kitchen than into the bedroom. The correlation between kitchen and bedroom in homes with gas stoves was quite strong. The gas stove appeared to be a major source of NO_2 within these homes, and the NO_2 did reach the bedroom from mixing of the air within the house, though, as mentioned above, the bedroom levels were about one-half the kitchen levels.

Stepwise regression analysis was performed on the gas and electric homes separately with the following variables: the presence of a kitchen vent, the presence of a gas drier, the type of air conditioner, the area of the house, whether the garage was attached, and the amount of smoking by the occupants. (All homes except two had gas hot water heaters, so it was not included as an explanatory variable.) In this exploratory analysis, none of these variables were significant predictors of NO_2 concentrations indoors, although subsequent analyses are planned.

DISCUSSION

The results of measuring week-long average NO_2 concentrations at three specific locations within homes for a one-year period indicated that the type of cooking stove used within the home was a significant predictor of the NO_2 concentrations indoors. The gas cooking stove was found to be a major source of NO_2. The NO_2 levels in the gas cooking homes were much higher than levels found outdoors or in electric cooking homes. The NO_2 levels in the gas cooking homes were higher in the kitchen than in the bedroom. In contrast, the NO_2 levels inside electric cooking homes were less than levels found outdoors. In addition, the NO_2 concentrations within homes with gas cooking stoves was undoubtedly not uniform over the one-week sampling period, and most homes likely had peak concentrations many times greater than the observed week-long average values.

The results are virtually identical to results reported by Spengler, *et al.* (2) for 137 homes in Portage, Wisconsin. The pattern shown in Figures 1 and 2 would suggest that gas stoves are a major source of NO_2, which is retained inside the home more during the winter season than the summer season, is mixed throughout the house, but is depleted by air exfiltration and deposition.

ACKNOWLEDGMENTS

Special thanks are due the homeowners in Topeka, Kansas, who graciously participated in this year-long study and diligently followed sampling instructions. Dr. P.B. Ryan contributed much expertise and support. A.M. Majahad and H. Miklas participated in an inter-laboratory audit.

This work was supported under general support provided to the Harvard AIr Pollution Health Study through NIEHS grant ES-01108 and Electric Power Research Institute contract RP1001-1.

REFERENCES

1. B.G. Ferris,Jr., F.E. Speizer, J.D. Spengler, D.W. Dockery, Y.M.M. Bishop, M. Wolfson, C. Humble, "Effects of sulfur oxides and respirable particles on human health: Methodology and demography of populations in study," *Am. Rev. Resp. Dis.* 120:767, 1979.

2. J.D. Spengler, C.P. Duffy, R. Letz, T.W. Tibbits, B.G. Ferris, "Nitrogen dioxide inside and outside 137 homes and implications for ambient air quality standards and health effects research," *Environ. Sci. Technol.* 17:164, 1983.

3. E.D. Palmes, A.F. Gunnison, J. DiMattio, C. Tomczyk, "Personal sampler for NO_2," *Am. Ind. Hyg. Assoc. J.* 37:570, 1976.

4. B.C. Cadof, S.F. Knox, J.A. Hodgeson, "Personal exposure samplers for NO_2," Draft report of the National Bureau of Standards, Washington, D.C., 1979.

5. A.J. Apling, K.J. Stevenson, B.D. Goldstein, R.J. Melia, D.H.F. Atkins, "Air pollution in homes: Validation of diffusion tube measurements of NO_2," Warren Spring Laboratory Report LR 311(AP), Herefordshire, England, 1979.

6. J.R. Girman, A.T. Hodgson, B.K. Robison, G.W. Traynor, "Laboratory studies of the temperature dependence of the Palmes NO_2 Sampler," Paper presented at the Third Annual National Symposium on Recent Advances in Pollutant Monitoring of Ambient Air and Stationary Sources, Raleigh, North Carolina, May 3-6, 1983.

7. F.C. Strong, "Regression line that starts at the origin," *Anal. Chem.* 51:298, 1979.

TABLE 1

Summary of NO_2 Concentrations in Kitchen, Bedroom and Outdoor Locations for All Week-long Samples in Homes with Electric and Gas Stoves

Location	N	Mean ($\mu g/m^3$)	Std.Dev. ($\mu g/m^3$)
ELECTRIC:			
Kitchen	460	12	6.1
Bedroom	461	11	6.8
Outdoor	456	17	6.6
GAS:			
Kitchen	425	69	45.2
Bedroom	422	43	33.5
Outdoor	408	19	5.9

TABLE 2

Summary of Annual Average* NO_2 Concentrations in Kitchen, Bedroom and Outdoor Locations in Homes with Electric and Gas Stoves

Location	N	Mean ($\mu g/m^3$)	Std.Dev. ($\mu g/m^3$)	Maximum ($\mu g/m^3$)
ELECTRIC:				
Outdoor	56	17	3.3	24
Kitchen	56	12	3.9	21
Bedroom	56	11	4.3	26
GAS:				
Outdoor	48	19	3.3	31
Kitchen	48	69	28.5	150
Bedroom	48	43	20.9	94

*Average of five or more valid observations of the eight sampling periods.

TABLE 3

Correlations Between Kitchen, Bedroom and Outdoor NO_2 Values at Locations in Homes with Electric and Gas Stoves*

	Outdoor	Kitchen
ELECTRIC:		
Kitchen	.36	-
Bedroom	.22	.64
GAS:		
Kitchen	.38	-
Bedroom	.26	.85

FIGURE 1

Figure 1: Average NO_2 concentrations at homes with electric cooking stoves for each month of the year for outdoor (± two standard errors of the mean), kitchen and bedroom locations.

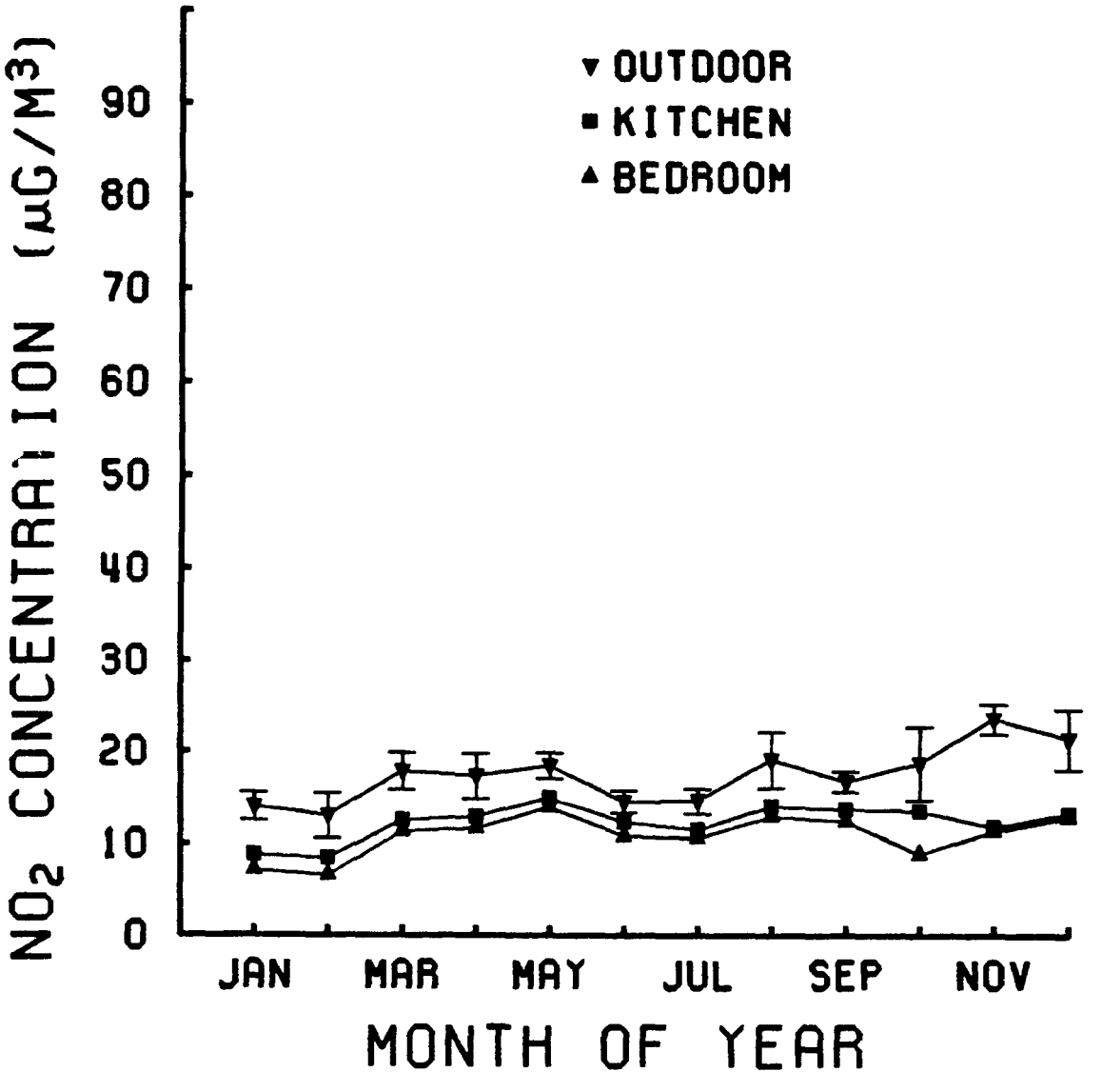

FIGURE 2

Figure 2: Average NO_2 concentrations at homes with gas cooking stoves for each month of the year for outdoor (± two standard errors of the mean), kitchen and bedroom locations.

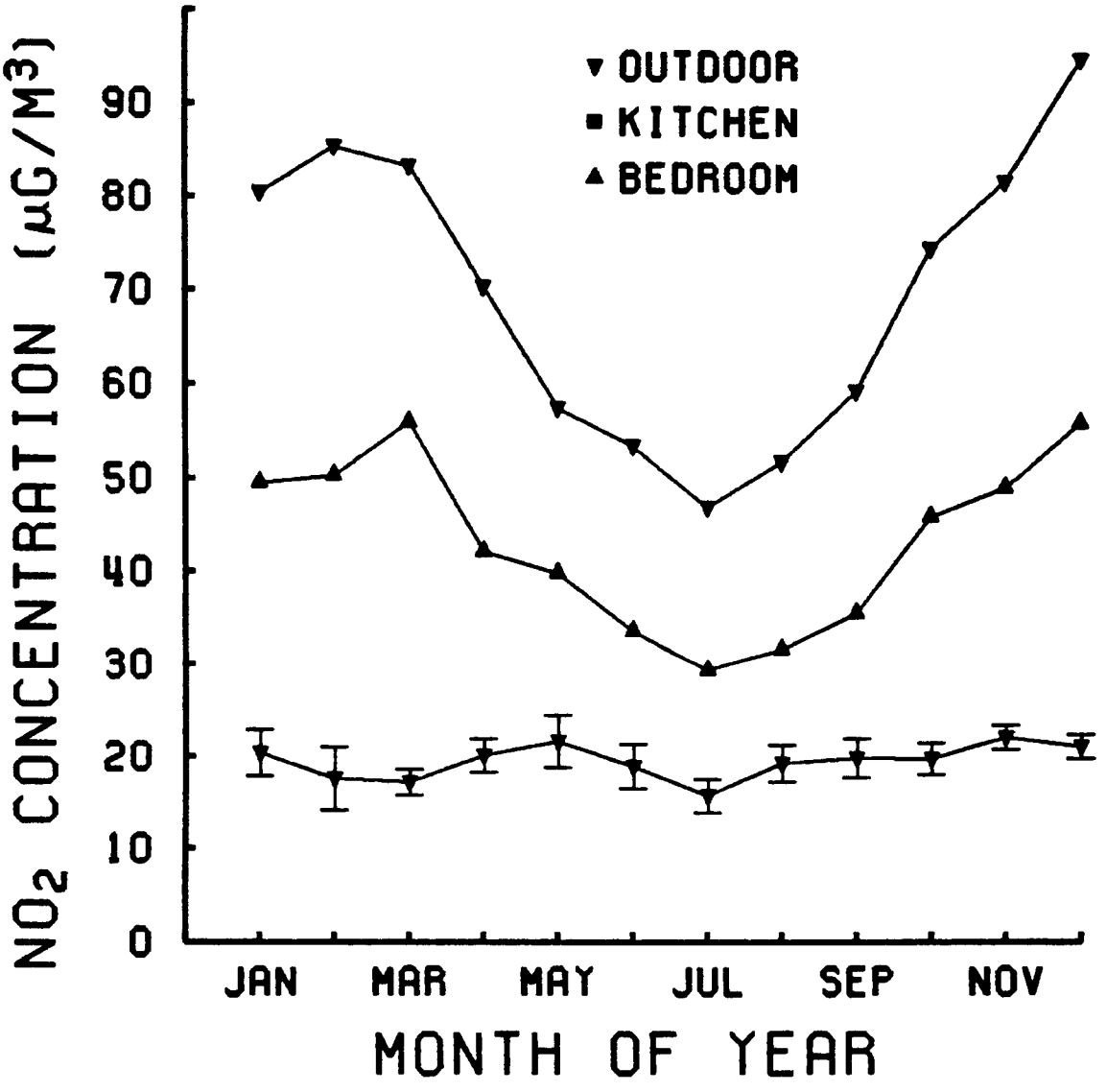

FIGURE 3

Figure 3: Distributions of annual average NO_2 concentrations in the kitchens of homes with electric and gas cooking stoves.

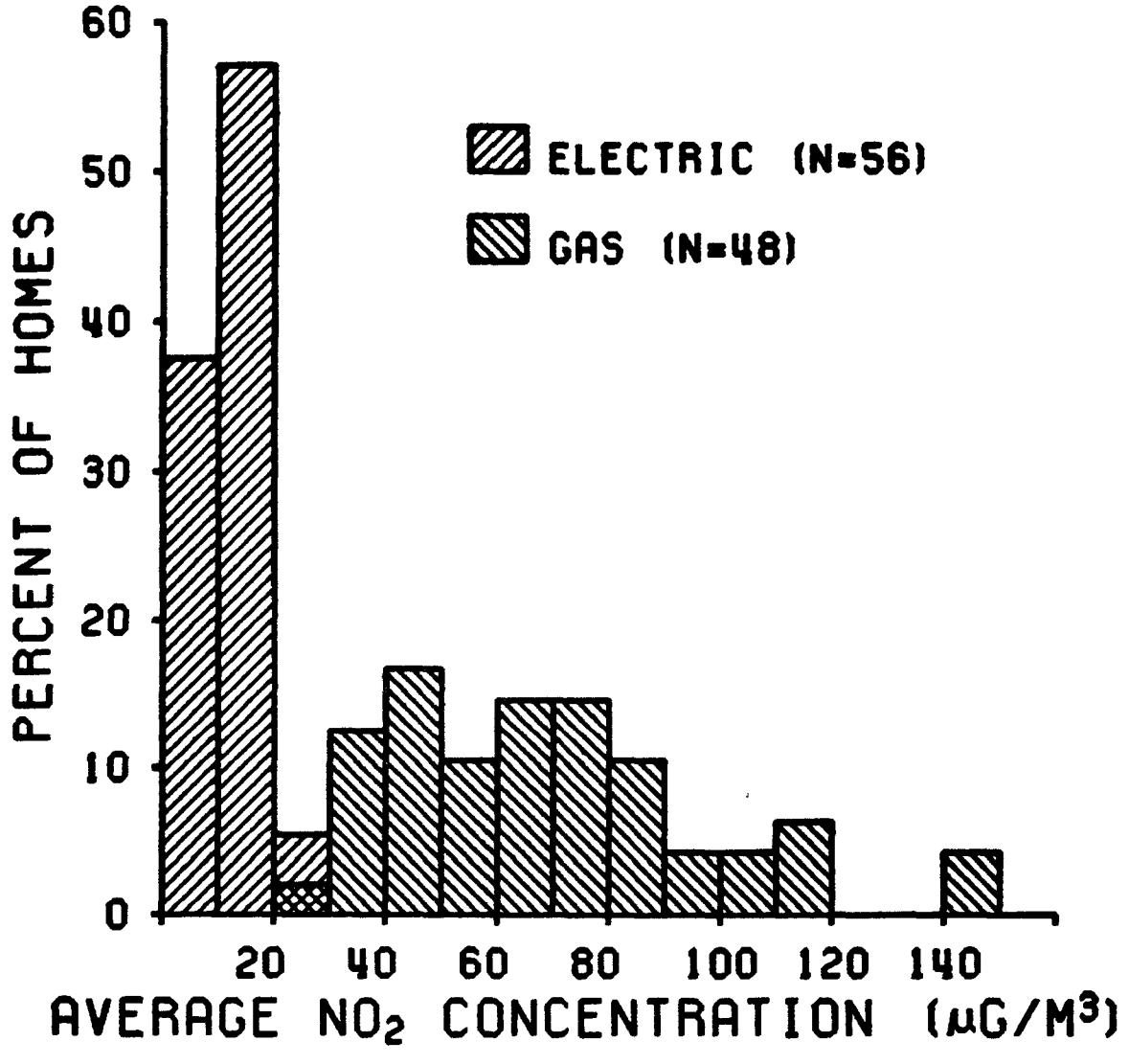

FIGURE 4

Figure 4: Plot of annual average NO_2 concentration in the kitchen of each home versus the annual average NO_2 concentration outside that home.

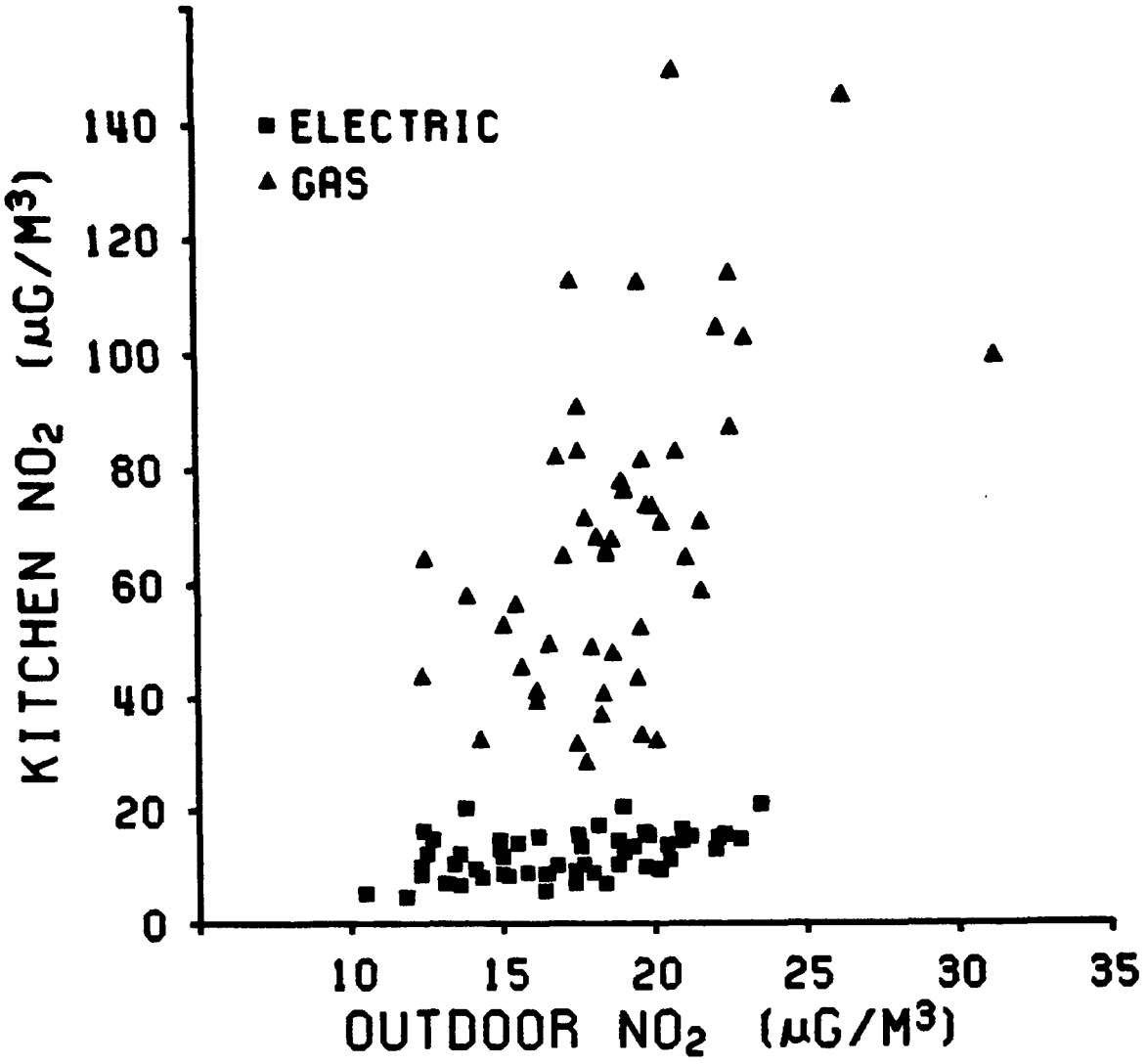

Estimated Distributions of Personal Exposure to Respirable Particles

Richard Letz, P. Barry Ryan and John D. Spengler

Department of Environmental Health Science and Physiology

Harvard School of Public Health

677 Huntington Avenue

Boston, MA 02115

INTRODUCTION

The Harvard Air Pollution Health Study is a prospective epidemiologic study involving about 20,000 people in six communities. Respiratory symptoms and pulmonary function have been measured on these people for about nine years (1). Outdoor air pollution measurements have been made in these communities to assess pollutant exposures. Exposure categories based on health questionnaire items (e.g., the presence of smokers or gas cooking stoves in the home) have been related to respiratory symptoms well as pulmonary function changes (2). Previous studies by our group were directed toward characterizing indoor pollutant concentrations associated with these simple dichotomous categories and attempted to identify better descriptors to categorize exposure (3).

Perhaps the best method of determining air pollution exposure for the people in our health study would be to do personal monitoring on every one. Our group has conducted personal monitoring studies of respirable particle (4) and nitrogen dioxide (5) exposures of some health study participants. However, personal monitoring on all participants is not feasible for many reasons. The most important reason is cost; i.e., personal monitoring is very expensive. Also, personal dosimeters are not available for all the pollutants of interest and all have (size, weight, measurement) limitations. (For a review, see (6).)

Experience with personal monitoring studies shows not only that personal monitoring expensive, but also that personal exposures can be poorly correlated with central site ambient air monitoring data. Also, current ambient air quality or personal exposure monitoring may not reflect past exposures well. Therefore, our group has focused on developing models of indoor pollutant concentrations (7) and personal exposures (8). Exposure models allow estimation of pollutant exposure for groups of people and time periods for which personal monitoring has not been conducted. A simple approach for estimating distributions of exposure to respir-

able particles (RSP) is presented in this paper. Some evidence for validation of the model with data from a personal monitoring study of adults in Kingston-Harriman, Tennessee, is presented, and the model is applied to provide estimates of RSP exposure for children in our six communities.

BASIC APPROACH

The general approach used in this paper is that of a time-weighted average concentration summed over microenvironments (9,10), i.e.,

$$E = \sum_i E_i = \sum_i f_i C_i \qquad (1)$$

where E is the mean pollutant exposure and E_i, f_i and c_i are exposure, fractions of time and pollutant concentrations, respectively, in the ith microenvironment. Pollutant concentrations are estimated by extrapolation from existing measurements or calculation from knowledge of source strengths, ventilation, removal and mixing volume. Our group has conducted indoor and outdoor monitoring in a large number of homes in our six cities (3) and has developed a framework for estimating indoor concentrations from outdoor concentrations (7,8):

$$C_i = p_i C_{OUT} + S_i \qquad (2)$$

where in the ith microenvironment, C_i is the concentration, p_i the "effective" penetration, and S_i the "effective" indoor source strength, and C_{OUT} is the pollutant concentration outdoors. The p_i and S_i are called "effective" because they include factors for air exchange as well as pollutant deposition due to chemical and physical action (See (7).) Effective penetration is affected by various home characteristics such as infiltration rate and presence of active surfaces for deposition. Indoor effective source strengths can be affected by human activities such as smoking and hobbies. The utility of expressing the relationship in this way is that indoor pollutant concentrations are considered to be a function of outdoor concentrations and two parameters that can be estimated from indoor/outdoor monitoring. This

approach allows extrapolation to locations other than those monitored, where outdoor pollutant concentrations may be different.

The approach outlined so far should allow estimation of mean exposures, given estimates of the microenvironment fractioned times (f_i) and pollutant concentrations (C_i). However, to calculate distributions one needs and estimate of the variance about his mean exposure. If not only the mean but also the variance of each parameter in the model is known, Gauss' law of error propagation (11) can be used to approximate the variance about the estimated mean exposure:

$$\mathrm{var}(E) \approx \sum_i \left[\frac{\partial E}{\partial C_i}\right]^2 \sigma_{C_i}^2 + \left[\frac{\partial E}{\partial f_i}\right]^2 \sigma_{f_i}^2 \qquad (3)$$

It should be noted that approximation should be good only if the uncertainties of the parameters are small relative to their means and the parameters are uncorrelated.

MODEL VALIDATION

A distribution of exposures to respirable particles was available from a personal monitoring study of 88 non-smoking adults in Kingston-Harriman, Tennessee (4). To predict this exposure distribution, we will use a model with 5 microenvironments: outdoors (OUT), indoors at home while awake (HA), indoors at home while asleep (HS), other non-home indoor environments (OI), and vehicular travel (T). Two distinct microenvironments are associated with the home because the RSP concentrations are substantially different indoors when people are active and when they are not (12). People generate particles with their activities; e.g., cooking, cleaning, smoking. The expanded expression for estimating mean RSP exposure thus becomes:

$$E = f_{HA} C_{HA} + f_{HS} C_{HS} + f_{OI} C_{OI} + f_T C_T + (1 - f_{HA} - f_{HS} - f_{OI} - f_T)\, C_{OUT} \qquad (4)$$

where E, f and C are as in Equation 1. Note that because the fractional times

must sum to unity, the fractional time spent in the last microenvironment is one minus the other fractional times. Thus, an n-microenvironment model has $2n-1$ free parameters.

Means and variances for fractional times, outdoor RSP concentrations and exposures were taken from tables in a report by Spengler, *et al.* (4). Personal exposures were monitored for three 24-hour periods using the Harvard/EPRI cyclone pump. The fractional times observed in the personal monitoring study are presented in Table I. The values agree well with those available from other sources (13,14). Data from our previous indoor/outdoor monitoring network (3) were used to estimate indoor pollutant concentrations. Annual average indoor RSP concentrations were regressed on outdoor RSP concentrations for 57 homes across 6 cities, yielding:

$$C_{IN} = 0.385\ C_{OUT} + 29.4\ (Smoking) + 13.8 \qquad (5)$$

where smoking is a 0-1 dichotomous indicator variable and C_{OUT} and C_{IN} are in $\mu g/m^3$. The mean outdoor concentration was 18 $\mu g/m^3$ with a standard deviation of 11 $\mu g/m^3$, while the mean indoor concentration was 28 $\mu g/m^3$ with a standard deviation of 21 $\mu g/m^3$. The root mean square error was 16 $\mu g/m^3$ from the regression model, or about 60% of the mean.

This analysis indicated that indoor RSP concentrations would be about 40% of outdoor values when there are no indoor sources from smoking and people's activities. The smoking source of 29.9 $\mu g/m^3$ and the 13.9 $\mu g/m^3$ source due to people's activities have to be adjusted upward because these values represent the contributions of these sources to the 24-hour integrated value. Both sources are assumed "off" during the HS fraction of time and "on" during the HA fraction of time. The adjusted effective smoking source for the HA microenvironment thus becomes the observed value, 29.9 $\mu g/m^3$, divided by the fraction of time spent at home awake (f_{HA}), 0.38, or equal to 78.7 $\mu g/m^3$. The source due to people's activities was

estimated to be 36.6 $\mu g/m^3$ (= 13.9 ÷ 0.38). Thus, for homes with non-smokers the indoor concentration was estimated as:

$$C_{HA} = .385(18) + 78.7(0) + 36.6 = 44.5. \quad (6)$$

The corresponding C_{HA} for homes with smokers would be 123.2 $\mu g/m^3$, and C_{HS} for both types of homes would be 7.9 $\mu g/m^3$. It was also assumed that C_{OI} is the same as C_{HA} in non-smoking homes, a conservative assumption, especially groups with occupational exposure or passive smoke exposure away from home.

In addition to mean RSP concentrations for the microenvironments, the variances about these means are needed as input for the model. An attempt to use the standard errors on the p_i and S_i estimated from the indoor/outdoor regression model (Equation 5) according to Gauss' law produced results that were inconsistent with observed values. It is likely that the estimates of the standard errors on the regression coefficients were poor because of the non-symmetric nature of the observed distributions and the violation of the assumption of homogeneity of variance. However, the violation of these assumptions should have little effect on the parameter estimates themselves. Results from indoor/outdoor monitoring (3,15) indicated that variances of indoor concentrations increase with increasing mean concentrations. The average error in the regression model was 16 $\mu g/m^3$ on an average indoor concentration of 28 $\mu g/m^3$, so 60% of the mean concentration for each microenvironment was used as the standard deviation for that C_i.

The observed RSP means and standard deviations for non-smokers living in homes with either non-smokers or smokers are presented in the first row of Table 2, and the corresponding predicted values are in the second row. The predicted value agree well with the observed values for both the means and standard deviations for both groups. They are slightly low, and this may be attributable to occupational exposures which would not be well-characterized by our assumption that the mean and variance for the C_{OI} is the same as the C_{HA}.

APPLICATIONS TO CHILDREN IN THE SIX CITIES

The children's 5-microenvironment model is the same as that presented for the adults except that the adults' other-indoor (OI) microenvironment is changed to a school (S) microenvironment. The fractional times for the children's model are presented in Table 3. These fractions were observed in an as-yet-unpublished personal monitoring study of children's exposure to NO_2 conducted in Watertown, Massachusetts, during the fall of 1982. They agree closely with values observed in another study in Portage, Wisconsin (5), and other values calculated from school hours and absence figures.

Indoor concentrations and their variances were calculated as for the adult model. Annual averages and (spatial) variances were taken from data available from our previous indoor/outdoor monitoring in each city (3). The means and standard deviations (spatial distribution) of outdoor RSP concentrations for each city as well as predicted mean exposures and their standard deviations are presented in Table 4. Exposure estimates are presented separately for children not living with smokers and children living with smokers. Note that although the mean outdoor concentrations of RSP vary by a factor of about four, estimated mean exposures for children living in non-smoking homes vary by less than factor of two. For example, the mean exposure of children in smoking homes where outdoor RSP concentrations are lowest (Portage) is higher than the mean exposure of children in non-smoking homes where outdoor concentrations are on average four times higher (Steubenville).

Distributions of exposures observed in our personal monitoring studies can be fit well with a gamma distribution. Gamma distributions have variances proportional to their means, cannot assume negative values, are generally skewed to the right, and approach the Gaussian distribution as the variance becomes small relative to the mean. Further, gamma distributions are additive in the sense that the

sum of two gamma distributions is itself a gamma distribution (16). Gamma distributions of predicted exposures of RSP for children living in homes with smokers and non-smokers in the cities with the highest and lowest outdoor concentrations are presented in Figure 1. The estimated percentage of children in our six cities having annual average RSP exposures greater than 75 $\mu g/m^3$ (the NAAQS for *TSP*), assuming gamma distributions with the predicted means and standard deviations, are presented in the last column of Table 4. A sizeable percentage of the children's population living in homes with smokers is seen to have exposures above the NAAQS for TSP, even in areas with low outdoor RSP concentrations.

DISCUSSION

This paper has been an attempt to estimate distributions of RSP exposure for children in our Harvard Air Pollution/Lung Health Study. Obviously, much work remains to be done. Model validation needs to be done with results from personal monitoring studies. Better estimates of the model parameters and especially their variances are needed. Some improvements can be made with analysis of existing data, but additional data on both pollutant concentrations and fractional times in other microenvironments are needed. Chemical and elemental analysis of indoor and personal RSP samples could be used as a means of quantifying source contributions. Also, there is a need to reconsider microenvironment definitions to minimize within-microenvironment variances rather than using arbitrary *a priori* schemes (10). Improvements to estimation of exposure variances may require attention to co-variances between model parameters. Finally, the implications of assumptions of the form of distributions of pollutant concentrations and personal exposures needs to be explored.

The large variance of exposure within exposure categories and the large overlap of observed, as well as predicted exposure distributions, has implications for

the power of epidemiologic investigations (18). This suggests that very large numbers of subjects are necessary to detect health effects differences between people grouped into exposure categories, even when the mean difference in pollutant concentrations between exposure categories appears large. Alternatively, it suggests that we might achieve greater efficiency by quantifying exposures well with personal monitoring on a much smaller number of subjects. Finally, this work points out the potential importance of indoor sources (e.g., percent of homes with smokers, amount smoked, etc.) as confounders in studies of the effects of outdoor air pollution across communities.

ACKNOWLEDGMENTS

This work was supported under general support provided to the Harvard Air Pollution Health Study through NIEHS grant ES-01108 Electric Power Research Institute contract RP1001-1, and EPA grant EPA 68-02-3466.

REFERENCES

1. B.G. Ferris,Jr., F.E. Speizer, J.D. Spengler, D.W. Dockery, Y.M.M. Bishop, M. Wolfson, C. Humble, "Effects of sulfur oxides and respirable particles on human health: Methodology and demography of populations in study," *Am. Rev. Resp. Dis.* **120**:767, 1979.

2. F.E. Speizer, B.G. Ferris,Jr., Y.M.M. Bishop, J.D. Spengler, "Respiratory disease rates and pulmonary function in children associated with NO_2 exposure," *Am. Rev. Resp. Disease* **121**:3, 1980.

3. J.D. Spengler, B.J. Ferris,Jr., D.W. Dockery, F.E. Speizer, "Sulfur dioxide and nitrogen dioxide inside and outside homes and the implications on health effects research," *Env. Sci. & Tech.* **13**:1276, 1979.

4. J.D. Spengler, R.D. Treitman, T.D. Tosteson, D.T. Mage, "Personal exposures to respirable particulates: A tale of two cities - Kingston and Harriman, Tennessee," Paper presented at the International Symposium on Indoor Air Pollution, Health and Energy Conservation, Amherst, Mass., October 13-16, 1981.

5. J.J. Quackenboss, M.S. Kanarek, J.D. Spengler, R. Letz, "Personal monitoring for nitrogen dioxide exposure: Methodological considerations for a community study," *Environ. Int.* **8**:249, 1982.

6. L.A. Wallace, W.R. Ott, "Personal monitors: A state-of-the-art survey," *J. Air Poll. Control Assoc.* **32**:601, 1982.

7. P.B. Ryan, J.D. Spengler, R. Letz, "The effects of kerosene heaters on indoor pollutant concentrations: A monitoring and modeling study," *Atmos. Environ.* in press, 1983.

8. K. Sexton, R. Letz, J.D. Spengler, "Human exposures to nitrogen dioxide: An indoor/outdoor modeling approach," *Environ. Res.* in press, 1983.

9. M. Fugas, "Assessment of total exposure to an air pollutant," Proceedings of the International Conference on Environmental Sensing and Assessment, IEEE #75-CH 1004-1 ICESA, Las Vegas, Nevada, 1975.

10. N. Duan, "Models for human exposure to air pollution," *Environ. Int.* **8**:305, 1982.

11. P.R. Bevington, *Data reduction and error analysis for the physical sciences*, McGraw-Hill, New York, 1969.

12. "Indoor pollutants," National Academy Press, Washington, D.C., 1981.

13. M.D. Koontz, J.P. Robinson, "Population activity patterns - St. Louis study," *Environ. Mon. Assess.* **2**:197, 1982.

14. F.S. Chapin, *Human activity patterns in the city*, Wiley-Interscience, New York, 1974.

15. J.D. Spengler, C.P. Duffy, R. Letz, T.W. Tibbits, B.G. Ferris, "Nitrogen dioxide inside and outside 137 homes and implications for ambient air quality standards and health effects research," *Environ. Sci. Technol.* **17**:164, 1983.

16. W.L. Hays, *Statistics for the social sciences*, Holt, Rinehart and Winston, New York, 1973.

17. C.M. Shy, D.G. Kleinbaum, H. Morgenstern, "The effect of misclassification of exposure status in epidemiological studies of air pollution health effects," *Proc. N.Y. Acad. Med.* **54**:1155, 1978.

TABLE 1

Time Fractions Used for 5-Microenvironment Adult's Model

Micro-Environment	Fractional Time	Standard Deviation
Home-Awake (f_{HA})	0.38	0.25
Home_Asleep (f_{HS})	0.30	0.05
Other-Indoors (f_{OI})	0.15	0.16
Vehicular travel (f_T)	0.05	0.06
Outdoors (f_O)	0.12	-

TABLE 2

Observed and Predicted Exposures to Respirable Particles in a Personal Monitoring Study in Kingston-Harriman, Tenn. (n=88)

	Non-Smoke Exposed		Smoke-Exposed	
	Mean ($\mu g/m^3$)	Std.Dev. ($\mu g/m^3$)	Mean ($\mu g/m^3$)	Std.Dev. ($\mu g/m^3$)
Measured Personal Exposures	36	22	67	51
5-Micro Model Estimates	34	21	63	45

TABLE 3

Time Fractions Assumed for

5-Microenvironment Children's Model

	Annual	School year	Summer
f_{HA}	0.40	0.40	0.40
(s.d.)	(0.20)	(0.20)	(0.20)
f_{HS}	0.30	0.30	0.30
(s.d.)	(0.10)	(0.10)	(0.10)
f_S	0.12	0.16	0.01
(s.d.)	(0.02	(0.03)	(0.0003)
f_T	0.03	0.03	0.03
(s.d.)	(0.03)	(0.03)	(0.03)
f_O	0.18	0.14	0.29

TABLE 4

Predicted Exposures to Respirable Particles for Children in Six Cities Using a 5-Microenvironment Model

City	OUTDOOR Mean*	OUTDOOR S.D.*	EXPOSURE Mean*	EXPOSURE S.D.*	% > 75 $\mu g/m^3$**
NON-SMOKE EXPOSED:					
Portage	11	1	26	15	1
Topeka	12	2	26	15	1
Watertown	19	2	30	17	2
Kingston	17	2	29	16	2
St.Louis	20	3	30	17	2
Steubenville	41	10	40	22	7
SMOKE-EXPOSED:					
Portage	11	1	56	41	25
Topeka	12	2	56	41	26
Watertown	19	2	60	42	28
Kingston	17	2	59	42	28
St.Louis	20	3	60	42	29
Steubenville	41	10	70	46	38

* in $\mu g/m^3$

** Assuming a gamma distribution with the predicted mean and standard deviation.

FIGURE 1

Figure 1: Estimated distributions of RSP exposure for children living in homes with and without smokers in Portage, Wisconsin, and Steubenville, Ohio.

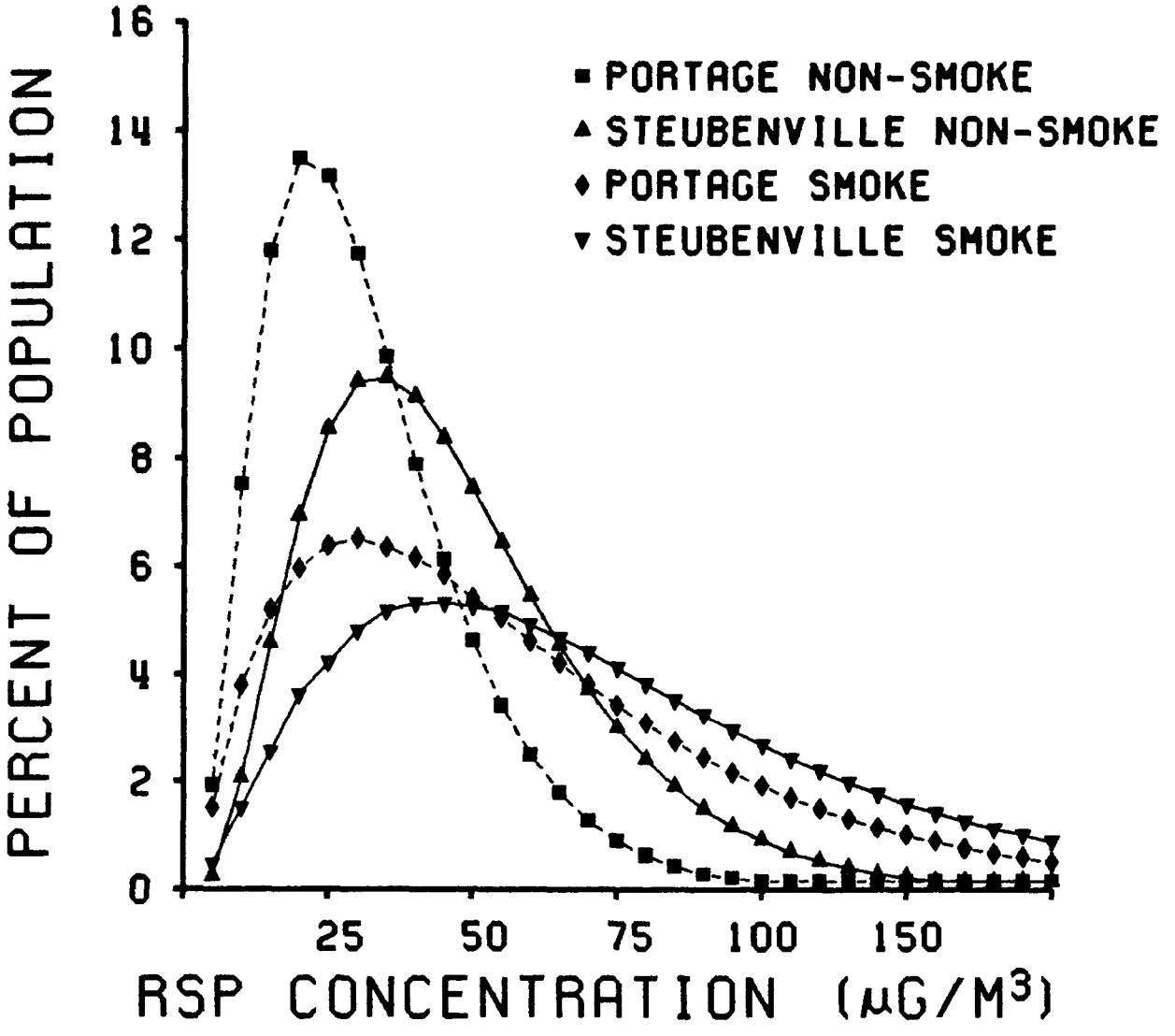

Empirical Models for Estimating Individual Exposures to Air Pollutants In a Health Effects Study

C. F. Contant, Jr., M.P.H.,

T. H. Stock, Ph.D.,

A. H. Holguin, M.D., M.P.H.,

B. M. Gehan, M.A.,

D. J. Kotchmar, M.D.,

P. A. Buffler, Ph.D., M.P.H.,

B. P. Hsi, Ph.D.

Although the research described in this article has been funded wholly by the United States Environmental Protection Agency through Grant R808738010 and Contract 2D5526NAEX to the University of Texas at Houston, it has not been subjected to the Agency's required peer and policy review and therefore does not necessarily reflect the views of the Agency and no official endorsement should be inferred.

In the spring of 1981, investigators at the University of Texas School of Public Health at Houston undertook a study of the effect of exposure to air pollution in asthmatics in the Texas Gulf Coast area. The goal of the Asthma Study was to examine the relationship between exposure to single pollutants and combinations of pollutants in the air and the frequency of occurrence of asthmatic attack in an asthmatic population. After extensive recruitment and screening, a panel of 52 medically managed extrinsic asthmatics, ranging in age from 7 to 55 years, was identified. The study subjects resided in two Houston neighborhoods, Clear Lake (n=31) and Sunnyside (n=21).

Twice a day, during the period of May through October, study subjects filled out log forms on which they reported their daily activities, as well as the occurrence of general symptoms, changes in medication usage and the results of a peak expiratory flow maneuver. The asthma specific symptoms, medication and peak flow data were summarized for each individual to provide an indication of whether an asthma attack had occurred in the twelve hour period.

Previous studies of ozone and asthma had used air monitoring data from a fixed monitoring station some distance away from residences to describe the exposure each individual received. The work of several authors (1,2,3) indicated that exposures differed among "micro-environments". As the use of personal monitors on all the study subjects for the course of the study was not feasible for both technological and cost reasons, it was deemed desirable to obtain exposure estimates for each individual using the micro-environment concept.

The approach taken was to estimate the pollutant concentration in each of certain broad groups of micro-environments using a regression model which describes the relationship of the fixed site data to these micro-environments. Exposure estimates were provided using the micro-environment specific estimates and the data collected from the study subjects concerning their movement through

the micro-environments. This regression model is based on the data obtained from a subset of the study population. The model for ozone will be described here.

To describe the micro-environment exposures a three-tiered monitoring system was developed. Details of this monitoring system have been presented by Stock et al elsewhere (4). The first level consisted of two fixed monitoring sites, each located in the center of one of the two study neighborhoods. All study subjects lived within 2.5 miles of a fixed monitoring site. The second tier consisted of a mobile monitoring station housed in a large van. Data were collected at each of twelve residences selected to be representative of the study subjects' residences; eight were in Clear Lake and four in Sunnyside. All these houses had some form of air-conditioning. The areas sampled were the den, kitchen and bedroom of each house and the area immediately outdoors. The same pollutants were monitored at both the fixed site and mobile van; ozone was measured with a chemiluminescence method instrument.

Personal monitoring provided the third tier of the sampling network. The ozone monitors were portable CSI Chemiluminescence samplers. Monitoring of ozone was labor intensive, requiring two research assistants to carry the monitors as they followed each study subject on his or her daily routine. For the younger study subjects the monitoring included some time in the classroom. Thirty of the 52 study subjects were involved in the personal monitoring, each for an average of sixteen hours on two separate days.

Figure 1 displays the ozone values as measured at the fixed site and indoors for one of the residences studied over a nine day period. Note that the indoor values are usually near zero. It would appear that little or no relationship exists. There is a slight problem is this interpretation. It is known that ozone follows a strong diurnal cycle outdoors.(Figure 2) A problem arises from this variation. The deviations around the outdoor diurnal pattern tend to be less than

the range of the pattern itself. That is, the variation about the one o'clock mean is smaller than the difference between the one o'clock mean and the eight o'clock mean. There might exist a relationship between the deviations from the one o'clock mean outdoors and the one o'clock mean indoors. The obvious relationship between the fixed site and outdoor mean would tend to inflate the amount of variation explained by the model (R-squared) for this regression beyond what it may actually be. Therefore, the regression model was calculated with "centered" data. The hour and site specific mean was subtracted from each hour and site specific observation and the regression was performed using the resulting values. Symbolically this model is:

$$(Y_{hr} - \bar{Y}_{hr}) = B\ (FS_{hr} - \bar{FS}_{hr})$$

where

Y_{hr} = hour specific ozone value (indoors or outdoors)

$\bar{Y}_{hr}$ = hour specific ozone mean (indoors or outdoors)

FS_{hr} = hour specific ozone value at Fixed Site

$\bar{FS}_{hr}$ = hours specific ozone mean at Fixed Site

B = regression coefficient

Because the data are "centered", this model will tend to be less sensitive to the effects of the diurnal variation and have more likelihood of detecting a small fixed site/indoor relationship. The coefficient is an estimate of the slope of the line relating the fixed site value to the outdoor or indoor value. Separate regressions for each residence were performed in which both the indoor and outdoor data for each residence were regressed on the fixed site data corresponding to the time periods during which the van was operating at the residence. The resulting coefficients were combined over the twelve residences to provide a summary measure. These residence specific values have been examined for differences which might relate to characteristics of the residence; no strong differences were found

for ozone.

The fixed site to outdoor summary coefficient is .78609, (see Table 1) which is significant at the 0.001 level. The R-squared value indicates that about 73 % of the variation in the outdoors ozone may be explained by the fixed site data. Surprisingly, the fixed site to indoor coefficient is also significant at the 0.001 level. However the coefficient is extremely small and the R-squared is only 2.1%. These coefficients were used with the hour specific means to provide an estimate of the ozone levels in each of several groups of micro-environments. To illustrate, this model would predict that a fixed site value of 100 PPB at one o'clock in the afternoon would increase the indoor ozone by only 0.24 PPB above its hour specific mean of 1.6 PPB. The outdoor to indoor coefficient is also significant, and approximately twice the fixed site to indoor coefficient. The very small R-squared is due to data from one residence; when this residence is deleted from the summary the R-squared increases to 7.9%. The reason for the anomalous data at this residence is not clear.

TABLE 1-RESULTS OF OZONE REGRESSIONS

	Summary beta	RSQ	P
Fixed site-outdoors	0.78609	73.6	<.001
Range		(38.1; 90.0)	
Fixed site-indoors	0.005934	2.1	<.001
Range		(0.0; 15.4)	
Outdoors-indoors	0.010119	0.4	<.001
Range		(0.0; 24.9)	

The exposure model also uses data concerning the movement of the study subjects through micro-environments. Activity patern data were collected using a section of the twelve hour log shown in Figure 3. For any hour the study subject could indicate whether he or she was in any or all of several locations.

Figure 4 presents an estimate of the distribution of time spent outdoors between 7:00 AM and 7:00 PM by the Clear Lake study subjects. Approximately 60% of the study subjects spent two hours or less outdoors on an average day. Patterns in the Sunnyside neighborhod were similar.

The exposure model was built using the measured activity data, the ozone values as measured at the fixed site, hour specific means, and coefficient values from regressions which provided estimates of the relationship between the fixed site values and the ozone values outdoors and indoors. The ozone exposure for each individual is determined by the subject's location and the estimated ozone concentration in that location. For this model it is assumed that there is no difference in ozone concentration within the various indoor locations and that the same holds true for the various outdoor concentrations. Also, it is assumed that a closed vehicle had the same concentration as that found indoors, while an open vehicle received the outdoors value. Therefore the several locations in the activity log were treated as two homogeneous groups: indoors and outdoors. Individuals who were in more than one group during an hour were assigned the mean of the estimated ozone level in each of the locations. These simplifications are required by the limits of the sampling scheme used in the outdoor/indoor monitoring.

Having generated the ozone exposure estimate for each individual it is of interest to compare these estimates to the values obtained from the personal monitoring activities. As the exposure model yielded one hour averages, the personal monitoring data, which were collected in five minute intervals, were reduced to one hour averages. To assess the accuracy of the exposure model two measures were calculated.

Mean Difference: $D = \frac{\Sigma (P - E)}{N}$

Mean Squared Difference: $MSD = \frac{\Sigma (P - E)^2}{N}$

where:

P = personal monitoring concentration.

E = exposure estimate, (Fixed Site or Exposure Model).

N = number of hours monitored.

The mean difference is simply the average difference between the personal monitoring value and the exposure estimate value generated for the same time period. In this case a negative mean difference indicates the exposure estimate is higher than the observed exposure, while a positive difference indicates that the exposure estimate underestimates the actual exposure. The mean squared difference is a measure of the error in the exposure model. If the differences center around zero the average difference may be small, but the model may still have a high degree of error, which the mean squared difference will detect. As it has been used so often in the past, the fixed site estimates are used as a comparison for the exposure model.

There were 417 hours of personal monitoring data available for comparison, for an average of 13.9 hours per subject. The average ozone exposure as determined by the personal monitoring was 15.96 PPB, with a standard deviation of 19.79 PPB. The average in Sunnyside was 19.31 PPB and that found in Clear Lake was 13.02. Loss of exposure estimates due to missing activity data was small, reducing the number of hours available to 406 from 417.

The results of the comparisons are shown in Table 2. Using the exposure model results in estimates which average 8 PPB below the ozone exposure actually

observed. The mean squared difference, 387.67 PPB^2, represents a reduction of 82.5% in the error found with the fixed site data. The average reduction in mean squared difference was 2077.5 PPB^2 per person. The difference between fixed site estimates and personal monitoring data tended to decrease as percent of time outdoors increased. The opposite trend was seen with the exposure model; the error increased as time outdoors increased.

TABLE 2-SUMMARY OF DIFFERENCES IN EXPOSURE ESTIMATES

Source of estimate	Mean difference	Mean squared difference
Fixed site only	-31.19 PPB	2218.24 PPB^2
Range	(-83.6; -2.8)	(70.8; 11378.4)
Exposure model	7.96 PPB	387.67 PPB^2
Range	(-7.52; 99.06)	(1.9; 10821.5)

The large range in mean squared differences indicates that the exposure model does not function uniformly across all subjects. The mean squared difference was smaller for 27 of the 30 individuals when the exposure model was used. For three subjects the fixed site actually provided a better estimate of ozone exposure than the exposure model. Two of these subjects live in the same residence which is the only residence in the study completely without air-conditioning. Apparently, a different fixed site to indoor relationship exists for this residence than for the other residences, accounting for the failure of the exposure model. When these two residences are removed from the analyses, the mean difference between the personal monitoring and exposure model is reduced to only 3.67 PPB. The mean squared difference becomes 230 PPB^2 which represents an 89.9% reduction from the fixed site estimates. This percentage reduction indicates that consideration of air-conditioning might explain 40% of the remaining error. When examining the fixed site to indoor coefficients, a slight air-conditioning effect was noted; but this difference was based on only two residences and due to the non-random

sampling scheme used to select the residences to monitor, it was unreasonable to include this effect in the model.

In conclusion, a simple ozone exposure model has been obtained based on activity data, fixed site monitoring data and fixed site to outdoor and indoor relationships estimated from the data. The purpose was to provide exposure estimates for all the health effect study subjects, using relationships obtained from only a subset of the subjects. Therefore, distinctions among micro-environments have been avoided except at the gross level and then made only when the data strongly supported these differences. For ozone, the only distinction was whether the subject was outdoors or indoors. It has been assumed that differences within the outdoor or indoor environments are small. However, there is evidence that this assumption is not true for some study subjects, resulting in a few serious errors in their estimated ozone exposure. This rather simple model resulted in an 82.5% reduction in the error when compared with the fixed site estimates. Improvements in this model would result from making more distinctions among the micro-environments, which would lead to a larger set of fixed site to micro-environment coefficients.

It is obvious that future health effects studies will need to include a monitoring experiment carefully designed to closely examine the differences among micro-environments. Choice of micro-environments to examine will depend on the characteristics of the pollutant and population being examined. It would appear that the largest determinant of ozone exposure in this study is whether the subject was indoors or not. While the model used in this study represents a significant improvement over exposure estimates used in earlier studies, further refinements to this model can be attained by careful design and interpretation of monitoring experiments.

REFERENCES

1. Fugas, M. Assessment of total exposure to an air pollutant. Proceedings of the International Conference on Environmental Sensing and Assessment, Paper No. 38-5, Vl. 2, IEEE #75 - CH 1004-1 ICESA, 1975.

2. Sexton, K., Letz, R. and Spengler, J. D. Human exposure to nitrogen dioxide: exposure modeling and risk assessment. APCA Paper 82-48.8. Paper presented at the 1982 Air Pollution Control Association Annual Meeting, New Orleans, Louisiana. 1982.

3. Duan, N. Models for human exposure to air pollution. Rand Note N-1884-HHS/RC. The Rand Corporation, Santa Monica, California. July 1982.

4. Stock, T., Holguin, A., Selwyn, B., Hsi, B., Contant, C., Buffler, P., Kotchmar, D. Exposure estimates for the Houston area asthma and runners studies. Lee, S., Mustafa, M., Mehlman, M. (eds.) In: Advances in Modern Environmental Toxicology. Vol 2. International Symposium on The Biomedical Effects of Ozone and Related Photochemical Oxidants. 1982.

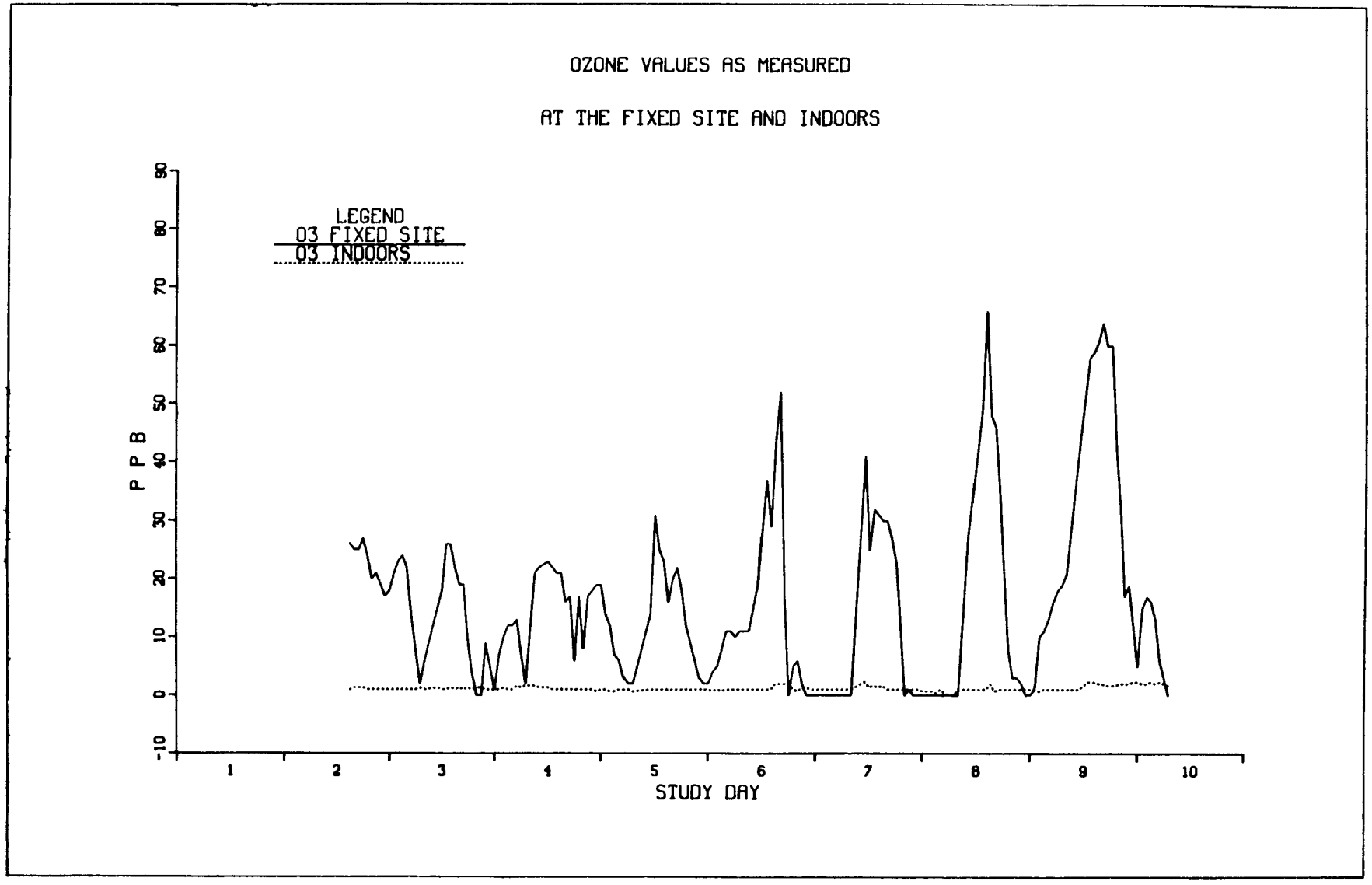

Figure 1. Plot of ozone values measured at the fixed site and indoors.

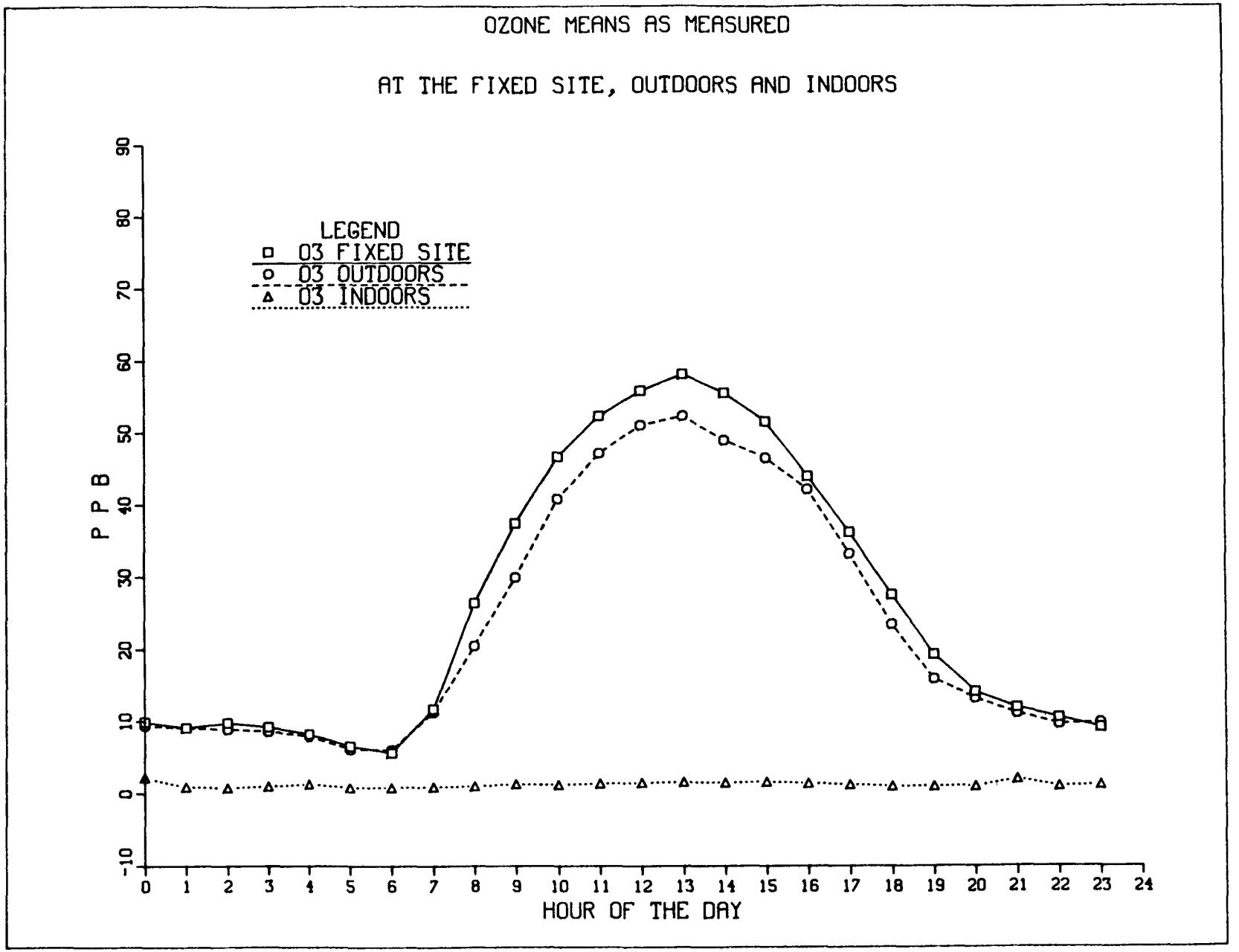

Figure 2. Plot of mean ozone values measured at the fixed site, outdoors and indoors.

PLACE		HOURS												
		morning					noon				evening			
		7	8	9	10	11	12	1	2	3	4	5	6	7
INDOORS	HOME													
	SCHOOL OR WORK													
	ELSEWHERE													
OUTDOORS	IN NEIGHBORHOOD													
	OUT OF NEIGHBORHOOD													
IN OPEN CAR, TRUCK OR BUS														
IN CLOSED CAR, TRUCK OR BUS														

Figure 3. Activity Data Log.

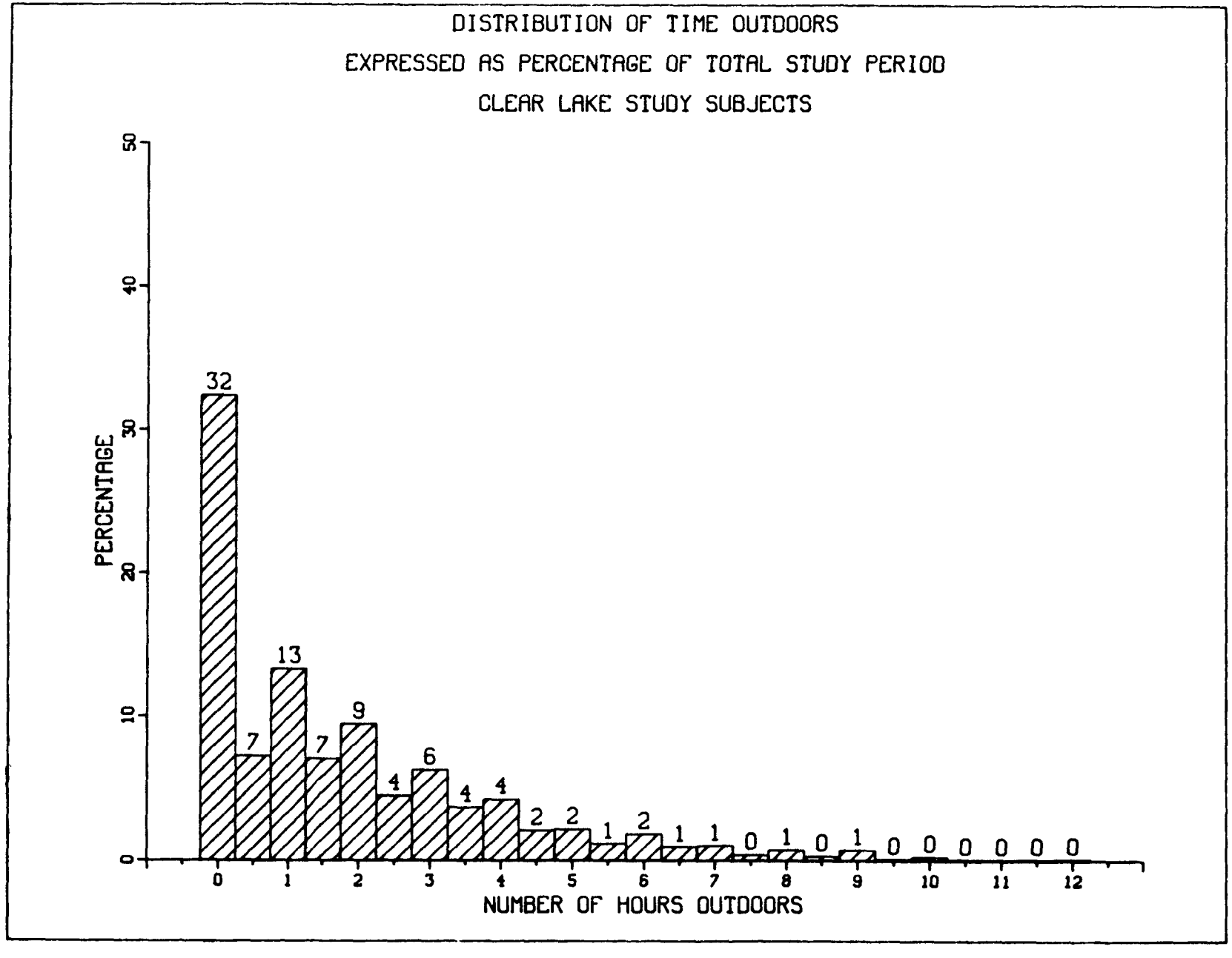

Figure 4. Distribution of daytime hours spent outdoors, May-October 1981, by Clear Lake subjects.

CARBON MONOXIDE EXPOSURES IN WASHINGTON, DC AND DENVER, COLORADO DURING THE WINTER OF 1982-83

by: Gerald G. Akland

Environmental Monitoring Systems Laboratory

Research Triangle Park, NC 27711

ABSTRACT

A study of exposures to carbon monoxide (CO) using Personal Exposure Monitors (PEMs) was conducted in Washington, DC and Denver, Colorado during the winter of 1982-83. The primary objective of the study was to validate a methodology for measuring the distribution of CO exposures in a representative sample of an urban population so that the risk to the entire population can be estimated. The methodology for selecting the participants and measurements of CO will be presented. Preliminary results indicated that for Washington, the median CO value was 6 ppm, and 1% of the values exceeded 35 ppm. For Denver, the median value was 8 ppm, and 3.5% of the values exceeded 35 ppm. After further statistical analysis, the participants' exposure data will be contrasted to fixed monitor exposure estimates, and an exposure profile for each city will be determined.

INTRODUCTION

The overall goal of EPA's exposure research program was to develop a methodology that precisely and accurately determined the public's exposure to air pollutants. We selected carbon monoxide (CO) for our exposure study because of available CO instrumentation, known sources, and known CO health effects.

Our study objectives were to (1) develop methodology to estimate urban population exposure to CO, (2) obtain exposure estimates and relate them to fixed site measurements, (3) develop methodology for selecting relevant microenvironments, (4) develop methodology for using Personal Exposure Monitors (PEM's) to analyze COHb in breath, and (5) develop an activity pattern data base.

Washington, DC and Denver, Colorado were chosen for the field study because they differ in elevation, past CO levels based on fixed site data, geographical area, administrative complexities (single or multiple state), and commuter patterns. The City of Denver requested a CO exposure study before EPA's selection. EPA hoped that the selection of Denver as a study area would satisfy EPA's research objectives and local/state needs for an exposure data base to assess control strategy alternatives.

Portable CO detectors have been designed for industrial or mining applications and do not have operational features or CO concentration ranges suitable for exposure studies. EPA decided to modify an existing industrial CO monitor, the General Electric PEM, Model CO-3.[1] This unit was readily

available, provided real-time data within the expected concentration range, was previously field tested, generally met the performance specifications, but lacked data logging capability. To provide the data handling features, the Magus Group, Inc. of Menlo Park, CA developed a microprocessor system. This system was integrated with the monitor and repackaged for the study by Rockwell International.

STUDY DESIGN

Personal CO exposure measurements were taken during November through February, the period of expected maximum ambient CO concentrations. PEMs were distributed each evening between 7 pm and 10 pm and collected 24-hr later.

Alveolar CO was collected at the end of each 24-hr sampling period. The participants took a deep breath and exhaled all air from their lungs. A second deep breath was taken and held for 20 sec. The first part of the breath was exhaled into the room and the last portion into a sample bag. The bag was sealed, returned to the laboratory, and attached to a specially calibrated GE monitor.

The Research Triangle Institute (RTI) selected the statistical sample of

---

[1]Mention of specific trade name does not imply product endorsement.

target population members for EPA as a two-phase sample: 1) data were collected for all members of a particular household (the screening sample) and 2) personal exposure data were collected for a stratified random sample of the screening sample household members. The second-phase sample was stratified to oversample those population members at high CO exposure risk.

The screening sample was selected as a two-stage area sample. For the first stage, area segments defined by 1980 Census block groups and enumeration districts were selected. Census geography variables were used to stratify the first-stage sample to assure geographic dispersion across the study area. The Donnelley Marketing Corporation[2] provided a list of the households in the selected area segments. A second-stage sample of 8643 households in Washington and 4987 households in Denver was selected from this list for the household screenings. Data on smoking, commuting time, occupation, presence of gas appliances in the home, and the presence of an attached garage were collected for all household members.

The second-phase sample of persons selected for personal exposure monitoring was stratified by the above variables. The sample size was 1773 persons in Washington and 1139 in Denver and was expected to yield 1000 and 500 interviews in Washington and Denver, respectively.

---

[2]The Donnelley Marketing Corporation sells lists of names, addresses, and telephone numbers of residents in many areas of the U.S. The sources of these lists are based upon telephone directories and vehicle ownership records.

WASHINGTON, DC

Fixed site CO data were collected at nine existing sites throughout urban Washington, DC. Fifty PEM's were delivered to the contractor for daily distribution of 20 units with 10 spares. Monitoring began November 8, 1982 and continued through February 24, 1983. PEM measurements were obtained from participants in the urban Washington, DC Standard Metropolitan Statistical Area (SMSA) who were at least 18 years of age at the time of the study. The estimated population size for this group is 1.12 million. RTI obtained the PEM and activity information. The Council of Governments, Washington, DC, was the site coordinator and supplied laboratory space for RTI.

DENVER, COLORADO

The study design for Denver was similar to that for Washington with two major differences. First, the Mayor of the City and County of Denver requested that such a study be performed in his city. As a result, local officials from the city, state, and EPA Regional office established a monitoring committee chaired by the Mayor's office to coordinate the study and establish new monitoring sites. Nine additional CO sites[3] were added to the existing six

[3]A major development effort was undertaken by Bill Basbagill of EPA Region 8 to build an inexpensive temperature-controlled box to house the instrumentation at the additional sites. For less than $50, Bill was able to construct a box which maintains temperatures within the required + 5°C.

telemetered sites in the study area. The Air Pollution Control Division of th State of Colorado operated all 15 sites (following uniform standard operating procedures except for the manual data reduction from the nine new sites). All fixed data, including meteorological data, flowed from the State to the Environmental Monitoring Systems Laboratory through the Regional Office.

The other change to the design was that 500 instead of 1000 participants were selected, but each participant carried the monitor for two consecutive days. Multiple measurements per participant were used to estimate the influenc of activity pattern on the overall exposure profile.

The PEM measurements were obtained from a sample of the non-institutionalized, non-smoking residents of the urban Denver SMSA who were at least 18 years of age at the time of the study. The estimated population size for this group was 245,000.

PEDCo conducted the exposure monitoring program. EPA provided 25 PEM's f a daily distribution of 10 units, with 5 instruments for replacements. Monitoring began on November 1, 1982, and continued through February 1983.

PRELIMINARY RESULTS

Data available for each participant include (1) data from the various questionnaires; (2) time the CO monitor button was pressed, the corresponding reading, and the corresponding activity diary information; (3) the CO readings on the hour for each of the 24 hours, and (4) the CO concentration in the breat

samples. In addition, fixed site monitoring data, meteorological data, and land use data were also collected.

Monitoring data, once validated, will be statistically analyzed. The statistical analysis will estimate the distribution of personal CO exposure, average time spent in various activities and at various locations, the significance of selected exposure factors, and the relationship between CO values measured by PEM's and simultaneous values reported by fixed-site monitors.

SAMPLING RESULTS AND RESPONSE RATES - WASHINGTON, DC

Between November 8, 1982 and February 24, 1983, 1455 households were interviewed. Of these, 944 (64.9%) agreed to participate, 184 (12.6%) refused to participate, and 198 (13.6%) were not interviewed for a variety of reasons. Of the 100 sampling periods originally planned, 98 were carried out. Two sampling periods (November 11 and 12) were cancelled due to equipment problems. A total of 814 subject days were completed. Twelve percent of the 944 participant days (130 days) were lost due to monitor malfunction.

Activity diaries had not been entered into the computer by the middle of April. A total of 870 breath samples were obtained and successfully analyzed for CO content. Twenty-two were lost because of leaks in the sample bag. The arithmetic mean of the 870 samples is 5.4 ppm with a standard deviation of 5.2 ppm.

Figure 1 presents an unweighted cumulative frequency distribution of the 638 maximum 1-hr PEM results (one value/subject/day) collected through the middle of January. This median is about 6 ppm, and 1% of the values exceed 35 ppm (fixed site data were not available for comparison). Interpretation of these data will be possible after further analyses of the completed data set. For this time period, 86% of all completed samples were valid within ± 10% and % 1.5 ppm based on pre- and post-sample calibration slopes and intercepts, respectively.

SAMPLING RESULTS AND RESPONSES RATES - DENVER, COLORADO

Of the 1000 eligible individuals in the primary and three supplementary samples, 424 agreed to be interviewed. In addition, 60 of the 139 eligible individuals identified through field screening agreed to be interviewed. Of these 485 eligible individuals, 454 were interviewed successfully and participated in the study.

A total of 1094 subject-days of participation were scheduled. The 454 individuals participating in the study yielded 900 subject-days; 446 subjects participated in two sampling periods, while eight subjects participated in only one sampling period.

Of the 900 activity diaries, 778 were accurate and complete. Significant omissions occurred in 66 diaries, primarily because of PEM failures. Diaries were filled out incorrectly in 52 cases.

A total of 895 breath samples were obtained and successfully analyzed for CO content. Thirty samples were lost because of leaks in the sample bag. The arithmetic mean of the 895 samples is 7.0 ppm with a standard deviation of 5.6 ppm.

Figure 2 is a preliminary unweighted cumulative frequency distribution of the maximum 1-hr PEM data (shown by solid line). The median is about 8 ppm, and 3.5% of the values exceed 35 ppm. The dashed line represents approximately 1000 daily maximum 1-hr per fixed site. The plot suggests that the distribution of maximum 1-hr PEM levels is slightly, but consistently higher than the corresponding distribution of daily fixed-site maxima, except at the upper decile where the difference is much greater.

Figure 3 is a quantile/quantile comparison of the permanent fixed CO monitors with the nine additional CO monitors. The plot is a simple cumulative distribution of 1-hr maximum fixed data from the permanent site (x-axis) and the corresponding distribution from the temporary sites (y-axis). The new sites have a larger percentage of lower values (< 6 ppm) than the permanent sites. Also, 80% of the permanent site values are less than 14 ppm (arrows on Figure 3). In contrast, 80% of the temporary site values are less than 12 ppm. This difference might be attributed to the downtown location of the permanent sites where traffic density is higher.

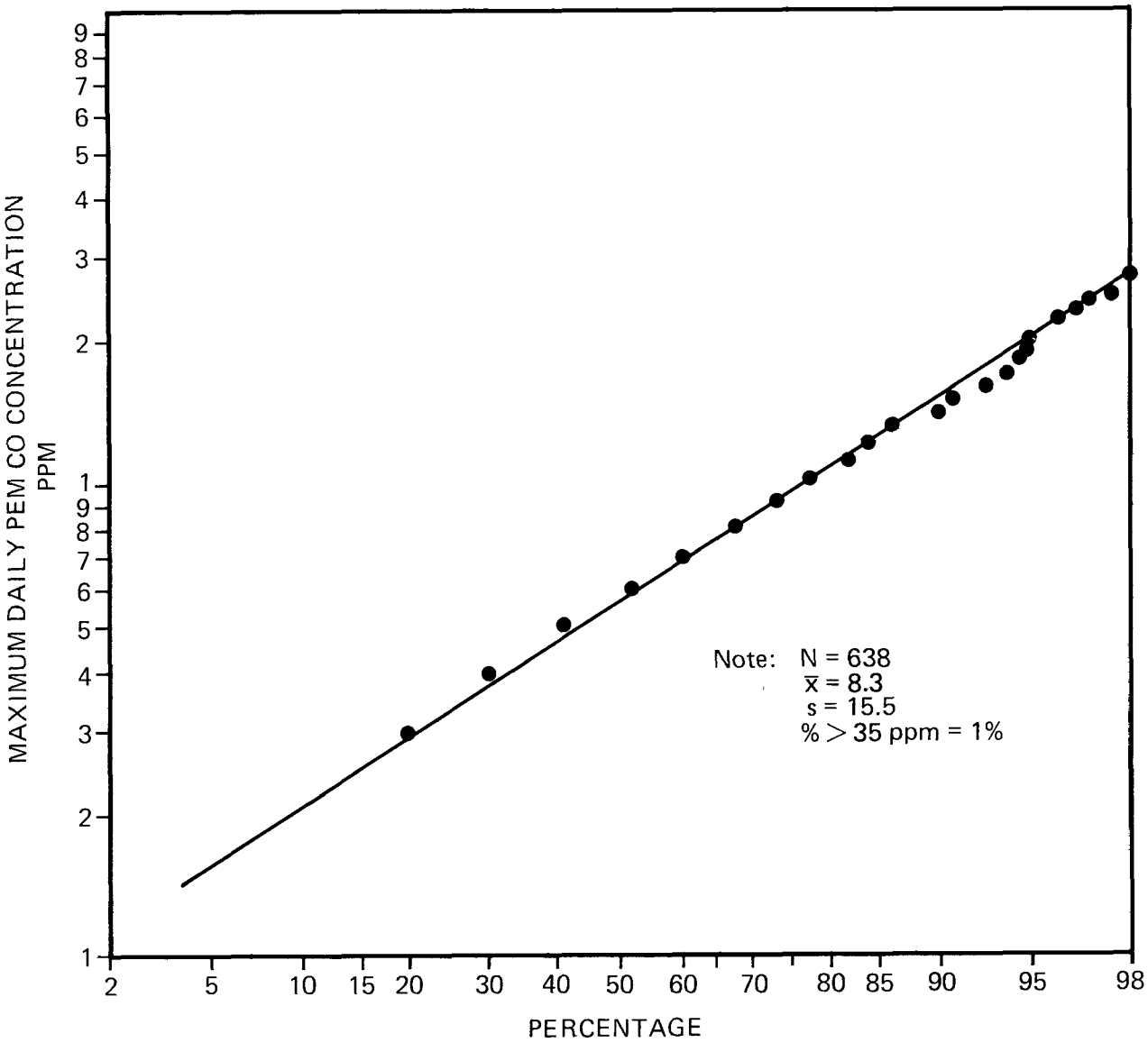

Figure 1. Cumulative Frequency Distribution of Maximum PEM Levels in Washington, DC.

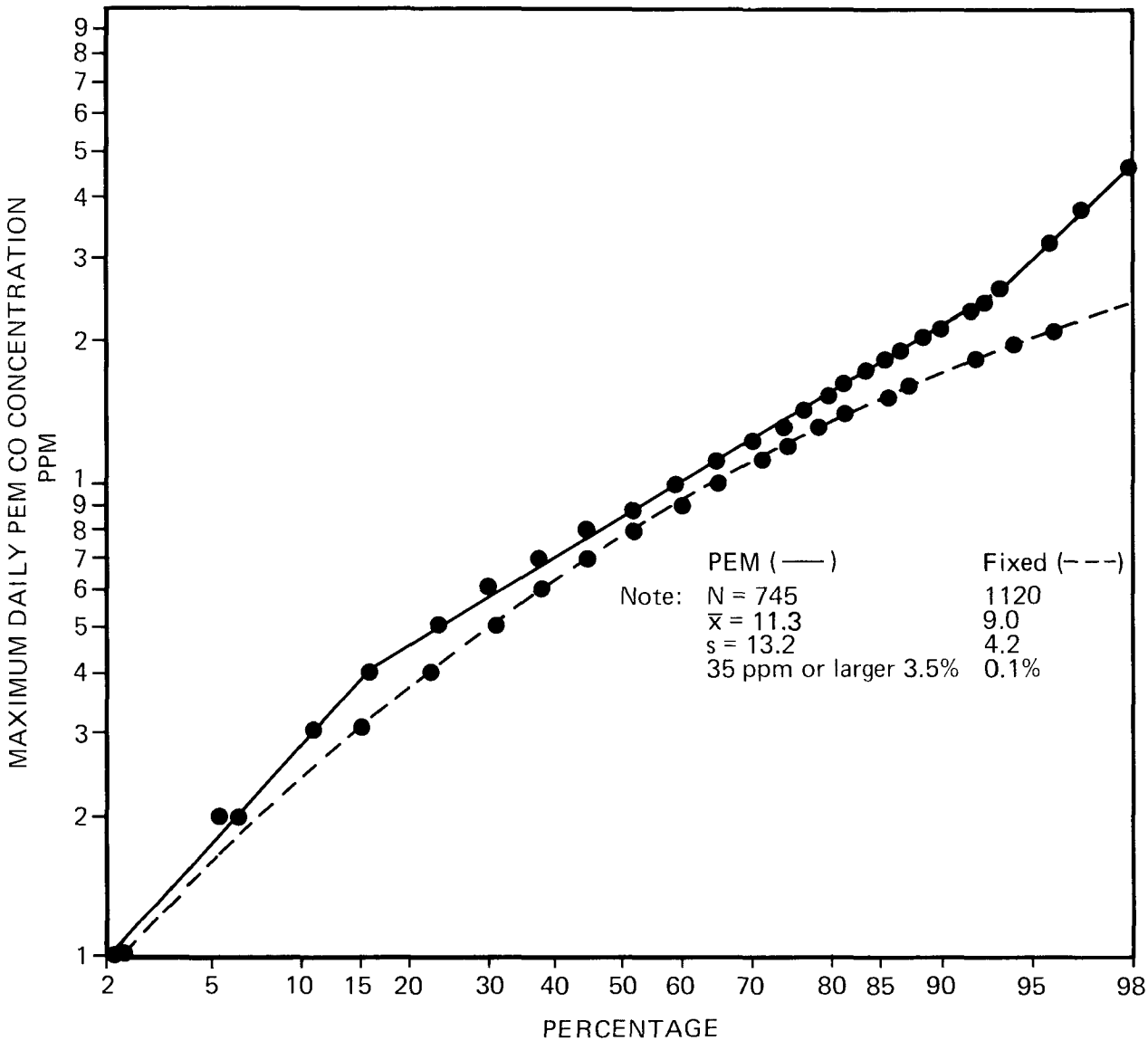

Figure 2. Cumulative Frequency Distribution of Maximum PEM Levels in Denver, Colorado.

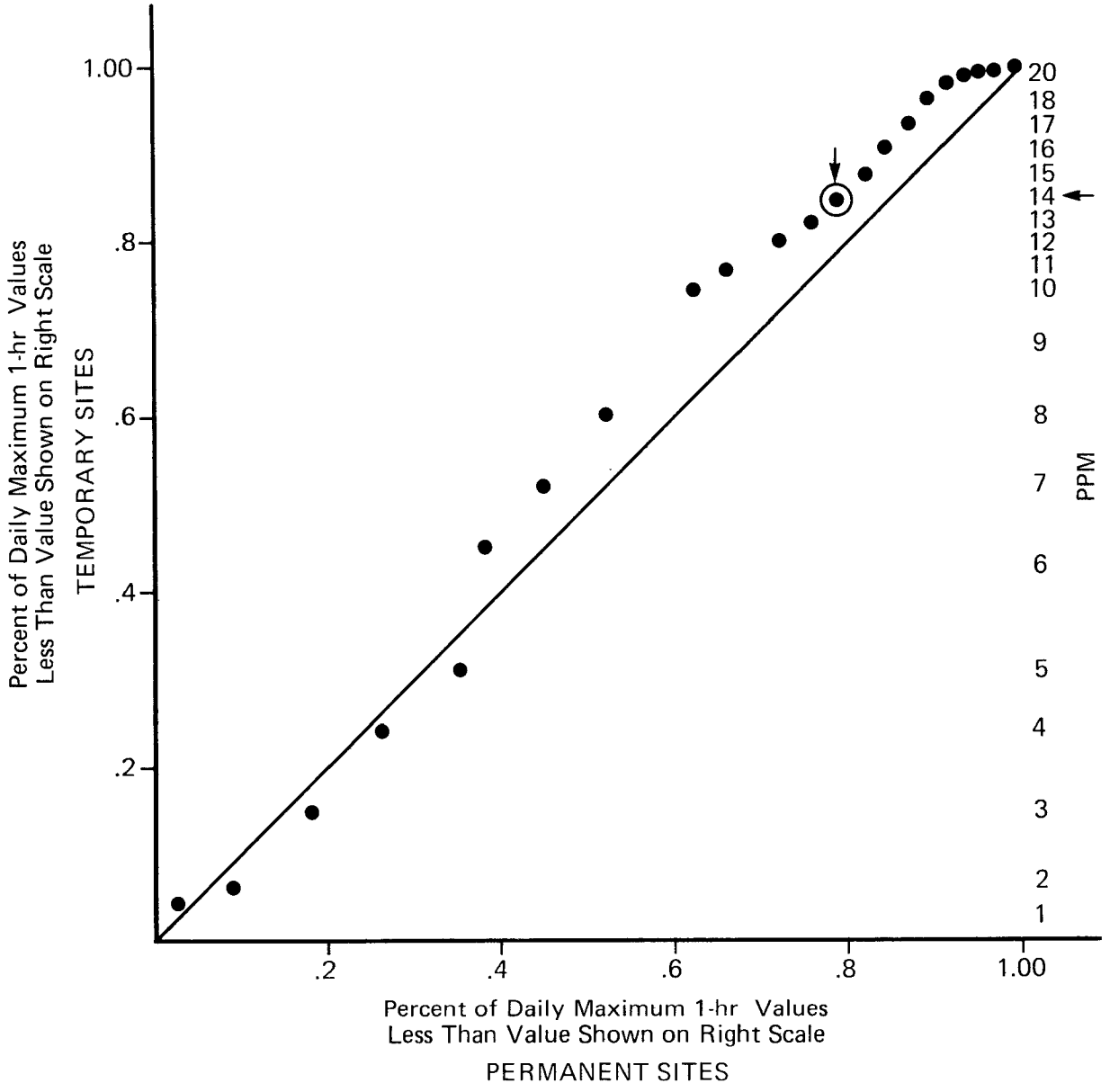

Figure 3. Quantile/Quantile Plot of Permanent vs. Temporary Sites in Denver, Colorado.

The following Washington and Denver data will be further analyzed: 1) questionnaire and diary responses, 2) analysis of personal CO exposure distribution, 3) relationships between breath, personal CO exposure, and activity patterns, 4) significance of selected exposure factors, and 5) fixed vs. PEM data.

SUMMARY AND CONCLUSIONS

Although interpretation of the study results is not possible at this time, we have shown that measuring exposures in an urban area is possible. The willingness of the public to carry monitors and prepare activity diaries has been demonstrated. Although the present monitoring system works, we propose the following improvements: 1) automatic data dumping, 2) keystroke entry of activity information, 3) adding programming capabilities, 4) repackaging to reduce size and weight, 5) improving battery life, size, and recharging time, and 6) modifying pump connections for easier replacement and cleaning.

We also believe a new city should be studied in the winter of 1983-84 to permit a more realistic test of normal cold temperatures, which were not experienced in the winter of 1982-83.

ACKNOWLEDGEMENTS

The complexities involved in the design and execution of this study necessarily mean that a number of individuals contributed to its success. The author thanks the individuals and organizations listed below:

City and County of Denver	Cooper Wayman and Jack Green
Region 8 - Denver	Bill Basbagill, Jim Lehr, Marshall Payne and Charles Stevens
State of Colorado	Steve Arnold, Rick Kramer, and Gordon MacRae
Washington, DC Council of Governments	Allen Delman and Trevis Markle
PEDCo	Ted Johnson and Tom Wey
RTI	Ty Hartwell, Ray Michie, Roy Whitemore, and Harvey Zelon
Rockwell International	Frank Burmann
EMSL/RTP	Ron Drago, Charles Rodes, and Robert Jungers

Personal Exposure to Nitrogen Dioxide

[1]James J. Quackenboss, [2]John D. Spengler, [1]Marty S. Kanarek, [3]Richard Letz, [1]Colin P. Duffy, and [1]Mark D. Lindsay

[1]Department of Preventive Medicine and
The Institute for Environmental Studies
University of Wisconsin
504 North Walnut Street
Madison, WI 53705

[2]Department of Environmental Health Sciences
Harvard School of Public Health, Boston, MA 02115

[3]Department of Physiology,
Harvard School of Public Health, Boston, MA 02115

Abstract

As part of a longitudinal air pollution/health study (Harvard Six Cities Study), personal exposure to NO_2, time spent in various locations and household concentrations were measured for nearly 350 individuals in the Portage, Wisconsin area for one week during both the summer and winter of 1981-1982. Average levels of NO_2 measured outside these homes were 13.55 $\mu g/m^3$ (S.D. 5.64) during the summer, and 15.35 $\mu g/m^3$ (S.D. 6.15) during the winter. Indoor concentrations in homes with gas stoves averaged about 20 $\mu g/m^3$ higher in the summer (mean I/O ratio 2.85) and 36 $\mu g/m^3$ (mean I/O ratio 3.93) in the winter than levels measured outside of the home. Personal exposures were closely related to indoor levels for households with gas stoves ($r=0.80$, $p<0.001$), and electric stoves ($r=0.65$, $p<0.001$). This may reflect the influence of spending nearly 65% of the average day at home in the summer compared with about 15% spent outdoors. An average of less that 5% of the their time was spent outdoors during the winter: the association between outdoor and personal levels of NO_2 was weakest during this season for both gas ($r=0.13$, $p<0.22$) and electric ($r=0.16$, $p<0.14$) stove groups. These measures of exposure and time allocation suggest that there is a wide range of variability in personal exposures to NO_2 that may not be adequately accounted for by simple stratifications based on cooking fuel type.

The work described in this paper was not funded by the U.S. Environmental Protection Agency and therefore the contents do not necessarily reflect the views of the Agency and no official endorsement should be inferred.

Personal Exposures to Nitrogen Dioxide

In the course of daily activities, individuals move about from location to location, breathing samples of the air from each. The amount sampled is determined, in part, by the duration of time spent there, while the magnitude of pollutant present in each location during the specific time periods is a complex function of the ambient background level, of the proximity to sources of pollutant generation and release, and of various mechanisms for removal or dilution. Nitrogen dioxide (NO_2) is formed as a byproduct of high temperature combustion.

Outdoor concentrations are closely related to the proximity of the sampled location to major sources, such as motor vehicle traffic and fossil fuel power plants, to meteorological factors influencing the transfer and dilution of NO_2, and to atmospheric conversion reactions (1). Indoor concentrations are driven, in part, by these outdoor levels as well as by usage patterns for sources of unvented or improperly vented indoor combustion (e.g. gas stoves and unvented kerosene space heaters), by air infiltration and ventilation rates, and by chemical reactions and adsorption or absorption of the gas on indoor surfaces (2,3).

Until recently, epidemiological studies of the health effects of air pollution have relied on measurements of "ambient" air quality that are obtained from fixed location monitoring stations, rather than on the actual exposures of the individuals whose health status is being tested, to draw inferences regarding possible exposure-response relationships (4-7). Several recent reports have indicated that such exposure measurements fail to adequately assess individual exposure (2,5,7,8-12). This inadequacy is acutely apparent for NO_2, since several reports have shown that NO_2

concentrations consistently exhibit a declining gradient as one moves from kitchens with gas stoves to non-kitchen areas in these homes, to outdoor locations nearby, and then to kitchen and non-kitchen locations inside households that use electricity for cooking (13-18). The importance of these departures from fixed station ambient air monitoring results is underscored by summaries of human activity pattern studies (19) indicating that an average of 90% of each day is spent indoors by employed men, while homemakers spent nearly 95% of their time indoors (2,20-23).

Physically, exposure may be defined as the pollutant concentration present at the exchange boundaries of a receptor during specified times. Ott (20) has incorporated both space and time dimensions by conceptualizing exposure as the event that "a person comes into contact with a pollutant." Contact is then specified as the intersection of an individual and a pollutant in the same location at the same time. Location may be narrowly defined in terms of a three-dimensional coordinate system (X, Y, Z), aggregated by existing environmental zones such as rooms or floors within a household, or more broadly classified as inside the home itself. With each level of averaging, some within zone variability may be lost, although these differences are likely to be smaller than those between zones (eg. between homes, or between indoor and outdoor locations) and are probably of minimal health significance (24). At a more general level, Duan (25,26) aggregates locations with homogeneous pollutant concentrations at specified times into microenvironments with concentrations γ_j, and then groups these to form a reduced number of microenvironment types for sampling and modelling purposes. Exposure may then represented as a linear combination of the individual's "sample" average for each microenvironment type (C_k), weighted by his or her time allocation to microenvironments of that type (t_k):

$$E = \Sigma C_k t_k, \quad (k = 1,\ldots,K \text{ microenvironment types}).$$

This model is a generalization of that proposed by Fugas (4) for deriving a "weighted weekly exposure" (WWE) estimate of total exposure by using the concentration measured at one location (γ_j) to represent the levels sampled by individuals in all microenvironments of the same type (C_k). This approach does not incorporate variability among samples collected by different individuals at distinct times, and is sensitive to a potential lack of independence between these individual sample concentrations and individual time allocations. This potential may be realized when pollutants are generated as a result of individual activities, such as cooking or smoking, that are likely to increase in frequency as more individuals are present at a given location. Personal exposure monitoring implicitly incorporates both the time spent in various microenvironments of each type (t_k), and the variability in air samples obtained by different individuals from each microenvironment type (C_k). This allows for direct evaluation of both variability and central tendency for human exposures, and for estimation of average sample concentrations (C_k) for each microenvironment type (26).

The development of a small, inexpensive, and reliable passive monitor for NO_2 by Palmes, et al. (27) has made a large-scale general population study of personal exposures to NO_2 practical. This potential, combined with concerns regarding the adequacy of current exposure assessment practices and with several recent reports advocating personal exposure studies as part of epidemiological investigations into the health effects of air pollution (2,5,8-11,28), have prompted our investigations. The objectives for this study were:

1. To examine the relationship between personal exposure and indoor and outdoor NO_2 concentrations.

2. To explore the association between household members in personal exposures.
3. To determine those household and individual characteristics that are most important in explaining variability in personal exposure.
4. To determine what types of measurements are needed to adequately assess personal NO_2 exposures.

Previous personal exposure studies have demonstrated differences between indoor, outdoor and individual exposures for NO_2 using smaller study populations (29), especially for gas homes (30,31) or those using unvented space heaters (32). Mean personal exposures for families with gas stoves have been shown to be closer to indoor than to outdoor levels, while those using elective stoves were indistinguishable from ambient outdoor measures. In addition, personal exposures to NO_2 were found to be closely related to other family members (30).

Methods

Individual exposure to NO_2, time spent in various locations, and household concentrations were measured for nearly 350 volunteers residing in 82 homes in the Portage, Wisconsin area for one week during both the summer and winter of 1981-1982 as a component of the exposure assessment activities for a longitudinal air pollution/health study (33). Households were separated into groups of approximately 10 homes each that were sampled during the same week-long period to allow for travel time and initial visits to each home. The protocol for these visits included a description of study objectives, and instructions for using the passive diffusion NO_2 monitors and for completing an activity diary. An example diary page was filled out for that day; this was checked for completeness and corrected with each subject to reduce recording errors. All household residents were asked to participate, although

this was not always possible. During the winter phase, short visits were made to each home to return their summer results and to encourage continued participation.

Sample Selection

The target population selected was that of families whose school-aged children were participating in the Harvard Six Cities Study from the Portage area. The basic sampling design was a stratified cluster sample (34) in which the primary sampling unit (cluster) was the family, and the secondary sampling units (elements within cluster) were individual family members. Households were stratified by type of cooking fuel used (gas or electricity). Letters describing the study and requesting volunteers were sent out to obtain approximately equal numbers of gas- and electric-cooking fuel homes. A postage-paid response postcard was provided, and non-respondents were contacted by telephone. A more detailed description of the study was sent to those indicating a willingness to consider participating in the study. From this pool of household units, approximately equal numbers of each cooking fuel type were randomly allocated (without replacement) into a group of homes that were then visited and sampled during the same week.

NO_2 Monitoring

Passive diffusion NO_2 dosimeters developed by Palmes et al. (27) were used to determine week-long average NO_2 concentrations for fixed household locations, and average exposures of individuals. These monitors are simple to use, have a good shelf life before and after exposure, and give results that are both accurate and reproducible (35). Extensive use has been made of these devices for monitoring indoor and outdoor levels of NO_2 (14-16,18,36,37).

Household monitors were placed by project staff outside near the home, in at least one bedroom on each floor, and in the kitchen at 4 to 6 ft. (1.2 to

1.8 meters) in height. Kitchen monitors were placed between 8 and 10 ft. (2.4 to 3.05 meters) from the stove. Indoor monitors were placed to avoid windows, corners, and heating vents; outdoor monitors were located on the shady side of the house, away from driveways, roads, and exhaust vents. Each participant was also assigned a monitor, his or her name was written on tape affixed to the top end, and the monitor identification number was recorded on the activity diary. Volunteers were instructed to wear their monitor at approximately breathing height by clipping it onto their shirt collar or lapel, to keep it outside of coats or jackets, and to keep their monitor nearby when not wearing it.

Integrated average NO_2 concentrations measured by the kitchen monitors and by bedroom monitors on the same floor were grouped together to give one compartment average. When appropriate, NO_2 measurements from non-kitchen floors were aggregated to give a second compartmental average. These two within home averages were then combined to yield a single household average for indoor NO_2 concentrations.

During the winter phase, integrated average NO_2 concentrations were measured inside of 17 schools that were attended by participating children. Monitors were placed in one classroom on each floor, and a school-wide average was estimated from these for the time period sampled. To allow for direct comparison with student's personal monitors, a time-weighted average for each week-long time period during which a group of households was concurrently sampled was calculated. This was done by weighting the school-wide average concentration by the proportion of the time these monitors were exposed that corresponded to each week-long personal monitoring sample period.

Monitors were prepared and analyzed at the Wisconsin State Laboratory of Hygiene using methods based on Palmes et al. (27) with modification by Wolfson

(38). Analyses of replicate pairs of these monitors, used for household measurements, has given a precision estimate of 1.68 $\mu g/m^3$ (18). Their sensitivity has been estimated as approximately 1128 $(\mu g/m^3)h$, with an accuracy of within 10% for these preparation and analysis procedures (39,40).

Survey Materials

For each day of the week-long sampling period, participants recorded the time periods they spent in each of 5 general location categories: (1) Inside of their home, (2) outside (any where), (3) inside of a motor vehicle, (4) inside at work or school, and (5) inside at other indoor locations. The reporting format was developed to derive week-long totals for the proportion of time spent in each category, and was field tested during a pilot study (31). In addition, time spent "cooking or helping to cook" and "near people who are smoking" was also recorded to obtain information about time spent near potential sources of NO_2. However, the lack of a clear relationship between time spent near stoves or smokers and the possible NO_2 emission rate for each (per unit of fuel or per cigarette) makes interpretation of these values difficult. During the winter phase, time periods near smokers at home were separated from those away from home, since the possible effect of smoking within the home on indoor NO_2 concentrations should be included by the monitors located there.

Participants were also instructed to record the amount of time each day that they did not wear their monitor and the location where it was left during this time period. These time periods were tabulated for several locations and the individuals monitored exposure was corrected using the measured concentrations for that location, weighted by the time the monitor was left there (31). For each day, a marginal total for the amount of time spent in each location category was estimated; week-long totals and proportions were derived

from these. Errors in recording leading to potential uncertainties in interpretation were also recorded, as a total number of hours in question.

In order to assess the validity (41) of this reporting procedure for determining average time allocation, a separate format 24-hour recall questionnaire derived from Chapin (42) was administered to a random sample of 12 subjects during the pilot study. For all 5 location categories, the correlation coefficients between the two responses for a one day period exceeded 94%. All 5 correlations were statistically significant with an overall error rate of α=0.025, using the Bonferroni method for non-orthogonal tests (43), indicating that these two methods give approximately the same results. Most discrepancies were due to the limitation of the diary format to 1/2-hour intervals. For longer term, week-long averages this reporting format should provide valid reports of time allocation.

A subject questionnaire was administered during the initial visit to ascertain individual demographic characteristics, smoking habits, and commuting patterns. Ventilation, heating and cooking systems for the workplace as well as potential sources of occupational NO_2 exposure (such as welding, gasoline or diesel engines, gas ovens or flames) were also requested. Characteristics of the schools were determined by interviewing the maintenance and engineering staff for each monitored school.

Household characteristics were detailed using an additional questionnaire that was completed by a parent and returned by mail to our office. This included questions regarding (1) sources, such as the fuels used for cooking, heating water and space heating, the presence of a stove or oven pilot light, and the household cooking patterns; (2) factors potentially influencing ventilation rates such as the kitchen exhaust fan's venting and usage, and the use of plastic on windows to reduce air infiltration, and neighborhood

characteristics. This questionnaire was developed for the study conducted by Spengler et al. (18).

Statistical Analyses

Personal exposures to NO_2 were compared with indoor and outdoor measurements using the sample means for each cooking fuel group, and Pearson product-moment correlation coefficients. As a result of the natural clustering of household members, the variance in individual exposures can be described by a standard Model II (random effects) ANOVA layout (with varying numbers of observations in each family): $\sigma_A^2 + \sigma^2$ where σ_A^2 is the variance component for random differences between households; σ^2 represents individual variability within households (44). From this formulation, an expression for the intra-family (intraclass) correlation between any two members of the same household was used to indicate the proportion of total variance that is associated with household factors that are shared by its members:

$$\rho = S_A^2/(S_A^2 + S^2), \text{ where}$$

$$S_A^2 = (S_b^2 - S_w^2)/\{[\Sigma n_j - (\Sigma n_j^2)/\Sigma n_j]/(N-1)\}$$

estimates σ_A^2, S_b^2 and S_w^2 are the between and within class mean squares, n_j is the number of observations from the jth household ($j=1,\ldots,a$; a is the number of homes), and N is the total sample size (45). Variance of the sample mean is estimated by $var(\bar{x})=S_b^2/N$; the standard error is s.e. $=\sqrt{var(\bar{x})}$ (45).

The relationship between personal NO_2 exposure and individual and household factors was evaluated using stepwise multiple linear regression analysis (46). Logarithms of the NO_2 concentration measurements were taken to compensate for heterogeneity of their variances (47). A pattern of increasing spread with increasing NO_2 concentrations has been previously reported

for indoor NO_2concentrations (18). Missing values for quantitative independent variables were filled to conform to a linear model (47,48) using the BMDP program PAM (49), and the error degrees of freedom appropriately reduced. However, the frequency of missing values was very small, both for individual-level variables (<1%) and for household-level variables (<6%; these cases were primarily missing outdoor monitors), so that these substitutions should have a minor influence on our results. As a consequence of the two-stage nature of this sample (individuals nested within household), a two-stage regression analysis was employed to evaluate household-level variables separately from those specific to the individual.

First, individual characteristics were fit, together with (a-1) indicator variables for household, to the log-transformed personal exposure data. Although this assumes a common slope across households relating these variables to exposure, it was impractical to fit independent slopes to each home given the limited number of observations in each. Averages for personal exposures in each home were adjusted to the same (mean) value for the individual-level variables selected in the stepwise procedure.

In the second stage of analysis, these adjusted household averages were used as response variable to fit a model for the home-level variables. The residual mean square (RMS) from this stage incorporates both the within household variability, and the random factors varying from home to home:

$RMS = S_A^2 + S_w^2/(N/a)$, where S^2 is the estimated among household component of the residual variance; S_w^2 estimates the within-household variance component and is given by the RMS from the first stage regression (49).

In order to compare the ability of various types of measurements to represent personal exposure a series of regression models were fit seperately

for the summer and winter data sets: (a) Outdoor NO_2 concentrations only; (b) Outdoor NO_2 measurements together with household characteristics; (c) Outdoor and indoor NO_2 measurements. Comparisons among these models were made using three summary indices:

(1) The Residual Mean Square (RMS) from the second stage regression; and

(2) The coefficient of variation (CV), using the geometric standard error from the RMS of the regression equation and the geometric mean;

(3) The multiple correlation coefficient, R^2 for the proportion of variance in the second stage data set that was explaned.

Quality Control

Replicate monitors were used for most homes. Allocation of these pairs was rotated between kitchen, bedroom, outdoor, and personal monitor locations. Inter-laboratory analyses of unknowns were compared between the Wisconsin and Harvard laboratories for both phases. All coding, data entry, and correction procedures were verified. For each variable, records having values exceeding two standard deviations from the mean were identified. These cases were then checked for transcription or calculation errors, or for possible explanations of their values.

Results

A total of 357 volunteers from 88 homes participated in the summer phase: 150 were from 38 gas-cooking fuel homes; 207 resided in 50 homes with electric stoves. Of this study population, 142 were classified as workers, 33 as non-workers, and 182 as students. During the winter phase there were 324 participants from 82 homes: 127 were from 34 gas-stove households; 197 were from 48 electric-stove households. There were 127 workers, 26 non-workers, and 171 students during this phase. Relative proportions for each of these three general population classifications were similar across both stove type classification and study phase.

Mean NO_2 concentrations are summarized in Table 1 for these homes and for the participants living there. Average levels of NO_2 measured outside these homes were generally quite low during both phases, with combined means of 13.43 $\mu g/m^3$ and 16.46 $\mu g/m^3$ NO_2 for summer and winter, respectively. The lower outdoor averages for gas stove homes may be attributable to 29 of these homes being located in rural areas, while only 9 were in Portage. In comparison, 38 of the electricstove homes were located in Portage and 12 were rural. The small numbers of households in the Gas-Urban and Electric-Rural cells did not allow for meaningful analysis of possible interactions between community and fuel type. Indoor NO_2 concentrations in homes with gas-stoves were consistantly higher during both the summer and winter phases than those measured outside or inside homes with electric-stoves. To permit comparison of indoor and outdoor levels, difference scores and ratios were calculated; their means are given in Table 1. Mean differences and ratios were largest for gas stove homes. For both gas- and electric-cooking fuel homes, absolute differences were greater in the winter than in the summer phase. Similar patterns are evident for the variability of these measurements: standard deviations were greater for the indoor measurements in the gas stove group,

and increased in the winter, along with the higher concentrations. Mean personal NO_2 exposures for families from homes with gas stoves were closest to, but somewhat below, average indoor concentrations in both their magnitude and variability. For families with electric stoves, the mean for personal exposure was somewhat closer to the outdoor mean in the summer, and between indoor and outdoor means for the winter. The mean of indoor measurements obtained at 17 schools during the winter phase was 15.87 $\mu g/m^3$, which is close to the outdoor mean NO_2 concentration.

Average personal exposures for each household are compared with levels measured outside the home in Figure 1. For the summer phase, there was considerable overlap in average personal exposure between families from homes with gas and electric stoves. In addition, this figure shows the large variability in these averages for personal exposure, especially in the winter phase for families with gas stoves. Linear correlation coefficients between average personal exposure and outdoor levels are shown in Table 2. These were $r=0.40$ ($p<0.001$) for the gas- and $r=0.35$ ($p<0.001$) for the electric-cooking fuel homes in summer, while in the winter the corresponding correlatins were only $r=0.13$ ($p>0.22$) and $r=0.16$ ($p>0.14$). These graphs and their associated correlation coefficients indicate that only a small portion of the variability in average personal NO_2 exposures between families can be accounted for by differences in measurements made outside their homes. In contrast, average indoor home NO_2 concentrations demonstrated a much closer association with the average personal exposures those living there, as is shown in Figure 2 and by the correlation coefficients in Table 2. This association was strongest in gas homes, $r=0.80$ ($p<0.001$) for both summer and winter.

Intra-class correlation coefficients are shown in Table 3 to indicate the proportion of variability in individual personal exposures that may be explained by common characteristics of those micro-environments shared by

individuals from the same home. Given the overall increase in variability in the winter phase relative to the summer phase, it is not surprising that these shared characteristics explained less of this variation in the winter than in the summer phase. However, for gas stove homes, the degree of association between members of the same household for personal exposure was too great to assume that individual measurements were independent--an assumption necessary for least squares regression analysis.

Part of this association may be attributable to time spent at home relative to other locations. Mean percentages for time spent in each of five locations is summarized in Table 4 for workers, non-workers and students during the summer and winter phases. Time spent inside at home was the largest mean proportion for all three groups, with overall mean percentages of 65.41% in the summer and 67.47% in the winter. This implies that the home is the principle location of exposure to air pollutants, although time spent in other locations can not be neglected when considering total integrated exposure. Specifically, time spent at work or school accounted for nearly 20% of the average day during the winter for students and workers, making this an important microenvironment contributing to NO_2 exposures. Working with or nearby welding, gas space heaters, or gasoline engines may be responsible for driving the winter phase personal NO_2 expsoures of 3 individuals from electric stove homes to levels exceeding many of the cases from gas stove homes. In contrast, time spent away from gas-cooking fuel homes may account for some of the overlapping in personal exposures between the two cooking fuel groups.

This activity data and NO_2 measurements were combined to form a partial time-weighted average (TWA) model. Home average indoor and outdoor levels were weighed by the proportion of time spent there, their total was compared with individual exposure measurements rather than the household averages.

The Pearson correlation coefficients were r=0.65 (R^2=0.42) for the gas cooking fuel group, r=0.37 (R^2=0.14) for the electric group in the summer. School exposures were estimated by weighing the school average indoor level by the time spent there for elementary, middle and high school students in the winter phase; this was added to the estimates for home and outdoor exposures. For students, correlations of these TWA estimates were r=0.83 (R^2=0.68) and r=0.68 (R^2=0.46), from the gas-and electric-fuel groups, respectively. Non-student correlations were 0.54 (R^2=0.29) for individuals from gas stove homes, and 0.32 (R^2=0.10) for those having electric stoves.

Individual and household characteristics were evaluated separately using a two stage, stepwise multiple regression analysis. Significant personal characteristics during the summer phase were: (a) full-time worker (vs. student or part-time); (b) commuting distance to and from work each day; (c) sex is female; and (d) working with or near gas furnaces, boilers, ovens, or flames. In the winter phase, significant predictors included (a) working with or near welding or cutting torches (arc or flame), and (b) the individual's age. Household characteristics were evaluated using the adjusted average personal exposures for each home as the response variable. The presence of a stove pilot light, outdoor NO_2 concentration, and having a gas clothes dryer were significant predictors for the summer data set, explaining 45% of the variation in the adjusted household averages for log transformed personal exposures (CV=6.7%, RMS=0.07). During the winter, the use of gas as the cooking fuel was the significance home-level predictor, with R^2=67.1 (CV=7.4, RMS=0.13).

For comparing the ability of distinct types of measurements to represent personal exposures, two additional models were fit. The first assumes that only outdoor NO_2 concentrations and a simple geographic classification (urban vs. rural) are available; the second assumes that indoor averages for

kitchen and non-kitchen zones, and an overall indoor average NO_2 concentrations are available. For the summer data, the first model had an R^2=11.7% (CV=7.16, RMS=0.101), compared with R^2=67.3% (CV=6.3, RMS=0.041) for the second model and with R^2=44.5% for the model based on home characteristics. Measurements of NO_2 outside the home gave an R^2=9.0% (CV=9.33, RMS=0.36) during the winter, compared with R^2=82.9 for the model using indoor NO_2 measurements, and with R^2=67.1 for the home characteristics model.

The coefficient of variation (CV) for 93 replicate pairs of Palmes' tubes was 4.52% for the summer phase. Absolute differences were less than 5 $\mu g/m^3$ in 98% of these pairs, with a precision estimate (square root of ½ the variance of the difference scores) of 1.0 $\mu g/m^3$. For the winter monitoring phase the CV was 4.99%, and the precision estimate was 1.32 $\mu g/m^3$ for 81 replicate pairs. Absolute differences were less than 5 $\mu g/m^3$ in 95% of these. Inter-laboratory comparisons gave a difference between means for the Wisconsin and Harvard laboratories of 1.16 $\mu g/m^3$ or 3.3% (S.D. of difference scores, 1.6 $\mu g/m^3$) for summer, and 3.29 $\mu g/m^3$ or 6.51% (S.D. of difference scores, 3.56 $\mu g/m^3$) for the winter phase, indicating generally good agreement between these labs.

Discussion

The relationships between mean indoor and outdoor NO_2 concentrations observed in this study compare favorably with several previous investigations in demonstrating the close association between the use of gas for cooking and elevated levels of NO_2 inside of homes, with the magnitude of departure from outdoor concentrations being greatest during the winter when both intentional ventilation and unintentional infiltration rates may be reduced, and stove use is likely to be increased (13-16,18,50). Conversely, average indoor NO_2 concentrations in electric stove homes were below those measured outdoors, possibly explained by the reactive nature of NO_2 (3). This difference was also increased in during the winter, suggesting that for NO_2 being inside these homes may be protective against exposure to outdoor levels. Given the proportion of time spent at home by our study population, the levels of NO_2 they are exposed to there contribute a major time concentration component to their total personal exposures. This impact is most apparent in both the mean comparisons and correlations between indoor and personal NO_2 exposures for the gas stove households. By comparison outdoor measurements are a poor estimator of personal exposures, especially during the winter when more time is spent indoors and the levels of NO_2 found there differ most from those outdoors.

These results have several consequences for epidemiological studies of the health effects of air pollutants, from both outdoor and indoor sources. By using only the outdoor component of exposure, several key confounding variables are omitted from consideration. These have been identified in our regression analyses for personal characteristics such as occupation and occupational exposures (welding, gas fire equipment), and as age and sex. For household characteristics, indoor NO_2 concentrations were closely associated

with individual exposure. The variability in these concentration measurements could only be partially represented by source (gas stove, pilot light, gas dryer) and ventilation factors of the home as related to personal exposures. Errors in the determination of the independent variable, exposure, may have especially serious consequences for the ability of health studies to derive an exposure-response relationship, since these errors may bias parameter estimates to falsely imply the presence or absence of an effect.

Were all cases to conform to their group means both for indoor NO_2 levels and for activity patterns, adjustment of ambient air pollution monitoring data to estimate personal exposures would be simple. However, measures of central tendency fail to convey information regarding the considerable variability observed here and by other investigators for indoor NO_2 concentrations. Yet this is precisely what is implied by statistically controlling for the presence of indoor sources in covariate-type analyses of the health effects of air pollution.

A similar problem is presented to those studies attempting to demonstrate health effects associated with the use of gas as opposed to electric stoves. Although the group means for personal NO_2 exposure diverge, this study demonstrates that there is a considerable overlap between these two groups. This overlap might be attributable to variability in exposures experienced in other locations, which in turn is related to the individual's own pattern of activities. Such misclassification of individual exposures will reduce the sensitivity of these studies. It also may explain some of the inconsistancies in their results, and of suggested modification of health impacts over time. Biological changes in children as they grown older may make them less susceptible to environmental challenges, but social changes may modify their exposures by altering their mobility patterns. As less time is spent at home

and more is allocated to school and other locations, this will alter the individual's total integrated exposure even though he or she remains classified as having a gas or electric stove.

Acknowledgements

The interest, cooperation, and hospitality of the participating families are greatly appreciated, as is the assistance given by the staff of the Pardeeville, Portage, and Rio school systems. We acknowledge the efforts of William Knight for his assistance with graphics and programming, of Dr. Mari Palta for her suggestions for data analysis, and Gary Hoffman at the Wisconsin State Laboratory of Hygiene for his assistance in the preparation and analysis of the monitors. This study was supported primarily by a grant from Wisconsin Power Companies, and through a cooperative agreement between the Environmental Monitoring Surveillance Laboratory (EMSL) of the U.S. EPA and the Harvard School of Public Health.

REFERENCES

1. National Academy of Sciences. Nitrogen oxides. ISBN 0-309-02615-6. National Academy of Sciences, Washington, D.C., 1977. 333 pp.

2. National Academy of Sciences. Indoor pollutants. ISBN 0-309-03188-5. National Academy Press, Washington, D.C., 1981. 537 pp.

3. Yocom, J.E. Indoor-outdoor air quality relationships. A critical review. J. Air Pollut. Control Assoc. 32: 500, 1982.

4. Fugas, M. Assessment of total exposure to an air pollutant. In: Proceedings of the International Conference on Environmental Sensing and Assessment. Vol. 2. IEEE #75-CH 1004-1 ICESA. Paper No. 38.5. Las Vegas, Nevada. September 14-19, 1975.

5. Morgan, M.G. and Morris, S.C. Needed: A national R+D effort to develop individual air pollution monitor instrumentation. J. Air Pollut. Control Assos. 27: 670, 1977.

6. Sexton, K., Letz, R. and Spengler, J.D. Human exposures to nitrogen dioxide: Exposure modeling and risk assessment. Paper 82-48.6 presented at the 75th Annual Meeting of the Air Pollution Control Association, New Orleans, Louisiana. June 20-25, 1982.

7. Lebowitz, M.D. Health effects of indoor pollutants. Ann. Rev. Public Health. 4: 203, 1983.

8. National Academy of Sciences. Energy in transition 1985-2010. ISBN 0-7167-1228-8. W.H. Freeman and Company, San Francisco, California, 1979. 677 pp.

9. U.S. Environmental Protection Agency. Air monitoring strategy for state implementation plans. EPA 450/2-77-010. U.S. Environmental Protection Agency, Office of Air Quality Planning and Standards, Research Triangle Park, North Carolina, 1977.

10. Chapter III - Environmental agents. In: Epidemiology of Respiratory Diseases Task Force Report, July 1979. U.S. Department of Health and Human Services. NIH Publication No. 81-2019. U.S. Government Printing Office, Washington, D.C., 1980.

11. Young, G.S., Hagopian, J.H., Hoyle, E.R. Potential health effects of residential energy concentration measures. Final Report. Report No. GRI-79/0097. Arthur D. Little, Inc., Cambridge, Massachusetts, 1981.

12. Hauser, T.R., Scott, D.R., and Midgett, M.R. Air monitoring: Research needs. Environ. Sci. Technol. 17: 86A, 1983.

13. Wade, W.A., Cote, W.A., and Yocom, J.E. A study of indoor air quality. J. Air Pollut. Control Assoc. 25: 933, 1975.

14. Palmes, E.D., Tomczyk, C., and DiMattio, J. Average NO_2 concentration in dwellings with gas or electric stoves. Atoms. Environ. 11: 869, 1977.

15. Melia, R.J.W., Florey, C. du V., Darby, S.C., Palmes, E.D., and Goldstein, B.D. Differences in NO_2 levels in kitchens with gas or electric cookers. Atmos. Environ. 12: 1379, 1978.

16. Goldstein, B.D., Melia, R.J.W., Chinn, S., Florey, C. du V., Clark, D., and John, H.H. The relation between respiratory illness in primary schoolchildren and the use of gas for cooking: II. Factors affecting nitrogen dioxide levels in the home. Int. J. Epidemiol. 8: 339, 1979.

17. Keller, M.D., Lanese, R.R., Mitchell, R.I., and Cote, R.W. Respiratory illness in households using gas and electricity for cooking: I. Survey of incidence. Environ. Res. 19: 495, 1979.

18. Spengler, J.D., Duffy, C.P., Letz, R., Tibbitts, T.W., and Ferris, B.G. Nitrogen dioxide inside and outside 137 homes and implications for ambient air quality standards and health effects research. Environ. Sci. Technol. 17: 164, 1983.

19. Szalai, A., (ed.). The Use of Time: Daily Activities of Urban and Suburban Populations in Twelve Countries. Mouton Publichers, The Hague, Netherlands, 1972.

20. Moschandreas, D.J., Zabransky, J., and Pelton, D.J. Comparison of indoor and outdoor air quality. Final Report. EPRI EA-1733. Electric Power Research Institute, Palo Alto, California, 1981.

21. Ott, W.R. Models of human exposure to air pollution. Technical Report No. 32. SIAM Institute for Mathematics and Society, Standford University, Standford, California, 1980. 67 pp.

22. Dockery, D.W. and Spengler, J.D. Personal exposure to respirable particulates and sulfates. J. Air Pollut. Control Assoc. 31: 153, 1981.

23. Moschandreas, D.J. Exposure to pollutants and daily time budgets of people. Bull. N.Y. Acad. Med. 57: 845, 1981.

24. Moschandreas, D.J., Zabransky, J., and Pelton, D.J. Comparison of indoor-outdoor concentrations of atmospheric pollutants. Final Report for the Electric Power Research Institute. GEOMET Technologies Inc., Gaithersburg, Maryland, 1980.

25. Daun, N. Micro-environment types: A model for human exposure to air pollution. Working Draft. WD-908-1-HHS. Rand Corporation, Santa Monica, California, 1981. 24 pp.

26. Duan, N. Models for human exposure to air pollution. N-1884-HHS/RC. Rand Corporation, Santa Monica, California, 1982. 15 pp.

27. Palmes, E.D., Gunnison, A.F., DiMattio, J., and Tomczyk, C. Personal sampler for nitrogen dioxide. Am. Ind. Hyg. Assoc. J. 37: 570, 1976.

28. Morris, S.C. Personal monitoring of air pollution exposures. Environ. Int. 5: 69, 1981.

29. Silverman, F., Corey, P., Mintz, S., Olver, P., and Hosein, R. A study of effects of ambient urban air pollution using personal samplers; a preliminary report. Environ. Int. 8: 311, 1982.

30. Dockery, D.W., Spengler, J.D., Reed, M.P., and Ware, J. Relationships among personal, indoor and outdoor NO_2 measurements. Environ. Int. 5: 101, 1981.

31. Quackenboss, J.J., Kanarek, M.S., Spengler, J.D., and Letz, R. Personal monitoring for nitrogen dioxide exposure: Methodological considerations for a community study. Environ. Int. 8: 249, 1982.

32. Nitta, H. and Maeda, K. Personal exposure monitoring to nitrogen dioxide. Environ. Int. 8: 243, 1982.

33. Ferris, B.G., Speizer, F.E., Spengler, J.D., Dockery, D.W., Bishop, Y.M.M., Wolfson, M., and Humble, C. Effects of sulfur oxides and respirable particles on human health: I. Methodology and demography of population in study. Am. Rev. Resp. Dis. 120: 767, 1979.

34. Kish, L. Survey Sampling. Wiley, New York, New York, 1965.

35. Palmes, E.D. Development and application of a diffusional sampler for NO_2. Environ. Int. 5: 97, 1981.

36. Palmes, E.D., Tomczyk, C., and March, A.W. Relationship of indoor NO_2 concentrations to use of unvented gas appliances. J. Air Pollut. Control Assoc. 29: 392, 1979.

37. Melia, R.J.W., Florey, C. du V., Morris, R.W., Goldstein, B.D., Clark, D., and John, H.H. Childhood respiratory illness and the home environment: I. Relations between nitrogen dioxide, temperature and relative humdity. Int. J. Epidemiol. 11: 155, 1982.

38. Wolfson, M.J. Modifications to the Palmes diffusion tube preparation and analysis methods. Quality Assurance Document, Vol. II. Harvard Six City Study, Harvard School of Public Health, Cambridge, Massachusetts, 1980.

39. Apling, A.J., Stevenson, K.J., Goldstein, B.D., Melia, R.J., and Atkins, D.H.F. Air pollution in homes: Validation of diffusion tube measurements of NO_2. Report LR311 (AP). Warren Spring Laboratory, Herfordshire, England, 1979.

40. Cadof, B.C., Knox, S.F., and Hodgeson, J.A. Personal exposure samplers for NO_2. Draft Report. National Bureau of Standards, Washington, D.C., 1979.

41. Gordis, L. Assuring the quality of questionnaire data in epidemiologic research. Am. J. of Epidem. 109: 21, 1979.

42. Chapin, F.S. Human Activity Patterns in the City. Wiley-Interscience, New York, New York, 1974.

43. Neter, J. and Wasserman, W. Applied Linear Statistical Models. Richard D. Irwin, Inc., Homewood, Illinois, 1974.

44. Snedecor, G.W. and Cochran, W.G. Statistical Methods. 7th ed. Iowa State Unviersity Press, Ames, Iowa, 1980.

45. Rosner, B. Donner, A., and Hennekens, C.H. Significance testing of interclass correlations from familial data. Biometrics. 35: 461, 1979.

46. Draper, N.R. and Smith, H. Applied Regression Analysis. 2nd ed. Wiley, New York, New York, 1981.

47. Weisberg, S. Applied Linear Regression. Wiley, New York, New York, 1980.

48. Donner, A. The relative effectiveness of procedures commonly used in multiple regression analysis for dealing with missing values. Amer. Statist. 36: 378, 1982.

49. Dixon, W.J. (ed.). BMDP Statistical Software 1981. University of California Press, Berkeley, California, 1981. 726 pp.

50. Daniel, C. and Wood, F.S. Fitting Equations to Data. 2nd ed. Wiley, New York, New York, 1980.

51. Cote, W. A., Wade, W.A., Yocom, J.E. A study of indoor air quality. Final report. EPA-650/4-74-042. U.S. Environmental Protection Agency, Washington, District of Columbia, 1974, pp. 282.

TABLE 1. INDOOR, OUTDOOR AND PERSONAL MONITOR NO_2 CONCENTRATIONS ($\mu g/m^3$) FOR BOTH PHASES AND STOVE TYPES

Phase	Stove	Location	Mean	S.D.	Mean I-O Diff	Mean I/O Ratio	a*
Summer	Gas	Indoor	29.60	11.67	17.90	2.85	(38)
		Outdoor	11.54	5.06			(38)
		Ave. Personal†	25.33	7.67			(38)
	Elect.	Indoor	12.33	4.89	-2.65	0.86	(50)
		Outdoor	15.17	5.62			(47)
		Ave. Personal†	17.93	4.91			(50)
Winter	Gas	Indoor	50.61	23.48	36.43	3.93	(34)
		Outdoor	15.35	6.15			(33)
		Ave. Personal†	44.02	16.65			(34)
	Elect.	Indoor	9.63	5.15	-7.71	0.60	(48)
		Outdoor	17.24	5.53			(47)
		Ave. Personal†	15.57	5.94			(48)

*Number of households (a).
†Average personal exposure for each household.

TABLE 2. PEARSON PRODUCT-MOMENT CORRELATION OF HOUSEHOLD AVERAGE PERSONAL NO_2 EXPOSURE WITH INDOOR AND OUTDOOR CONCENTRATIONS*

Phase	Stove	Location Indoor	Outdoor	Kitchen	a
Summer	Gas	0.80	0.40	0.78	(38)
	Elect.	0.66	0.35	0.69	(50)
Winter	Gas	0.80	0.13†	0.75	(34)
	Elect.	0.65	0.16†	0.65	(48)

*All p-values (that r=0) <0.001 except as noted.
†p>0.22.
†p>0.14.

TABLE 3. INTRACLASS CORRELATION (ρ) BETWEEN MEMBERS OF THE SAME HOUSEHOLD FOR PERSONAL NO_2 EXPOSURE

Phase	Stove	ρ	S_A^2	S^2	a*	N†
Summer	Gas	0.63	45.67	26.62	38	150
	Elect.	0.24	12.82	40.48	50	206
Winter	Gas	0.50	194.51	194.29	34	127
	Elect.	0.19	16.88	71.73	48	197

*Number of households.
†Number of valid personal exposures.

TABLE 4. MEAN PERCENT TIME SPENT IN VARIOUS LOCATIONS FOR 3 POPULATION GROUPS

Phase	Location	Population Group			Combined Totals
		Workers	Non-Workers	Students	
Summer	Home	59.32	75.22	68.34	65.41
	(S.D.)	(11.92)	(12.11)	(12.46)	(13.28)
	Outside	12.33	12.91	14.96	13.73
	(S.D.)	(9.13)	(9.87)	(9.31)	(9.35)
	Motor Vehicle	5.79	4.43	3.30	4.39
	(S.D.)	(4.22)	(2.72)	(4.26)	(4.28)
	Work/School	15.52	0.19	4.40	8.41
	(S.D.)	(10.87)	(0.76)	(7.81)	(10.60)
	Other Indoors	7.04	7.24	9.00	8.06
	(S.D.)	(6.38)	(6.38)	(9.57)	(8.2)
	N	137	32	177	346
Winter	Home	66.07	83.25	66.14	67.47
	(S.D.)	(11.41)	(8.39)	(10.12)	(11.47)
	Outside	3.31	1.87	3.86	3.49
	(S.D.)	(5.35)	(2.01)	(3.29)	(4.17)
	Motor Vehicle	5.62	4.25	3.25	4.24
	(S.D.)	(5.56)	(2.50)	(2.57)	(4.14)
	Work/School	18.64	3.04	19.47	17.85
	(S.D.)	(10.36)	(7.05)	(7.49)	(9.70)
	Other Indoors	6.36	7.59	7.27	6.95
	(S.D.)	(6.00)	(5.34)	(6.19)	(6.05)
	N	127	26	176	329

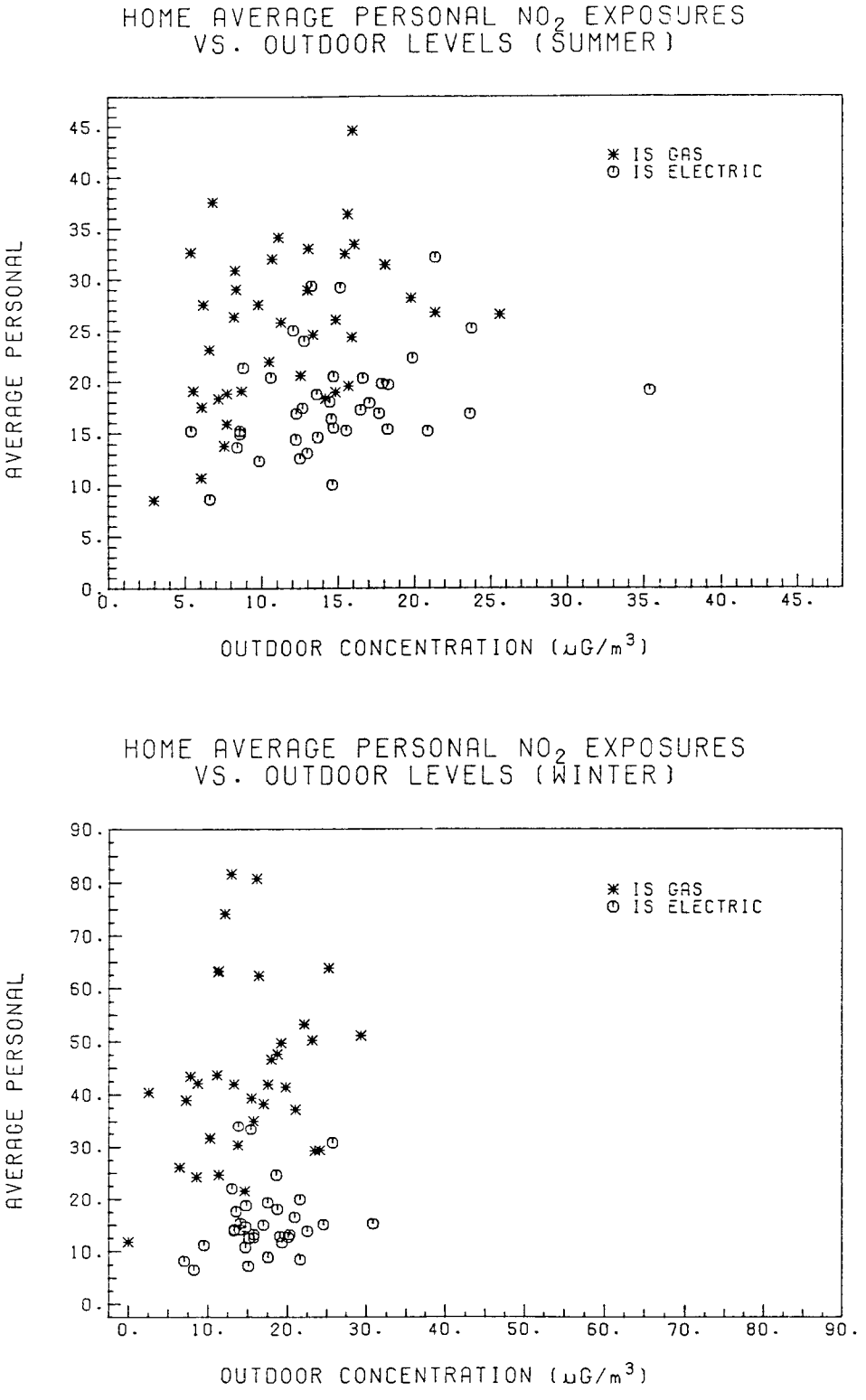

Figure 1. Average personal NO_2 exposure for each household compared with outdoor concentrations for summer and winter.

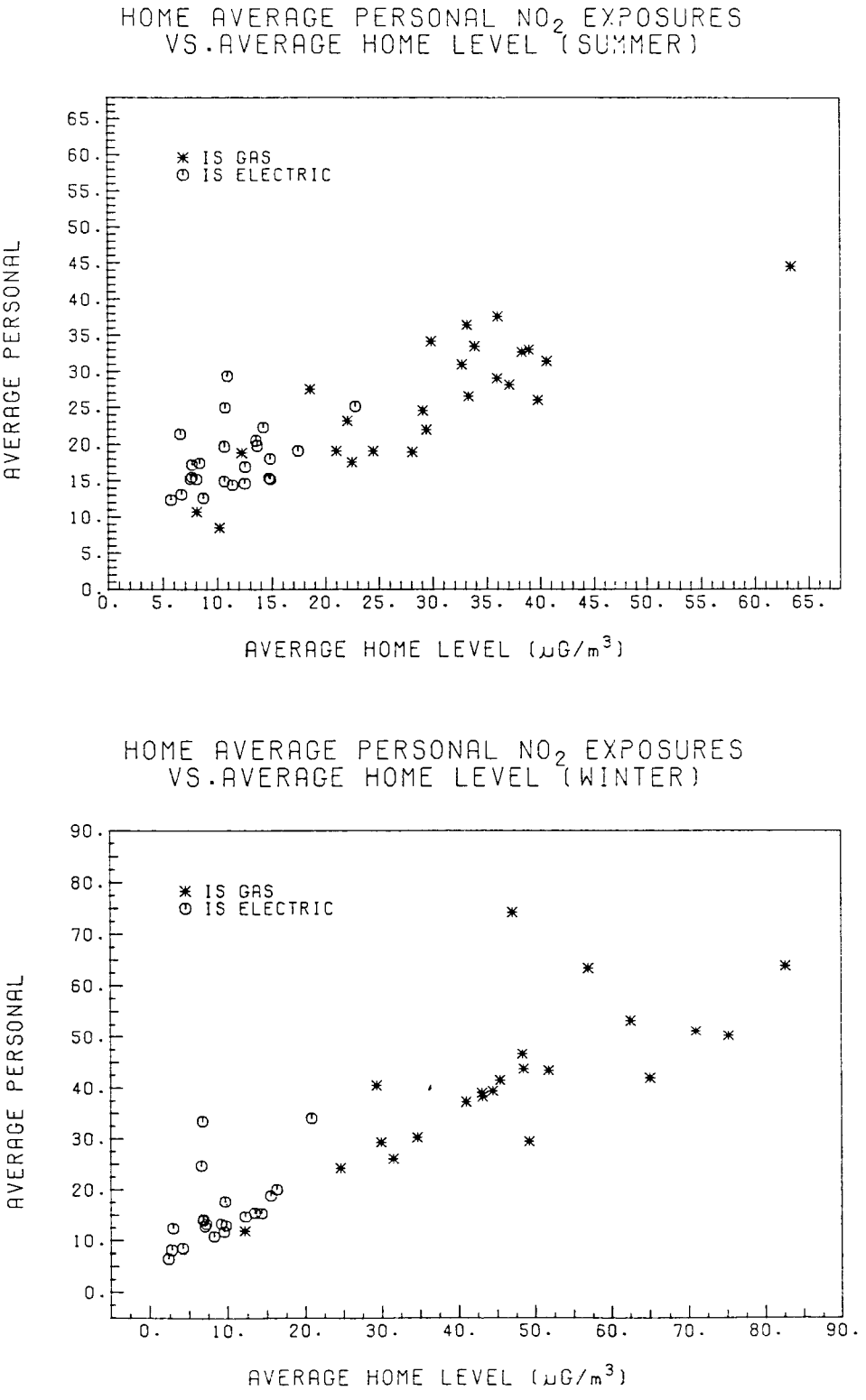

Figure 2. Average personal NO_2 exposure for each home compared with average indoor concentrations for summer and winter.

COMPARISON OF PERMEATION AND DIFFUSION-TYPE PASSIVE SAMPLERS VERSUS CHARCOAL TUBE COLLECTION OF SELECTED GASES

BY

PHILIP W. WEST, Ph.D. and A.S. Lorica, Ph.D.

WEST-PAINE LABORATORIES, INC.

7979 GSRI AVENUE

BATON ROUGE, LOUISIANA 70820

AND

JOHN W. STORMENT, C.I.H.

WESTERN ELECTRIC COMPANY

9595 MANSFIELD ROAD

SHREVEPORT, LOUISIANA 71130

ABSTRACT

A study has been made of the performance characteristics of permeation-type samplers (REAL, Inc.), diffusion-type devices (3M and DuPont) and charocal tube collection of four gases of interest. The gases studied were Freon 113, trichloroethylene, 1,1,1-trichloroethane, and perchloroethylene. Concentrations of the gases were ten, fifty, one hundred, and one hundred fifty per cent of the respective TLV's with face velocities of 50 and 500 ft. per minute. Temperatures of 20°C and 30°C, and relative humidities of 30% and 80% were included.

Passive monitors are recommended. The permeation-type monitors were essentially free of problems arising from environmental variables and gave consistently good results. They can be considered the most reliable, accurate, and generally satisfactory devices for personal monitoring as determined for the gases studied. The diffusion-type samplers were found to show errors of as much as 99% when used in humid atmospheres, but were generally satisfactory for use in atmospheres having humidities below 80 percent.

INTRODUCTION

Previous studies of the performance characteristics of passive monitors have been limited to diffusion-type samplers such as the DuPont Pro-Tek and 3M 3500 badges (1,2). The permeation-type passive monitor developed at Louisiana State University, by West and his co-workers (3,4,5,6,7,8) has yet to be studied alongside the diffusion-type monitors and the charocal tube. It was the purpose of this investigation to compare the performances of the diffusion-type monitors, represented by 3M and DuPont Pro-Tek, the permeation-type monitors, represently by REAL Minimonitor (Reizner Environmental Analytical Laboratory, P.O. Box 3341, Baton Rouge, Louisiana 70821), and the charocal tube in an atmosphere containing four organic chlorine compounds encountered in the dry-cleaning industry and in metal degreasing, namely, Freon 113, (1,1,2-trichloro-1,2,2-trifluoroethane), 1,1,1-trichloroethane, trichloroethylene, and tetrachloroethylene (a.k.a. perchloroethylene).

EXPERIMENTAL

Organic Vapors and their Concentrations

Test mixtures of the following compounds representing approximately 10%, 50%, 100%, and 150% of their respective TLV's were made by injecting appropriate amounts of the pure liquids which were either AR grade or were spectroscopic quality.

Freon 113 - For spectroscopic use.

1,1,1-Trichloroethane - MCB Reagents, 98% by GC.

Trichloroethylene - Certified ACS Reagent; Fisher Scientific Co., Chemical Mfg. Division, Fairlawn, N.J. 074010

Perchloroethylene - For spectroscopic use.

Standard Gas

The standard gas that was used to calibrate the GC gas results was supplied by Gas Analytical Services, Inc. 10172 Mammoth Ave. Baton Rouge, Louisiana 70814, according to the following specifications: Freon 113, 109 - 121 ppm; 1,1,1-trichloroethane, 46.0 - 48.1 ppm; trichloroethylene, 18.0

- 18.3 ppm; and perchloroethylene, 18.6 - 20.8 ppm.

The Exposure Chamber

The exposure chamber was an elongated toroid, closed loop type designed by West-Paine Laboratories, Inc. The chamber main body, with a volume of 80 L, was made of 1/8" and 3/8" Teflon-coated "Lucite" SAR, E.I. DuPont de Nemours Co., Inc. The Teflon-coated inside surface of the chamber served to minimize adsorption of the test vapor molecules. The chamber was essentially an assembly of two parrallel long arms of rectangular cross-section, joined together at each end by a U-joint, one of which housed the blower used to mix and circulate the mixture of gaseous test species.

The monitors were placed in the two long arms of the chamber which were accessible through removeable but tight-fitting covers.

Face velocity was measured with Datametrics Dresser 100 VT Air Velocity and Temperature Meter with the probe inside the chamber operative on the hot-wire anemometer principle.

A "Linseis" LS 64 Linear Strip Chart Recorder used in connection with a Type "K" thermocouple gave a continuous print-out of the temperature inside the chamber.

Two "Neptune" Dyna Pumps, Model 2, Universal Electric Co. Michigan, equipped with Teflon diaphragms were located outside the chamber. One pump was used in the network to sample automatically the gas mixture inside the chamber; the other was used to draw the gaseous mixture inside the chamber through the charocal tubes and back to the chamber through Cole-Parmer flowmeter, Model FM 042-15 with 150 mm flowtube and stainless steel float, Cole-Parmer Instrument Co.,Chicago, IL 60648.

A Perkin-Elmer Gas Chromatograph Sigma 115 System continuously monitored the concentrations of the organic pollutants in the chamber. A 15' x 1/8" x 0.012" GC column was used packed with 20% SP-2100 - 0.1% carbowax 1500 on Chromosorb W, HP 80/100 mesh.

The gas sampling network consisted on one 10-port Valco Air-Activated gas sampling valve. Two 10-mL sampling loops were connected to this valve such that one loop was continuously being flushed with fresh samples as the other was loading sample onto the analytic column. A 3-way ASCO 832061 stainless steel body, stainless steel seat ASCO solenoid, controlled through the GC data processor was used to sample the pollutant mixture inside the chamber.

The relative humidity inside the chamber was continuously monitored with a Lab-Line Electro-hygrometer, Lab-Line Instruments, Inc. Melrose Park, IL.

Experimental Procedure

Exposure of Monitors, Desorption and GC Analysis

Five to ten monitors were positioned inside the chamber facing the gas flow and at sufficient distance from the blower motor to avoid turbulent flow. A measured amount of each liquid organic pollutant was injected into the injection port with the appropriate Hamilton GC syringe. After the last liquid had been injected, the blower motor and GC sampling network were immediately activated and the starting time recorded. Only mixtures of the four organic pollutants representing either 10%, 50%, 100%, or 150% TLV of each pollutant were used. By means of an "MSA Ventilation Smoke Tube Kit" Part No. 458481, Mine Safety Appliances Co., Pittsburgh, PA 15208, instantaneous mixing inside the chamber was observed when the blower was run at a speed that would give an air flow of 500 ft/min.

The monitors were exposed to the pollutant mixture for more than five hours. After exposure, the monitors were taken out of the chamber for immediate analysis or set aside in the freezer for later study.

The analyses involved desorption with either one mL (for charcoal tubes), three mL (for diffusion-type monitors) or five mL (for REAL monitors) of pre-cooled carbon disulfide, GC grade, J.T. Baker Chemical Co., Phillipsburg, N.J. 08865, followed by the GC separation and

determination of the pollutants in the carbon disulfide solution after at least an hour of contact between the CS_2 and the adsorbent taken from each monitor. A second chromatographic run of this solution was made and the results were averaged for each pollutant. The order of elution was: 1) Freon 113; 2) 1,1,1-trichloroethane; 3) trichloroethylene; and 4) perchloroethylene.

In addition to the predetermined amount of pollutants introduced into the chamber, the face velocity, temperature, and relative humidity were also controlled. Two face velocities were used: 1) 50 ft/min, to correspond to the air flow in a laboratory where there is little movement of air or personnel; and 2) 500 ft/min, to simulate air motion in a laboratory where a great deal of relevant movement takes place. The temperature either at $30^{o} \pm 2^{o}C$ or $20^{o} \pm 2^{o}C$. The relative humidity was kept either in the 20 - 40% or 70 - 90% range except that at low temperature the relative humidity was maintained in the 60 - 70% range.

In experimental runs where the chamber leaked as shown by an uncharacteristically rapid decrease in the concentrations of the pollutants measured,volumes of the pure liquids were subsequently injected into the chamber to restore as closely as possible the initial concentrations.

For the calibration of the REAL Monitors, each monitor was filled with 1.35 g of activated charcoal (20 - 40 mesh, Lot 382, supplied by REAL, Inc.). The permeation constant, k, of each monitor for each pollutant was determined by exposing the monitor to a mixture of all four pollutants for the same length of time used in the actual experimental run.

The sampling rates for the charocal tubes ranged from 2.09 mL/min to 22 mL/min, depending upon the concentration of the pollutant mixture. The sampling rate used was the maximum possible without breakthrough of the pollutants.

RESULTS

The k values used in the calculations for the permeation-type REAL monitor are given in Table 1.

TABLE I - Permeation Constants, k*

Monitor No.	Freon 113		1,1,1-Trichloroethane		Trichloroethylene		Perchloroethylene	
1	504	532	181	194	116	87.6	64.4	90.6
2	492	500	175	182	114	82.9	65.5	89.2
3	468	511	174	187	117	87.3	67.2	95.9
4	491	509	178	177	115	80.6	66.3	86.9
5	638	683	225	236	137	105	76.6	110
6	432	446	153	150	96.1	66.1	56.1	72.8
7	479	538	173	183	108	82.8	61.1	93.7
8	485	537	178	184	112	84.1	65.1	95.9
9	493	594	179	198	116	89.5	64.6	101
10	447	491	162	167	109	77.9	62.7	95.2

* The first column is for values at 30°C and 30% R.H.; the second, for 20°C and 60 - 70% R.H.

The temperature effect on the permeation constant noted by West and co-workers (3,4,8) is evident for Freon 113, perchloroethylene, and 1,1,1-trichloroethane. The k values for trichloroethylene, on the other hand, decreased with temperature which could mean a decrease in its mass transfer rate through the permeable membrane with increase in temperature. The following summary of the range of values of the coefficient of variation of the permeation constants gives an indication of the precision involved.

	Freon 113	1,1,1-trichloroethane	Trichloroethylene	Perchloroethylene
Coefficient of Variation	5.0 - 11	9.5 - 15	2.2 - 8.4	15 - 23

The percentage relative error, which by definition, is the absolute error divided by the true value, expressed in percentage, is given in Table

2. It might be pointed out that the true value was taken to be the value given by the GC sampling network. By absolute error is meant the difference between the value shown by a particular monitor and the true value.

At 30°C and 26 - 28% relative humidity and 500 ft/min face velocity, the diffusion-type 3M 3500 and the REAL minimonitor showed good accuracy. The other diffusion-type monitor, DuPont Pro-Tek, did not perform as well as 3M and REAL. However, at 50 ft/min face velocity, the DuPont Pro-tek had improved accuracy. The 3M and REAL devices also performed well at 50 ft/min face velocity but the latter seemed less able to hold perchloroethylene (9). At 20°C the REAL monitor performed excellently for all pollutants studied. This behavior towards perchloroethylene, also shown by the charcoal tube, might be characteristic of activated charcoal, the absorbent used in these monitors. This view is supported by a series of experiments involving the use of different kinds of activated charcoal in the REAL minimonitor, which gave consistently low values for perchloroethylene.

At high relative humidity, which often attends the actual use of these personnel monitors, only the REAL monitor and the charcoal tube continued to function well; the DuPont and 3M monitors apparently could not retain the pollutant molecules in the presence of a large number of highly polar water molecules.

The coefficient of variation of the TWA values had the following range of values:

Charcoal tubes, 3.3 - 16;

3 M, 1.3 - 18;

DuPont, 1.7 - 26;

REAL, 2.4 - 18

It might be pointed out that the frequency of occurrence of the higher values was relatively low. The confidence in passive monitors inspired by impressive evidence presented in recent publications (1-8)

seems to be justified.

Using an error ceiling of 35% and the data in Table 2 as basis for comparison of the overall performance of the three passive monitors studied, it can be seen that only 16% of the REAL data go beyond the error ceiling as compared with 27% and 41%, respectively, for the 3M and DuPont data. Of the three passive monitors included in this investigation, the permeation-type REAL minimonitor showed, on the whole, dependable performance. Indeed, it might be convenient and timely to adopt the permeation-type REAL monitor as standard in place of or at least equivalent to the charcoal tube.

CONCLUSIONS

1. Passive monitors, whether diffusion - or permeation-type, are as reliable as the charocal tube.
2. Of the three passive monitors included in this work, only the permeation-type REAL minimonitor continued to perform well at high relative humidity.
3. On the whole, therefore, the permeation-type REAL monitor came out with a better performance and it might now be time to adopt it as standard in place of the charcoal tube.

ACKNOWLEDGMENTS

Financial support from the following organizations is gratefully acknowledged:

Council for International Exchange of Scholors, Eleven Dupont Circle, N.W. Suite 300, Washington, D.C. 20036, which administers the Fulbright-Hays Fellowships, supported Dr. Lorica for 11 months;

Philippine-American Educational Foundation, 12th Floor, Magsaysay Center, 1680 Roxas Blvd., Manila, Philippines, underwrite the travel expenses of Dr. Lorica to and from the United States.

University of the Philippines, Quezon City 3004, Philippines, granted sabbatical and research leaves consecutively to Dr. Lorica.

Louisiana State University, Baton Rouge, LA 70803-1804, U.S.A., where Dr. Lorica was visiting scholar.

West-Paine Laboratories, Inc. 7979 GSRI Avenue, Baton Rouge, LA 70820, U.S.A., supported Dr. Lorica upon termination of CIES funding.

The work described in this paper was not funded by the U.S. Environmental Protection Agency and therefore the contents do not necessarily reflect the views of the Agency and no offical endorsement should be inferred.

REFERENCES

1. Feigley, Charles E. and Chastain, James B. An experimental comparison of three diffusion samplers exposed to concentration profiles of organic vapors Am. Ind. Hyg. Assoc. J. 43(4): 227
2. Voelte, D. R. and Weir, F. W. A dynamic-flow chamber comparison of three passive organic vapor monitors with charcoal tubes under single and multiple solvent exposure conditions Am. Ind. Hyg. Assoc. J. 42(12): 845 (1981).
3. Reiszner, K. D. and West, P. W. The collection and determination of sulfur dioxide incorporating permeation and the West-Gaeke procedure Environ. Sci. Technol. 7: 526-32 (1973).
4. McDermott, D. L., Reiszner, K. D. and West, P. W. Development of long-term sulfur dioxide monitor using permeation sampling Environ. Sci. Technol. 13: 1087 (1979).
5. Bell, D. R., Reiszner, K. D. and West, P. W. A permeation method for the determination of average concentrations of carbon monoxide in the atomsphere Anal. Chim. Act 77: 245-254 (1975).
6. Nelms, L. H., Reiszner, K. D. and West, P. W. A personal vinyl chloride monitoring device with permeation technique for sampling Anal. Chem. 49: 994-998 (1977).

7. Hardy, J. K., Dasgupta, P. K., Reiszner, K. D. and West, P. W. Personal chlorine monitor utilizing permeation sampling Environ. Sci. Technol. 13: 1090-1093 (1979).

8. Ryan, Roland L. and West, Philip W. A hydrogen fluoride personal monitor using permeation sampling Am. Ind. Hyg. Assoc. J. 43: 640-44 (1982).

9. Gergory, E.D. and Elia, V.J. Sample retentivity properties of passive organic vapor samplers and charocal tubes under various conditions of sample loading, relative humidity, zero exposure level periods and a competitive solvent. Am. Ind. Hyg. Assoc, J. 44: (2) 88 - 96 (1983).

TABLE 2
PERCENTAGE RELATIVE ERROR

50 Ft/MIN FACE VELOCITY

		10% TLV		50% TLV		100% TLV		150% TLV	
FREON 113	C. Tube	-2.2	+13	-18	+11	-3.8	-2.2	+22	+3.3
	3M	-9.7	-76	-1.8	-88	-16	-85	-38	-87
	DuPont	-4.9	-89	-25	-95	-47	-92	-69	-91
	REAL	+3.6	+3.2	-8.0	+5.4	-5.8	-5.0	-17	-6.8
1,1,1 TRICHLOROETHANE	C. Tube	+3.3	+16	-17	+16	-0.5	+1.6	-14	+9.0
	3M	-13	-26	-14	-46	-17	-44	-5.6	-53
	DuPont	-11	-48	-24	-74	-30	-68	-35	-64
	REAL	-19	-14	-18	-17	-25	-21	-8.2	-7.2
TRICHLORO-ETHYLENE	C. Tube	+18	+27	-8.0	+33	+14	+11	-14	+24
	3M	-28	+14	-28	-10	-20	+5.1	+24	-4.6
	DuPont	-23	+28	-26	+13	-13	+14	+19	+24
	REAL	-13	+11	-25	+12	-18	+4.2	+5.1	+6.9
PERCHLORO-ETHYLENE	C. Tube	-24	-14	-41	-18	-26	-24	-46	-23
	3M	-19	-7.3	-24	-12	-19	-16	-6.8	-25
	DuPont	+1.7	+37	-8.4	+8	+4.8	+4.5	+12	+18
	REAL	-46	-37	-38	-33	-50	-40	-39	-39

500 Ft/MIN FACE VELOCITY

		10% TLV		50% TLV		100% TLV		150% TLV	
FREON 113	C. Tube	+7.6	+5.7	-24	-12	-5.5	+3.4	-1.7	+4.2
	3M	+5.3	-80	+1.3	-85	-11	-88	-25	-84
	DuPont	-7.5	-91	-18	-93	-53	-94	-57	-94
	REAL	-1.2	-1.0	-9.7	+17	-13	+3.2	-12	-10
1,1,1 TRICHLOROETHANE	C. Tube	+13	+12	-22	-9.4	+0.5	+28	+4.6	+9.2
	3M	+8.7	-25	-2.0	-46	-3.9	-49	-8.6	-45
	DuPont	+9.0	-56	-2.4	-72	-18	-76	-21	-77
	REAL	-2.6	+0.8	-12	-2.4	+0.7	-3.4	-2.4	-0.3
TRICHLORO-ETHYLENE	C. Tube	+30	+16	-13	+2.7	+13	+39	+16	+18
	3M	-8.7	+36	-16	-6.9	-25	0	-8.0	+0.8
	DuPont	+7.1	+106	-6.0	+22	+12	+23	-8.2	+24
	REAL	0.0	+20	-3.8	+42	-1.1	+36	+5.1	+41
PERCHLORO-ETHYLENE	C. Tube	-15	-17	-47	-37	-28	-11	-25	-24
	3M	-18	0	-12	-27	-31	-24	-9.3	-18
	DuPont	+36	+99	+45	+28	+58	+23	+35	+68
	REAL	-3.2	+20	-13	-10	-1.5	-7.8	+3.5	+1.2

NOTE: At each TLV the left column gives values at 30% R.H., right column values at 80% R.H.

SESSION V

ACID DEPOSITION

AUTOMATED ACQUISITION, FILTERING AND REDUCTION OF ION CHROMATOGRAPHIC DATA

RICHARD C. GRAHAM, JOHN K. ROBERTSON, AND JEFFREY S. POULIN

SCIENCE RESEARCH LABORATORY

US MILITARY ACADEMY

WEST POINT, NEW YORK 10996

In the past several years, few problems have received the national and international attention that acid precipitation has received (1,2). For informed decisions about pollution control strategies to be reached by policymakers, large amounts of data on the chemical composition of precipitation must be amassed. This data must address and be able to define trends in chemistry and hopefully to delineate sources of pollution from which acid is derived. Trends in the spatial and temporal variability of precipitation are being addressed by national networks such as the National Atmospheric Deposition Program, the MultiState Atmospheric Precipitation Sampling Program, and the Canadian Sampling Program (3). In addition to these deposition oriented networks, a need exists to sample a storm from beginning to end on a systematic basis such as reviewed by Robertson et. al. (4). An intensity weighted sampler used by the Science Research Laboratory at the US Military Academy collects one sample of 7 ml volume every 0.01" of precipitation. For each sample collected a rather complete ionic chemistry workup is desired so as to obtain pH, concentration of major cations (monovalent and divalent) and major anions. With average precipitation of 47" per year at West Point, it became obvious early in our effort that we must

automate as much as possible every aspect of our data collection, storage, and processing effort. We chose to begin our automation effort with the ionic chemistry analysis since this would represent the largest savings of time.

INSTRUMENTATION

Since the originally designed DIONEX Model 14 was initially only capable of determining either anions or cations, a second detector and associated circuitry were obtained from DIONEX and the system replumbed to allow for use of both sets of columns at the same time. Anion analyses are performed using the 500 mm x 3 mm or two 250 mm x 3 mm separator column(s) followed by a 6 x 250 mm suppressor column. The eluent is the 0.0024 M $NaHCO_3$/0.003M Na_2CO_3 prepared by diluting 2 gms of each anhydrous salt to 8 liters using > 15 megohm-cm deionized water. Monovalent cation (Na^+, NH_4^+, K^+) analysis was performed using a 6 x 250 mm separator column followed by a 9 x 250 mm suppressor column. A 0.007 M HNO_3 eluent is prepared by dilution of 55 ml 1 N HNO_3 solution to 8 liter using > 15megohm-cm deionized water. Deionized water is obtained from a Millipore water treatment system consisting of a reverse osmosis column, carbon adsorption column, two mixed bed strong ion exchange resins and a 0.2 micron particulate filter.

A Varian 8055 liquid chromatographic autosampler was added to enhance the DIONEX capabilities. A Valco ACV-10-UHPa-N60 10 port sampling valve with two 100 microliter sampling loops was used to allow the simultaneous injection of a single sample onto each of the sets of columns on the ion chromatograph. The sampling valve is plumbed as in Figure 1.

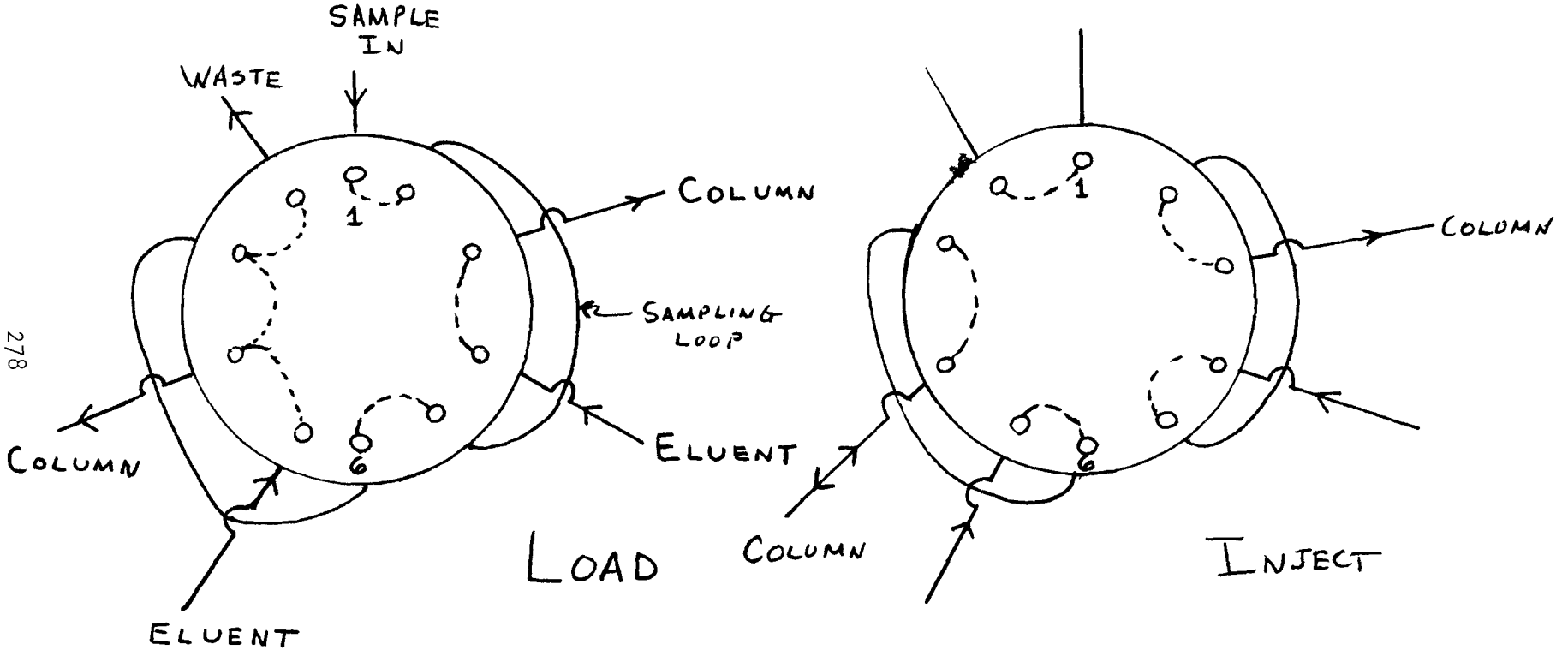
SAMPLE IN
WASTE
COLUMN
SAMPLING LOOP
ELUENT
COLUMN
ELUENT
1
6
LOAD
COLUMN
COLUMN
INJECT

The original sampling loop as supplied by DIONEX was left in the eluent flow line as the ion chromatograph is used both for research and for teaching.

OBJECTIVES

The objectives defined at the outset of the project were as follows:

1. To provide a physical link between the DIONEX and a microcomputer.
2. To provide a link between the Varian Autosampler and a microcomputer.
3. To convert the analog signal from the DIONEX to a digital signal for input to the microcomputer.
4. To have the autosampler signal the microcomputer when a sample is injected.
5. To read the rack and vial number of the sample being analyzed.
6. To provide a sample control system.
7. To store the digital information for later processing.
8. To smooth the digital data by an accepted technique.
9. To process the smoothed data to obtain peak height, peak area and retention time of each peak.
10. To sort the output file from objective 9 to include sample identification data from the sample control system.
11. To transfer the sample data from the microcomputer to a mainframe computer for archival, statistical analysis, etc.

To date all but objectives 6, 10 and 11 have been fully implemented. Programming efforts on the remainder are continuing. We are also pursuing a means to accomplish objective 9 simultaneously with the acquisition of the analog data which will require a foreground/background programming effort.

The overall system is shown as block flow charts in Figure 2 and 3. The program operation can be divided into four sections -- Administrative, Data Acquisition, Data Storage, and Data Processing. Each of the subsystems will be discussed in subsequent paragraphs.

Administrative

The administrative portion of the code is an interactive session allowing the analyst to enter run conditions, date, number of samples to be analyzed, number of wash vials, source of sample, etc. The answers to the questions asked during the session control the naming of two types of data storage files -- a file containing the sample identification, run conditions, etc. and a second which contains the digital chromatographic data. It is anticipated that as the software continues to develop that the header file will be accessed to determine if the sample being analyzed is a standard or not, and then using the standards for construction of calibration charts. If the sample is an unknown, then the peak height will be converted to concentration. At this time, the conversion of peak heights to concentration still requires some "manual" manipulations of the data files. Work is ongoing to fully automate this process. The data files are dynamically created during the run as the rack and vial number are read at the autosampler.

Data Acquisition

To write the computer code for the acquisition of data from the ion chromatograph and from the autosampler, the internal workings of the

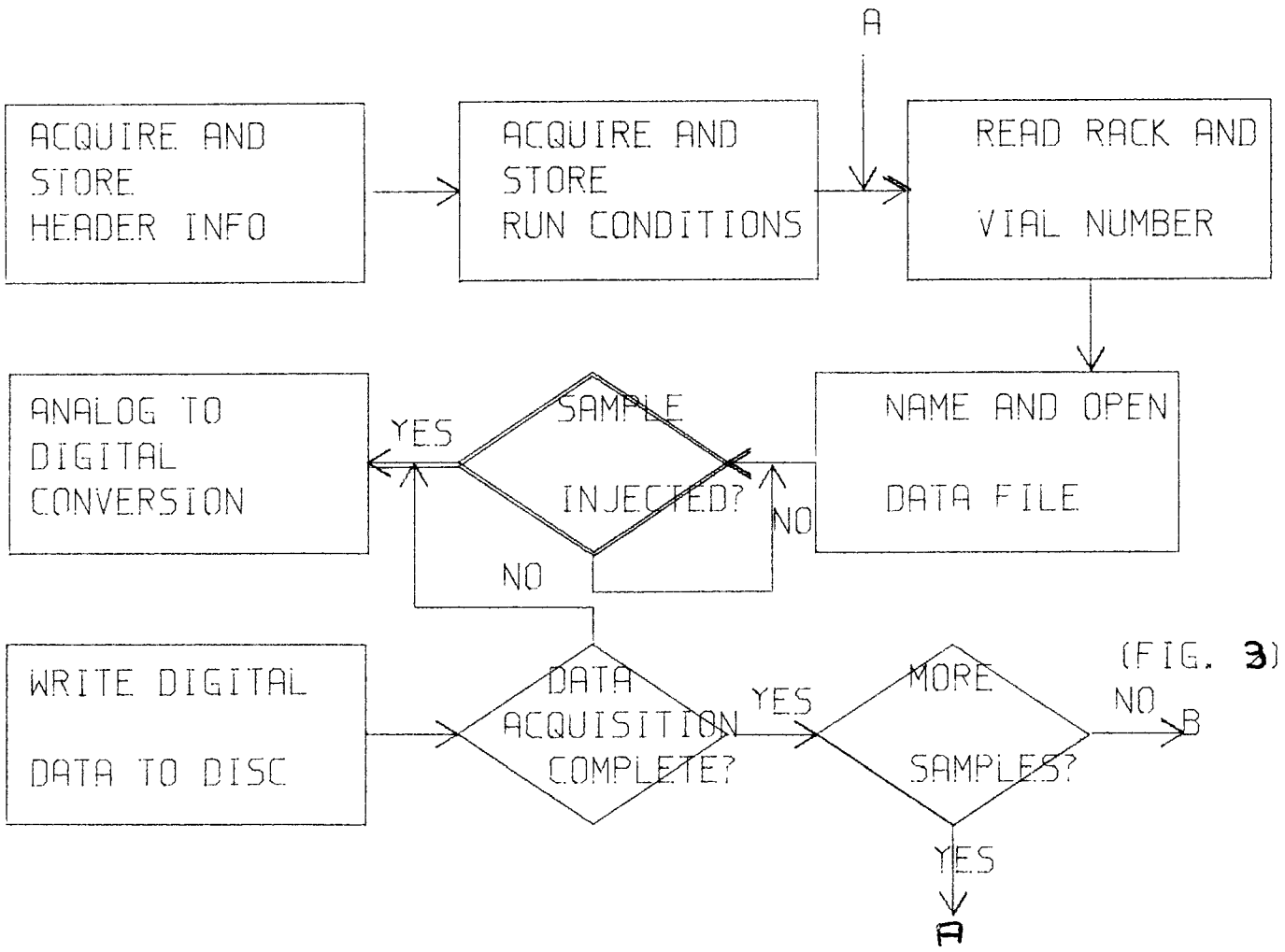

FIGURE 2 FLOW CHART FOR ADMINISTRATIVE, DATA ACQUISITION, AND DATA STORAGE

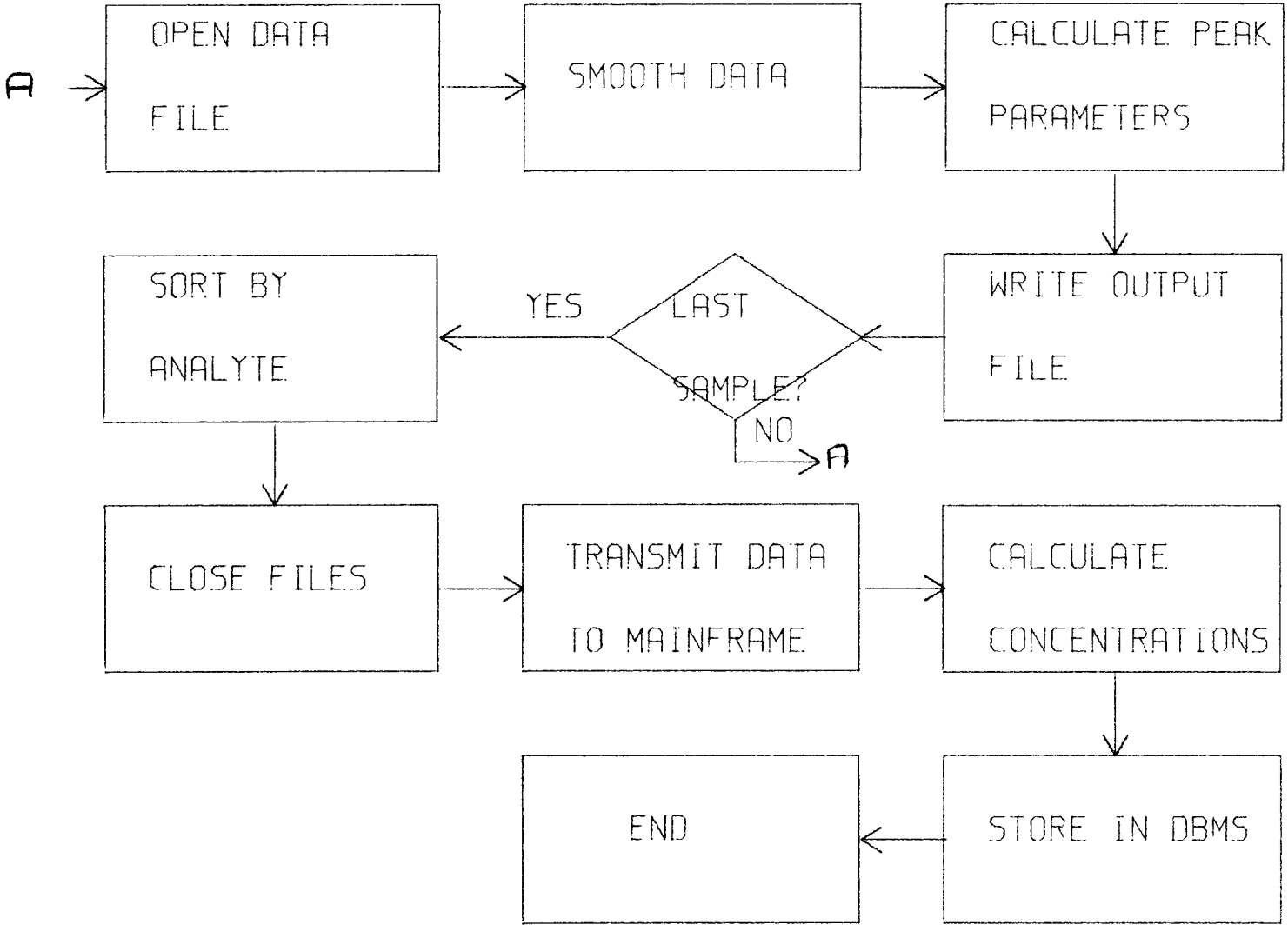

FIGURE 3 FLOW CHART FOR DATA PROCESSING

autosampler had to be completely understood. The timing of actions in the program had to be closely linked to the sequencing of events occurring in the autosampler and to the signals from the ion chromatograph. The autosampler is placed in operation by depressing the multiple/single run button. As the rack rotates under the injection needle, the program delays for several seconds. When the needle has pierced the septum, the rack and vial number information is available as 5 bit binary coded decimal (BCD) output on the interface cable. This information is read by a parallel digital board on the microcomputer and is immediately used to dynamically name and open a data file for the chromatographic data. Since the inject cycle on the autosampler allows for flushing of the tubing carrying sample to the injection loops, the program waits for a signal from the autosampler that the Valco valve has turned to the inject position (See Figure 1).

The signal is quite weak and required that an amplifier circuit be built (Figure 4) which could be detected by the Schmitt Trigger on the Minc. The 0-1 volt signal from the DIONEX is fed via 22 gauge copper wire to the preamplifier on the MINC which allows programmable "autogaining" of the preamplifier. The signal is then fed through the internal bus structure of the MINC to the analog to digital converter. The Schmitt Trigger on the MINC initiates the acquisition and conversion of the analog signal to digital form. Simultaneously a realtime clock is triggered to maintain the time of a run and also to control the timed acquisition of data. The clock module generates interrupts to the processor to signal that an Analog-Digital conversion must be made. Data acquisition requires that buffers be initialized and subsequently filled with the converted data. Data acquisition continues until

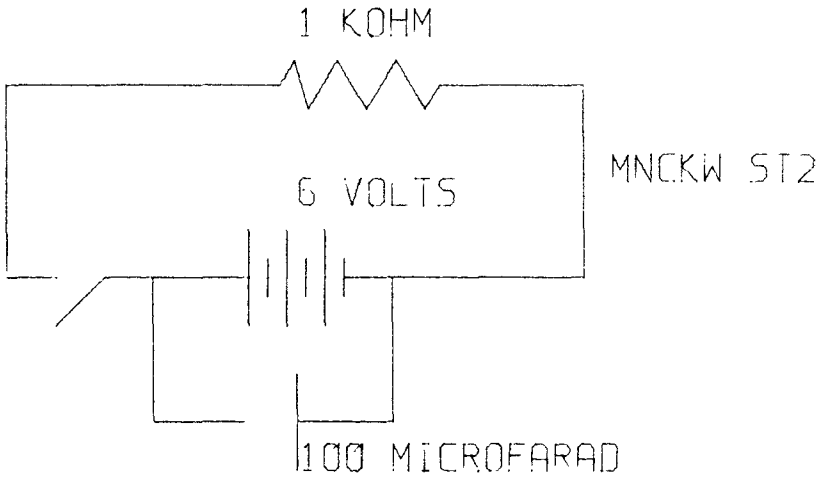
1 KOHM
MNCKW ST2
6 VOLTS
100 MICROFARAD

the run time as specified by the operator is exceeded. The data as acquired is in integer form, and must, therefore, be converted to floating point. All of the buffer management and integer to floating point conversion is handled by system subroutines. The preceding is continued until the rack and vial number that are read indicate that a stop pin has been encountered, at which time data acquisition ceases and data processing begins.

Data Storage

After the data is acquired from the DIONEX and is resident in the memory of the microcomputer, the data is transferred to either a floppy disc or the hard disc of the microcomputer system. The files as explained earlier are named and opened as the rack and vial number of the sample are read from the autosampler.

Data Processing

Data is smoothed using a modified Savitzky-Golay smoothing technique (5,6). The particular technique is a seven point moving box car average. Hacker, et. al. (7) and Walraven (8) indicate that significant shift in the position of a peak may be caused by a single pass of such a smoothing routine. They also showed that insignificant loss of peak height and no resultant peak shift would occur if the algorithm smoothing the peaks were to include four passes--the first and third from time equal zero to end of run, and two and four from time equal to the end of run to zero.

The expression for the filter function is:

$$y(n+3)=\frac{(x(n-3)+x(n-2)+\ldots+x(n+2)+x(n+3))}{7} \qquad (1)$$

where y(n+3) is the value of the filtered data point and the x(n-3), etc. are the values of the unfiltered data points.

The transfer function, H(f), of this filter formula exhibits unity gain for low frequency output. Higher frequencies are greatly attenuated so that almost no high frequency "noise" appears in the output data. For the moving average filter, the transfer function is:

$$H(f)=A+2\sum_{K=1}^{M} A\cos 2 K f t \qquad (2)$$

where f = the frequency of the input data and t = the sampling rate. For a seven point filter, K=3 and M=2. This gives the transfer function:

$$H(f)=\frac{1+2\cos 2 f t + 2\cos 4 f t + 2\cos 6 f t)}{7} \qquad (3)$$

A graph of H(f) versus 2 ft enables visualization of the filtering action

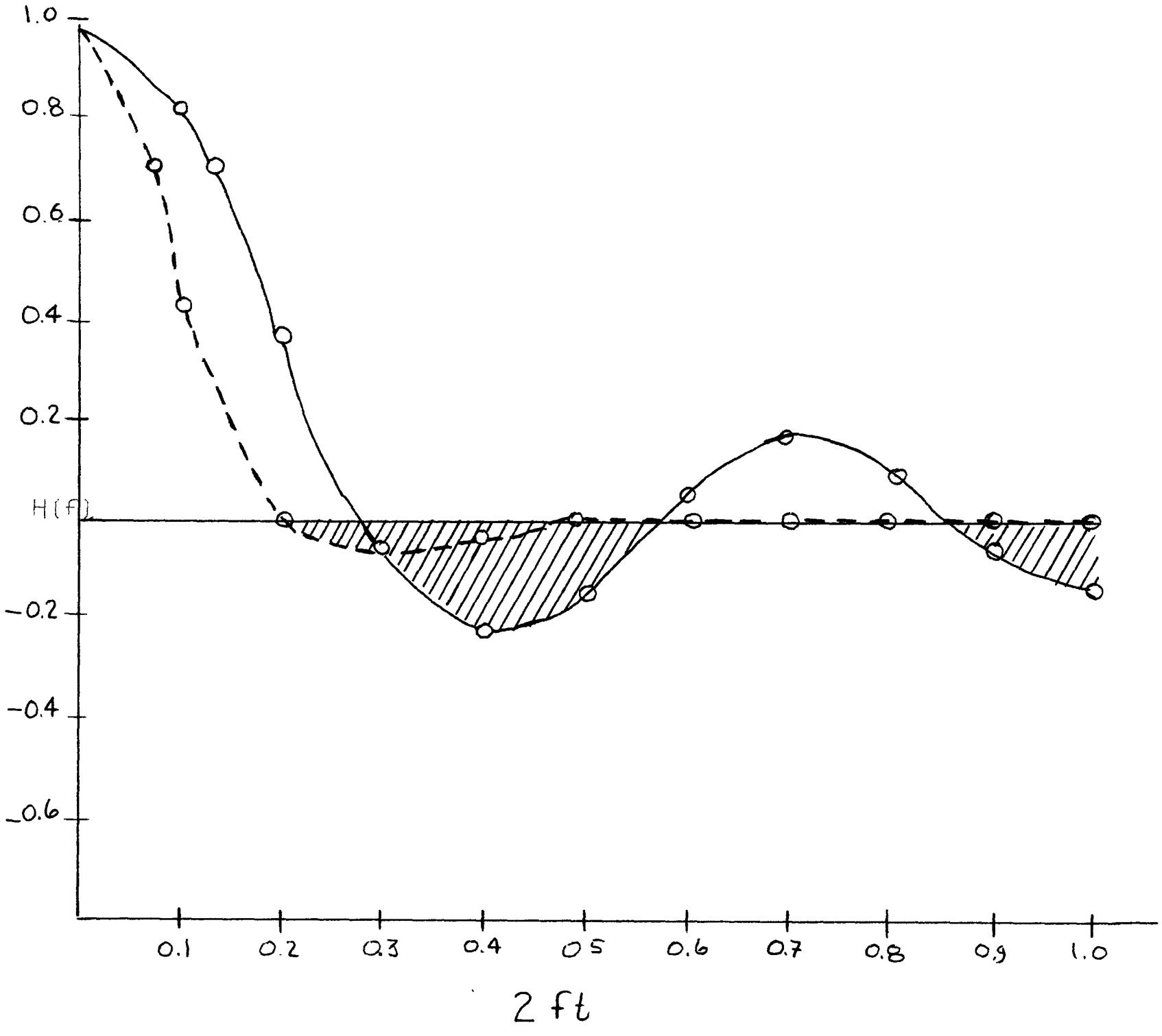
1.0
0.8
0.6
0.4
0.2
H(f)
-0.2
-0.4
-0.6
0.1
0.2
0.3
0.4
0.5
0.6
0.7
0.8
0.9
1.0
2 ft

The dashed graph represents the transfer function of the smoothing filter employed in the program. It represents the effect of four passes of the moving average formula on the data. The solid graph represents the effect of one pass. As can be seen, the effect of four successive applications of the filter is that noise above a frequency component (2 ft) of 0.20 is for all practical purposes eliminated.

Whereas for the single pass, only those frequency components of 2 ft equal to 0.28, 0.56 and 0.85 are eliminated. In the region between these values, the frequency components are passed and for the region $0.28 \leq 2\ ft \leq 0.56$, the amplitude is reversed, thus subtracting from the net signal.

The peak height, peak width, retention time, and several other parameters were determined using chromatography peak processing routines on the MINC. After all of the peaks have been identified and the peak areas tabulated, the data is transferred via a Network communications package to a larger mainframe system for conversion of the peak heights to concentrations using a linear least squares fit of peak height vs. concentration calibration curve. The resulting concentrations and other sample identification data are stored on the mainframe using the RIM-5 data base system. Data retrieval and subsequent statistical analysis of data are accomplished on the mainframe.

Future work

In the future, we plan to streamline the working of the program to allow more efficient use of the computer resources and to allow for simultaneous processing and acquisition of data. Several other routines for the sorting and merging of data are currently being written.

REFERENCES

1. Carter, J., Environmental Priorities and Programs, Message to the Congress, 2 August 1979.

2. Memorandum of Intent Between the Government of Canada and the Government of the United States of America Concerning Transboundary Air Pollution, signed 5 August 1980.

3. Wisneiski

4. Robertson, J.K., R.C. Graham and T.W. Dolzine, Chemistry of Precipitation from Sequentially Sampled Storms, EPA 600/4-80-004, US Environmental Protection Agency, Research Triangle Park, NC, 1980, 117 pages.

5. Savitzky, A., and M.J.E. Golay, Smoothing and Differentiation of Data by Simplified Least Squares Procedures, Anal. Chem. 36:1627,1964.

6. Steiner, J., Tremonia and DeHour, Comments of the Smoothing and Differentiation of Data by Simplified Least Squares Procedure, Anal. Chem. 44:1909,1972.

7. Hacker, H., R.C. Graham, and J.K. Robertson, Interfacing a Digital MINC-11 Microcomputer with a Polarograph, Proceedings of the Digital Equipment Computer Users Society Symposium, Los Angeles, 1981, p.467-473.

8. Walraven, R., Digital Filters, Proceedings of the Digital Equipment Computer Users Society, San Diego, California, 1980, p.827-834.

DESIGN AND TESTING OF A PROTOTYPE

RAINWATER SAMPLER/ANALYZER

Richard J. Thompson
School of Public Health
University of Alabama in Birmingham
Birmingham, AL 35294

A device for the collection and analysis of rainwater has been conceptualized; component parts are undergoing testing. The sampler will record the temperature, pH, conductivity and volume of collected rain samples and note the time of capture/analysis. Ions from samples of known volume will be trapped for subsequent laboratory analysis.

Performance characteristics will be presented which are designed to meet the short-term needs of meteorological modeling and atmospheric chemists as well as the long-term needs of soil scientists.

The collection and analysis of precipitation matter is vital to the definition and understanding of the "acid rain" problems. It has been shown that there are grave problems in the monitoring of rainwater (1,2), and that samples decay on standing (2-10). Even in laboratories which should be among the best, the measurement of all constituents in all samples varies by over a factor of 2 and some constituents measurements in some samples varies by over a factor of 10 in both rain (5) and synthetic deposition samples (11). This could mean that there is potentially an error of at least ± 0•3 and as much as ± 1•0 pH units in the monitoring data being collected today. Even in data from the National Atmospheric Deposition (NADP) program one may note a difference of one pH unit between field and laboratory measurements for some samples.

The errors existent in monitoring the chemical constituents of rainwater, pH, and conductivity are largely ignored, although this problem has been addressed in the literature (1,8,9). It has been shown that phosphate, nitrate and ammonium are unstable, in the order given (3,4,5,10). Cooling (5,6) or freezing (4) collected samples is said to promote stability. Storage in glass or polyethylene is claimed not to affect stability (5).

One solution to the vexing problem of identifying change sample stability is to follow the NADP procedure (contributed by the author) of measuring pH and conductivity in the field and in the laboratory. Another advance would be to isolate chemical constituents in a manner such that decay is avoided. Another need is for sequential, sampling rather than the bulk samples collected in the NADP, the NOAA-WMO-EPA network (the oldest national network) and other networks (2,8).

A number of sequential samplers have been devised (6,12,13,14) one of which measures pH (14). None of the samplers, however, measures conductivity, nor provides for the immobilization of chemical contents, although one design

provides for refrigeration to reduce temperature in order to minimize biological activity and chemical decay (6).

In table 1, characteristics of the Rainwater Sampler/Analyzer (RWSA-1) are shown. The RWSA-1 designed is intended to avoid most of the problems given above. Measurements will be made of pH, conductivity, ionic composition, and acidity. Stored samples will be analyzed to determine decay.

The capabilities of the RWSA-1 are given in table 2. Note that the sampler capabilities address the needs of both meteorologists for short-term data and biologists and ecologists for seasonal data. Also addressed is the need for the determination of sample stability.

In table 3, the operational features include operator control to allow for varying intensities of rain. The storage of cations and ions (on ion exchange resins) is a novel feature of this device. The designed operating range of -50°F to +50°F is of course subject to proof in the field. The micro-processor control of measurements and the operator processor control of sampling options is also a novel feature.

The engineering of the electronics for this device and its construction are from venture capital. The objectives of the testing of the prototype is given in table 4. As noted, modification of the RWSA-1 is a possibility which field test results may dictate. This project will commence when prototypes are available.

In table 5, a portion of the planned future studies is given. The last item given, "show applicability of RWSA-1 to generating data for quality assurance program development is direly needed and may prove to be a notable advance in "acid-rain" work.

Due to the demonstration of storage effects from some samples from some sites, it would obviously be of interest to monitor rain samples at a site for

a year before tailoring a quality assurance program to that site. Because of the unique nature of sites and of rain samples, only from a year's data can a meaningful site specific quality assurance program be developed.

The sequential collection of samples and concommittant measurement of pH and conductivity is shown in diagram 1. In diagram 2, the interfacing of the various components around the micro-processor is depicted.

Although the National Acid Deposition Plan does not make mention of, nor allude to, any monitoring difficulties (15), those of us who have had to deal with "real-work" precipitation monitoring programs are aware of the problems mentioned above. The RWSA-1 may prove to be of significant help in making precise the data for the chemical monitoring of precipitation. Without more precise monitoring data, defensible relationships between cause and effect of "acid-rain" will not be possible. If non-metal oxides go up, "acid-rain" must come down, but the relationship between emissions and deposition will not be convincingly demonstrable without monitoring data more precise than that currently obtainable.

The work described in this paper was not funded by the U.S. Environmental Protection Agency and therefore, the contents do not necessarily reflect the views of the agency and no official endorsement should be inferred.

Acknowledgment: The purchase of prototypes described and the bench and field testing are to be performed under NOAA contract No. NAOLRA00125, Design and Testing of a Prototype Rainwater Sampler/Analyzer.

TABLE 1 - RAINWATER SAMPLER ANALYZER-1

CHARACTERISTICS

SENSOR-OPENS COLLECTOR COVER TO RAIN/SNOW

TWO COLLECTORS AND TWO CHANNELS

CHANNEL I - WILL MEASURE pH, CONDUCTIVITY AND TEMPERATURE

CHANNEL II - WILL MEASURE VOLUME AND PASS SAMPLES THROUGH COLUMNS

COLLECTOR SIZE VARIABILITY WILL PERMIT RWSA-1 USE IN AREAS OF DIFFERENT RAINFALLS

ONE TO TEN UNITS OF RAIN CAN BE LOADED ON EACH COLUMN

SIX COLUMNS ARE AVAILABLE ON THE RWSA-1 PER SEQUENCE

AN AUXILIARY MODULE (AM) CAN BE COUPLED TO THE RWSA-1 TO EXTEND THE COLLECTION CAPABILITY TO 12 COLUMNS

THE RWSA-1 (AND AM) CAN BE POWERED BY 110 VAC OR BY AN OPTIONAL BATTERY PACK

OPTIONAL HEATED VERSIONS FOR RAIN/SNOW COLLECTION

DESORBER OPTION TO INTERFACE WITH ION CHROMATOGRAPH

CLOSED COLLECTION SURFACES OF TEFLON

IONS LOADED ON RESINS FROM FIXED VOLUMES

MICRO-PROCESSOR CONTROLLED BY OPERATOR

ALL DATA RECORDED AND PRINTED

TABLE 2 - RWSA-1 CAPABILITIES

DETERMINE RAINWATER COMPONENTS IN "REAL-TIME"

"REAL-TIME" MEASUREMENT OF CONDUCTIVITY, pH, TIME, DATE & TEMPERATURE

DETERMINE RAINWATER COMPONENT PROFILE OF RAIN EPISODES

DETERMINE DEPOSITION - EPISODE AND ANNUAL

DETERMINE SEASONAL COMPOSITION VARIATION

STORE BULK SAMPLE TO ALLOW THE DETERMINATION OF SAMPLE STABILITY FOR EACH SAMPLE

TABLE 3 - RWSA-1 OPERATIONAL DESIGN FEATURES

COLLECTOR CONTROL TO ACCOMMODATE RAINS OF VARYING INTENSITY OR AMOUNT

BOTH ACTIONS AND ANIONS STORED

"AS IS" RAINWATER SAMPLED FOR OTHER ANALYSES

OPERATES BETWEEN +50°F AND -50°F

MEASUREMENTS MICRO-PROCESSOR CONTROLLED

COLLECTION OPTIONS PROGRAMMABLE BY OPERATOR

TABLE 4 - PROTOTYPE TEST OBJECTIVES

COMPLETE RWSA "BENCH-MODEL"

DEVELOP "BENCH-MODEL" TEST PROTOCOL

TEST "BENCH-MODEL" FOR PERFORMANCE AND RELIABILITY

MODIFY AS NEEDED TO RWSA-1

DEVELOP A FIELD-TEST PROTOCOL FOR THE RWSA-1

FIELD-TEST TWO RWSA-1 COPIES FOR PERFORMANCE PRECISION AND RELIABILITY

MODIFY RWSA-1 AS NEEDED

RETEST (IF MODIFIED) AND COMPARE WITH OTHER SAMPLING SYSTEMS

DEMONSTRATE VIABILITY OF STORED RESINS

DEMONSTRATE DEVICE CAPABILITY TO PROFILE EPISODES

TABLE 5 - FUTURE STUDIES

DETERMINE EPISODE PROFILES AT SELECTED HIGH EMISSION LOCALES

DETERMINE EPISODE PROFILES AT SELECTED INTERMEDIATE EMISSION LOCALES

DETERMINE EPISODE PROFILES AT SELECTED BACKGROUND EMISSION LOCALES

DETERMINE CAUSE OF SAMPLE DECAY

BENCH TESTING BY OTHER LABORATORIES

FIELD TEST AT OTHER LABORATORIES

COMPARE WITH OTHER SYSTEMS

SHOW APPLICABILITY OF RWSA-1 TO GENERATING DATA FOR QUALITY ASSURANCE PROGRAM DEVELOPMENT

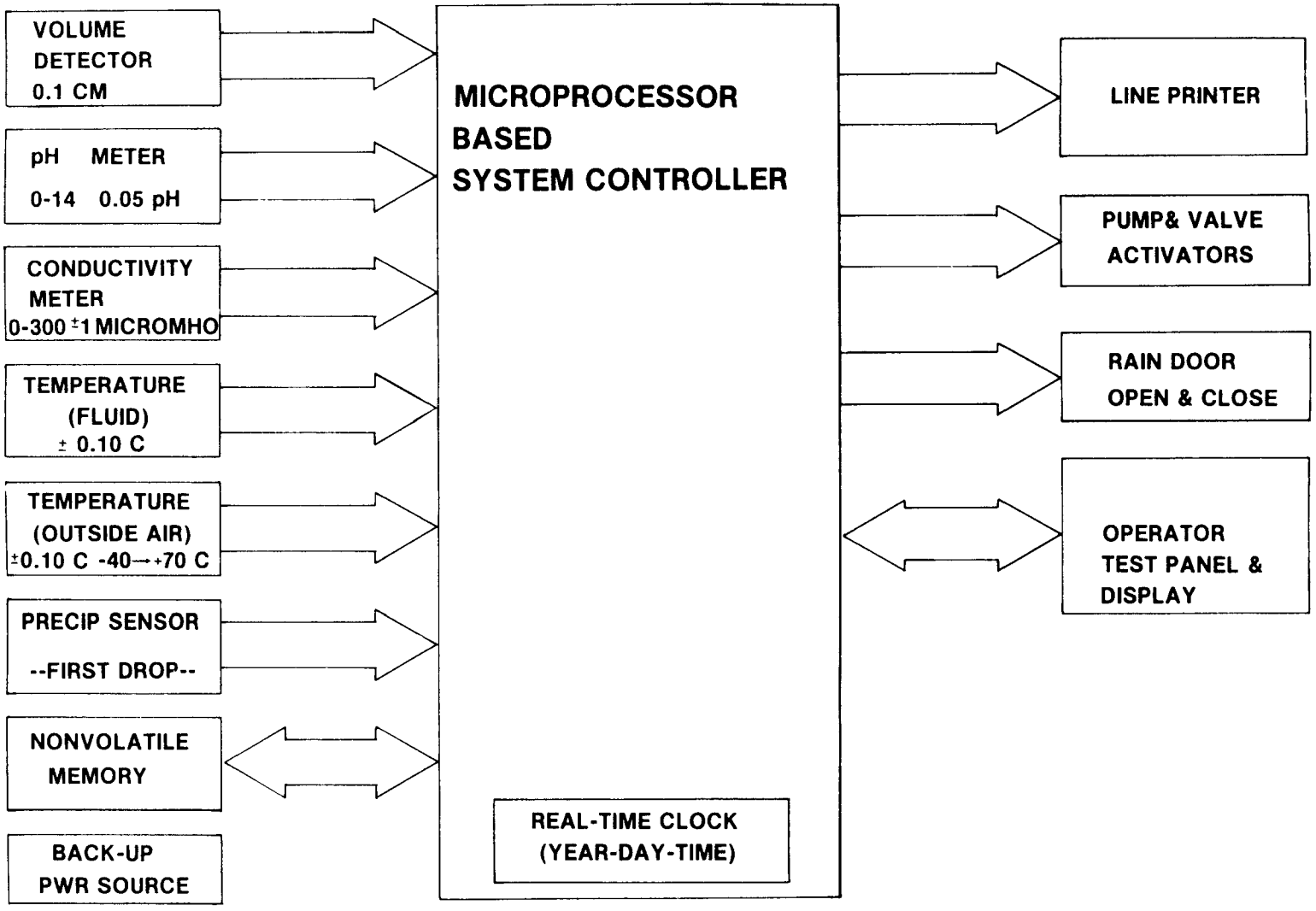
VOLUME DETECTOR 0.1 CM
pH METER 0-14 0.05 pH
CONDUCTIVITY METER 0-300 ±1 MICROMHO
TEMPERATURE (FLUID) ± 0.10 C
TEMPERATURE (OUTSIDE AIR) ±0.10 C -40→+70 C
PRECIP SENSOR --FIRST DROP--
NONVOLATILE MEMORY
BACK-UP PWR SOURCE
MICROPROCESSOR BASED SYSTEM CONTROLLER
REAL-TIME CLOCK (YEAR-DAY-TIME)
LINE PRINTER
PUMP& VALVE ACTIVATORS
RAIN DOOR OPEN & CLOSE
OPERATOR TEST PANEL & DISPLAY

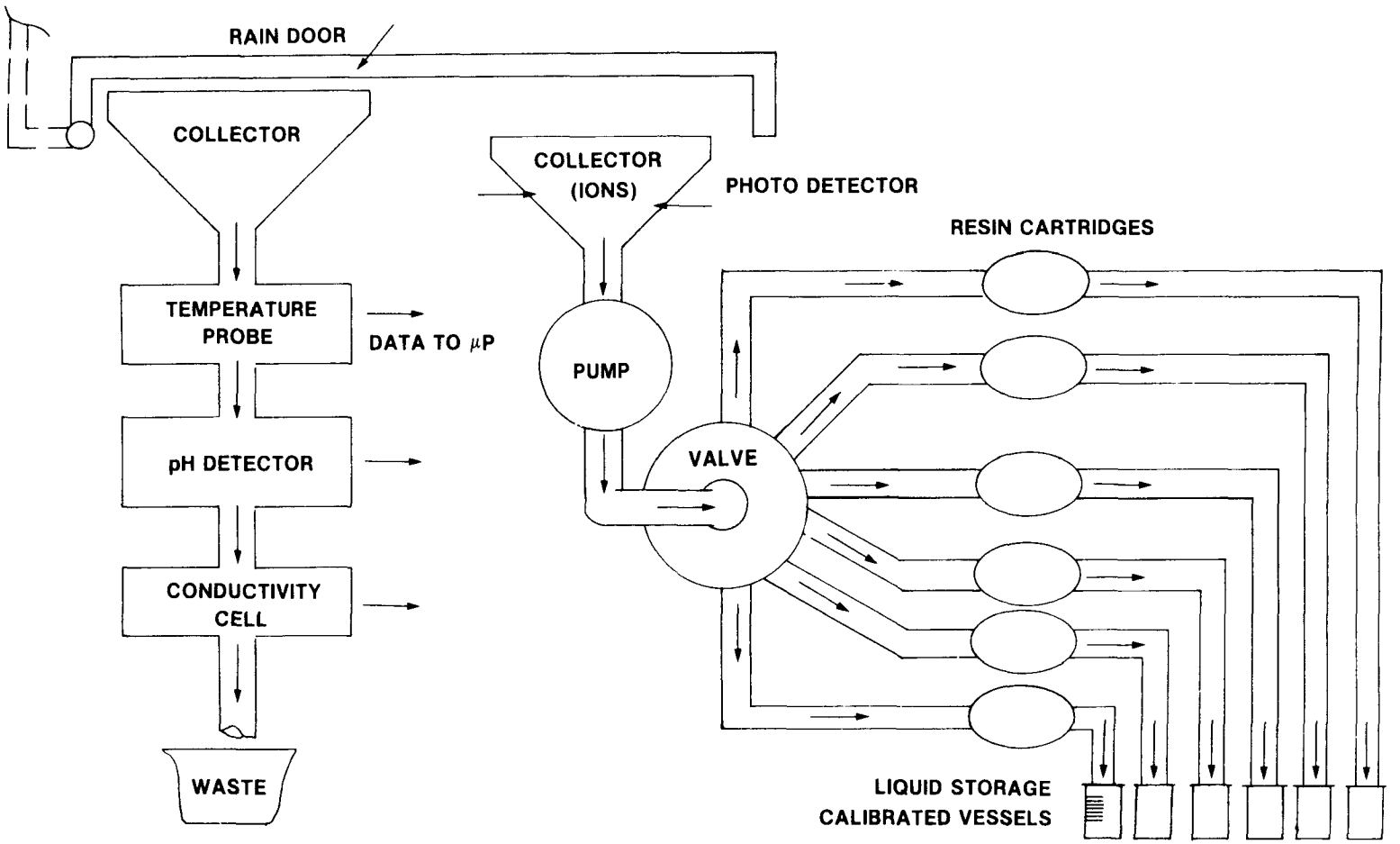
RAIN DOOR
COLLECTOR
COLLECTOR
(IONS)
PHOTO DETECTOR
RESIN CARTRIDGES
TEMPERATURE
PROBE
DATA TO μP
PUMP
pH DETECTOR
VALVE
CONDUCTIVITY
CELL
WASTE
LIQUID STORAGE
CALIBRATED VESSELS

REFERENCES

1. Tyree, S.Y., Jr. Rainwater Acidity Measurement Problems. Atmos. Environ. 15:57, 1981.

2. Thompson, Richard J. The Sampling and Analysis Techniques in Current Use in the EPA/NOAA/WMO Precipitation Network. WMO Special Environmental Report No. 10. Air Pollution Measurement Techniques, WMO No. 460, Geneva, 1967. p. 40.

3. Feeley, Herbert W. et. al. The Chemical Analysis of Deposition Samples. Environ. Meas. Lab. Environ 0 1980, EML 391. I-43-I-74.

4. Mueller, K.P. et. al., Deposition Atmos. Poll. Proc. Colloq. 1981. via C.A. 97:203034q.

5. Linkaityte, E. et. al. Change in the Composition of [atmospheric] Precipitate Samples in Relation to the Conditions of Time & Storage. Zashch. Atmos. Zagryaz. 3:38,1976. via C.A. 87:28105h

6. Coscio, M.R., Pratt, G.C. and Krupa, S.V., An Automatic, Refrigerated, Sequential Precipitation Sampler. Atmos. Environ. 16:1939, 1982.

7. Lewin, Ella E. and Torp, Ulrik. Influence of Contamination on the Analysis of Precipitation Samples. Atmos. Environ. 16:795, 1982.

8. Hansen, D.A. and Hidy, G.M. Review of Questions Regarding Rain Acidity Data. Atmos. Environ. 16, 2107 (1982).

9. Jervis, T.R., Rainfall Acidity: Natural Variance and Subsequent Time Dependence of pH. Atmos. Environ. 13:1601, 1979.

10. Peterson, D.L. et. al. For. Res. Rep. (Univ. Ill. Urbana-Champaign. Agri. Exp. Sta. Dept. For.) 1979, 79.

11. Feeley, Herbert W. and Bogen, Donald C. The Chemical Analysis of Deposition Samples. An Interlaboratory Comparison. Environ Q (US Dept Energy Environ. Meas Lab) 1978. I,3-43.

12. Asman, Willem A.H., Draft Construction and Operation of a sequential rain sampler. Water, Air, Soil Pollut., 13:235, 1980.

13. Raynor, Gilbert S. and McNeil, John P., An Automobile Sequential Precipitation Sampler. Atmos. Environ. 13:149, 1979.

14. Lopez-Gonzalez, Jose Alberto, Determination of raviations in the Chemical Composition of rainfall in several regions of Texas through the use of an automated sequential sampler and analyzer. Dissertation, University of Texas, Austin, 1982. via Diss. Abstr. Int. B. 43:809, 1982.

15. National Acid Deposition Plan, Prepared by the Interagency Task Force on Acid precipitation Draft January, 1981, Dr. Cris Bernabo, Executive Secretary, Council on Environmental Quality, Washington, D.C.

ORGANIC ACIDITY IN PRECIPITATION FROM REMOTE AREAS OF THE WORLD

William C. Keene

James N. Galloway

J. David Holden

Department of Environmental Sciences

University of Virginia

Charlottesville, Virginia 22903

INTRODUCTION

The anthropogenic emissions of SO_2 and NO_x into the atmopshere has caused widespread acidification of precipitation in Northern Europe and eastern North America (1,2). The study of precipitation chemistry developed largely in response to this perturbation, and consequently most research has focused primarily on major inorganic chemical constituents. The organic constituents, and particularly carboxylic acids, have received relatively little attention. Carboxylic acids are a common constituent of aerosols and precipitation (3). In industrialized regions of the Northern Hemipshere, these acids make a negligible contribution to the free acidity of precipitation (4,5,6,7,8). However, evidence suggests that formic and acetic acids are a major source of free acidity in precipitation from remote regions of the world (9,10). This paper reports a summary of current findings regarding organic acidity in precipitation collected by the Global Precipitation Chemistry Project (GPCP).

Study Site, Collection Procedures and Analytical Protocol

The (GPCP) was established in 1979 to determine the composition of precipitation, and processes that control the composition, in remote regions of the world. To date, 5 stations have been established. They are Katherine, Australia; San Carlos de Rio Negro, Venezuela; Poker Flat Research Range, Alaska; St.George's, Bermuda; and Amsterdam Island in the Indian Ocean. Galloway et al. (9) gave detailed descriptions of the sites, sample collection procedure and analytical protocol.

Samples were collected by event in scrupulously washed polyethylene containers. Immediately after a sample was collected, the pH's of two aliquots were measured at the field site. If sufficient volume remained, the sample was divided into two 250 ml aliquots. One aliquot was treated with chlorcform to prevent biological activity during sample storage and shipment to the University of Virginia. The other aliquot was left untreated.

During the first two years of operation, samples were analyzed for the following major inorganic species: H^+, Ca^{2+}, Mg^{2+}, Na^+, K^+, NH_4^+, SO_4^{2-}, NO_3^-, Cl^- and SiO_4^{-4}. PO_4^{3-} was measured only in samples from San Carlos de Rio Negro.

Development of Hypothesis

Ion balances calculated from inorganic data suggested that unmeasured proton doners contributed significantly to the free acidity of precipitation at certain sites (9,10). Comparisons between pH measured in the field and in the laboratory suggested that these acids were present when samples were collected and that, in the absence of chloroform, they were consumed by biological activity prior to analysis. It was hypothesized that weak organic acids were the unmeasured proton doners and the substrate for biological activity.

METHODS

Keene et al. (10) developed accurate and precise techniques to measure organic anions and total acidity in the samples. Ion Exclusion Chromotography (11) was used to identify and quantify organic acid anions. Formate and acetate were found in all aliquots which had been treated with a biocide. Citrate,

propionate, glycolate and/or lactate were observed infrequently and always at very low concentrations. Succinate, butyrate and valarate were not found. Therefore, the technique was optimized for the quantification of formate and acetate and was verified by standard additions, replicates, comparisons with free acidity and comparisons with total acidity.

A technique incorporating Johansson's (12) modifications of Gran's (13) functions was developed to measure total acidity. Because organic acids dissociated throughout the titration below pH 7.00, it was impossible to differentiate strong from weak acidity using Gran's technique. Measurements of total acidity were verified with replicates and comparisions with calculated total acidity.

DISCUSSION

Keene et al. (10) presented a small set of direct measurements on precipitation samples collected at Katherine, Australia between 9 December 1981 and 26 January 1982. Results showed that the loss of free acidity in untreated aliquots was directly proportional to the concentrations of dissociated organic anions in treated aliquots (Figure 1). On a volume weighted basis, formic and acetic acids contributed 64% of the free acidity and 63% of the total acidity in the 12 samples. Unmeasured proton donors contributed 21% of the measured total acidity.

The volume weighted averages and ranges of H^+ and the sum of dissociated organic anions are compared for 3 sites in Figure 2. The large range in both H^+ and ΣRCO_2 for precipitation from Amsterdam Island resulted from a single low volume event which

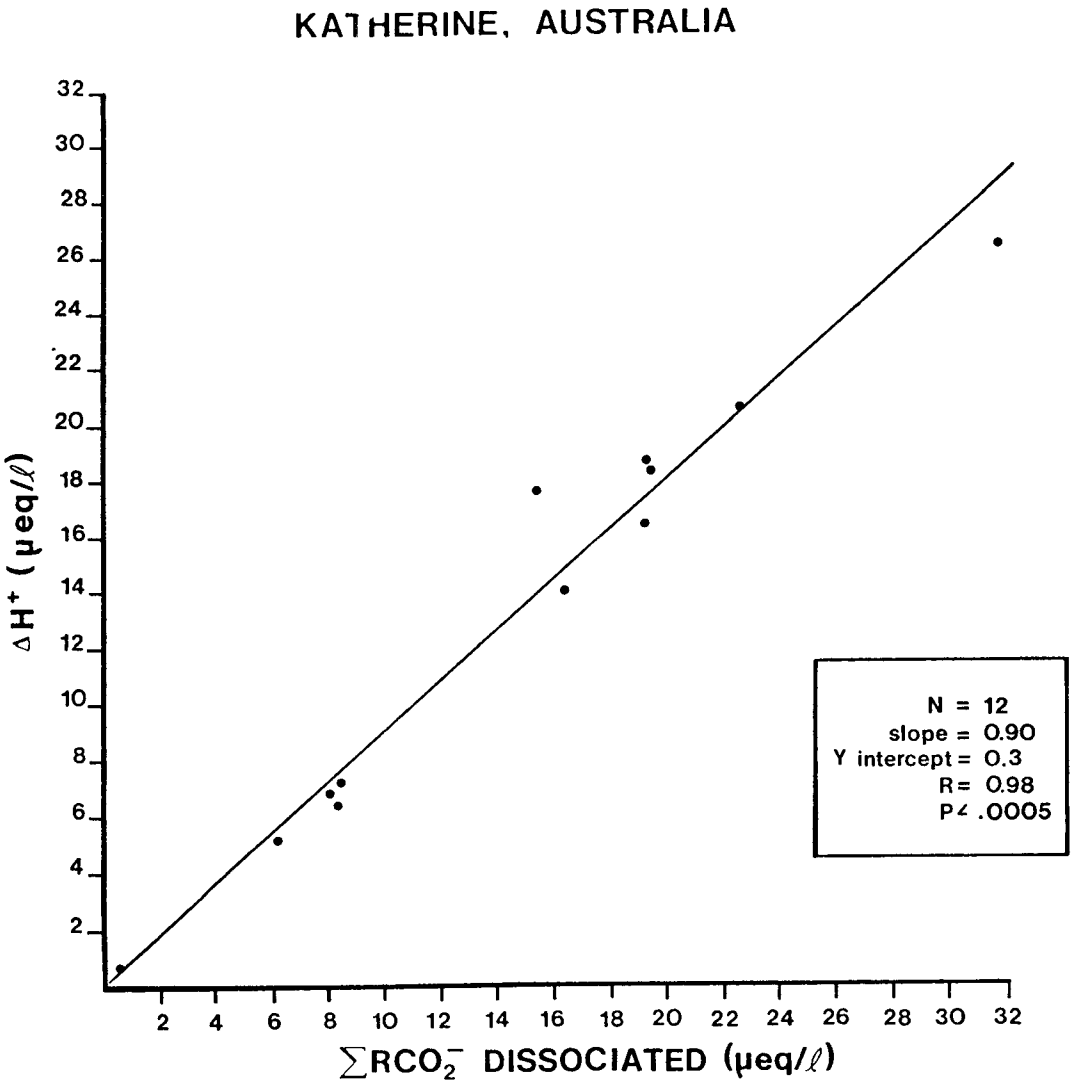

Figure 1. Plot of the sum of dissociated organic anions (ΣRCO_2^-) in treated aliquots versus the difference between H^+ (ΔH^+) in treated and untreated aliquots of precipitation from Katherine, Australia.

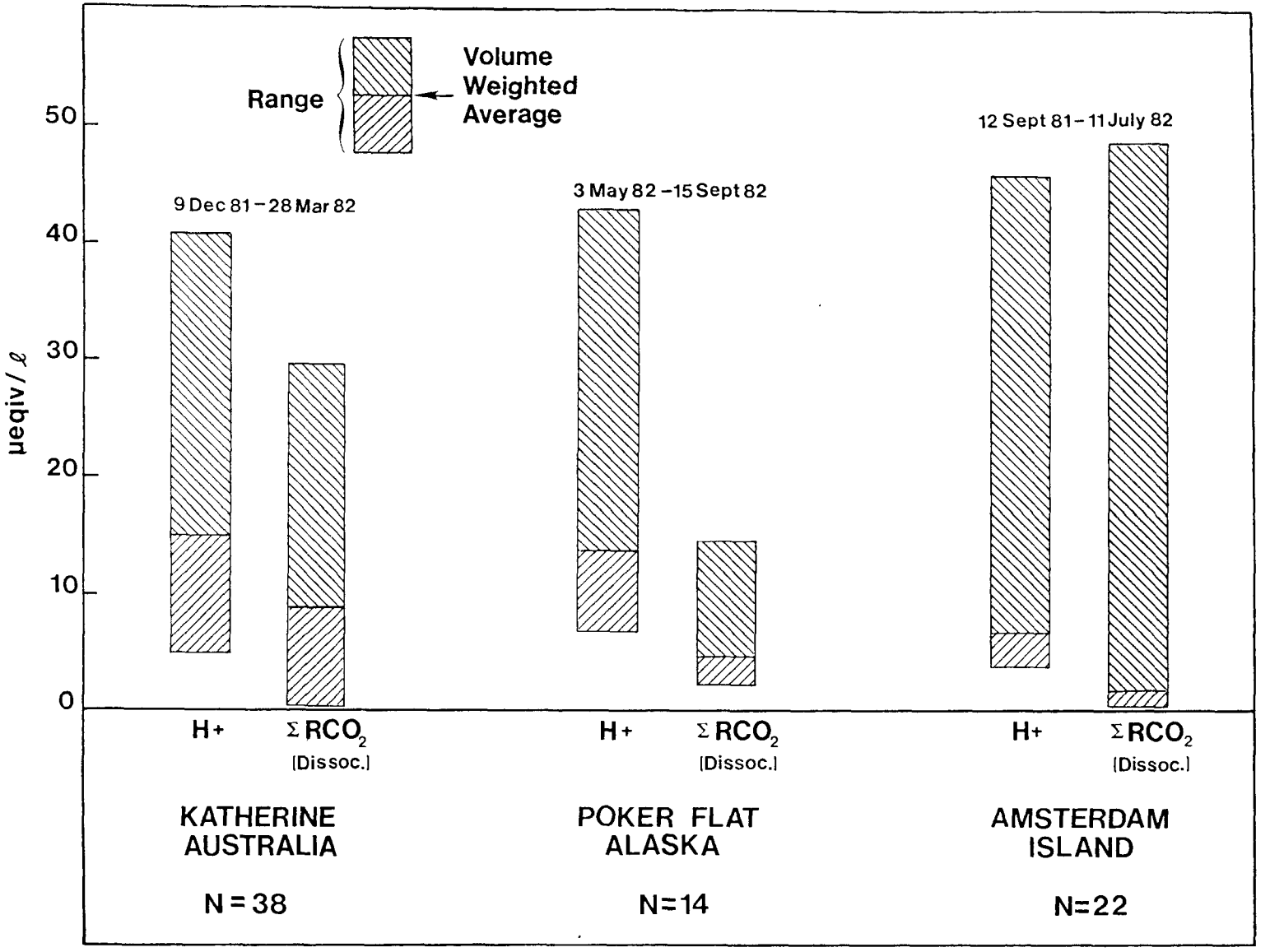

Figure 2. A Comparison of the volume weighted averages and ranges of H^+ and dissociated organic anions (ΣRCO_2) in treated aliquots of precipitation from 3 sites in the GPCP.

contained high concentrations of formic and acetic acids. Although the sample may have been contaminated, we had no justifiable reason for excluding if from the analysis. On a volume weighted basis, organic acids contributed 59% of the free acidity in precipitation at Katherine, 34% at Poker Flat and 25% at Amsterdam Island. Low volume events tended to have higher absolute and relative concentrations of organic acidity.

The regression of ΔH^+ vs ΣRCO_2^- (Figure 1) indicated that ΔH^+ could be used to estimate the organic acidity of treated aliquots in which formate and acetate had not been measured. Two assumptions were implied when using this estimate: (1) Organic acids were the only constituents, contributing to free acidity, which disappeared from untreated aliquots; and (2) these acids were completely consumed in untreated aliquots. Keene et al. (10) demonstrated that these assumptions were satisfied for samples from Katherine. A similar comparison of ΔH^+ and ΣRCO_2^- for samples from Amsterdam Island indicated that the assumptions were also satisfied for that site. However, results from Poker Flat suggested that the second assumption was not satisfied, resulting in an underestimte of ΣRCO_2^-. We speculated that because of the relatively short time interval between collection and analysis of samples from the site, all organic acids had not been consumed in untreated aliquots. Data was not available to evaluate the validity of the assumptions for samples from San Carlos and Bermuda.

H^+ is compared with ΔH^+, for the 5 GPCP sites, in Figure 3. On a volume weighted basis, organic acids accounted for most of the variability in free acidity from site to site. Strong mineral acidity, as estimated from the difference between H^+ and ΔH^+, was

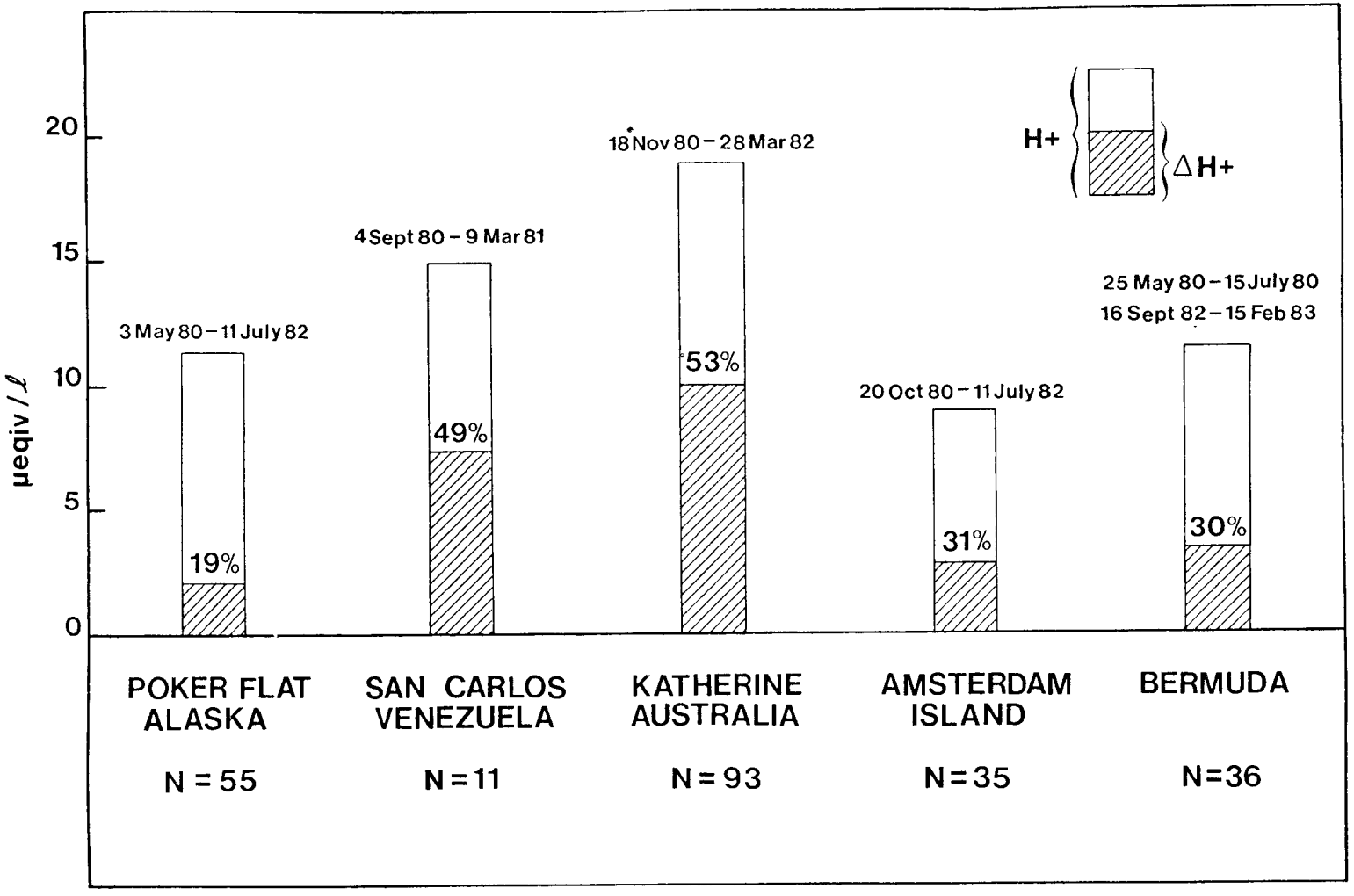

Figure 3. A comparison between the volume weighted average of H^+ in treated aliquots and that of the difference between H^+ (ΔH^+) in treated and untreated aliquots of precipitation from the 5 sites in the GPCP.

relatively constant at all sites. When interpreting these results, three factors were considered.

1. Approximations of ΣRCO_2^- based on ΔH^+ underestimated organic acidity in precipitation at Poker Flat.

2. At Amsterdam Island, 15% of the original free acidity in precipitation was neutralized by seasalt alkalinity (14).

3. Precipitation on Bermuda contained a significant anthropogenic component of strong mineral acidity (15). The free acidity of precipitation at the site was also neutralized by seasalt alkalinity.

Considering these factors, as well as actual measurements and estimates based on ΔH^+, we arrived at 4 conclusions regarding precipitation acidities at GPCP sites. All conclusions were based on volume weighted averages.

1) Free acidities at the five sites ranged from a minimum of 9 μeq/ℓ at Amsterdam Island to a maximum of 19 μeq/ℓ at Katherine.

2) Organic acidities at the 2 oceanic sites ranged from 2 to 3 μeq/ℓ and contributed 25 to 30% of the free acidities.

3) Organic acidities at terrestrial sites ranged from 5 to 10 μeq/ℓ and contributed 35 to 60% of the free acidities.

4) Strong mineral acidities ranged from 7 to 9 μeq/ℓ at all sites.

ACKNOWLEDGEMENTS

We thank Howard Clark in San Carlos de Rio Negro, Mike Cogan and Charles Lasater at Poker Flat Research Range, Andre Gaudry on Amsterdam Island, Tim Jickells on Bermuda and Judy Locke in Katherine for the excellent jobs they have done operating field stations for the GPCP. We also thank Carl O. Moses and M. Robbins Church for valuable comments during the investigation and Linda Zieler and Klaus Scott for assistance with sample analysis

and data reduction. Funding was provided by the National Oceanic and Atmospheric Administration, the Environmental Protection Agency, and the U. S. Department of Energy. The Academic Computing Center at the University of Virginia, Charlottesville, provided computer facilities for data reduction.

REFERENCES

1. Likens, G. E. and Butler, T. J. Recent acidification of precipitation in North America. Atmos. Enivron., 15: 1103, 1981.

2. Glass, N. R., Arnold, D. E., Galloway, J. N., Hendrey, G. R., Lee, J. J., McFee, W. W., Norton, S. A., Powers, C. F., Rambo, D. L. and Schofield, C. L. Effects of acid precipitation. Env. Sci. Tech., 16: 162A, 1982.

3. Graedel, T. E. and Weschler, C. J. Chemistry within aqueous atmospheric aerosols and raindrops. Rev. Geophys. Space Phys., 19: 505, 1981.

4. Galloway, J. N., Likens, G. E. and Edgerton, E. S. Acid precipitation in the Northeastern United States: pH and acidity. Science, 194: 722, 1976.

5. Lunde, G., Gether, J., Gjos, N. and Lande, M.-B. S. Organic pollutants in precipitation in Norway. Atmos. Environ., 11: 1007, 1977.

6. Hoffman, W. A., Jr., Lindberg, S. E. and Turner, R. R. Some observations of organic constituents in rain above and below a forest canopy. Environ. Sci. Tech., 14: 991, 1980.

7. Barcelona, M. J., Liljestrand, H. M. and Morgan, J. J. Determination of low molecular weight volatile fatty acids in aqueous samples. Anal. Chem., 52: 321, 1980.

8. Likens, G. E., Edgerton, E. S. and Galloway, J. N. The composition of organic carbon in precipitation. Tellus (in press), 1983.

9. Galloway, J. N., Likens, G. E., Keene, W. C. and Miller, J. M. Composition of precipitation in remote areas of the world. J. Geophys. Res. 18: 8771, 1982.

10. Keene, W. C., Galloway, J. N. and Holden, J. D. Measurement of weak organic acidity in precipitatin from remote areas of the world. J. Geophys. Res., (in press), 1983.

11. Dionex Corporation. Analysis of inorganic anions and organic acids in carbonated beverages. Application No. #25, Sunnyvale, Ca., 1980.

12. Johansson, A. Automatic titration by stepwise addition of equal volumes of titrant. Analyst, 95: 535, 1970.

13. Gran, G. Determination of the equivalence point in potentiometric titration. Part II. Analyst, 77: 661, 1952.

14. Galloway, J. N., Gaudry, A., Likens, G. E., Lambert, G. and Miller, J. M. Composition of rain on Amsterdam Island, Indian Ocean. (in preparation), 1983.

15. Jickells, T. C., Knap, A. H., Church, T. M., Galloway, J. N. and Miller, J. M. Acid precipitation on Bermuda. Nature 297: 55, 1982.

A FIELD INTERCOMPARISON OF PARTICLE AND GAS DRY DEPOSITION MEASUREMENT AND MONITORING METHODS.

Donald A. Dolske and Donald F. Gatz
State Water Survey Division
Illinois Department of Energy and Natural Resources
Champaign, Illinois 61820-9050

Abstract

From 3 through 30 June, 1982, concurrent dry deposition flux measurements were performed using various currently available techniques. Researchers from more than a dozen U.S. and Canadian institutions gathered at a site near Champaign, Illinois. The Illinois State Water Survey (SWS) coordinated the field program and collected ambient meteorolgical and pollutant concentration data. Micrometeorological methods used included eddy correlation, eddy accumulation, particle concentration variance, and concentration profiles / modified Bowen ratio computations. Deposition flux collection methods using surrogate surfaces such as polyethylene buckets, funnels, and plastic or Teflon disks were also used. The principal species for which deposition was measured were particles, particulate sulfur, sulfate, and nitrate, as well as gaseous nitric acid, sulfur dioxide, and ozone. An overview of the experiment is presented, with a preliminary examination of some early results.

Introduction

Refinement in the ability to accurately measure dry deposition of airborne pollutants has been the object of much recent research. Detailed model descriptions of the transport, transformation, and fate of airborne materials must include reliable estimates of dry deposition rates. To date no consensus has been reached regarding a routine and practical method by which dry deposition can be monitored [1]. This intercomparison of monitoring and measurement methods was an approach to the verification of deposition determinations from several of the methods now available.

The intercomparison experiments were conducted from 3 through 30 June, 1982, (Julian Dates 154 through 181) at a 32 hectare (800 m X 400 m) field site, 14 km southwest of Champaign, Illinois. Figure 1 shows plan views of the site and the location of the participant experiments. The methods included in the field program and the participating research organizations are listed in Table 1. Vegetation at the site consisted of grass, 25 to 30 cm high. The surrounding farm fields were planted in soybeans and corn, and the local topography is essentially flat. Prevailing winds in the region during June are south to southwest, so the linear arrangement and spacing of instruments provided the best potential to minimize interferences between experiments.

Table 1. EXPERIMENTS IN THE JUNE, 1982 DRY DEPOSITION INTERCOMPARISON

Method	Organization	Acronym
Eddy-Correlation	Atmospheric Environment Service (Canada)	AES
	Battelle Pacific Northwest Laboratory	PNL
	Oregon State University	OSU
	Argonne National Laboratory	ANL
Variance	Governors State University	GSU-V
Eddy-Accumulation	USEPA/Environmental Science Research Lab.	EPA
	Atmospheric Environment Service (Canada)	AES
Gradient	Concord Scientific Corporation (Canada)	CSC
	The Colorado College	TCC
	Battelle Pacific Northwest Laboratory	PNL
Filtration/Model	University of Illinois, Medical Center	UIMC
	Ontario Ministry of the Environment (Canada)	MOE
Surrogate Surfaces	Carnegie-Mellon University	C-MU
	USDOE/Environmental Measurements Laboratory	EML
	Governors State University	GSU-B
	University of Illinois, Medical Center	UIMC
Vegetation Washing	Oak Ridge National Laboratory	ORNL

Figure 1A. Plan view of intercomparison field site.

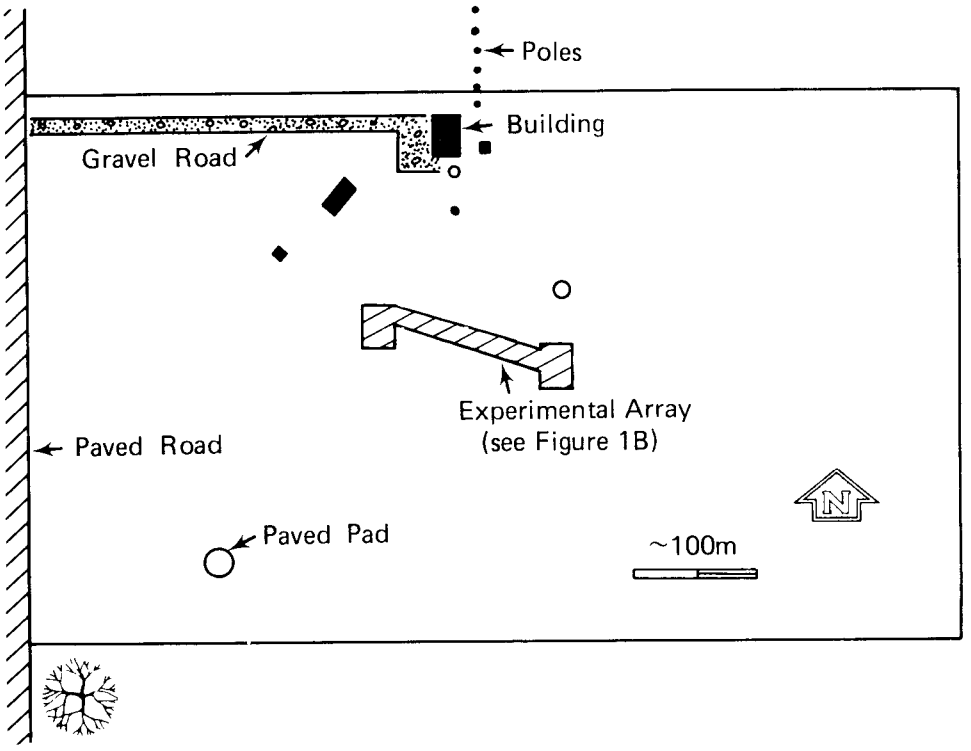

Figure 1B. Plan view of instrumentation array.

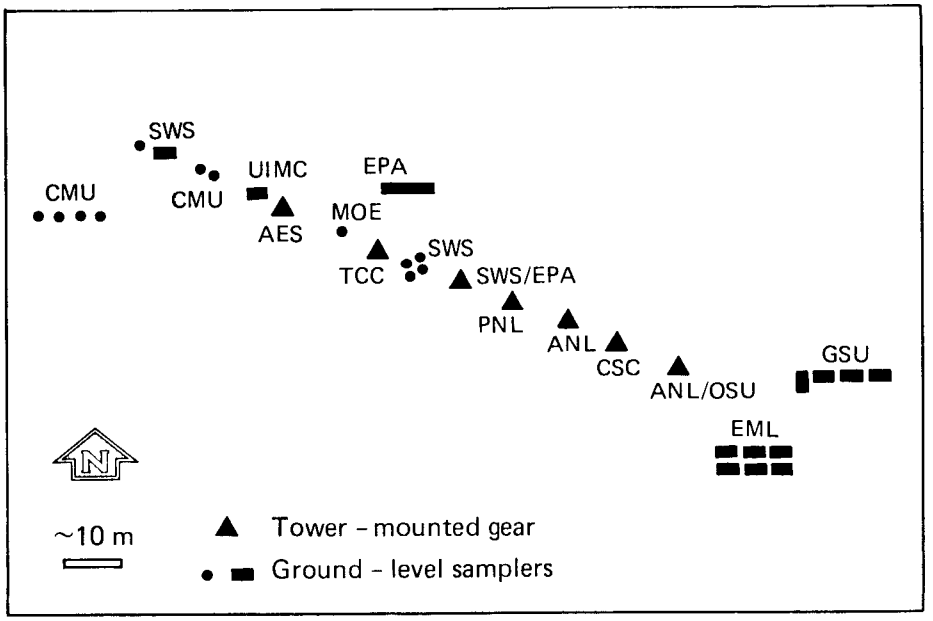

Each of the deposition measurement experiments was set up at the field site as normally used by the participating researchers. A sampling protocol was agreed upon which maximized the comparability of the results. Most ambient pollutant concentration measurements and deposition collection on surrogate surfaces were done at a height of 1.5 m above the ground. Eddy correlation and eddy accumulation measurements were done at 6.0 m or 3.0 m, while concentration gradients were monitored at the 0.75, 1.5, 3.0, 6.0, and 9.0 m heights. For experiments with collection periods 12 h or longer, primary sample change times of 0700 and 1900 CDT were specified. Micrometeorological experiments, with much shorter continuous collection periods, generally operated whenever conditions would allow. The month of June 1982 featured frequent periods of light rain and winds from unfavorable directions. Sampling was impossible for about 25 percent of the month, when northerly winds created improper fetch conditions because of site buildings and the instrument array orientation. Figure 2 is a plot of the times during the month when each experiment was actively collecting data. The times indicated probably overestimate the actual amount of valid samples, but are an indication of the temporal density with which flux measurements were made during the intercomparison field program.

FIGURE 2. PERIODS OF DATA COLLECTION DURING JUNE, 1982.

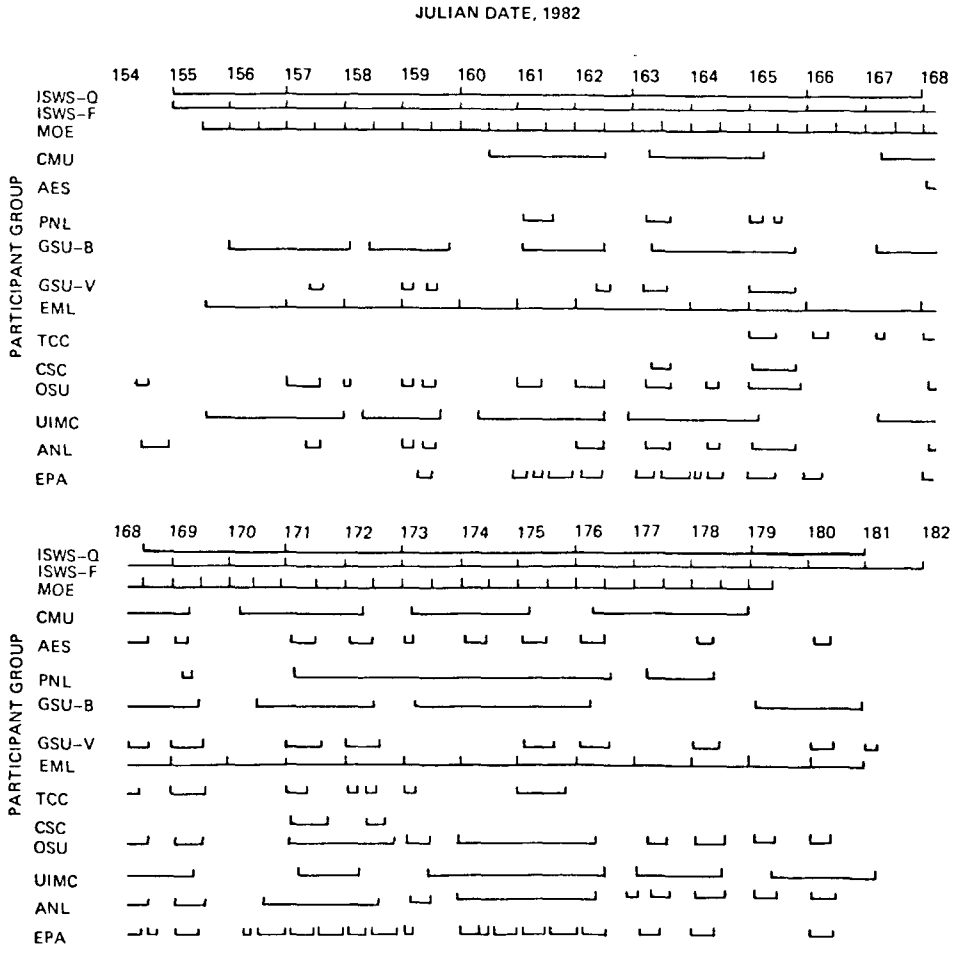

Results

The discussion presented here is based on a partial set of results. Data from some of the experiments has yet to be fully analyzed; however, some points of general interest are apparent in the data so far reported to SWS. It must be noted that dry deposition rates are strongly dependent on prevailing meteorological conditions and characteristics of the receiving surface. These experiments were conducted over a grassy field during a one-month period. Applying these results to other surfaces and other seasons calls for awareness of the limitations of

such an extension. Table 2 shows the range and overall mean deposition velocities, v_d , found for several chemical species by some of the methods used in the intercomparison. These results do not necessarily reflect one-to-one temporal correspondence in the data, as indicated in Figure 2. A sample by sample comparative analysis must be completed before direct and quantitative relationships between methods can be defined.

The values of v_d shown in Table 2 are comparable to measurements made during September, 1981 at the same site [2]. Good agreement among most of the methods is apparent for sulfate and particulate sulfur, with v_d of about 0.2 to 0.3 cm/s. Some short time scale variations, i.e. on the order of minutes, were observed in the magnitude and direction of size resolved total particle fluxes. Diurnal trends were evident in many of the measurements. Deposition of gaseous pollutants showed very strong diurnal variations, with v_d near zero at night and up to several cm/s during daylight hours. For both sulfur dioxide and nitric acid vapor, the daytime deposition rate was not limited by vegetative canopy resistance to mass transfer. Particulate sulfur and sulfate v_d near zero were also observed at night, while v_d up to 1.0 cm/s were observed during daylight hours. Size fractionated aerosol samples and calculated deposition velocities suggest that large (diameter > 2.0 μm) particle associated sulfate may account for 20 to 50 percent of the total sulfate flux.

It is very likely that the overall averaged v_d results depend on the response of each method to a number of highly variable factors. There remains much detail to be carefully screened and analyzed before firm conclusions and comparisons can be drawn. The temporal resolution and particle size sensitivity of each experiment must be considered before the good agreement between the various measurement methods can be termed significant.

TABLE 2. OVERALL RESULTS FROM SEVERAL DEPOSITION MEASUREMENTS.

P.I.	METHOD	PARAMETER	V_d, cm-s^{-1}	RANGE
CMU	Teflon disk	$SO_4^=$	.22 ± .1	(.17 - .42)
	Teflon disk	NO_3^-	1.0 ± .4	(.5 - 1.8)
	Petri dish	$SO_4^=$	.35 ± .2	(.18 - .61)
	Petri dish	NO_3^-	2.5 ± .8	(1.4 - 3.8)
GSU	GLAD bulk	$SO_4^=$	.14 ± .1	(.01 - .44)
	Aerochem 301	$SO_4^=$	.17 ± .1	(.03 - .31)
EML	Aerochem 301	$SO_4^=$	.40 ± .2	(0.1 - 1.0)
PNL	Profile	Particulate S	.3 ± .2	-
ANL	Eddy-correlation	Particulate S	.25 ± .2	(0.1 - 0.8)
TCC	Profile	HNO_3	3.0 ± 1.1	(1.1 - 4.9)
CSU	Profile	SO_2	1.8 ± 1.8	(0.0 - 7.0)

Acknowledgements

Coordination of the intercomparison study and partial support for the participants was provided by the Illinois State Water Survey, under a cooperative agreement with the U.S. Environmental Protection Agency, CR808863. In addition, a number of U.S. and Canadian government agencies and other institutions funded the efforts of several particpants.

References

1. Hicks, B.B., M.L. Wesely, and J.L. Durham. "Critique of methods to measure dry deposition." Workshop Summary Report, EPA-600/9-80-050. USEPA / ESRL, Research Triangle Park, NC, 1980. 83pp.
2. Dolske, D.A., and D.F. Gatz. A field intercomparison of sulfate dry deposition monitoring and measurement methods: preliminary results. In Proceedings of ACS Acid Rain Symposium, Las Vegas, NV, March 1982. Ann Arbor Science Publishers, in press.

A COMPARISON OF AMBIENT AIRBORNE SULFATE CONCENTRATIONS DETERMINED BY SEVERAL DIFFERENT FILTRATION TECHNIQUES.

Donald A. Dolske and Gary J. Stensland
Water Survey Division
Illinois Department of Energy and Natural Resources
P.O. Box 5050, Station A
Champaign, Illinois 61820-9050

Abstract

Ambient airborne concentrations of sulfate, total particulate sulfur, and sulfur dioxide gas were measured at a rural Champaign County, Illinois, site from 3 through 30 June, 1982. Several different filtration techniques were used concurrently to collect pollutants 1.5 meters above ground in a grass - covered 32 hectare field. Filter changes were sychronized at 12 or 24 hour intervals. Single stage filters and multiple stage series filter pack methods with Nuclepore, Teflon, Nylon, and cellulose fiber materials were used. Comparisons are made between the results of methods employing different filter materials, exposure schedules, and extraction and analysis techniques. Preliminary results show large differences in concentrations determined by Teflon and Nuclepore filter methods.

Objectives

During June, 1982, a field intercomparison of dry deposition measurement methods was held at Champaign, Illinois [1]. The Illinois State Water Survey (SWS) collected ambient meteorological and air pollutant concentration data in support of the flux measurements made by research groups participating in the intercomparison. Several different filtration methods were used concurrently to measure concentrations of chemical species of interest. Most of the methods provided sulfur concentration results, in addition to various other species. Because all ambient air sampling was synchronized with the flux measurement

schedule, the sulfate, particulate sulfur, and sulfur dioxide concentration data from commonly used filtration methods can conveniently be compared. Earlier comparisons of the field performance of cellulose fiber (Whatman 41) and polycarbonate membrane (Nuclepore) [2] indicated rather small differences in sulfate collection efficiency. The present study extends that result by comparisons to Teflon and Nuclepore filters.

Methods

Eight filtration methods were used continously from 3 through 30 June, 1982. Flame photometric sulfur monitors were also operated at the rural site, 14 km southwest of Champaign, Illinois. Results from measurements made with dichotomous samplers using Teflon filters, a high-volume sampler using 20 X 25 cm type A glass fiber filters, and cascade impactors using Teflon substrates have not yet become available. The five methods for which data are available are summarized in Table 1.

Exposure conditions for the first two filter types listed in Table 1 were carefully matched. The 1.0 μm Teflon (Membrana Corp., Zefluor), and 0.8 μm pore diameter Nuclepore filters were mounted in 37 mm diameter open face holders and exposed facing down under inverted 30 cm diameter funnels 1.5 m above ground. The volume of air sampled was calculated from initial and final flow rates for every daily sample. Every fourth day, a dry test meter was inserted into the vacuum line and the actual air volume sampled was recorded. The sample volumes

determined by these two methods agreed within about two percent. To minimize the possibility of overloading or clogging the filters, the 37 mm pairs were exposed on a half-hour on, half-hour off cycle. Filters were changed daily at 0700 CDT, resulting in 720 minutes of active sampling time per 24 h period. Field and laboratory blank filters were collected every fifth day. The filters were extracted in 30 ml of pH 3.0 hydrochloric acid and agitated for 12 h. Sulfate analysis was performed by automated colorimetry [3]. The sulfate results from these filters are referred to here as SWSTSO4 (Teflon) and SWSNSO4 (Nuclepore).

Table 1. FILTER TYPES USED AT CHAMPAIGN, JUNE, 1982.

	Filter Type	Filter Size	Typical Flow Rate (L / min)	Sample Volume (cu.m)	Reference Label
1.	1.0 μm Teflon	37 mm	24.	17.5	SWSTSO4
2.	0.8 μm Nuclepore	37 mm	24.	17.5	SWSNSO4
3.	0.4 μm Nuclepore	2 X 4 mm	0.8	1.15	SWSPS
4.	Filter pack:	47 mm	28.	38.	
	1.0 μm Teflon				SWSFPSO4
	Treated cellulose				SWSFPSO2
5.	Filter pack:	47 mm	18.	26.	
	2.0 μm Teflon				MOEFPSO4
	Nylon				MOEPFSO2
	Treated cellulose				MOEFPSO2

Two circular streaker samplers (PIXE International Corp.) were operated continuously during the month. 0.4 μm Nuclepore filters mounted in a plastic frame rotated past a 2 X 4 mm Teflon vacuum orifice at 1 mm/h. The filters were changed weekly. Elements were determined by proton induced x-ray emission (PIXE) at 2 mm intervals, so that a

total sulfur concentration moving-average value was determined for each 2 h period. The flow rate was limited to 0.8 L/min by the pores of the filter, which act as critical orifices. The 2 h data were averaged over 24 h periods from 0700 CDT, to correspond with the other results presented here. The streakers were sometimes co-located at 1.5 m above ground level, and at other times one sampler was moved to 6.0 m above ground. All of the data were averaged together, ignoring the differences in sampler height, to arrive at the ambient 24 h values used in this comparison. The 24 h averaged particulate sulfur results are referred to as SWSPS.

A two-stage series filter pack, consisting of a 1.0 μm Teflon particle filter and a second stage sulfur dioxide absorbing filter was mounted in a 47 mm open face plastic holder, and exposed under an inverted funnel at 1.5 m above the ground. The sulfur dioxide absorbing filter was a double layer of cellulose fiber material (Whatman 41) which had been treated with a saturated solution of potassium carbonate in 25 percent (v/v) glycerol and water. Mean flow rate and dry test meter determinations of sample volumes, and filter blank collection were performed as with the SWSTSO4 and SWSNSO4 filters. The filter packs were run continuously, with daily filter changes at 0700 CDT. The Teflon filters were extracted in 35 ml of dilute sodium carbonate / sodium bicarbonate buffer for 60 minutes with ultrasound. The cellulose filters were extracted in 30 ml of the same buffer, but with the addition of 0.05 percent hydrogen peroxide. After 30 min of ultrasonic agitation, 10 ml of additional buffer plus peroxide was added, followed

by 30 min of agitation. These solutions were then analyzed for sulfate by ion chromatography [4]. The Teflon filter sulfate result is referred to as SWSFPSO4, and the treated cellulose filter sulfur dioxide result as SWSFPSO2.

The Ontario Ministry of the Environment provided three-stage filter packs consisting of a 2.0 μm Teflon particle filter, 1.0 μm Nylon (Membrana Corp., Nylasorb) nitric acid absorbing filter, and a double layer of potassium carbonate / glycerol treated cellulose (Whatman 41) sulfur dioxide absorbing filter. Eight filter holders were mounted under a shelter 1.5 m above ground. Seven 12 h samples, and one field blank were collected for each 3.5 day period. A sequential air sampler (Metrex Instruments, Ltd.) recorded air volume sampled for each filter pack, and sequenced filters at 0700 and 1900 CDT each day. For comparison with the 24 h samples from other methods, means of the two daily 12 h concentrations were calculated. The Teflon filters were extracted in 25 ml of distilled water for 15 minutes in an ultrasonic bath. The Nylon filters were also ultrasonically extracted, but 25 ml of 0.003 N sodium hydroxide was used. The cellulose filters were ultrasonically extracted 30 min in 0.05 percent hydrogen peroxide, then an additional 25 ml of fresh peroxide solution was added prior to the final 15 min of agitation. The liquid samples were analyzed for sulfate by ion chromatography. The Teflon filter sulfate result is referred to as MOEFPSO4, and the total of sulfur detected on the Nylon and cellulose filters, attributed to sulfur dioxide, as MOEFPSO2.

Results and Discussion

The overall arithmetic mean concentrations for 23 days in June, 1982 when all five methods had valid samples are listed in Table 2. Note that the units for all species are μg of sulfur / cu.m. The range in sulfate sulfur observed was 0.20 to 7.67 μg/cu.m; for sulfur dioxide, the range was 0.27 to 5.49 μg/cu.m.

Table 2. MEAN AND (MEDIAN) CONCENTRATIONS (μg/cu.m) FOR 23 DAYS.

SULFATE		PARTICULATE SULFUR		SULFUR DIOXIDE	
SWSFPSO4	2.45 (2,05)	SWSPS	1.82 (1.51)	SWSFPSO2	2.42 (2,20)
SWSTSO4	2.33 (2.09)			MOEFPSO2	2.56 (2,59)
MOEFPSO4	2.19 (1.82)				
SWSNSO4	1.28 (1.19)				

SWSFPSO4 and MOEFPSO4 are plotted in Figure 1 [5], showing the consistent good agreement between the filter pack methods. A Bartlett method [6] regression line, MOEFPSO4 = SWSFPSO4 * .906 + .005, suggests that the 2.0 μm Teflon filter slightly undercollects sulfate relative to the 1.0 μm filter. The possibility of some "missed" sulfate is further supported by the sulfur dioxide results, discussed below. These two sets of filters were extracted and analyzed independently by separate laboratories. An interlaboratory exchange of a blind sample series for sulfate gave results that agreed within three percent. Thus, the analytical procedures should not contribute to the differences in the final concentration determination. Figure 2, a plot of SWSTSO4 and SWSFPSO4, compares two sets of 1.0 μm Teflon filters. The exposure

schedules, flow rates, and extraction methods, and analytical techniques were different, yet there is good agreement between these two sets of concentration data. The regression line is SWSTSO4 = 1.09 * SWSFPSO4 - .335.

Figure 1. RESULTS OF TWO FILTER PACK METHODS FOR SULFATE.

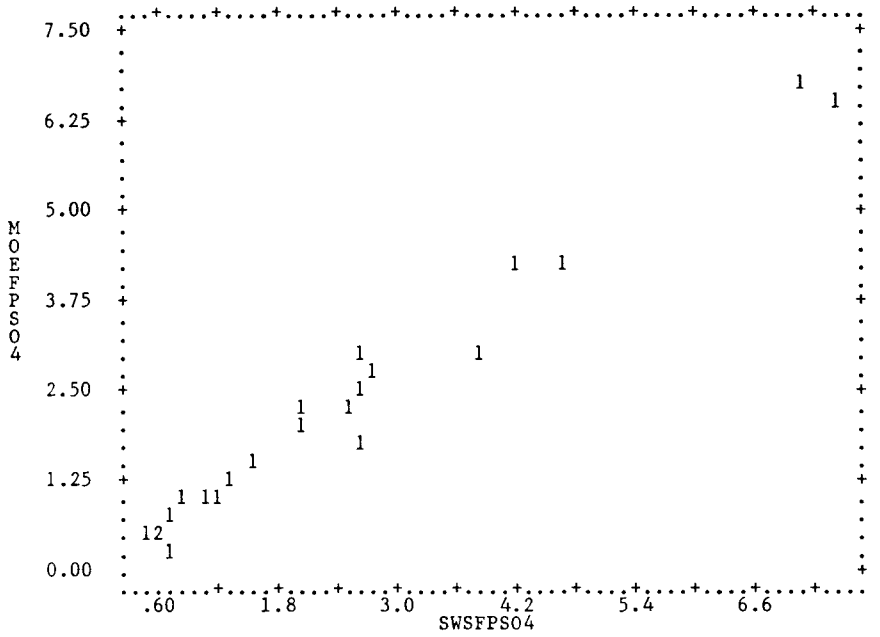

Figure 3 compares SWSTSO4 with SWSNSO4, the 37 mm diameter filters exposed, extracted, and analyzed under carefully matched conditions. The regression line, SWSNSO4 = SWSTSO4 * .437 + .277, does not show the good agreement found in Figures 1 and 2. The 0.8 μm Nuclepore filter seems to undercollect sulfate relative to all the Teflon methods by about 50 percent. Confidence region calculations show the data to be less tightly grouped than in the Teflon method comparisons.

Figure 2. RESULTS OF TWO 1.0 μm TEFLON FILTER SAMPLING METHODS.

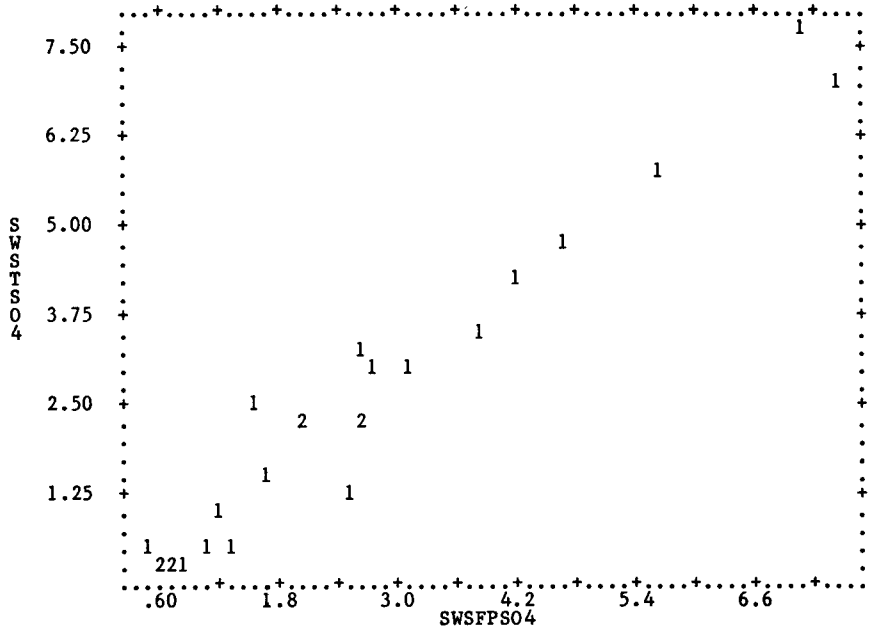

Figure 3. RESULTS OF MATCHED - EXPOSURE TEFLON AND NUCLEPORE FILTERS.

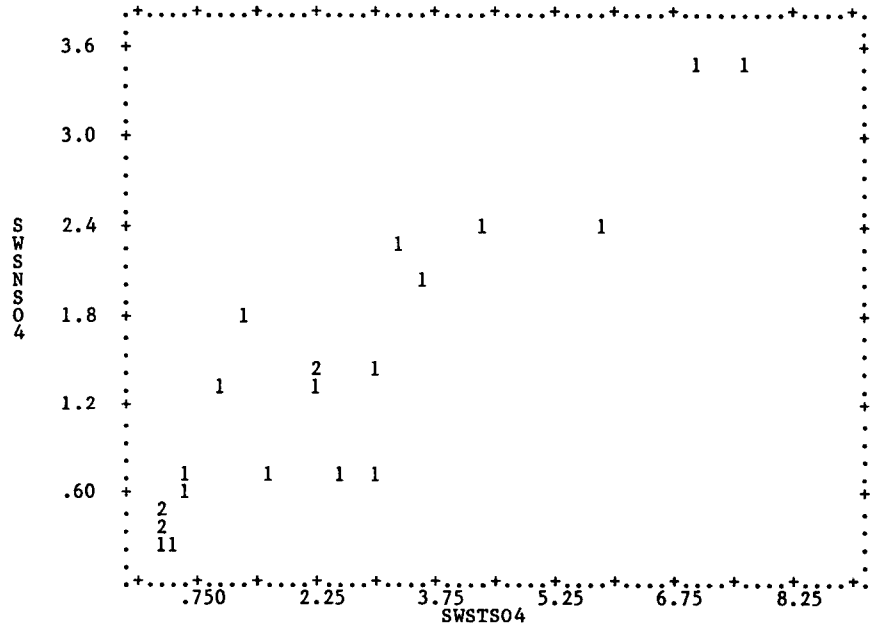

The relatively low sulfate determinations by the 0.8 μm Nuclepore filters are probably due to poor small particle collection, rather than extraction and analysis problems. Figure 4 compares the total particulate sulfur collected on a 0.4 μm Nuclepore filter, SWSPS, with

the daily mean sulfate sulfur from the three Teflon filter methods, SO4BAR. The regression line is SWSPS = SO4BAR * .687 + .243, again demonstrating an apparent undercollection. The PIXE elemental analysis does not involve an extraction step. In both Figure 3 and 4, the greatest percentage differences between the Teflon filter methods and the Nuclepore filters occur at higher concentrations. Dichotomous sampler data from this site in September, 1981, show that the percentage of sulfur in the small aerosol fraction increases during episodes of high total sulfate concentration. This also supports the idea that differences between the Teflon and Nuclepore filters are due to undercollection. Further interpretation of these comparisons will be greatly aided by the completion of the data set. The additional methods include size fractionated samples of several kinds, and other filter media.

Figure 4. PARTICULATE SULFUR AND MEAN SULFATE RESULTS.

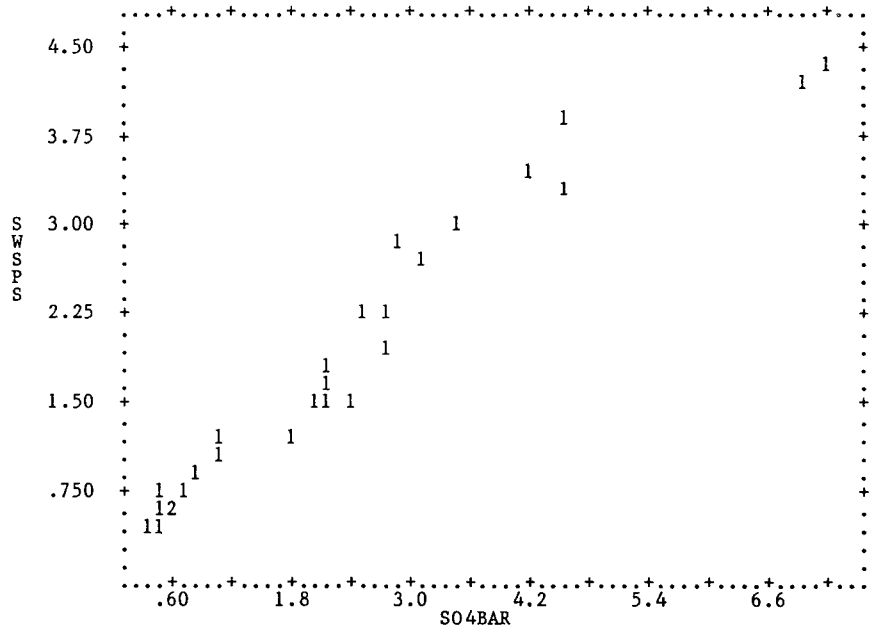

Acknowledgements

This work was supported by the US Environmental Protection Agency through Cooperative Agreement 808863, and by the US Department of Energy through contract number DEAS0276EV01199. Walter Chan of the Ontario Ministry of the Environment generously provided the filter pack data which were collected under the auspices of the Acidic Precipitation in Ontario Study.

References

1. Dolske, D.A. and D.F. Gatz. A field intercomparison of particle and gas dry deposition measurement and monitoring methods. This Proceedings. 1983.

2. Stensland, G.J. and J.D. Bartlett. Measurements of atmospheric nitrate, sulfate, ammonium, and calcium using various filter setups. Proc. 72nd APCA meeting. Cincinnati, OH. 1979.

3. Peden, M.E., L.M. Skowron and F.M. McGurk. "Precipitation sample handling, analysis, and storage procedures." USDOE Research Rept. 4, C00-1199-57. Illinois State Water Survey, Urbana, IL. 1979.

4. Dionex Corporation. "System 12 analyzer operation and maintenance." Sunnyvale, CA. 1979.

5. All plots in this text were generated by BMDP statistical software. Univ. California, Berkeley, CA. 1983.

6. Smith, M.V., R.W. Shaw, Jr. and R.J. Paur. An alternative to least squares statistics for comparison of duplicate measurements. Atmos. Env. 17(1): 65-71. 1983.

Comparison of Surrogate Surface Techniques for Estimation of Sulfate Dry Deposition

John J. Vandenberg and Kenneth R. Knoerr, Duke University School of Forestry and Environmental Studies, Durham, N.C., 27706.

Surrogate surfaces, often used to estimate the dry deposition of sulfate to vegetation, were simultaneously exposed within and above a hardwood forest canopy. Surfaces representing both rough and smooth textural types included deposition buckets, petri dishes, filter paper, Teflon configurations and polycarbonate membranes. The dry deposition rate of sulfate was correlated across the surface types and the magnitude of the deposition rates were compared. The petri dish and filter plate surfaces were found to represent the best devices for the estimation of dry deposition to smooth and rough artificial surfaces, respectively. Further work is now needed to relate the dry deposition to surrogate surfaces to that on natural surfaces.

This study was a cooperative effort of the Duke University School of Forestry and Environmental Studies, the Aerosol Research Branch of the U.S. Environmental Protection Agency, and the Research Triangle Institute. This paper has been reviewed in accordance with the U.S. Environmental Protection Agency's peer and administrative review policies and approved for presentation and publication.

Comparison of Surrogate Surface Techniques for Estimation of Sulfate Dry Deposition

Natural vegetation is thought to be effective in removing atmospheric pollutants through dry deposition as well as wet deposition processes (1,2). However, difficulties related to the leaching of internal plant sulfate have limited the accurate assessment of the dry deposition component of pollutant removal by natural surfaces. Although a number of researchers have relied upon surrogate deposition surfaces to estimate the flux rate of many materials (3-5), little work has been done to intercompare the surfaces. In our study, the dry deposition rates of sulfate particles to artificial surfaces within and above a mature hardwood forest were measured over an annual range of synoptic weather conditions. Sampling levels were at heights of 1, 12, 25, and 36 m above the forest floor, corresponding with the forest floor region, the region between overstory and understory canopies, the area of canopy closure, and above the forest foliage, respectively.

Surrogate surfaces representing both rough and smooth textural types included 28.6 cm diameter polyethylene deposition buckets, 9 cm diameter polystyrene petri dishes with and without Whatman 41 cellulose filters taped inside, 9 cm wide by 27 cm long Teflon sheets in both solid bar form and as Teflon sheets affixed to a stainless steel core, 4.7 cm diameter Nuclepore #111105 polycarbonate membranes held in circular filter holders, and a sheet of Pallflex E70-2075W cellulose-glass filter paper held within a stainless steel frame to expose a 13.2 cm by 18.2 cm rectangular portion of filter paper. Ambient concentrations of sulfate and sulfur dioxide were monitored at the top and bottom of the tower with U.S. EPA high-volume samplers and Huey sulfation plates, respectively, with all chemical analysis performed by USEPA and Research

Triangle Institute laboratories.

For periods when on-site high-volume samples were not available, ambient sulfate concentrations were estimated from measurements made by the Research Triangle Institute (RTI), Research Triangle Park, N.C., some 14 miles away. Comparison of simultaneous high-volume measurements made at the Duke Forest and RTI sites demonstrated a strong relationship in the ambient sulfate concentration at these locations.

The dry deposition rates of sulfate to the artificial surfaces were evaluated on the basis of their magnitude and precision. Correlation coefficients calculated for the dry deposition rate of sulfate to the various surrogate surfaces were generally positive, with a number of significant coefficients as shown by asterisks in Table 1. Blank positions in Table 1 indicate insufficient sample size or interference from outlier points which biased the interpretation of the coefficients and were therefore excluded from further consideration. Those correlations which were shown by plots of the data values to indicate strong trends between the sampling surfaces are underscored.

A grouping of the surrogate surfaces was made based on the correlation coefficients. One group, characterized by generally smooth, low profile surface types, was composed of the Teflon configurations, the petri dish surfaces and the polycarbonate membrane. A second group, having smooth surfaces with a greater profile in each dimension included the inner and outer surfaces of the deposition buckets. One other surface with a low profile and a relatively rough texture, i.e. the filter plate, comprised a separate type. In the first two groups, strong and significant correlations between the surfaces tended to tie each group together, while the filter plate type was seen to respond in a unique manner. Ambient concentration of the sulfur oxides and sulfate deposition rates to the surrogate surfaces were not well correlated.

For diverse reasons, several of the techniques (i.e. deposition buckets, Teflon surfaces and polycarbonate membranes) were found to have limited reliability. In general, these surrogate surface types demonstrated a high degree of data variability and low levels of net accumulation of sulfate dry deposition relative to background amounts. In contrast, the petri dish and filter plate surrogate surfaces demonstrated a high degreee of precision and adequate surface accumulations. Thus the petri dish and filter plate surfaces were found to represent the best devices for the estimation of dry deposition to smooth and rough artificial surfaces, respectively. Average dry deposition rates to these samplers during the season of the year with foliage on the trees were 13.6 and 53.6 ug $SO_4^{2-}/m^2/hr$, respectively. Average deposition rates for all the surrogate surfaces during the foliated season of the year are shown in Table 2.

The wide range of surface deposition rates estimated from the variety of deposition surfaces emphasizes the uncertainty of the individual measurement techniques as well as the dependency of sulfate dry deposition on surface characteristics. In spite of these limitations, the use of surrogate surfaces provides at least an approximate estimate of sulfate flux rates not currently obtainable from natural surfaces. A critical research need is studies emphasizing surface deposition on natural vegetation. Such studies should provide a relationship between the deposition to surrogate surfaces in this and other studies to that on natural surfaces.

Table 1. CORRELATION COEFFICIENTS FOR EACH COMBINATION OF SURROGATE SURFACES.

	Bucket Inside	Bucket Outside	Solid Teflon Downfacing	Solid Teflon Upfacing	Steel Teflon Downfacing	Steel Teflon Upfacing	Petri Dish Filter	Petri Dish	Polycarbonate Membrane
Filter Plate		.35	.31	.14	.36	.29		-.27	.22
Polycarbonate Membrane		.50			.25	.61*+	.52	.33	
Petri Dish	.05	.07			.47*	.61*	.90*		
Petri Dish Filter	-.14	-.27	.34	.02	.55	.77			
Steel Teflon Upfacing	.42*	.24	.57	.28	.69				
Steel Teflon Downfacing	.13	-.02	.65*	.48					
Solid Teflon Upfacing	.33	.50	.82*						
Solid Teflon Downfacing		.82*							
Bucket Inside	.88*								

*Asterisks indicate significant coefficients at the $p \leq 0.05$ level.
+Correlations which were shown by plots of the data points to indicate strong trends between sampling surfaces are underscored.

TABLE 2. MEAN DEPOSITION RATES OF SULFATE TO SURROGATE SURFACES EXPOSED WITHIN THE FOREST FOLIAGE

Surface	Mean Deposition Rate ug $SO_4^=/m^2/hr$	Sample Size
Filter Plate	53.6	21
Petri Dish	13.6	15
Petri Dish Filter	45.7	3
Polycarbonate Membrane	34.8	10
Steel Core Teflon Upfacing	7.0	21
Steel Core Teflon Downfacing	1.6	21
Solid Core Teflon Upfacing	6.4	8
Solid Core Teflon Downfacing	3.0	8
Bucket Inside	32.3	13
Bucket Outside	5.4	13

REFERENCES

1. Smith, W.H. Air pollutants and forests: Interactions between air contaminants and forest ecosystems. Springer-Verlag, New York, 1981. 379 pp.

2. Hill, A.C. Vegetation: a sink for atmospheric pollutants. J. Air Poll. Control Assoc. 21: 342-346, 1971.

3. Hicks, B.B., M. L. Wesely, and J. L. Durham. Critique of methods to measure dry deposition: Workshop summary. U.S. Environmental Sciences Research Laboratory, Research Triangle Park, N. C., 1980. 71 pp.

4. Nihlgard, B. Precipitation, its chemical composition and effect on soil water in a beech and spruce forest in south Sweden. Oikos 21: 208-217, 1970.

5. Schlesinger, W., and W. Reiners. Deposition of water and cations on artificial foliar collectors in fir-krummholz of New England Mountains. Ecology 55: 378-386, 1974.

Dry Deposition of Sulfate Within a Hardwood Forest Canopy

Vegetation provides a major surface area available for the deposition of atmospheric gaseous and particulate pollutants and may therefore provide an important sink for sulfur oxides. As particles and gases such as sulfate and sulfur dioxide flow through a forest environment the deposition processes of sedimentation, impaction, and diffusion take place. These deposition processes result in a decrease in the ambient concentration of these pollutants within and beneath the forest canopy. Previous studies have found most of the deposition of particles to be on the canopy foliage rather than to the ground surface (1). Ideally, such deposition to the foliage should be observed as a decreasing pollutant concentration gradient from above the forest canopy to the forest floor (2). Vertical differences in ambient pollutant concentrations and deposition rates may therefore reveal the sink or source role of a forest.

Direct measurements of sulfate dry deposition to natural surfaces have been hindered by technique difficulties and the leaching of foliar sulfate, leading to the use of surrogate deposition surfaces. In our study, canopy flux estimates were made based on petri dish and filter plate surfaces which represent oposite ends of the surface texture spectra. Natural leaf surfaces may have collection properties somewhere between them. These surrogate surfaces were also chosen as adequate surface representatives because they provide deposition estimates in which more confidence can be placed than with a number of other techniques. The choice of these surrogate surfaces is examined in another paper by the authors in this volume.

The total dry sulfate flux to the canopy was estimated as the summation of the flux to the top and bottom of the collectors multiplied by the mean leaf area per unit ground surface, plus the deposition to the unit ground surface.

The forested research site has a leaf area index (defined as the plan surface area of leaves per unit ground surface area) between 4 and 7 (3). Taking an average value of 5.5, this figure was multiplied by a typical deposition rate for each surface type to estimate a flux rate for the upwards facing leaf surface area. Our data were not detailed enough to define a vertical distribution of deposition rates associated with the vertical distribution of leaf area. Thus an average deposition rate was used for calculations with the total surface area to estimate the total sulfate dry deposition rate.

In previous studies the deposition of aerosols to upwards facing surfaces has been found to range from 0.17 to 19 times greater than the deposition to similar downfacing surfaces (4, 5). In the present study the sulfate deposition to upwards facing Teflon surfaces averaged 3.2 times the deposition to downwards facing Teflon surfaces, a value similar to that found for lead deposition to Teflon disks (up/down = 4.0) (6). For our purposes, on the basis of these Teflon surface measurements, we used a factor of 0.31 to estimate sulfate deposition to the downwards facing surface area of leaves. The deposition to the ground was estimated on the basis of the rate to the upfacing surfaces and unit ground surface.

A review of climatological data revealed that during the seven months when the trees were foliated (April through October) rainfall occurred approximately 7% of the time (7). The flux rate calculations were therefore adjusted by this amount through a multiplication by 0.93 to calculate the flux of sulfate aerosols during only dry events. The calculations of the dry flux of sulfate to the foliated oak-hickory-tulip poplar canopy during 1981 based on the petri dish flux rates is shown in Table 1 and that based on the filter plate flux rates in Table 2.

The sulfate flux rate totaled 5.3 and 21.0 kg $SO_4^=$/ha/(foliated canopy during 1981) for the petri dish and filter plate surfaces, respectively. These values may be modified to represent the elemental sulfur present in the sulfate particles ($SO_4^=$-S) through a division by three to compensate for the molecular weight of sulfur and oxygen in the sulfate molecules. This conversion yields flux rates of 1.8 and 7.0 kg $SO_4^=$-S/ha/(foliated canopy) for the petri dish and filter plate surfaces, respectively. These values compare favorable with other sulfate dry deposition estimates based in part on petri dish deposition rate measurements of 4.8 kg $SO_4^=$-S/ha/(foliage of a chestnut oak canopy) (8).

TABLE 1. CALCULATION OF THE MEAN TOTAL DRY SULFATE FLUX RATE TO A FOLIATED FOREST CANOPY ON THE BASIS OF PETRI DISH SURROGATE SURFACE FLUX RATES

Total flux rate = (upfacing flux + downfacing flux + ground flux)

Mean flux rate to petri dish surfaces during foliated periods = 13.6 ug $SO_4^=/m^2/hr$

Mean leaf area index = 5.5

Upfacing flux to downfacing flux ratio = 1 : 0.31

Upfacing leaf flux = 5.5 x 13.6 = 74.8 ug $SO_4^=/m^2/hr$

Downfacing leaf flux = 5.5 x 13.6 x 0.31 = 23.2 ug $SO_4^=/m^2/hr$

Ground surface flux = 1 x 13.6 = 13.6 ug $SO_4^=/m^2/hr$

Dry flux rate to canopy during foliated period = 112 ug $SO_4^=/m^2/hr$

Total dry flux to canopy during the foliated period = 5.3 kg $SO_4^=/ha/$(foliated canopy during 1981)

TABLE 2. CALCULATION OF THE MEAN TOTAL DRY SULFATE FLUX RATE TO A FOLIATED FOREST CANOPY ON THE BASIS OF FILTER PLATE SURROGATE SURFACE FLUX RATES

Total flux rate = (upfacing flux + downfacing flux + ground flux)

Mean flux rate to filter plate surfaces = 53.6 ug $SO_4^=/m^2/hr$ during foliated periods

Mean leaf area index = 5.5

Upfacing flux to downfacing flux ratio = 1 : 0.31

Upfacing leaf flux = 5.5 x 53.6 = 298.4 ug $SO_4^=/m^2/hr$

Downfacing leaf flux = 5.5 x 53.6 x 0.31 = 91.4 ug $SO_4^=/m^2/hr$

Ground surface flux = 1 x 53.6 = 53.6 ug $SO_4^=/m^2/hr$

Dry flux rate to canopy during foliated period = 440 ug $SO_4^=/m^2/hr$

Total dry flux to canopy during the foliated period = 21.0 kg $SO_4^=/ha/$(foliated canopy during 1981)

REFERENCES

1. Raynor, G.S., J.V. Hayes, and E.C. Ogden. Particulate dispersion into and within a forest. Boundary-Layer Meteorology 7: 429-456, 1974.

2. Sehmel, G.A. Particle and gas dry depostiion: a review. Atmos. Environ. 14: 983-1011, 1980.

3. Christensen, Norman. Duke University Department of Botany, personal communication, 1982.

4. Little, P. Deposition of 2.75, 5.0 and 8.5 um particles to plant and soil surfaces. Environ. Pollut. 12: 293-305, 1977.

5. Aylor, D.E. Deposition of particles in a plant canopy. J. App. Meteor. 14: 52-57, 1975.

6. Elias, R.W., and C. Davidson. Mechanisms of trace element deposition from the free atmosphere to surfaces in a remote high sierra canyon. Atmos. Environ. 14: 1427-1432, 1980.

7. NOAA. National Oceanic and Atmospheric Administration, Environmental Data and Information Service, National Climatic Center, Asheville, North Carolina. Local Climatological Data, Monthly Summary for Raleigh-Durham Airport, North Carolina, 1981.

8. Lindberg, S.E., R.C. Harriss, R.R. Turner, D.S. Shriner, and D.D. Huff. Mechanisms and rates of atmospheric deposition of selected trace elements and sulfate to a deciduous forest watershed. ORNL/TM-6674, Oak Ridge National Laboratory, Oak Ridge, TN., 1979.

SESSION VI

ORGANIC POLLUTANTS

EVALUATION OF SOLID SORBENTS FOR COLLECTION OF VOLATILE ORGANICS IN AMBIENT AIR

by

L. J. Hillenbrand and R. M. Riggin

BATTELLE
Columbus Laboratories
Columbus, Ohio 43201

ABSTRACT

The procedure is based on the equilibrium adsorption model of Dubinin-Radushkevich and the adsorption kinetics model of Wheeler and Robell. The method has had some success in correlating and predicting the relative adsorbability of various organic species on charcoal and has been used to describe the adsorption of hazardous vapors at low concentrations in air.

The very low vapor concentrations being employed, i.e., parts per billion, extend the application of the model to very low sorbent loadings and also tend to emphasize calibration and reproducibility uncertainties arising from the high-gain detector sensitivities that must be employed. From the plots of breakthrough time-versus-sorbent weight, the sorbent capacity and sorption kinetics are obtained.

When adsorption is completed, a programmed temperature rise is used to desorb the vapor. A complete and facile desorption of the vapor almost certainly implies that the vapor adsorption is limited to physical processes and the prediction procedure for the adsorption of a new vapor is based on this fact. Once a few reference vapors have been tried, the adsorption of the others may be predicted.

The results indicate that a detailed evaluation of a candidate sorbent can be obtained through the method investigated in this program.

This paper has been reviewed in accordance with the U.S. Environmental Protection Agency's peer and administrative review policies and approved for presentation and publication.

EVALUATION OF SOLID SORBENTS FOR COLLECTION OF ORGANIC VAPORS IN AIR, L. J. Hillenbrand and R. M. Riggin, Battelle, Columbus Laboratories, 505 King Avenue, Columbus, Ohio 43201.

The problem of sampling atmospheric organic vapors by adsorption at parts per billion concentration imposes several special requirements on the sorbent to be used. Tenax GC resin has been widely employed; nevertheless, some field problems have arisen implying difficulties with complete desorption of some vapors and candidate replacement resins have been suggested. This Work Assignment is concerned with the demonstration of a protocol suitable for qualifying such resins. Since the resin is to be used in a permeation bed configuration, we prefer a model that uses that configuration to describe vapor breakthrough characteristics.

The procedure used is based on the equilibrium adsorption model of Dubinin-Radushkevich[1] and the adsorption kinetics model of Wheeler and Robell[2]. The method has had some success in correlating and predicting the relative adsorbability of various organic species on charcoal and has been used to describe the adsorption of hazardous vapors at low concentrations in air. The plan for our program is intended to

- Demonstrate that the Model is Applicable
- Describe the Critical Parameters
- Obtain Numerical Values for Adsorption Capacity and Kinetics of Selected Reference Vapors
- Demonstrate Use of the Model for Predicting Performance of Untested Vapors.

This presentation will concentrate on the first two of these needs; work is continuing on a variety of systems for demonstration of the full scope of the applications possible.

Whatever model is used, several special circumstances must be recognized. First, since the volatile organic vapors to be sampled typically are in parts per billion concentration, the partial pressure of the vapor may be 10^{-6} to 10^{-5} that of its saturation vapor pressure ($P/P_o < 10^{-5}$) and such low partial pressures place restrictions on the adsorption models that are applicable. Second, in most cases the sorption is to be accomplished in the presence of relatively overwhelming amounts of atmospheric moisture and the need for H_2O rejection has been one of the factors that led to the use of the low surface energy organic resin sorbents. Further, since the sorbed vapors must be readily and quantitatively desorbed by moderate increased in temperature, we infer that chemisorption mechanisms generally will be unacceptable. Acceleration of the desorption by temperature rise can be tolerated only to the extent that no appreciable degradation occurs at the same time.

For the model as applied by Jonas[3], the time of breakthrough (t_b) of a vapor passing through a given bed of absorbent is expressed by

$$t_b = \frac{W_e}{C_o Q} \left[W - \frac{\rho Q}{k_v} \ln (C_o/C_b) \right] \qquad (1)$$

where

C_o/C_b = the ratio of the inlet concentration of adsorbate vapor to the breakthrough concentration, in consistent units. C_o alone is in g/cm^3.

Q = gas volume flow rate, cm^3/min

W = weight of adsorbent, g

W_e = the kinetic level of bed saturation achievable at chosen C_o/C_b; g/g

k_v = pseudo first order rate constant for the adsorption process in that bed, min^{-1}

ρ = bulk density of the packed bed, g/cm^3.

This can be arranged to form

$$t_b = a + bW \tag{2}$$

where

$$a = -\frac{W_e \rho}{C_o i_v} \ln (C_o/C_b) \tag{3}$$

and

$$b = W_e/C_o Q \tag{4}$$

Experimental values of t_b are obtained as a function of bed weight, W, for a fixed value of C_o/C_b. The value of W_e is derived from Equations (2) and (4) using known values of C_o and Q. Equation (3) then can be used to obtain the value of the adsorption rate constant since all the other quantities are known. The volume flow rate, Q, and the values of C_o and C_b are used as independent variables with values that are set by the adsorption conditions of interest.

The method of procedure is a simple one. Using the apparatus shown schematically in Figure 1, the procedure is as follows:

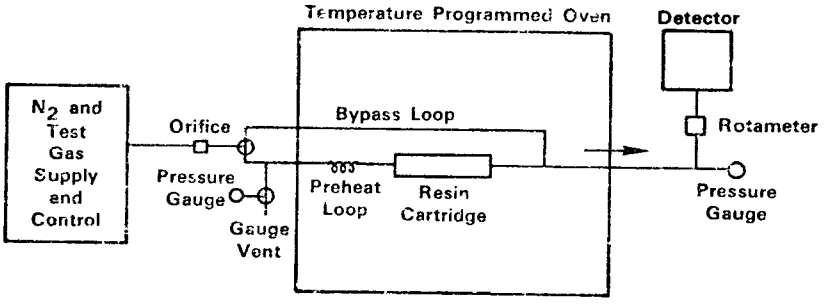

Figure 1. Arrangement of Apparatus.

The method of procedure is a simple one:

(1) A reference resin (Tenax GC) is characterized using a few vapors that also will serve as references in later work. The characterization involves adsorption of the vapor on resin columns of different length (weight) so that a correlation of breakthrough time and bed weight can be produced for a specified breakthrough concentration.

(2) Following each adsorption trial, the vapor is desorbed by a programmed temperature rise and the completeness of desorption is tested following various periods of storage for the sorbed vapor.

(3) The full adsorption capacity of the reference resin is tested by several experiments in which the resin bed weight is held constant and vapor concentration is varied.

The kinetic sorption capacity for the given inlet vapor concentration is determined by plotting variations of t_b with W for some chosen value of C_b/C_o, and we note that under these high sensitivity recording conditions the midpoints of the breakthrough curves, see for example Figure 2, are more precisely defined than points near the start of the breakthrough profile. We tested the constancy of slope for several values of C_b/C_o in order to determine the validity of using the more precise portion of the curve for this purpose.

The kinetic model identifies the rate constant, k_v, as a pseudo first order constant that pertains to the initial portion of the breakthrough curve where sorbent site occupancy is low so that the available concentration of sorbent "sites" is constant and nearly equal to the initial sorbent capacity. At later portions of the curve both vapor and sorbent site concentrations are varying so that the pseudo first order constant will be found to vary as the level of occupancy of the resin is allowed to vary according to the point,

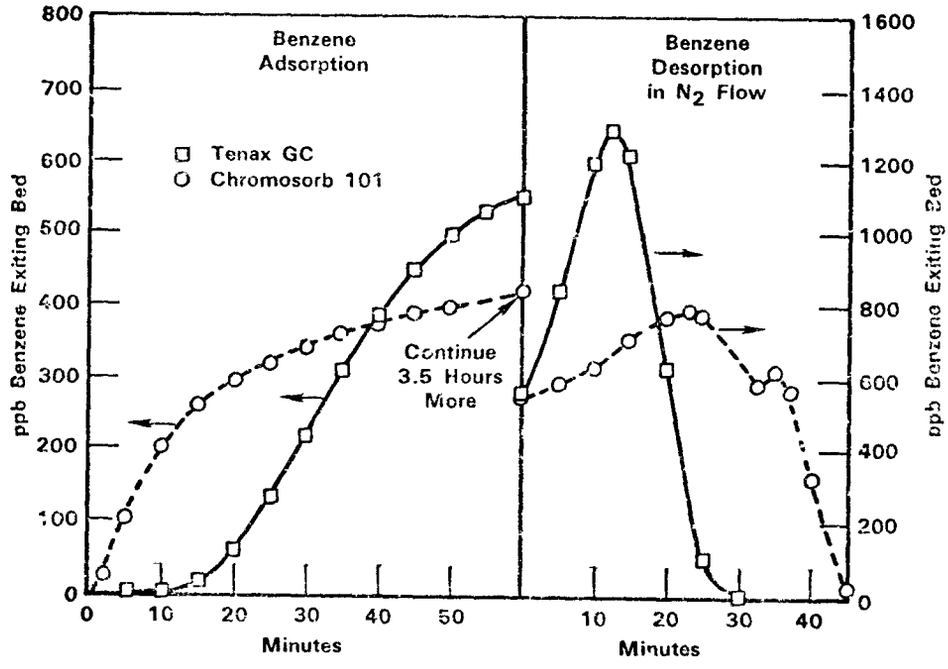

Figure 2. Comparison of Breakthrough and Desorption Curves for Two Different Sorbents.

C_b/C_o, chosen for the analysis. In this report the points for C_b/C_o = 0.05, 0.10, 0.20, and 0.50 have been tried for evaluation of k_v. The C_b/C_o value of 0.05 represents the lowest concentration that it appears possible to analyze with reasonable accuracy under these high sensitivity conditions.

When adsorption is completed, a programmed temperature rise is used to desorb the vapor. A complete and facile desorption of the vapor almost certainly implies that the vapor adsorption is limited to physical processes and the prediction procedure for the adsorption of a new vapor is based on this fact. The same basis for prediction applies to the several reference vapors employed so that once one reference vapor is tried the adsorption of the other two might be predicted. However, the matter is not quite this simple since the presence or absence of dipolar character in the vapor complicates the basis by which the physical adsorption is predicted. In prior work with

carbon sorbents, this feature has been handled by keeping a simple model for prediction of the adsorption and by using reference vapors that characterize nonpolar, moderately polar, and highly polar adsorbates. For the present study, these are being represented by benzene, 1,2-dichloroethane, and acetone vapors.

For the study of benzene vapor sorption by Tenax GC, resin bed depths of 1.0, 3.0, 5.0, and 6.5 inches were tried. The 1.0-inch bed depth proved to be too close to the critical value, for which breakthrough begins immediately, and was abandoned. For the remaining three bed depths, initial benzene vapor concentrations of 120 and 580 ppb were employed and the breakthrough times were measued at C_o/C_b equal to 20, 10, 5, and 2, corresponding to 5, 10, 20, and 50 percent vapor concentration breakthrough. This multiplicity of inlet and breakthrough concentrations permitted several analyses of the adsorption kinetics for improved precision of the kinetic constants. In Figure 2, the results for Chromosorb 101 illustrate a sorbent with good sorption capacity but with poor sorption kinetics so that appreciable breakthrough concentrations appear very quickly.

Only the averages of individual determinations are plotted in Figure 3 for the adsorption of benzene on Tenax GC. The lines represent the least square slopes determined from the complete set of data and the expected straight line relationship between t_b and W is illustrated. Similar data were obtained for 1,2-dichloroethane vapor. The slope b, for the data at C_b/C_o = 0.5, 0.2, and 0.05, was found to be independent of the choice of C_b/C_o for both benzene and 1,2-dichloroethane. These vapors showed complete desorption and no abnormalities were experienced either during adsorption or desorption of the vapors from the resin. The data for acetone demonstrated

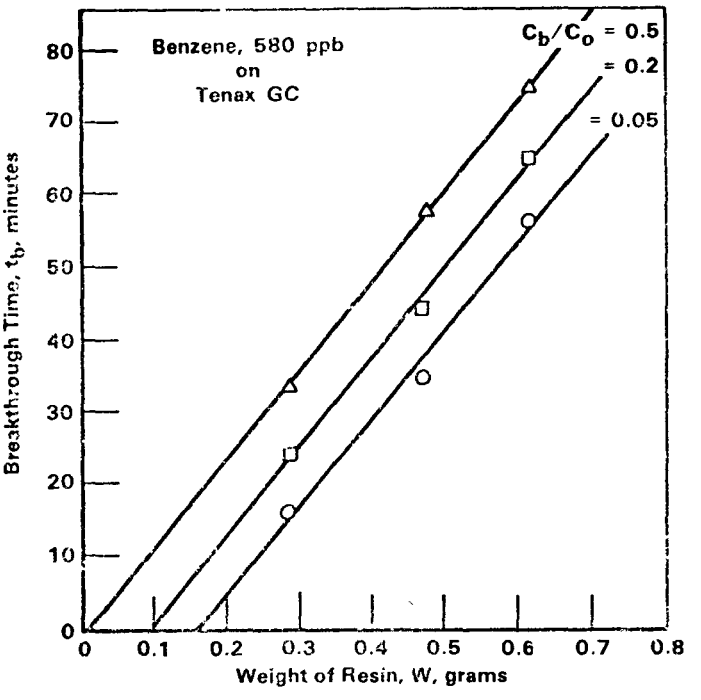

Figure 3. Variation in Breakthrough Time With Sorbent Bed Weight.

otherwise and are discussed separately.

For acetone, we note that whereas the vapor is rapidly adsorbed, the adsorption capacity of the resin for this vapor is comparatively small, see Figure 4.

It further was noted that the desorption peaks for this highly dipolar vapor, acetone, average only 78.0 percent of the size of the adsorption peaks and extraneous high molecular weight species appear in the desorption curve, see Figure 5. It is striking that the extra peaks, representing high molecular weight but unknown species, on the average were found to be equal in size to the adsorption peak for acetone in this FID system.

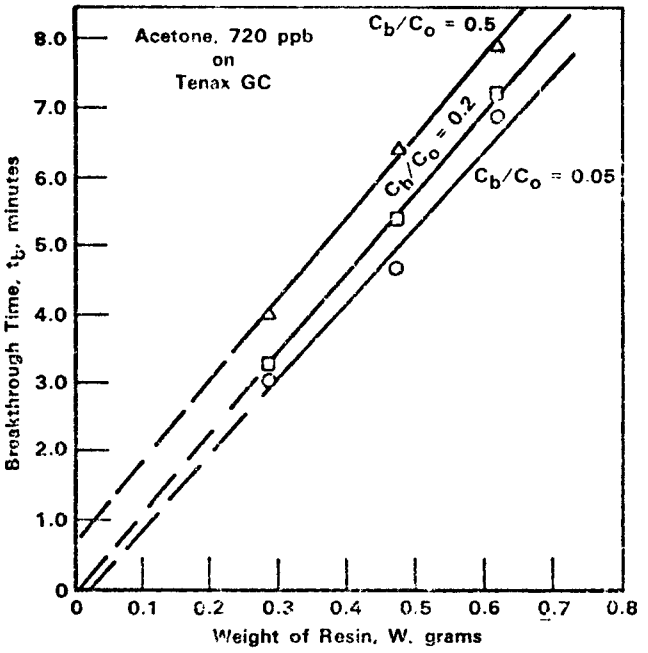

Figure 4. Variations in Breakthrough Time for Acetone on Tenax GC

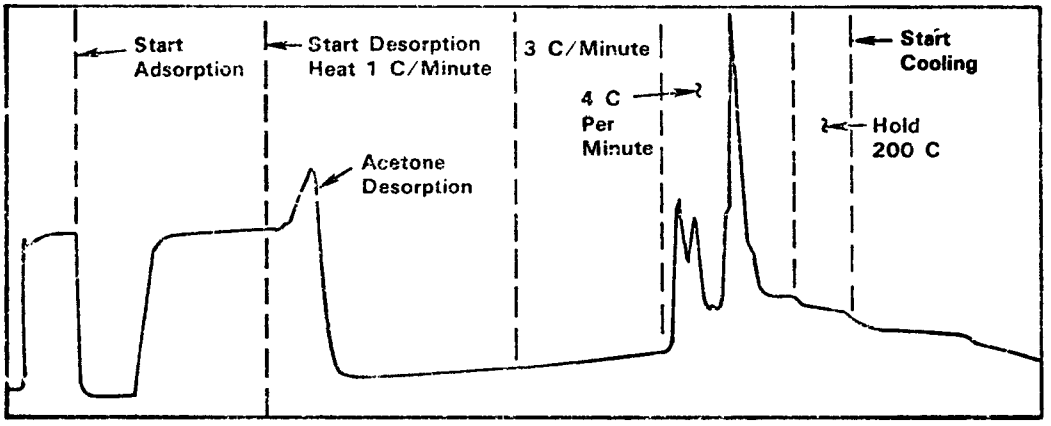

Figure 5. Sample Tracing of Recorder Plot for Acetone Adsorption and Desorption.

The spectrographic grade acetone used in this work, and its mixture with zero N_2 in the charge cylinder, were analyzed and no obvious explanation for these peaks based on pre-existing impurities was found. We currently favor

the conclusion that the artifact peaks represent species desorbed from the resin by acetone and roughly in proportion to the amount of acetone taken up.

The data presented illustrate that the Wheeler and Robell model is a good representation of sorbent-sorbate systems that behave as required for the present application. The data for Chromosorb 101, and for acetone, illustrate some of the deviations in performance that are unacceptable and which become readily recognizable once the features of the model are understood. Table 1 is a summary of the slope (b), and intercept (a), values obtained. The nearly 5-fold change in benzene concentration had no effect on capacity estimate, and the pseudo first order nature of the rate constant is confirmed by the intercept values. Table 2 shows relative values of the rate constant as obtained and as anticipated from a simple kinetic model.

TABLE 1. SLOPE AND INTERCEPT VALUES OBTAINED FOR VAPORS ON TENAX GC

	Benzene		1, 2-Dichloroethane
y (ppb)	580	120	640
a (minutes)			
at C_b/C_o = 0.05	-19.3	-18.6	-13.7
= 0.20	-12.0	-11.6	-8.95
= 0.50	-1.46	-1.46	-2.90
b (minutes/g)			
at C_b/C_o = 0.05	121.0	121.5	103.6
= 0.20	123.9	127.5	103.3
= 0.50	124.4	134.6	102.8

$$k_v = \left(\frac{W_c\ \rho}{C_c}\right)\left[\frac{\ln (Co/Cb)}{a}\right]$$

TABLE 2. RELATIVE VALUES OF THE RATE CONSTANT (k_v) OBTAINED FOR VAPORS ON TENAX GC.

C_b/C_o	For Benzene at		1, 2-Dichloroethane
	580 ppb	120 ppb	at 640
0.05	1.00	1.04	1.41
0.20	0.86	0.90	1.16
Predict	1.00	1.00	0.89

$$k_v\,[C_v] = k[C_s][C_v]$$

Under physical adsorption conditions, monolayer adsorption of vapor on relatively open surfaces will be extremely small at the low values of P/P_o employed here ($< 10^{-5}$). The Dubinin-Radushkevich isotherm indicates that the major part of the adsorption should occur in the micropores, especially those with diameters < 30 Å. According to that isotherm, see Figure 6, a plot of ε^2 versus the equilibrium amount of vapor sorption (W_v = liquid cc of sorbate (g sorbent) is a straight line with slope K/β^2 and the intercept W_o is the apparent total adsorption capacity available. If the system is well behaved, W_e (from the earlier kinetic treatment) should equal $W_v d_1$ where d_1 is the liquid density of the adsorbate. The series of experiments described with W constant and various partial pressures of vapor were made for the purpose of testing this isotherm and obtaining the values of the constants. It is satisfying to note that, for benzene on Tenax GC, W_e does equal $W_v d_1$. Figure 7 shows the anticipated straight line relationship.

For reference vapors, we can set $\beta = 1.00$ and so evaluate K. The process of prediction for untested vapors, or for arranging the vapors in sequence of sorbability, is based on estimating values of β for those vapors. This aspect

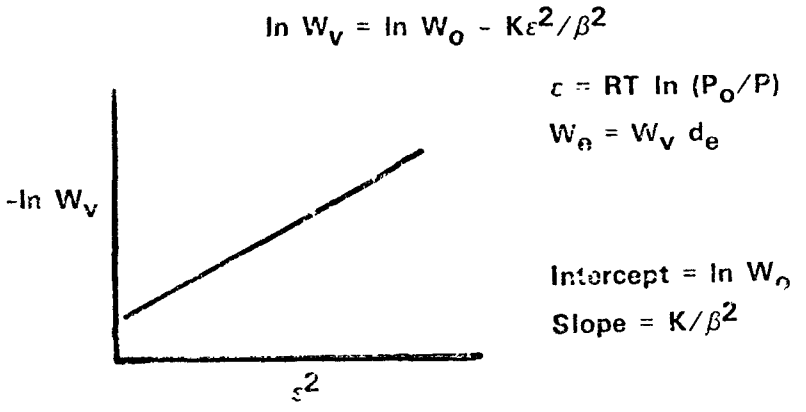

Figure 6. The Equilibrium Adsorption Isotherm.

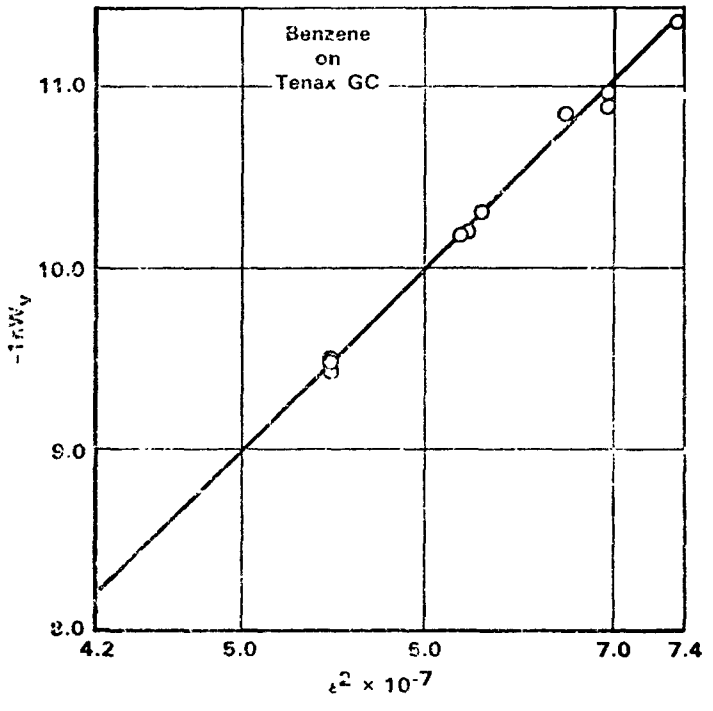

Figure 7. The Isotherm Data for Benzene on Tenax GC at 31 C.

is currently under study in our continuing program.

The features that give Tenax GC the good kinetics for adsorption and desorption of vapor are revealed by further examination of its structure. Table 3 lists bulk densities, and He- and Hg-displacement densities for the two resins, and gives comparative pore volumes estimated from these. The

TABLE 3. DENSITY AND PORE VOLUME ESTIMATES FOR TENAX GC AND CHROMOSORB 101.

Sorbent	Densities, g/cc			
			d_{Hg}	
	d_b	d_{He}	<70μ	<12μ
Tenax GC	0.158	1.10_2	0.295	0.335
Chromosorb 101	0.346	1.05_5	0.400	0.596

	Pore Volumes, cc/g			
	Total	<70μ	<12μ	<300A
Tenax GC	5.42	2.48	2.08	0.034
Chromosorb 101	1.94	1.55	0.729	0.010

two resins differ most significantly in the large conduit pores (e.g., > 70 microns in diameter) for which Tenax GC has almost 3.0 cc/g whereas Chromosorb 101 has about 0.4 cc/g. These are the pores that give ready access to the micropores in Tenax GC. We note that, for benzene on Tenax GC, the apparent total pore volume available, W_o, is 0.0183 cc/g which is about one-half of the micropores < 300 Å. The cumulative pore volume distribution for Tenax GC shown in Figure 8 indicates that W_o corresponds to the pore volume available in Tenax GC below about 110 Å. This comparison is clearly an oversimplification but is qualitatively consistent with the expectations of the Dubinin-Radushkevich isotherm.

Electron microscopy photographs of Tenax GC show it to have a worm-like structure with diameters below 0.5 microns. These structural elements apparently are nonporous since their peripheral surfaces roughly account for the total surface area available, 25.5 m^2/g. Thus, the pores are interstices between irregular cylindrical elements and these are easily available through the very low density arrangement provided. Presumably, a competitive adsorbent must provide an open structure with similar accessibility.

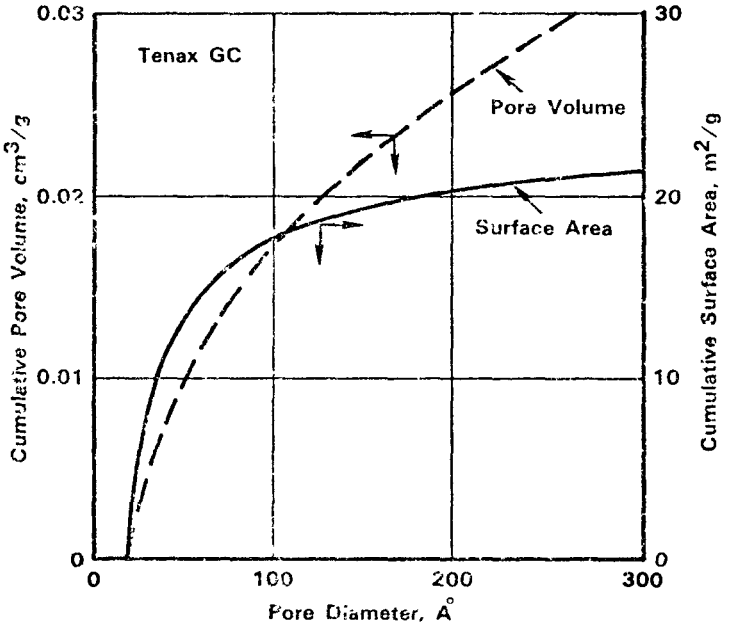

Figure 8. Cumulative Surface Area and Pore Volume Distributions for Tenax GC.

This work has been funded under a Work Assignment from the Environmental Monitoring Systems Laboratory of the Environmental Protection Agency.

REFERENCES

(1) Dubinin, M. M., Chem. Rev. 60, 235-41 (1960).

(2) Wheeler, A., and Robell, A. J., J. Catalysis 13, 299-305 (1969).

(3) Jonas, L. A., and Rehrmann, J. A., Carbon 11, 59-64 (1973).

DETECTION OF ENVIRONMENTAL POLLUTANTS USING PIEZOELECTRIC CRYSTAL SENSORS

Mat H. Ho
Department of Chemistry
University of Alabama in Birmingham
Birmingham, Alabama 35294

ABSTRACT

In recent years, coated piezoelectric crystal sensors have become of increasing interest for detection of trace amount of pollutants from ambient air. Not only are they highly sensitive detectors, but they are also simple, inexpensive, low power consumption, light-weight and portable devices.

The principle of the detector is that the frequency of vibration of an oscillating crystal is decreased by the adsorption of a gaseous sample onto its coated surface. The decrease in frequency is a measure of the amount of gas adsorbed. This linear relationship between frequency change and added mass enables a piezoelectric crystal to be used as a sorption analytical detector with a detection limit of about 10^{-10}g. The selectivity of detector can be achieved by coating the crystal with a substance which selectively adsorbs the pollutant one want to detect.

In this paper, we report new methods and coatings for the specific detection of mercury, organophosphorus pesticides, and formaldehyde. The effect of flow rate, amount of coating, cell configuration, and practical instrument suitable for use as personal monitor will be presented. The use of immobilized enzyme as coating for sensitive and specific detection of formaldehyde will also be described.

I. PRINCIPLE

It has been known for a long time that the depostion of a small mass of material on the surface of a piezoelectric crystal oscillator lowers its resonant frequency. In the early days of communication, it was common practice to lower the frequency of a piezoelectric quartz crystal by applying graphite or ink onto its surfaces. When more graphite or ink applied, the frequency of vibration is lowered. This observation has also been used by crystal manufacturers to adjust the frequency of the crystals. However, no quantitative relationship between the deposited mass and the change of frequency had been investigated until the late 1950's. This relationship and the theoretical basis for piezoelectric mass measurement were derived by Sauerbrey (1,2) and Stockbridge (3). The mass sensitivity of AT-cut, quartz crystals vibrating in the thickness-shear mode can be obtained from the following equation:

$$\frac{\Delta F}{\Delta M_q} = - 2.24 \times 10^{-6} \frac{F_q^2}{A}$$

where ΔF is the change in the resonant frequency, in Hz, caused by a change in the mass ΔM_q of the electrically-driven portion of the crystal, ΔM_q is the change in mass of the electrically-driven portion of the crystal in g, F_q is the basic resonant frequency of the crystal before any foreign mass is added in Hz, and A is the area of the electrically-driven portion of the crystal in cm^2. Sauerbrey (1,2) made the fundamental assumption that deposition of any foreign mass, which behaves in the same way as a quartz increment of equal mass, ΔM_q, will cause the frequency shift Δf. Sauerbrey also successfully tested this equation by coating the quartz crystal with a thin, evenly distributed film of metal, weighing the crystal with film on a microbalance and monitoring the frequency change. For commercially available 9 MHz, AT-cut, quartz crystals having an electrode area of 0.20 cm^2, the mass sensitivity is 907 Hz/μg. For 15 MHz

crystal having an electrode area of 0.10 cm^2, the mass sensitivity is 5040 Hz/μg.

The quantitative relationship between the deposited mass and the change of frequency of piezoelectric quartz crystals give them wide-spread application as transducers for mass detection (4). The use of coated piezoelectric quartz crystals as sorption detectors for toxic gases in air has been reported (5-7). The principle of the detector is that the frequency of an oscillating crystal is decreased by adsorption of a foreign material on its coated surface. A sampled gas is adsorbed by a coating on the crystal's surface which is specific for that gas, thereby increasing the mass on the crystal and decreasing the frequency. The frequency shift is proportional to the concentration of sampled gas. The interest in coated piezoelectric crystals for detection of environmental pollutants has been increased recently due to their properties of high sensitivity, rapid response, low cost, low power consumption (which can be operated on rechargeable batteries), light weight and portability for field use that are inherent in the piezoelectric detection method, in spite of some limitations.

II. APPARATUS

A schematic diagram of the experimental setup with the piezoelectric quartz crystal sensor is shown in Figure 1. The coated crystal was housed in the detector cell and was driven in its fundamental frequency by an oscillator (International Crystal Mfg. Co., Oklahoma City, Oklahoma). The oscillator was powered by a Heathkit variable power supply (Model IP-28). The frequency output from the oscillator was monitored by using a digital readout frequency meter (Heath Schlumberger, Benton Harbor, Michigan). The frequency change could be read on either the frequency meter or recorded by adapting a digitalto-analog converter (DAC) circuit to the output of the frequency meter. Standard concentrations of the test atmosphere were prepared by the saturation, diffusion and permeation methods for Hg, organophosphorous compounds and formaldehyde,

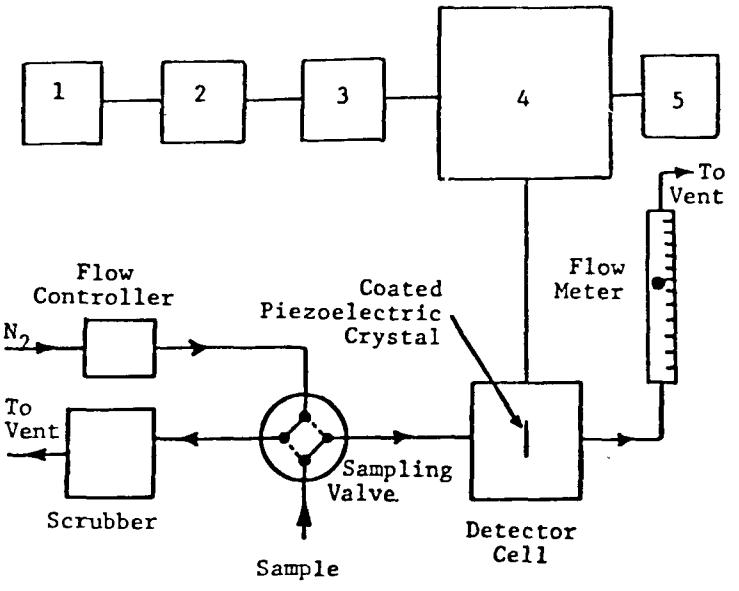

Figure 1. Schematic Diagram of the Exprimental Setup.

(1) Recorder; (2) Digital-to-Analog Converter; (3) Frequency Meter;

(4) Oscillator; (5) Power Supply

respectively (8). Samples from the generation system were introduced into the detector cell by a 4-port sampling valve (Varian Instrument Div., Palo Alto, California). Diffusion cell and permeation tube were obtained from Analytical Instrument Development, Inc., Avondale, Pennsylvania.

A typical piezoelectric crystal consists of a quartz plate, electrodes, and holder as shown in Figure 2. In order to be successfully used as sensor in the detection of gases, the crystal must possess several important characteristics such as stable frequency output, low temperature coefficient, high mass sensitivity and inert to its environment. An AT-cut, quartz crystal is a material that best meets these requirements. The crystals used in these studies were 9 MHz and 15 MHz with vacuum- deposited gold electrodes located on the center of each side of the quartz plate. Figure 3 shows the design of the detector cell. This design provides the best contact between the coating and the gas stream since the sample is split into two equal streams which directly

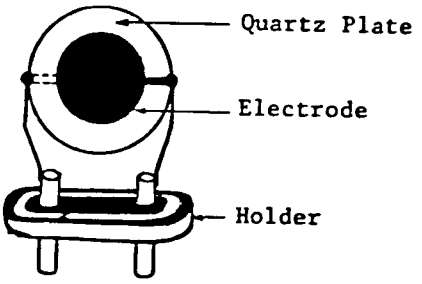

Figure 2. Piezoelectric Quartz Crystal

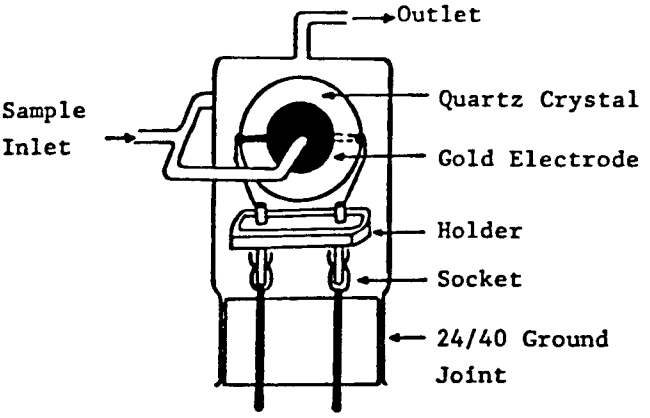

Figure 3. Detailed Design of Dectector Cell

and simultaneously impinge on both sides of the coated crystal. The cell was made from Teflon or Pyrex ground joint glass and the crystal is connected to the oscillator through a socket. This enabled not only the rapid and easy removal of crystals for exchanging or recoating, but also provided a sealed detector cell as well as optimum electrical contact. Several techniques such as vacuum deposition, dipping, painting with a small brush or cotton swab, or dropping with a microsyringe can be used to apply the coating onto the surface of the piezoelectric crystal.

Figure 4 shows the schematic diagram of the portable detector which is capable of field use. The device contains a coated sensing crystal, a reference crystal, an air sampling pump and solid-state electronics with digital display of the frequency differences. Since the sampled gas was adsorbed only on the surface of the coated sensing crystal, the frequency output was directly proportional to the concentration of gas. Rechargeable nickel-cadmium batteries, which are capable of eight hours continuous operation, provide all power for the electronics and for the sampling pump (Anatole J. Sipin Co., New York). In operation, nitrogen or clean air was first allowed to pass through the detector cell until the baseline frequency became stable. The

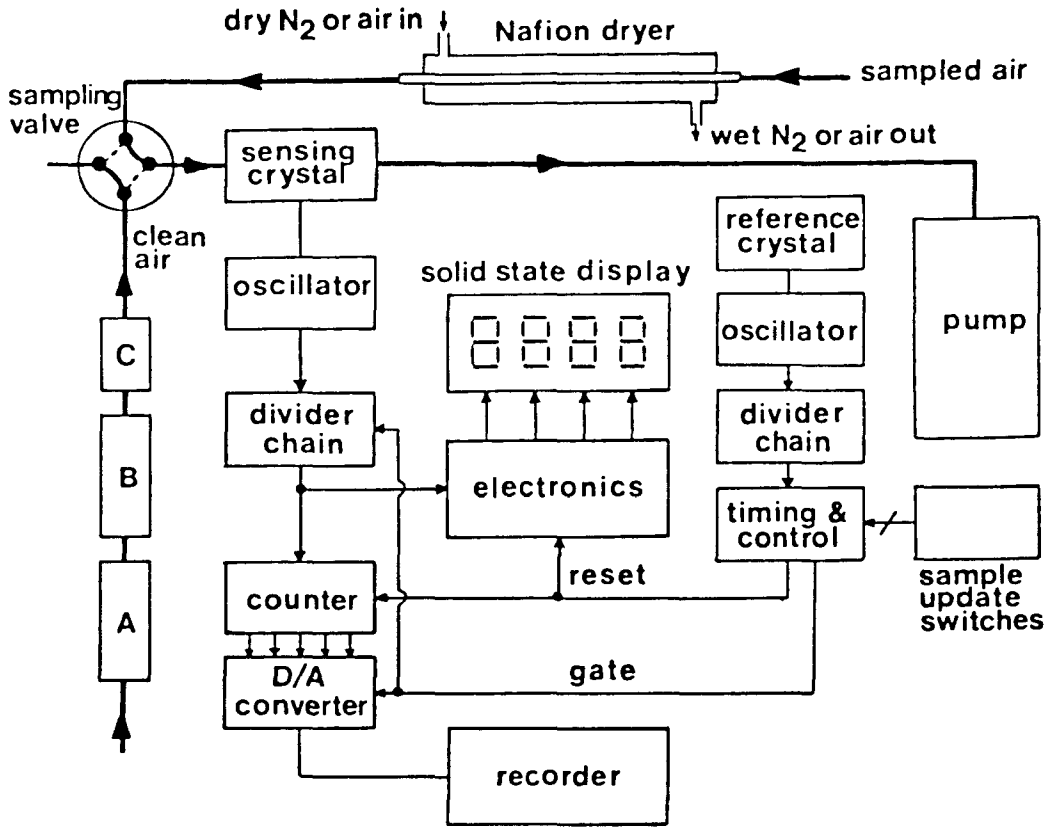

Figure 4. Schematic Diagram of the Portable Piezoelectric Detector

sampling valve was then rotated to introduce the sampled air into the detector cell, where the interaction between sampled gas and the coating occured. The frequency response was taken as the frequency difference between the baseline before sampling and the steady frequency after equilibrium was established. The sampling valve was then rotated again and clean air was allowed to pass through for desorption. For the detection of Hg, thermodesorption was used to remove Hg on the gold coated crystal.

III. DETECTION OF MERCURY

The ability of gold to adsorb and almagamate mercury is well known (6,9-11). Gold is also one of the metals used to make the electrode on commercially available crystals. Mercury is adsorbed on the surface of gold electrodes,

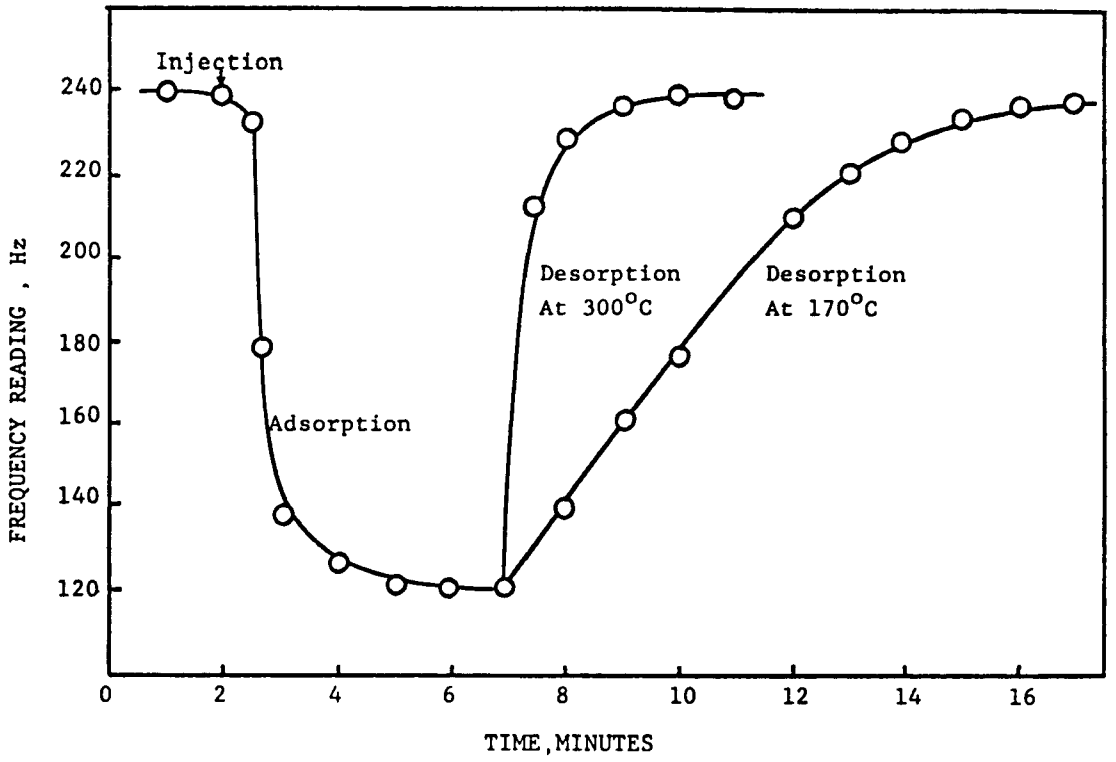

Figure 5. Adsorption - Desorption Curves of Mercury

causes an increase in the mass of the crystal, therefore decreasing the frequency. Mercury is then desorbed by thermal desorption and the frequency returns back to the original baseline as shown in Figure 5. Since the sensitivity of the detector depends on the mass of mercury adsorbed on the surface of gold electrode, the collection efficiency of the gold coated crystal was studied. Gold electrode should be fresh for the best collection efficiency and a commercially available gold electrode crystal can be used after heat cleaning (7). The effect of flow rate on the sensitivity was also studied. The volume of the sampled air was kept constant while the flow rates were varied from 30 ml/min to 250 ml/min. Below 100 ml/min the flow rate did not affect the sensitivity. At high flow rates the collection efficiency is decreased due to the incomplete adsorption of mercury. At 200 ml/min the collection efficiency is about 15% lower than that at 90 ml/min. The optimum flow rate was found to

be 100 ml/min. The configuration of the detector cell also affected the sensitivity. Several cell configurations were investigated and the design as shown in Figure 3, is the most sensitive one since it provides the best contact between the gold electrode and the sampled air stream (6). For best precision, the crystal should be desorbed after each measurement. We observed that if the crystal is desorbed immediately after each measurement the lifetime of the crystal is much longer. This may be due to the migration of mercury into the inner layers of the gold film during storage; it is difficult to desorb completely this mercury.

The linear range of the detector is from 5 ng to 100 ng as shown in Figure 6. Increasing the surface area of the gold electrode will increase the linear range of the detector. However, the mass sensitivity will decrease, since the mass sensitivity of the crystal is inversely proportional to the electrode's area. The detector responds to mass rather than to concentration

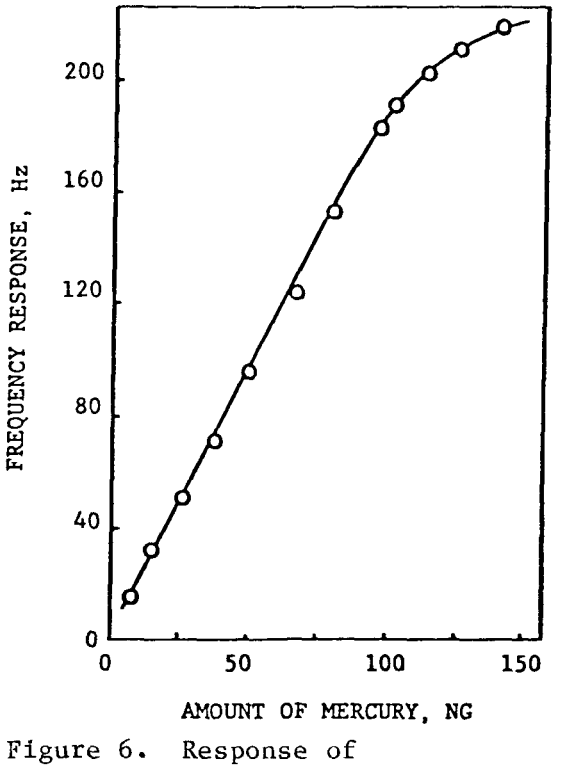

Figure 6. Response of Detector to Mercury

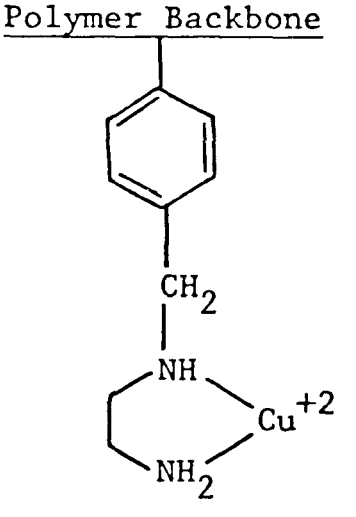

Figure 7. Structure of XAD-4-Cu^{2+}-diamine

and the larger volume of sample, which gives the larger amount of mercury, will increase the frequency response. Therefore, various concentrations in the ppm and ppb ranges can be detected by varying the sampling times. This will further enhance the usefulness of the detector. Since gold is well known as a highly specific adsorber for mercury, the detector is free of the interferences usually observed in cold vapor atomic absorption. H_2S and Cl_2 only slightly interfer at high concentrations (> 100 ppm). However these two interferents can be eliminated by collecting mercury from sampled air with a gold coated quartz collector. Mercury is then released from the collector by heating and is carried with carrier gas into the detector cell.

IV. DETECTION OF ORGANOPHOSPHORUS PESTICIDES

It has been known for many years that copper complexes can catalyze the hydrolysis of phosphorus ester (12,13). In an aqueous solution the overall reaction occurs in two steps: first, the copper complex binds reversibly to the phosphorus esters and second, the adduct product is irreversibly broken down by hydrolysis. In air, where the content of water is low, the second step is unlikely to occur.

Guilbault et al (14) showed that XAD-4-Cu^{2+} - diamine, a polymer bonded copper complex as shown in Figure 7 can be used as a sensitive and selective coating for detection of organophosphorus compounds. In this study, the crystal was first coated with polyhexadecylmethacrylate and then a finely ground powder of XAD-4-Cu^{2+} - diamine was sprayed onto the crystal. The excess XAD-4-Cu^{2+} - diamine was wiped out with a soft tissue paper. Since polyhexadecylmethacrylate is a highly viscous liquid, XAD-4-Cu^{2+} - diamine adhered strongly onto the surface of the crystal. For organophosphorus pesticides, diisopropyl methylphosphonate (DIMP) was chosen as the model compound because of its low toxicity and other reasons as shown elsewhere (15). The standard concentrations of

DIMP for test atmospheres were generated by the diffusion method. No significant interference was noted, except that responses are observed with DS-2 and high humidity. DS-2 is a decontamination solution for organophosphorus compounds and other chemical warfare agents. This response is expected, since DS-2 contains amines and may form a complex with the copper coating. The calibration curve for DIMP is shown in Figure 8.

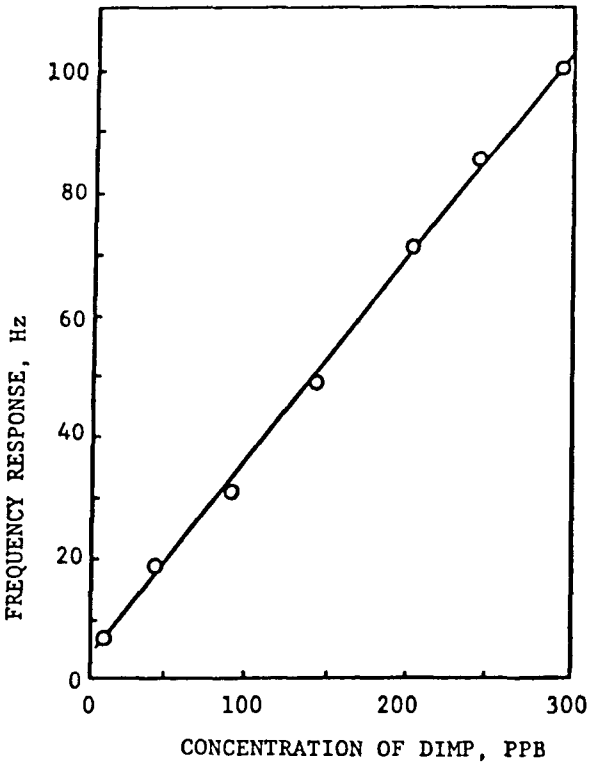

Figure 8. Frequency Response of Detector to DIMP

V. DETECTION OF FORMALDEHYDE

Due to the high sensitivity, coated piezoelectric crystals can be used as gravimetric sensors for measuring toxic gases in the atmosphere. The only drawback in this type of detector is the selectivity. The specificity of the detector is dependent on the coating materials. In this study, enzymes were immobilized on the piezoelectric crystal for assay of substrates directly in the

gas phase, entirely analogous to their use in solution. The specificity of enzymes is well known and this investigation represents the first attempt to use an immobilized enzyme as a coating for piezoelectric crystal sensors. The enzyme formaldehyde dehydrogenase catalyzes the oxidation of formaldehyde, in the presence of co-factor NAD^+, to form formic acid and NADH. Glutathione was also used as a co-factor. Formaldehyde dehydrogenase, NAD^+ and glutathione were immobilized onto the crystal using glutaraldehyde and albumin (16). The detector is highly selective toward formaldehyde with little response to acetaldehyde and alcohols. As low as 0.1 ppm concentration of formaldehyde could be detected. However, more studies are needed to improve the precision, response time, reversibility and a stability of the enzyme coating. The mechanism involved in this type of gas phase enzymatic reaction is not fully explained.

REFERENCES

(1) Sauerbrey, G. Z. Phys. Verhandl 8: 113, 1957.

(2) Sauerbrey, G. Z. Z. Phys. 115: 206, 1959.

(3) Stockbridge, C. D. Resonance Frequency versus Mass Added to Quartz Crystal. In: K. H. Behrndt (ed.), Vacuum Microbalance Techniques. Vol. 5. Plenum, New York, 1966. p. 193.

(4) Czanderna, A. W. and Lu, C. S. Applications of Piezoelectric Quartz Crystal Microbalances. Elsevier Scientific Publishing Co., New York, 1983.

(5) Hlavay, J., and Guilbault, G. G. Applications of the Piezoelectric Crystal Detector in Analytical Chemistry. Anal. Chem. 49: 1890, 1977.

(6) Ho, M. H., Guilbault, G. G., and Scheide, E. P. Determination of Nanogram Quantities of Mercury in Water with a Gold Plated Piezoelectric Crystal Detector. Anal. Chim. Acta. 130: 141, 1981.

(7) Ho, M. H., Guilbault, G. G., and Rietz, B. Detection of Carbon Monoxide in Ambient Air With a Piezoelectric Crystal. Anal. Chem. 54: 1998, 1982.

(8) Nelson, G. O. Controlled Test Atmosphere. Ann Arbor Science, Ann Arbor, Michigan, 1980.

(9) McNerney, J. J., Buseck, P. R., and Hanson, R. C. Mercury Detection by Means of Thin Gold Films. Science 178: 611, 1973.

(10) Bristow, Q. An Evaluation of the Quartz Crystal Microbalance as a Mercury Vapour Sensor for Soil Gases. J. Geochem. Explor. 1:55, 1972.

(11) Scheide, E. P., and Taylor, J. K. Piezoelectric Sensor for Mercury in Air. Environ. Sci. Tech. 8: 1097, 1974.

(12) Gustofson, R. L., Chaberek, L. S., and Martell, A. E. A Kinetic Study of the Copper(II) Chelate Catalyzed Hydrolysis of Disopropyl phosphorofluoridate. J. Amer. Chem. Soc. 58: 598, 1963.

(13) Epstein, J. and Rosenblatt, D. H. Kinetics of Some Metal Ion Catalyzed Hydrolysis of Isopropylmethyl-phosphorofluoridate at 25°C. J. Am. Chem. Soc. 80: 3596, 1958.

(14) Guilbault, G. G., Affolter, J., Yutaka, T., and Kolesar, E. S., Jr. Piezoelectric Crystal Coating for Detection of Organophosphorus Compounds. Anal. Chem. 53: 2057, 1981.

(15) Ho, M. H., and Guilbault, G. G. Portable Field Detector for Organophosphorus Pesticides. Anal. Chim. Acta, in press.

(16) Carr, P. W., and Bowers, L. D. Immobilized Enzymes in Analytical and Clinical Chemistry. John Wiley and Sons, New York, 1980, pp. 148-191.

ACKNOWLEDGEMENT

The author gratefully acknowledge the financial support of the National Institute of Health, Division of Research (Grant S07-RR05349-20) and the UAB Graduate School Faculty Research Grant (Grant 82-8509).

NOTICE

The work described in this paper was not funded by the U.S. Environmental Protection Agency and therefore the contents do not necessarily reflect the views of the Agency and no official endorsement should be inferred.

REDUCED-TEMPERATURE PRECONCENTRATION OF VOLATILE ORGANICS FOR GAS CHROMATOGRAPHIC ANALYSIS: SYSTEM AUTOMATION*

by: W. A. McClenny
U.S. Environmental Protection Agency
Research Triangle Park, North Carolina 27711

J. D. Pleil
Northrop Services, Inc.
Environmental Sciences
Research Triangle Park, North Carolina 27709

ABSTRACT

An automated system for unattended repetitive sampling and analysis of volatile organic compounds in ambient air has been designed and evaluated. The sampling and analysis scheme involves preconcentration of analytes from whole air at reduced temperature and subsequent thermal desorption and capillary column gas chromatographic analysis. This paper describes the system's components and operating procedures. Temperature versus time profiles measured at the trapping surface document the stability of the trap temperature during sample collection, as well as the rapid trap temperature changes, i.e., 3.5 minutes for +120°C to -150°C during cooling of the trap and 1.0 minute for -150°C to +100°C during thermal desorption. The system will be evaluated as a semi-real-time monitor for volatile organics and as a central system for analysis of air samples collected in small-volume metal containers.

INTRODUCTION

Preconcentration of target gases prior to analysis increases the effective sensitivity of standard monitoring techniques. Solid sorbants such as Tenax are currently used to selectively sorb gaseous organics while passing the major constituents of ambient air, including H_2O. Thermal desorption from Tenax onto a cryogenic trap (cryo-focusing) is used to further concentrate the gaseous organics. Subsequent heating of the trap releases the organics in a sample volume many times (10^3 to 10^5) smaller than the original whole air volume.

*This paper has been reviewed in accordance with the U.S. Environmental Protection Agency's peer and administrative review policies and approved for presentation and publication.

Direct semi-real-time monitoring of organics can be accomplished by sampling directly onto a reduced temperature surface, usually a section of small diameter metal tubing filled with small glass beads. However, water vapor condensation typically plugs a trap with only 200 to 300 ml of ambient air collected. Recently, Nafion tubing has been used successfully to dry the ambient air prior to condensation while quantitatively passing volatile organics (M. W. Holdren, private communication, 1982). It is therefore possible to directly cold-trap larger air volumes, e.g., 1 to 10 liters, in a range comparable to the volumes collected with solid sorbants.

We are currently investigating the feasibility of reduced-temperature trapping and have found that automation greatly facilitates run-to-run repeatability and eliminates the tedious manual procedures involved in sampling and analysis. This paper (1) describes a system design for automated operation and (2) documents certain aspects of the system's performance. We envision the use of this system as a semi-real-time monitor of volatile organics in ambient air. With minor modification, the system can also be used to analyze ambient air samples collected in reusable, small volume metal cylinders (e.g., 2-ℓ aluminum cylinders) and shipped to a central location.

Previous research conducted to condense extremely large air samples for analysis by long path absorption - Fourier transform infrared (Hanst et al. 1979) has provided useful information on the subject of cryogenic trapping. In particular, extrapolations of the Clausius-Clapeyron equation were used to furnish conservative estimates of target compound vapor pressures at reduced temperatures.

EXPERIMENTAL PROCEDURE

The system includes a Hewlett-Packard (HP) Model 5880A gas chromatograph (GC) which is operated with a preconcentrator rather than a sample loop. The preconcentrator (Figure 1) consists of a 20-cm section of 0.32-cm OD, 0.22-cm ID nickel tubing formed into a circular winding and threaded onto a 250-W cylindrical resistive element. During use, a stainless steel shell encapsulates the trap and is further sealed with heat-resistant tape and glass fiber insulation to prevent escape of liquid nitrogen (N_2) into the surrounding volume. Small 25-W cartridge heaters are sandwiched between small aluminum plates for each pair of outlet tubes to provide a heat source and thermal inertia to eliminate "cold" spots in the outlet lines. The central 10-cm portion of the trap is filled with 0.85 grams of 60/80 mesh Pyrex glass beads. The trap is further characterized by the flow rate for a given pressure drop: 40 cm^3/min for approximately 3 psig as measured prior to use. Each trap is used as indicated in the flow path schematic shown in Figure 2. The trap enclosure and a Seiscor valve are placed on an aluminum base plate that is insulated from and placed directly over the GC oven. An aluminum box is attached to the base plate to enclose all sample handling elements. Rope heaters, regulated to maintain +70°C, are attached to all lines through which the sample flows.

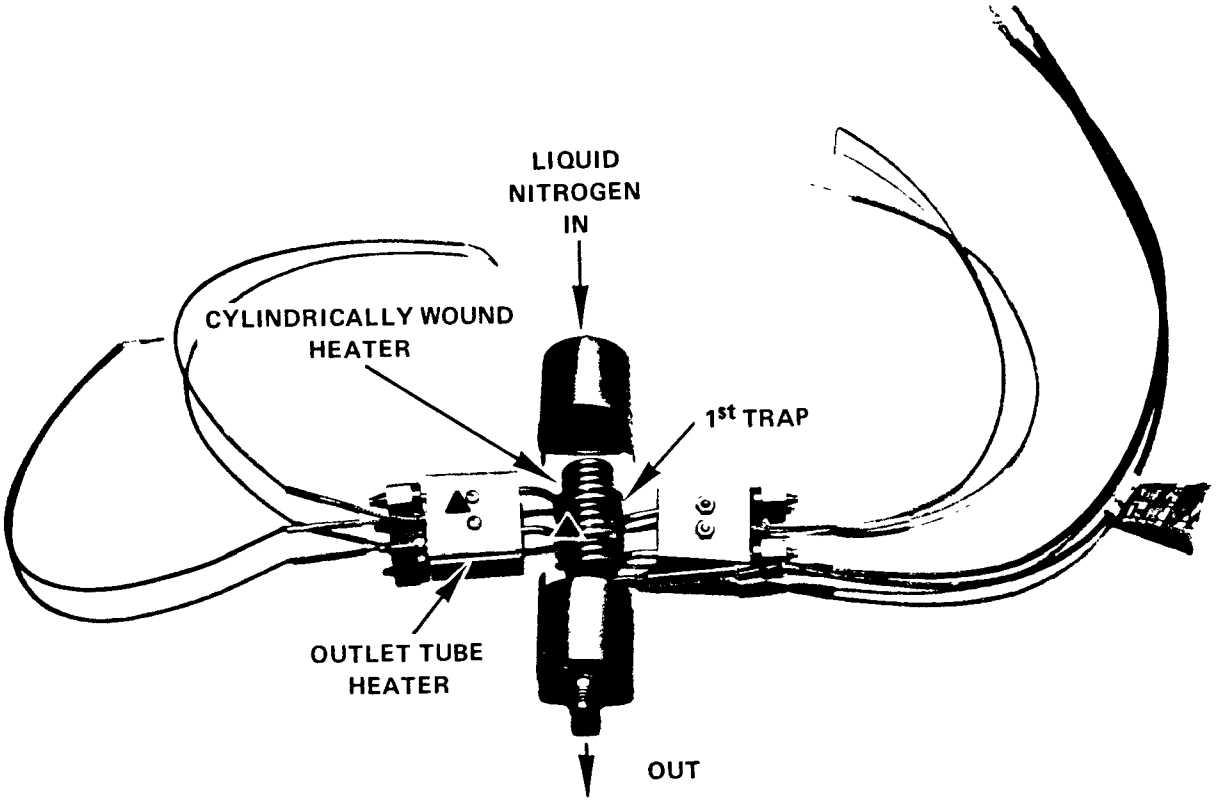

Figure 1. Unit for trapping gaseous organics at reduced temperatures with subsequent thermal desorption; Δ indicates thermocouple positions.

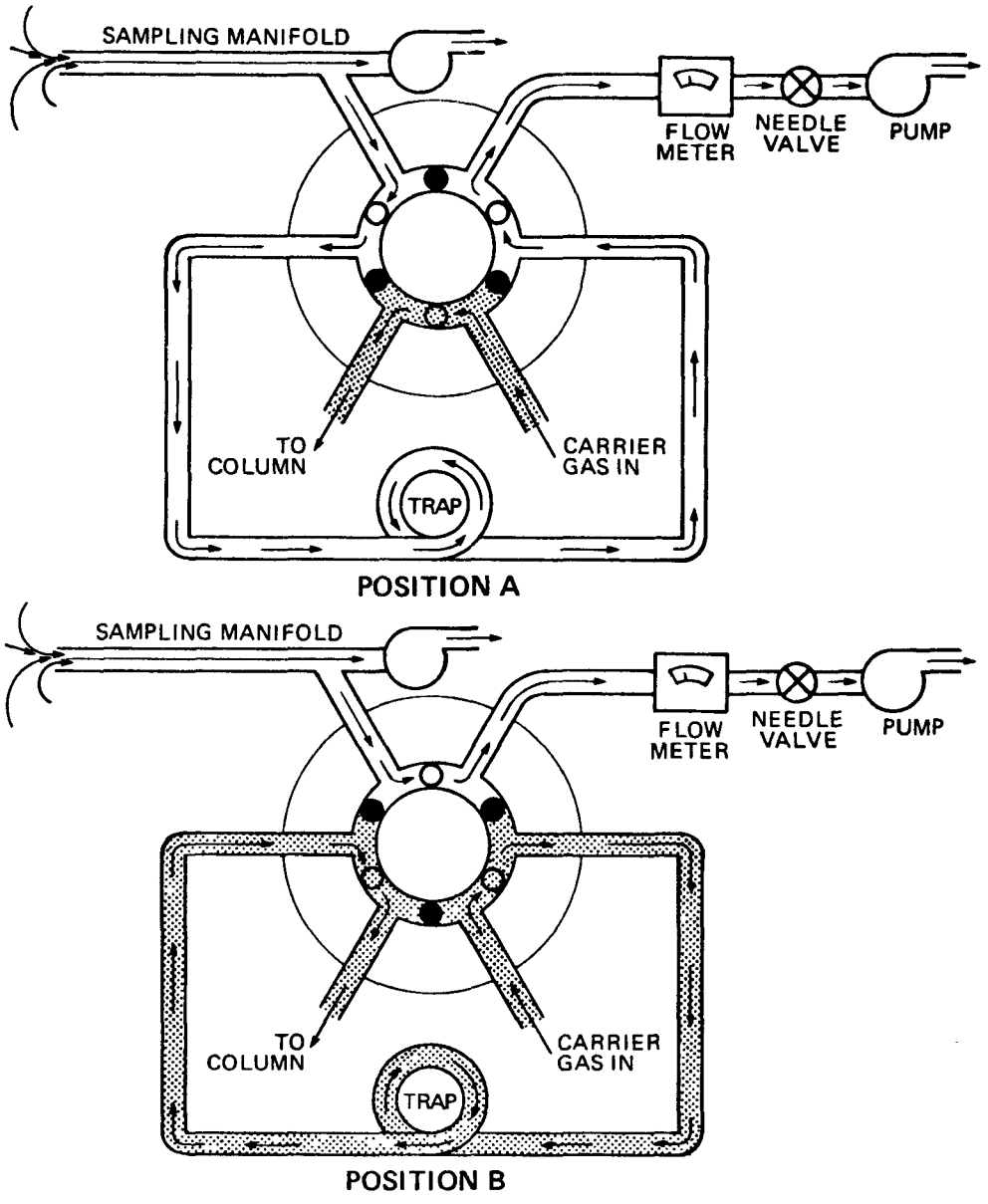

Figure 2. Flow path schematic showing cross-section of a six-port Seiscor valve in sampling (A) and desorbing (B) positions.

The set point network of a Nutech Model 320A cryogenic trapping/thermal desorption system (Nutech Corporation, 1982) controls the coooling and heating of the trap volume by releasing liquid N_2 into the trap enclosure or by passing current through the heater. The liquid N_2 is vented from the aluminum box.

The individual events during a system cycle are under microprocessor control from the HP 5880A. The run table listing for the sampling/analysis sequence is given in Table 1 along with the GC oven temperature profile. The input parameters are specified by the operator during system initialization. External valve controls, available on the GC as +24-V d.c. outputs, are used to change positions of the Seiscor valve (Valve 1 in listing) and to change the operational mode of the Nutech 320A from cooling to heating (Valve 3). Since the Basic language programming option is not included on our unit, Instruction 5 in the Run Table is used to reset and start successive cycles.

TABLE 1. HP 5880A LISTINGS FOR RUN TABLE AND OVEN TEMPERATURE PROFILE

Oven temperature profile			Run Table	
			Time (min)	Status/action
1.	Initial value	= -50°C	1. 0.50	Valve 1 on
2.	Initial time	= 3.00 min	2. 1.00	Valve 3 off
3.	Program rate	= 8.00°C/min	3. 5.00	Valve 3 on
4.	Final value	= 150°C	4. 10.00	Valve 1 off
5.	Final time	= 7.00 min	5. 35.00	Start valve 4 on
6.	Post value	= -50°C	6. 35.00	Stop
7.	Post time	= 10.00 min		

RESULTS

Table 2 shows the events occurring during the sequence of repetitive preconcentration /analysis runs. The steps are also shown in Figure 3. The two traces in Figure 3, one placed in thermal contact with the trap and one placed in the GC oven, record thermocouple outputs.

Figure 3 shows that stable trapping temperatures of -150°C can be achieved with cool-down times of 3.5 min. Additional thermocouples were placed (1) near the fittings at the output of the trap, (2) near the connector leading from the Seiscor valve into the GC oven, and (3) in the air space of the box that covers the preconcentrator and valves. Temperature readings during system operation indicated that these temperatures are controlled within the following ranges: 100 ± 20°C, 55 ± 5°C, and 55 ± 5°C, respectively.

Detailed information on the system and a discussion of the condendsation of a list of volatile organics is given by Pleil (1982).

TABLE 2. EVENTS OCCURRING DURING SEQUENCE OF ANALYSIS RUNS

Cycle	Time (min)	Status/action
A	0	Trap is at -150°C, oven at -50°C; Seiscor valve is in position B (see Figure 2) as sampling continues.
B	0.5	Instruction #1 of Run Table switches Seiscor valve to position A (see Figure 2). Sampling ends with 35.5-min sampling time. Carrier gas (N_2) is directed through trap at 3.0 cm^3/min flow rate.
C	1.0	Instruction #2 of Run Table activates relay in Nutech 320A to begin rapid heating of trap. Desorbed gases are retrapped on the column head.
D	3.0	Temperature programming begins at 8°C/min and continues for 25 min, reaching +150°C at the end. Recording and display of chromatograph occurs on HP thermal printer.
E	5.0	Instruction #3 of Run Table deactivates relay in Nutech 320A to begin cooling trap.
F	10.0	Instruction #4 of Run Table switches Seiscor valve to position B (see Figure 2) so that sampling begins.
G	28.0	Temperature programming ends with oven at 150°C. Final time instruction in oven temperature profile (OTP) holds oven temperature at 150°C for 7 min.
H		Run Table instruction program is reset, post time in OTP is set for 10 min, during which elution times and peak areas are printed. Post value instruction in OTP causes oven to begin cooling.
I	45.0	At end of post time, next run begins.

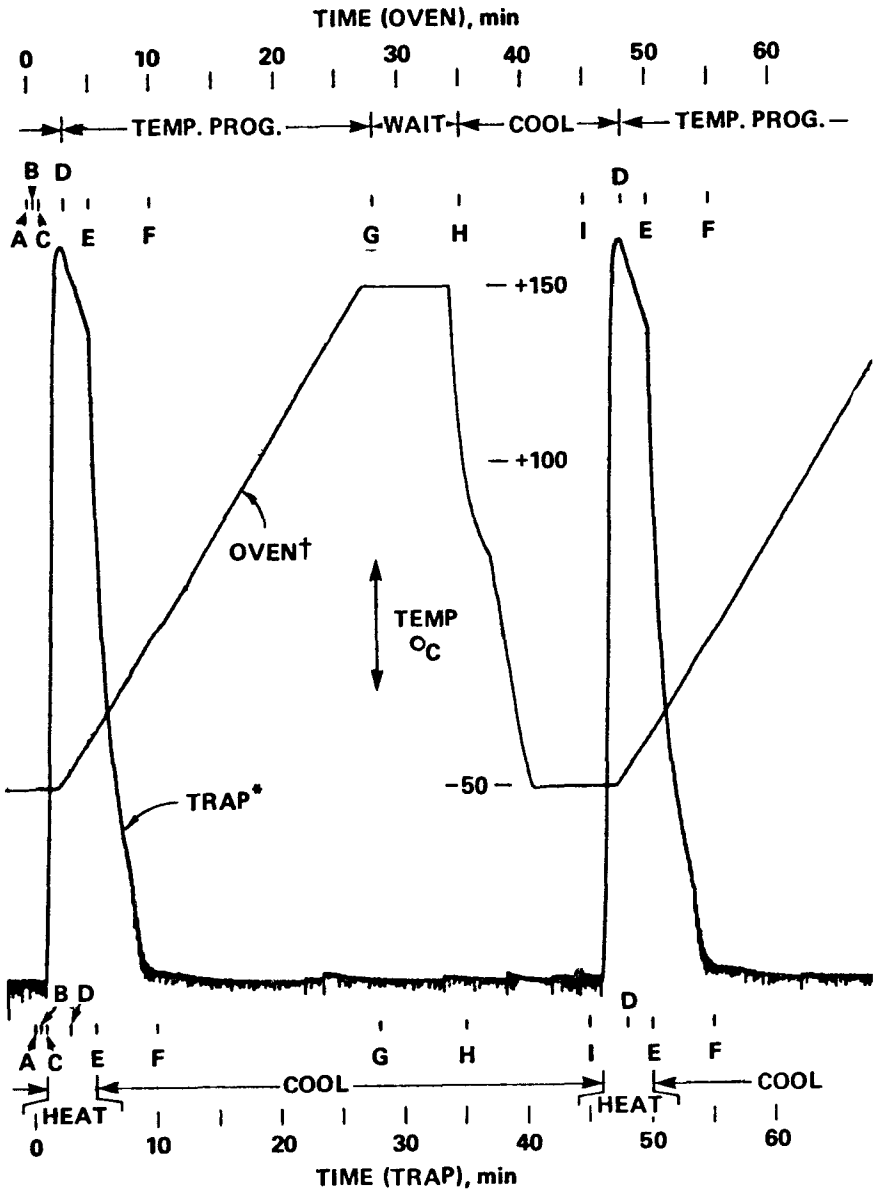

Figure 3. Temperature - time profiles for trap and oven. *Trap temperatures are approximate. †Recorder pens offset by 1.0 min. For explanation of cycle steps A through I, see text.

REFERENCES

1. Brown, R. H. and C. J. Purnell (1979) J. Chromatog., 178:179.

2. Hanst, P. L., L. L. Spiller, D. M. Watts, J. W. Spence, and M. F. Miller (1975) J. Air Poll. Control Assoc., 25:1220.

3. Nutech Corporation (1982) Nutech Model 320A Operating Manual, Nutech Corporation, 2806 Creek Road, Durham, North Carolina 27704.

4. Pleil, J. D. (1982) Technical Report TN-82-02, July 1982, Northrop Services, Inc.-Environmental Sciences, P. O. Box 12313, Research Triangle Park, North Carolina 27709.

DETECTION AND DETERMINATION OF POLYCHLORINATED BIPHENYLS IN AMBIENT AIR

E. Singer, M. Sage, T. Jarv and R. Corkum

Ministry of the Environment of Ontario, Air Resources Branch

Toronto, Ontario, Canada, M5S 1Z8

Abstract

High resolution gas chromatography with simultaneous analysis on two columns of different polarity with computer assisted data reduction and correlation was applied to the analysis of Polychlorinated Biphenyls (PCB's) in ambient air.

A method of identification of individual PCB congenors based on retention indices (RI's) was developed, as well as quantification of congenors, which are unavailable to be used as standards.

A standard, based on a mixture of commerical Aroclors, was synthesized and all major peaks in the mixture were identified and quantified.

A set of rules for the reduction of data from two columns of different polarity was established. As well, a programme was written for the miroprocessor controlled HP 5880 gas chromatograph. The program controls the gas chromatograph, the HP Autosampler 7672A, initiates the recalibration, performs the data reduction, correlation of the peaks, prints the reports and stores all the GC data and reports on a magnetic tape.

Ambient air samples from a survey of PCB's across the Province of Ontario were analyzed using methodologiies employing packed columns, single capillary columns, and dual capillary columns of different polarity and some of the results are reported.

The detection and determination of PCB's in environmental samples is a highly complex task. There are 209 possible congenors of PCB's, 102 of which have been identified in commercial Aroclor mixtures, and are therefore likely to be encountered in environmental samples. The major approach to the analysis was until recently low or medium resolution gas chromatography (1,2,3) utilizing packed columns coupled with detection by electron capture (EC) detector or mass-spectrometry (MS). The results were then quantified by peak or pattern matching with commercial Aroclors or their mixtures. The disadvantages of this technique, when applied to environmental (and mainly air) samples are obvious.

1. It is assumed that the ratio of individual PCB congenor in the vapour phase is identical to the ratio in the liquid phase, which is unlikely. The boiling points of PCB congenors spread over the range of more than 150°C and it is likely that the vapour pressure will spread over a range of several orders of magnitude as well.

2. It is assumed that the ratio of individual PCB congenor does not change after exposure to the environment. However, individual PCB congenors have different chemical and physico-chemical reactivities, so it is likely that the composition will change with the length of the exposure to the environment.

3. It is assumed that all interfering compounds can be removed from the sample during the clean-up procedure and if any stay in, they can be resolved from the PCB congenors and thus the PCB peaks can be identified and quantified with high degree of confidence.

However, the efficiency of the clean-up procedures, even for samples of "clean" air, can be questioned as well. It has been estimated (4) that in the concentration range individual PCB congenors might be present in "clean" ambient air, about 10^6 organic compounds could be present at similar levels. Only a fraction of these low level impurities were identified. It is a reasonable assumption that a significant number may not be removed by the clean-up procedure and some, which were not removed, may have on a given column retention times close to the retention times of the PCB congenors and may be detected by the EC detector as well.

The identification and quantification of individual PCB congenors in a complex matrix was not too practical until rescently. With the commercial availability of capillary columns of good and reproducible quality, gas chromatographs designed for work with capillary columns, and computer controlled instrumentation and signal processing, the introduction of high resolution gas chromatography into routine laboratory work became realistic although there were still some open questions. Mainly,

1. Only a limited number of individual PCB congenors, as they were identified in Aroclors, were commercially available.

2. The commercially available fused silica capillary columns, suitable for this analysis could not resolve all the PCB congenors, unless the run would be extended over extremely long periods of time.

3. There still remained the possibility that some impurities, present in the air sample and not removed by the clean-up procedure may be identified as PCB's.

The first problem was identification of the individual PCB congenors. Sissu and Welti (5) reported in 1971 that the RI of PCB's can be calculated by summing up the ½RI for the two substituted rings. We decided to extend their idea to capillary columns under temperature programmed condition using the formula of Said and Hussein (6). The calculated ½RI's for different chlorine substitution and two different liquid phases are in Table 1. A comparison of measured and calculated RI's of a number of PCB congenors is in Table 2.

Table 1. HALF RETENTION INDICES OF POLYCHLORINATED BIPHENYLS

Cl-Substitution	OV-1 ASYM PARENT	OV-1 SYM PARENT	SE-54 ASYM PARENT	SE-54 SYM PARENT
0-	676	676	690	690
2-	791	790	811	808
3-	860	860	877	878
4-	866	870	885	889
2,3-	983	984	1005	1004
2,4-	955	954	972	972
2,5-	954	947	972	965
2,6-	905	897	926	917
3,4-	1056	1066	1076	1088
3,5-	1013	-	1030	-
2,3,4-	1166	1174	1188	1197
2,3,5-	1140	1141	1159	1162
2,3,6-(2,5,6)	-	1065	-	1085
2,4,5-	1128	1124	1145	1140
2,4,6-	1042	1028	1057	1042
3,4,5-*	-	-	-	-
2,3,4,5-	1331	1330	1350	1349
2,3,5,6-	1242	1207	1260	1222
2,3,4,6-	1254	1251	1272	1279
2,3,4,5,6-	1448	1414	1464	1428

* not commercially available

TABLE 2. COMPARISON OF MEASURED AND CALCULATED RI's FOR SOME PCB's

CONGENOR	OV-1			SE-54		
	MEASURED	CALCULATED		MEASURED	CALCULATED	
		ASYM.	SYM.		ASYM.	SYM.
2,2',5	1739	1745	1737	1774	1783	1773
2,3',5	1810	1813	1808	1845	1849	1843
2,4',5	1824	1820	1817	1860	1856	1854
2,3',4'	1844	1847	1856	1881	1887	1895
2,2',4,6	1828	1833	1818	1859	1868	1849
2,2',3,5'	1931	1936	1931	1970	1977	1970
2,2',4,5'	1903	1908	1902	1939	1944	1937
2,3',4',5	2010	2009	2014	2048	2048	2053
2,2',3,5,6	2021	2034	1997	2054	2071	2029
2,2',3,4,5'	2117	2120	2121	2157	2160	2162
2,2',4,4',6	1990	1996	1982	2022	2029	2013
2,2',4,6,6'	1927	1947	1925	1961	1982	1959
2,2',3,3',4,5	2312	2313	2314	2352	2354	2353
2,2',3,4,5,5'	2270	2284	2278	2305	2322	2314
2,3,3',4,4',5	2405	2386	2396	2446	2426	2437
2,2',3,5,5',6	2170	2196	2154	2203	2231	2187
2,2',3,4,5,5',6	2375	2401	2361	2405	2436	2393
2,2',3,4,4',5,6'	2354	2372	2359	2384	2406	2391
2,2',3,3',4,4',6	2405	2421	2424	2444	2460	2475
2,2',3,4,4',5,6,6'	2435	2489	2442	2463	2521	2469
2,2',3,3',4,5',6,6'	2430	2497	2458	2460	2532	2501
2,2',3,3',4,4',5,6,6'	2635	2702	2664	2665	2736	2706
2,2',3,3',4,4',5,5',6	2752	2778	2744	2783	2814	2777

Although the agreement between the measured and calculated values of RI is very good - generally better than 0.5% - there are some differences depending on whether symmetric or asymetric parents are used. To get the best possible answer we set in Table 3 simple rules for the calculation of RI's using either symetric or asymetric parents, depending on the structure of the polychlorinated biphenyl.

TABLE 3. RULES FOR PREDICTING THE RI's OF PCB CONGENORS

PCB CONGENOR	OV-1		SE-54	
	ASYM. PARENTS	SYM. PARENTS	ASYM. PARENTS	SYM. PARENTS
Mono-chloro				
x=1; y=0	*		*	
Di-chloro				
x=2; y=0	*		*	
x=1; y=1		*		*
Tri-chloro				
x=3; y=0	*		*	
x=2; y=1	4- 3,4-	*	4- 3,4-	*
Tetra-chloro				
x=4; y=0	*		*	
x=3; y=1		*		*
x=2; y=2	3,4-	*	3,4-	*
Penta-chloro				
x=5; y=0	*		*	
x=4; y=1	*		*	
x=3; y=2		*		*
Hexa-chloro				
x=5; y=1	*		*	
x=4; y=2		*		*
x=3; 6=3		*		*
Hepta-chloro				
x=5; y=2		*		*
x=4; y=3		*		*
Octa-chloro				
x=5; y=3		*		*
x=4; y=4		*		*
Nona-chloro				
x=5; y=4		*		*
Deca-chloro				
x=5; y=5		*		*

Note: x = no. of chlorines on one ring
y = no. of chlorines on other ring
* use these types of parents to generate the retention index for the PCB whose composition is denoted by x and y.
4-; 3,4- these are exceptions to the * rule, use the parents of the column they are located in to generate the best retention index.

The next problem was the quantification of the unavailable congenors. Some relative response factors were already reported in literature (7). We investigated the relative response factors of the commercially available PCB congenors and some of the data are presented in Table 4.

TABLE 4. RELATIVE RESPONSE FACTORS OF SOME PCB CONGENORS

CONGENOR	REL. RESPONSE	CONGENOR	REL. RESPONSE
2-	21	2,2',4,6,6'-	313
3-	1	2,2'4,5,'6-	340
4-	11	2,2',4,4',6-	355
	AVG.=11	2,2',3,4,6-	351
		2,2',3,5,6-	364
2,2'-	48	2,3',4,5',6-	381
2,5-	206	2,2',4,5,5'	395
2,3-	224	2,3',4,4',6-	369
3,5'-	150	2,2',3,4',5-	427
3,3'-	82		AVG.=336
3,4'-	166		
	AVG.=146	2,2',4,4',6,6'-	367
		2,2',4,4',5',6-	351
2,4,6-	289	2,2',3,5,5',6-	378
2,2',5-	211	2,2',3,4,4',6-	341
2,4,5-	326	2,2',3,4,5,6'-	399
2,3',5-	319	2,2',4,4',5,5'-	401
2,4',5-	308	2,2',3,4,5,5'-	400
	AVG.=290	2,2',3,4,4',5-	440
		2,2',3,3',4,5-	370
2,2',6,6'-	224	2,2',3,3',4,4'	344
2,2',4,6-	352	2,3,3',4,4',5-	291
2,2',6'-	248		AVG.=371
2,3',4,6-	320		
2,2',5,5'-	320	2,2',3,4,5,5',6-	402
2,2',4',5-	335		
2,4,4',6-	527		
2,3,5,6-	361	2,2',3,3,5,5',6,6'-	378
2,2',3',5-	388	2,2'3,3',4,5',6,6'-	290
2,3',5,5'-	351	2,2',3,4,4',5,6,6'-	366
2,2'3,3'-	371		AVG.=345
2,3,4,5-	296		
2,3'4,'5-	358		
3,3',4,4'-	287		
	AVG.=338		

In this table the response of 3-monochlorobiphenyl is taken as unity. The relative response factors of tri- to octachloro biphenyls are fairly close, in the average about 340, however, there are large differences between relative response factors of mono-and dichlorobiphenyls. Luckily all mono- and a significant number of dichlorobiphenyls are commercially available. For the quantification of the rest of the PCB's we decided to take either the measured response factor (if available) or the average of the response factors of the two available PCB congenors bracketing in the congenor whose standard is not available.

The goals were not only positive identification and quantification of the individual biphenyls but also automation of the procedure, so it could be run on a microprocessor controlled GC - in our case a HP 5880A with dual terminals and level IV programming. This goal required a standard with as many identified and quantified PCB congenors as possible. This was achieved by combining Aroclors 1016, 1221 and 1254 (EPA Depository #9324, 9382 and 9533) in a single solution in the ratio of 2:3:2. For the identification and quantification, these Aroclors and their mixture were run on two capillary columns of different polarity simultaneously. Individual PCB congenors were identified with the help of ½RI's and quantified as mentioned before.

The last goal was the increase in confidence of positive identification and quantification of the PCB congenors. RT or RI on a single phase does not unequivocally identify an organic compound. It is estimated that the confidence of positive identification is about 60% for a packed column and relatively simple matrix and does not increase significantly for a high resolution capillary column. However, the confidence increases dramatically to about 90% if the sample is run on two columns of different polarity.

During our work fused silica columns came on market which simplified significantly our task. With this type of columns, we were able to mount two columns of identical lengths and I.D. but with different liquid phase into the same injection port and attach to two different EC detectors. This, with proper programming, simplified significantly our task. The correlation of the data from the two chromatograms was performed by the GC -microprocessor as well.

The programme, written for the HP 5880A, does the following:

1. controls the GC parameters
2. controls the HP-Autosampler 7672A
3. recalibrates the GC after a preset number of samples with weight averaging of the retention times and reponse factors
4. after analysis prints the reports from each column with the tentatively identified PCB congenors
5. correlates the gas chromatograms and prints the final report
6. stores all data and reports on a magnetic tape

For the correlation of the two gas chromatograms, we decided on a set of rules, under which the programme handles and correlates the peaks, tentatively identified and quantified on each column as PCB congenors. The rules are:

1. The retention time of the peak must be within narrow limits (usually $\pm$0.1%) of the expected retention time of the PCB congenor, otherwise the peak is rejected.

2. If the peak for a given PCB congenor is identified on both columns and the quantities are within limits (usually ±20%), the average is calculated and printed followed by the word "confirmed".

3. If the peak for a given PCB congenor is identified on both columns, but the quantities are not within given limits, then the lower value is taken as the result, followed by word "interference" (we assume that the higher value is caused by a coeluting impurity).

4. If a peak is identified as a given PCB congenor on one column only, the value is rejected and identified by the words "not PCB".

5. Although the used capillary columns have very high resolving power, some PCB congenors can not be resolved at all or can be resolved on one column only. If this happens, then the determined quantities of unresolved PCB congenors on one or both columns are summed up and evaluated under identical criteria.

The method was tested on individual Aroclors, Aroclor mixtures and synthetic ambient air samples. The results were within ±15% of the expected values.

We performed in Ontario two surveys for PCB's, in 1979 and 1980, to increase our data base for the background levels in ambient air.

All samples were collected on "Florisil" cartridges over 24 hour period at flow rates between 10-15 litre/min. The cartridges were extracted by pentane, boiled down in a Kuderna-Danish apparatus to a volume of 2 ml, cleaned up on a "Florisil" microcolumn,

and the final extract was boiled down in a Kuderna-Danish apparatus to a 1 ml volume with iso-octane (1 ml) as keeper. Processed samples were sealed in glass ampoules before they were analysed. Table 5 shows some data, obtained from the 1979 survey, as analysed by different gas chromatographic techniques. The processed samples were analysed by packed column (Dexil 400/Anachrom Q, 9 feet long, 1/8" O.D.), fused silica capillary columns - 50 m, 0.2 mm I.D. - with different liquid phases and by the dual column technique.

TABLE 5. COMPARISON OF RESULTS BETWEEN PACKED COLUMN, GC^2 AND GC^2 X 2

SAMPLE #	SAMPLE CODING	PACKED COLUMN	SINGLE CAPILLARY COLUMN			DUAL COLUMN
			SP-2100	OV-1	SE-54	OV-1/SE-54
1	HAM-I	317	11	11	7.0	3.3
2	HAM-I	173	4.8	5.2	4.1	1.4
3	HAM-I	52	8.7	0.7	1.6	0.2
4	HAM-I	68	20	5.9	9.7	1.9
5	HAM-U	28	1.6	2.5	1.0	0.02
6	HAM-U	128	2.4	3.8	3.0	0.9
7	HAM-U	31	3.6	2.3	1.7	0.2
8	HAM-U	25	4.4	2.2	1.6	0.2
9	KIN-U	3.6	4.3	12	6.5	0.08
10	KIN-U	9.3	3.3	5.2	2.7	0.3
11	LON-S	35	11	9.4	9.1	6.3
12	MIS-U	155	7.3	3.7	2.7	0.9
13	MIS-U	40	5.1	3.2	2.8	0.05
14	MIS-U	20	1.4	3.3	1.9	0.3
15	MIS-U	6.7	2.4	3.4	3.3	0.2
16	MOO-R	33	2.5	2.9	1.1	0.1
17	MOO-R	27	4.7	3.1	1.7	0.3
18	NAN-R	96	4.9	3.7	1.7	0.1
19	NAN-R	28	11	4.6	2.4	1.1
20	SAR-I	1615	6.8	4.3	6.5	2.1
21	SAR-U	115	3.5	3.7	14	0.6
22	SAR-U	58	4.6	6.1	4.3	0.6
23	STC-R	78	14	4.2	2.5	0.5
24	STC-R	15	1.9	4.7	4.2	2.0

Concentration ng/m^3

The data for total PCB's on the medium resolution packed column are about an order of magnitude, or more, higher than the data from the single capillary columns. The reason for it is, in our opinion, the low resolving power of the packed column with many impurities, which were not removed by the clean-up procedure, identified as PCB's.

There seems to be a fair agreement between the data for total PCB's obtained on capillary columns with different liquid phases. However, on closer examination we see that some PCB congenors are identified on one type of column only and their presence can not be confirmed on the other types of columns. The reason for it is, in our opinion, that although capillary columns have very high resolving power, many impurities present in ambient air may not be removed by the clean-up procedure and because of very close RT under given gas chromatographic conditions on a given column, they may be identified as PCB congenors and thus the reported data might be biased high.

The data from the dual column analysis with the elimination of PCB congenor which can not be confirmed on both columns and quantification based on individual PCB congenors are, in our opinion, closer to the true value than the results from a single capillary column analysis.

The work described in this paper was not funded by the U.S. Environmental Protection Agency and therefore the contents do not necessarily reflect the views of the Agency and no official endorsement should be inferred.

REFERENCES

1. Association Off. Anal. Chem. Methods 29.018.

2. Sawyer, L.D. Quantitation of Polychlorinated Biphenyl Residues by Electron Capture Gas-Liquid Chromatography: Reference Material Characterization and Preliminary Studies. J. Assoc. Off. Anal. Chem. 61, 272 (1978).

3. Sawyer, L.D. Quantitation of Polychlorinated Biphenyl Residues by Electron Capture Gas-Liquid Chromatography: Collaborative Study. J. Assoc. Off. Anal. Chem. 61, 282 (1978).

4. Lewis, R.G. Accuracy and Trace Organic Analysis. National Bureau of Standards Special Publication 422, pp. 17-20.

5. Sissons, D. and Welti, D. Structural Identification of Polychlorinated Biphenyls in Commercial Mixtures by Gas-Liquid Chromatography, Nuclear Magnetic Resonance and Mass-Spectrometry. J. Chromatog. 60, 15 (1971).

6. Said, A.S. and Hussein, F.H. The Absolute Retention Index in Chromatography. Part I. J. High Res. Chromatog. and Chromatog. Comm. 257 (1978).

7. Hutzinger, O., Safe, S. and Titko, V. The Chemistry of PCB's. CRC Press Inc. 1974.

A Cost-Effective Procedure to Screen Air Samples for Polyaromatic Pollutants[a]

T. Vo-Dinh[b], G. C. Colovos[c], T. J. Wagner[d], and R. H. Jungers[e]

Health and Safety Research Division
Oak Ridge National Laboratory
Oak Ridge, TN 37830

ABSTRACT

The use of simple and cost-effective luminescence techniques for screening ambient air particulate samples is described. Two analytical methods, synchronous luminescence and room temperature phosphorescence, are employed to monitor the content of polynuclear aromatic (PNA) species in air particulate extracts collected at two wood-burning communities. The validity and efficacy of this cost-effective screening approach are demonstrated via comparison of the screening data with results obtained by detailed gas chromatography/mass spectrometry and high-performance liquid chromatography. The results of this field study demonstrate that a simple and cost-effective screening procedure can be used to obtain PNA spectral profiles as a basis to rank air samples according to their PNA content and/or to determine whether these samples have similar PNA compositions.

This paper has been reviewed in accordance with the U.S. Environmental Protection Agency's peer and administrative review policies and approved for presentation and publication.

---

[a]Research sponsored jointly by the US Environmental Protection Agency under Interagency Agreement No. ERD-82-190 and the Office of Health and Environmental Research, US Department of Energy under Contract No. W-7405-eng-26 with the Union Carbide Corporation.

[b]Instrumentation and Measurements Group, Health and Safety Research Division, Oak Ridge National Laboratory, Oak Ridge, TN 37830.

[c]Rockwell International, *Energy Systems Group, Environmental Monitoring Service Center, Newbury Park, CA 91320*

[d]PEDCo Environmental, Inc., Cincinnati, OH 45246.

[e]Data Management and Analysis Division, US Environmental Protection Agency, Environmental Monitoring Systems Laboratory, Research Triangle Park, NC 27711.

I. INTRODUCTION

Many routine air monitoring programs involving large numbers of samples require that the decision as to the levels of accuracy and sensitivity of the analytical methods be governed by cost-benefit consideration. Before selection of the groups of samples to be analyzed in detail or the types of methods to be employed, it is desirable to have some screening procedure available that can provide an overall profile of major components. Such a screening step may obviate the need to perform unnecessary and costly detailed analyses.

This field study evaluated the efficacy of two simple and rapid analytical techniques, synchronous luminescence (SL) and room temperature phosphorescence (RTP), for routine screening of samples for PNA content (3-6). The SL and RTP techniques were used to monitor PNA compounds in cyclohexane extracts of air particulate samples collected in two wood-burning communities. The luminescence screening procedures conducted at Oak Ridge National Laboratory ranked all samples on the basis of their PNA content (7). The efficacy of the screening procedure was evaluated by comparing the SL and RTP results with data obtained from independent gas chromatography/mass spectrometry (GC/MS) and high-performance liquid chromotography (HPLC) analysis performed by PEDCo Environmental, Inc. and by Rockwell International, respectively. The results of this field evaluation showed that the luminescence screening procedure constituted an effective tool for ranking air samples for their PNA content and could serve to reduce the number of GC/MS analyses needed to characterize PNA compounds in ambient air.

II. EXPERIMENTAL

Ranking Procedures

The screening procedure evaluated in this research project is based upon RTP and SL (3-6). Because most of the PNA compounds fluoresce and/or phosphoresce, this ranking protocol is based upon the gross intensity of the total peak height of the SL and RTP bands. The full details of the screening protocol are described elsewhere (7). In this study the SL technique was applied to fluorescence measurements.The four major steps involved in the protocol are: 1) serial dilution of the sample extracts, 2) SL measurements, 3) RTP measurements, and 4) ranking the samples.

A simple computer program was developed to calculate a ranking index for SL and RTP screening. This program receives as inputs the peak height intensities of a preselected number of emission bands in the SL and RTP spectra, the sensitivity factor of the detector, the dilution factor of the sample, and the peak height of a given band of a known reference standard sample. These peak height intensities are then corrected to the reference standard, normalized to the unity sensitivity scale of the spectrometer, and original dilution (1:1) of the sample, and summed. The summed value of the peak height for each sample is stored in a one-dimensional array and used as a basis for ranking.

The SL ranking index is a relative number proportional to the total peak height of the six SL emission bands monitored at 316, 336, 360, 404, 434, and 472 nm. The RTP ranking index is obtained as a relative

number proportional to the average peak height of RTP emission using excitation at 290, 343, and 390 nm. These three wavelengths were found to excite most PNA compounds of interest in this study.

III. RESULTS AND DISCUSSION

Figures 1 and 2 show some typical SL spectra using $\Delta\lambda$ = 3 nm for six samples in the first series and illustrate the principle of SL screening. The background signal of the solvent blank is given in Figure 2d for comparison purposes. The samples, identified by a 5-digit alphanumeric code, correspond to diluted cyclohexane extracts from air particulate samples collected outdoors at different locations in a residential community. Visual examination of Figures 1 and 2 led readily to the qualitative ranking of CG654>CG543>CG626>CG634>CG573>CG656. Sample CG654 had the highest PNA content since a 50-fold diluted sample exhibited an SL emission intensity equivalent to that of a 10-fold diluted solution in other samples. It is interesting to note that samples CG543 showed three emission bands between 400 and 500 nm similar to those in sample CG626 with some additional bands at the spectral region <400 nm. This feature is an indication that sample CG626 contains fewer small-ring species (less than 4 benzene rings) than sample CG543.

According to their RTP intensities, the six samples in this first series were ranked as follows: CG654>CG543>CG634>CG626>CG573>CG656. Table I summarizes the results of gross ranking for the six air particulate extracts investigated in this first sample series and compares the SL and RTP screening results with data obtained by PEDCo

using GC/MS measurements. The SL/RTP ranking results were in good agreement with GC/MS data for the six samples from this first series of field samples.

Another series of field samples consisted of ten air particulate extracts randomly picked among the samples sent to ORNL. The SL spectra were similar to those observed with the first sample series, showing six major emission bands at approximately 316, 336, 360, 404, 434, and 472 nm. The RTP spectra of the field samples were also similar to those studied previously and exhibited a broadband and featureless structure with the maximum emission between 500 and 600 nm. Table II gives the results of the calculation of the SL Ranking Index for this series of field samples.

This second series of field samples were independently analyzed by PEDCo using GC/MS for ten specific PNA compounds used previously in the standard reference mixture, viz, phenanthrene, anthracene, fluoranthene, pyrene, benz[a]anthracene, chrysene, triphenylene, benzo[a]pyrene, benzo[e]pyrene, and perylene. The "total" content for the ten PNA compounds obtained by GC/MS was compared to the SL/RTP composite ranking index as shown in Table II. The correlation between the SL/RTP ranking results and the GC/MS data is illustrated in Figure 3. As depicted in Figure 3, there is a "linear" correlation between the SL/RTP ranking index and the total content for the ten PNAs analyzed by GC/MS.

Further information of analytical interest could also be provided by the spectral structure of the SL profiles. Examination of the SL profile of samples CG642 and CG635 shows that the intensity is higher

for wavelengths >360 nm where the emission of most PNAs having more than three benzenoid rings occurs. The GC/MS data on Table II for samples CG642 and CG635 are in good agreement with this qualitative prediction. Since the GC/MS analyses dealt mainly with high-number ring PNAs, the total PNA content obtained by GC/MS for CG642 and CG635 are relatively higher than those obtained with the other samples. Note that the data for samples CG642 and CG635 (triangular dots on Figure 3) correspond to another correlation line with a higher slope. This result demonstrates that the SL profile can be used not only to provide an index for ranking but also to provide useful information concerning the ring size of the PNA constituents in the sample.

Another series of air particulate sample extracts, previously ranked by SL and RTP, were also analyzed by Rockwell International using HPLC. The comparative results are illustrated in Figure 4. The results of this field study demonstrate the efficacy of the SL/RTP procedures to provide a ranking based solely on the total intensity of the luminescence profile without requiring any physical sample separation. Use of this ranking procedure will reduce the cost of pollution control and human exposure assessment by reducing the number of unnecessary analyses by more sophisticated and more expensive techniques.

References

[1] Greenberg, A., Yokoyama, R., Giorgio, P., and Canova, F., Analysis of Polynuclear Aromatic Hydrocarbons on the Airborne particulates of Urban New Jersey, in Polyaromatic Hydrocarbons, ed. Bjorseth and A. J. Dennis, Batelle Press, p. 193 (1980).

[2] Funke, W., Romanowski, T., Konig, J., and Balfanz, E., Detection of High Molecular Polycyclic Aromatic Hydrocarbons in Airborne Particulate Matter Using MS, GC, and GC/MS, in Polyaromatic Hydrocarbons. eds. M Cooke, A. J. Dennis, and G. L. Fisher, Batelle Press, p. 305 (1982).

[3] Vo-Dinh, T. Multicomponent Analysis by Synchronous Luminescence Spectrometry, Anal. Chem. 50: 396(1978).

[4] Vo-Dinh, T. Synchronous Excitation Spectroscopy, in Modern Fluorescence Spectroscopy, Volume 4, ed. by E. L. Wehry, Plenum Press, NY, 1981.

[5] Vo-Dinh, T. Room Temperature Phosphorimetry for Chemical Analysis, John Wiley and Sons, Inc. Publishers, New York (1984).

[6] Vo-Dinh, T., and Gammage, R. B. Singlet-Triplet Energy Difference as a parameter of Selectivity in Synchronous Phosphorimetry, Anal. Chem. 50: 2054 (1979).

[7] Vo-Dinh, T., and Bruewer, T. B. Field Evaluation of a Cost-Effective Screening Procedure for Polynuclear Aromatic Compounds in Ambient Air Samples, (Final Report, Interagency Agreement No. ERD-82-170, U.S. Environmental Protection Agency) Oak Ridge National Laboratory, Oak Ridge, TN (1983).

Table I. Comparison between SL/RTP result and GC/MS data.[a]

SL & RTP Ranking (ORNL)	CG654>	CG543>	CG626>	CG634>	CG573>	CG656
GC/MS Analysis (PEDCo)[b]						
Phenanthrene	52	180	70	44	42	19
Anthracene	0	0	0	0	0	0
Fluoranthene	1015	446	238	96	63	60
Pyrene	1253	479	221	86	65	61
Benz[a]anthracene	1608	408	135	0	0	0
Chrysene/ Triphenylene	2437	731	260	66	0	59
Benzo[e]pyrene	1120	278	152	0	0	0
Benzo[a]pyrene	1539	297	0	0	0	0
Perylene	166	51	0	0	0	0

[a]SL/RTP measurements were conducted at ORNL; GC/MS measurements were conducted at PEDCo.

[b]GC/MS data = μg/mL.

Table II. Comparison between the SL/RTP ranking results and GC/MS data for the 2nd sample series.

Sample	SF Index	RTP Index	SL/RTP Ranking Index	GC/MS Data μg/mL
CG616	90	35	125	2.197
CG545	75	25	100	2.264
CG627	65	20	85	1.119
CG560	55	20	75	0.727
CG619	65	10	75	1.094
CG629	20	15	35	0.056
CG624	15	5	20	0.134
CG533	15	1	16	0.260
CG642[a]	45	15	60	2.390
CG635[a]	20	2	22	0.414

[a]The SF profile of these two samples indicate a different PNA composition with relatively higher content of PNA with 4 rings and up.

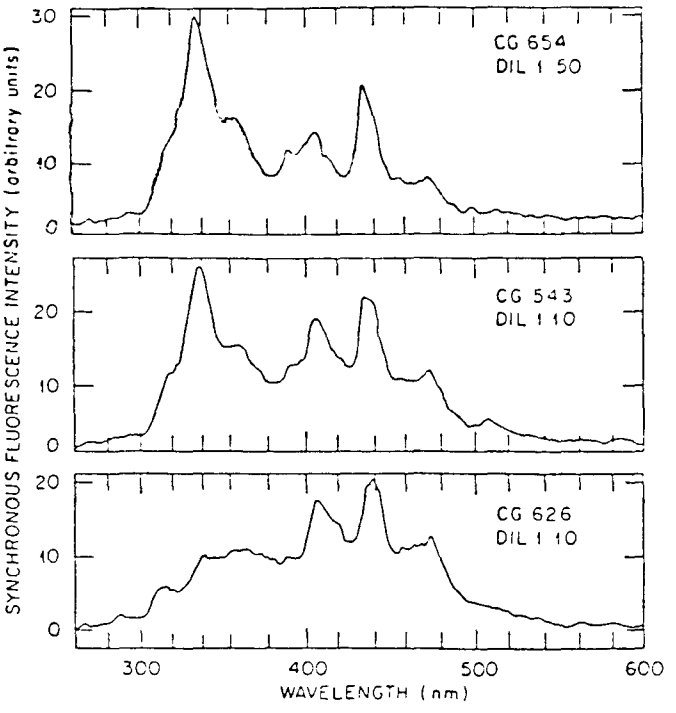

Figure 1: Synchronous luminescence profiles of several extracts of ambient air particulate samples.

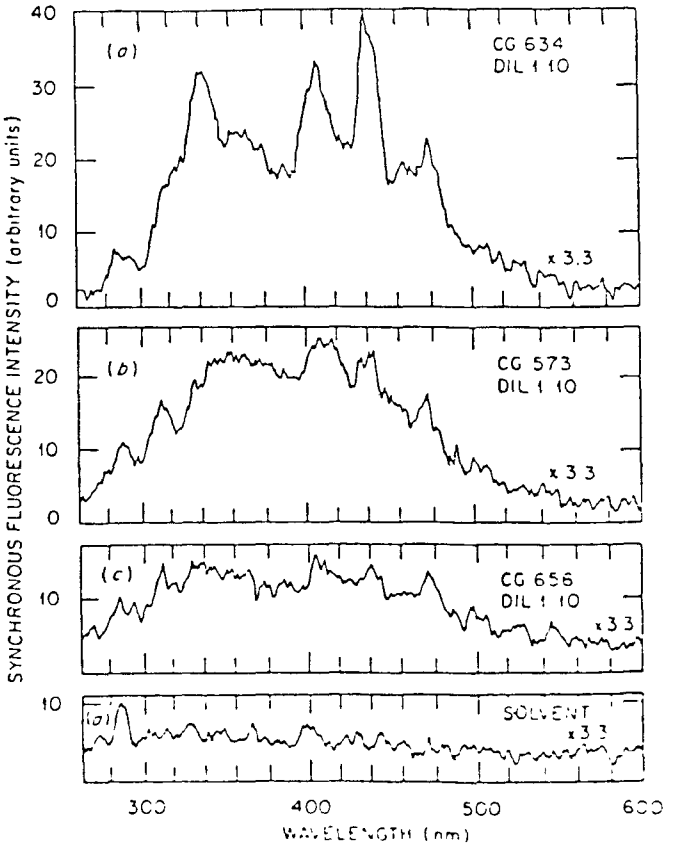

Figure 2: Synchronous luminescence profiles of several extracts of ambient air particulate samples.

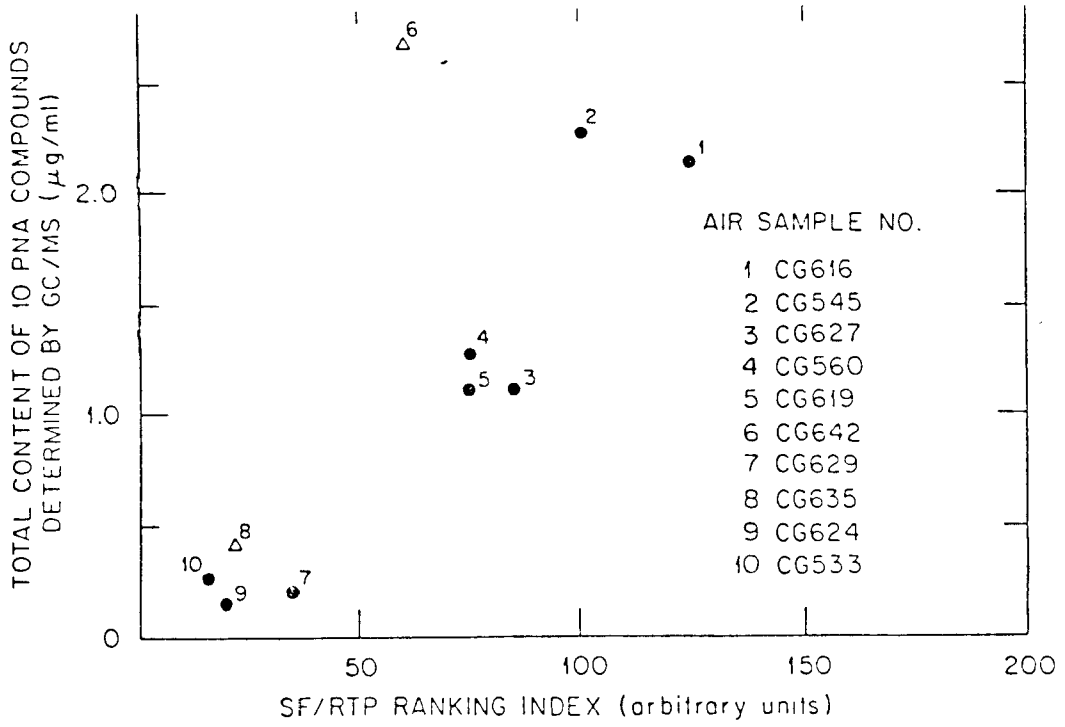

Figure 3: Correlation between SL/RTP ranking results and GC/MS data for several air sample extracts.

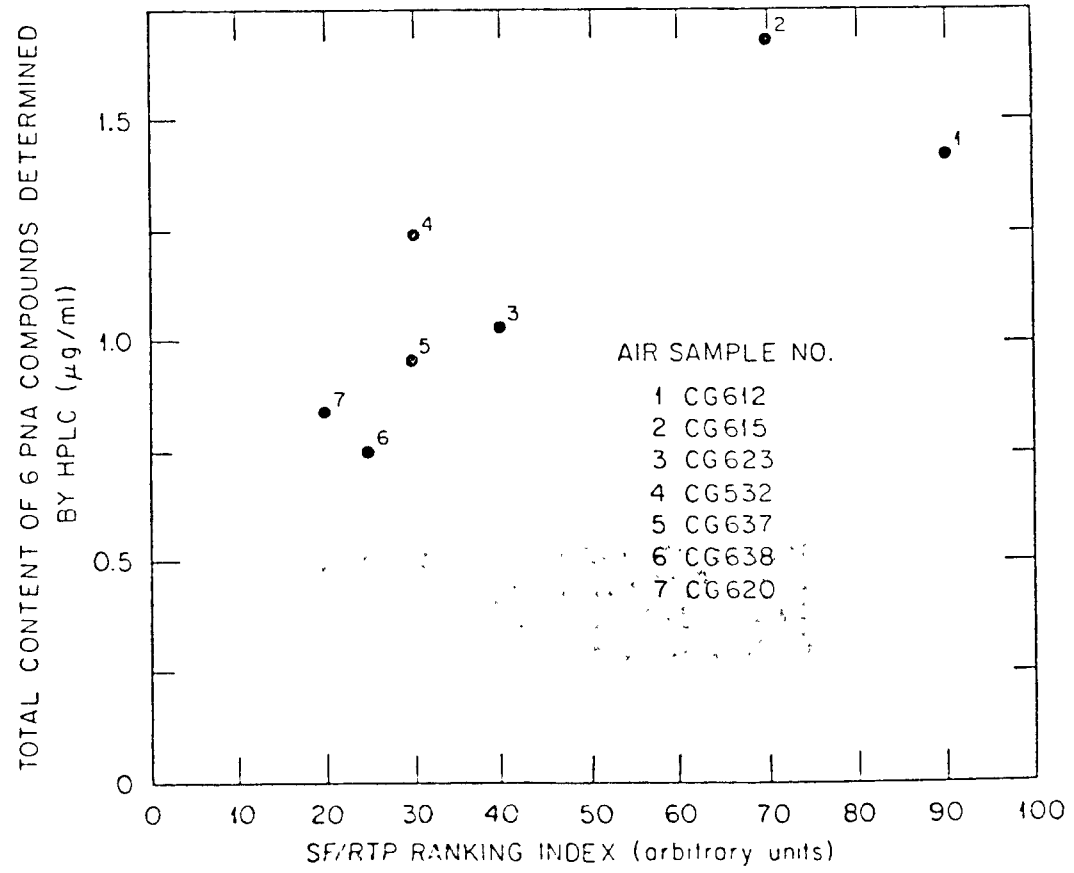

Figure 4: Correlation between SL/RTP ranking results and HPLC data for several air sample extracts.

☆USGPO: 1983 — 759-102/0805